



**Extraction of Marine *Chlorella* sp. and Potential Applications of the
Extracted Residue**

Muhammad Amin

**A Thesis Submitted in Fulfillment of the Requirements for the Degree of
Doctor of Philosophy in Chemical Engineering**

Prince of Songkla University

2019

Copyright of Prince of Songkla University



**Extraction of Marine *Chlorella* sp. and Potential Applications of the
Extracted Residue**

Muhammad Amin

**A Thesis Submitted in Fulfillment of the Requirements for the Degree of
Doctor of Philosophy in Chemical Engineering**

Prince of Songkla University

2019

Copyright of Prince of Songkla University

Thesis Title Extraction of Marine *Chlorella* sp. and Potential Applications
of the Extracted Residue

Author Mr. Muhammad Amin

Major Program Chemical Engineering

Major Advisor

.....
(Assoc. Prof. Dr. Pakamas Chetpattananondh)

Examining Committee:

.....Chairperson
(Assoc. Prof. Dr. Kamchai Nuithitikul)

.....Committee
(Assoc. Prof. Dr. Pakamas Chetpattananondh)

.....Committee
(Assoc. Prof. Dr. Sukritthira Ratanawilai)

.....Committee
(Assoc. Prof. Dr. Kulchanat Prasertsit)

.....Committee
(Asst. Prof. Dr. Suratsawadee Kungsanant)

The Graduate School, Prince of Songkla University, has approved this thesis as fulfillment of the requirements for the Doctor of Philosophy Degree in Chemical Engineering.

.....
(Prof. Dr. Damrongsak Faroongsarng)
Dean of Graduate School

This is to certify that the work here submitted is the result of the candidate's own investigations. Due acknowledgement has been made of any assistance received.

.....Signature
(Assoc. Prof. Dr. Pakamas Chetpattananondh)
Major Advisor

.....Signature
(Mr. Muhammad Amin)
Candidate

I hereby certify that this work has not been accepted in substance for any degree, and is not being currently submitted in candidature for any degree.

.....Signature
(Mr. Muhammad Amin)
Candidate

Thesis Title	Extraction of Marine <i>Chlorella</i> sp. and Potential Applications of the Extracted Residue
Author	Mr. Muhammad Amin
Major Program	Chemical Engineering
Academic Year	2018

ABSTRACT

In this work, marine *Chlorella* sp. was explored in various perspectives from biomass preparation and extraction through applications of its extracted residue. The experiments were divided into three sections as follows.

Section-I. Effect of drying methods for biomass preparation. Marine *Chlorella* sp. biomass cultivated in 25 m³ open pond was harvested by flocculation after 7 days, washed to remove contamination and vacuum filtered to prepare wet paste. This paste (90% moisture) was divided into five parts to be processed for; (I) fresh paste-FP, (II) stored wet paste-SWP, (III) sun drying-SD, (IV) oven drying-OD, and (V) freeze drying (FD). The total processing time (hours) accounted for biomass drying was observed as 72, 40 and 24 h with energy expanse of 14.07, 590 and 1094 MJ/kg for SD, OD and FD, respectively to obtain biomass with moisture content of 8-9%. The biochemical analysis showed that FD biomass had highest accumulated lipid (10.68%), protein (22.1%) and energy (275.4 kcal) while carbohydrates were slightly lower than OD and SD but significantly higher than FP biomass.

Section-II. Optimization of extraction by ultrasonication. Effects of various extraction factors including temperature (30-40 °C), time (60-120 min), biomass to solvent ratio (1/10-1/25 g/ml), solvent to solvent ratio (ml/ml), extraction cycles and solvent type on lipid yield (LY) were investigated. The results showed that with single extraction and single solvent recovery (1-1-cycle) process the LYs from fresh and stored paste were 11.7% and 6%, respectively, while freeze-dried biomass produced an 18.5% LY. The energy consumption was 6,000 MJ/kg lipid for the wet route and 8,200 MJ/kg lipid for the dry route in the 1-1-cycle process. The LY of the 2-1-cycle process using methanol/hexane (2/1 v/v) with a biomass to solvent ratio 1/20 g/ml was 31% and considered as a base case scenario of this study, which is 40.3% and 9.7% greater than those of the 1-1-cycle and 2-2-cycle, respectively. At developed optimized

condition extraction of OD and SD biomass shown 27% and 22% LY, which is 12.90% and 29.1% lower than the base case value. Extracted lipids from OD, SD and FD were further scrutinized for their biochemical composition, fatty acids, free fatty acids (FFA) and chlorophyll contents. Moisture in all samples was observed lower than 10% and the ash contents were recorded as 10-11%. The protein (5.9%-7.1%) contents were also almost similar. However, the crude lipid, which is main component for biodiesel production was found highest in SD extract (53.1%), followed by FD extract (46%) and lowest in OD extract (34.3%). The carbohydrates were 41.65%, 19.87% and 32.13%, while energy contents (calories) were calculated as 500, 570 and 585 for OD, SD and FD, respectively. Total fatty acids were observed between (63%-66%) in dried extracts. SD biomass seems superior among the lipid extract of biomass, however sun drying is time consuming process and not a suitable choice in tropical regions. Moreover, SD biomass has an odor. The FD biomass was rich green, with regular structure and no burning spots observed at its surface. Due to these features along with high lipid yield, high crude lipid contents and longer period storage capability it was selected for further processing.

Section-III. Assessment of extracted marine *Chlorella* sp. residue (EMCR) potential for the recovery of energetic and non-energetic products with their applications. EMCR was recycled for (i) biochar production with its application for heavy metals and yellow dye-145 abatement and (ii) bio-oil production via microwave pyrolysis assisted with EMCR derived biochar as a microwave absorber (MA). The resulting biochars were enriched with O containing functional groups. They are attractive for removal of heavy metals and anionic dyes. The surface areas of biochar prepared at 450, 550 and 650 °C were 266 m²/g, 355 m²/g and 151 m²/g, respectively. BC-450 was applied for Cr(VI), Zn(II) and Ni(II) removal by conventional adsorption (CA) and ultrasonic adsorption (UA). UA was found 1.1-1.3 higher adsorption capacity than CA in much shorter time. The maximum adsorption capacity was found as 27.45 mg/g for Ni(II) in UA. BC 550 applied for yellow dye removal by ultrasonication was highly efficient and shown an equilibrium achievement at 1 min. with 99.9% removal efficiency.

The EMCR was also subjected to microwave pyrolysis (MWP) for bio-oil production with investigation of temperature (350-450 °C), time (20-40 min) and MA loading (10-

30 wt.%) at fixed microwave power of 850 W. BC-450 prepared in earlier step was introduced as MA for the first time. The pyrolysis condition was optimized to obtain maximum bio-oil yield using the Response Surface Methodology (RSM) based on Central Composite Design (CCD). The optimum condition was 350 °C, 15% MA loading and 40 min, which yielded 46% bio-oil. The bio-oil mainly composed of nitrogenated (30.37%), phenols (17.56%), furans and aromatics (5.56%), esters (17.62%), acids (12.18%), alcohols (6.07%), ketones/aldehydes (2.88%), sugar (2.30%) and alkenes (0.5%) compounds. Although, a high N containing compounds restricting the bio-oil utilization as a fuel but it could be an attractive feedstock for chemical and petrochemical industry. The results showed a high feasibility of applying EMCR as the feedstock for biochar and bio-oil production. The EMCR derived biochar presented great efficiency as the microwave absorber. The recycling of EMCR could improve the environmental and economy of *Chlorella* based algal industry.

Keywords: Marine *Chlorella* sp, ultrasonic, lipid extraction, extracted residue, biochar, Microwave pyrolysis, bio-oil

ACKNOWLEDGMENT

In the Name of **ALLAH**, THE benevolent and THE clement, all the praises and thanks to **ALLAH**, for the blessing of life and wisdom for never neglecting me, who gave me courage every time during my research work and in whole life. Countless salutation upon The Holy Prophet HAZRAT MUHAMMAD (صلى الله عليه وسلم), the city of knowledge and blessing for an entire creature who has guided his Ummah to seek knowledge from cradle to grave, and enabled me to win the honor of life.

My journey to obtain a PhD degree ends with the successful completion of this thesis. In this journey, I did not travel in vacuum or darkness but were kept on track and been seen through to completion with the support, guidance and encouragement of numerous people including my family, friends, colleagues, teaching and non-teaching staff of Chemical Department.

First and foremost, I would like to express my honest, sincere, and heartfelt gratitude to my advisor **Assoc. Prof. Dr. Pakamas Chetpattananondh**, Head of Department of Chemical Engineering, Faculty of Engineering, Prince of Songkla University, who gave me the opportunity to study Ph.D program. I am thankful for her continuous support during Ph.D study, research, patience, motivation, inspiration, enthusiasm, and immense knowledge. Her tutelage helped me all the time during research work and in writing manuscript and thesis. I could not have imagined having a better advisor or mentor for my Ph.D study than her. I am short of words to express adequately my appreciation and gratitude to her.

I extend my thanks to **Assoc. Prof. Dr. Sukritthira Ratanawilai**, head for graduate studies, Department of Chemical Engineering, Faculty of Engineering, Prince of Songkla University for her continuous help and support during the entire program and specifically her guidance during my research proposal examination. I am also thankful to **Assoc. Prof. Dr. Kulchanat Prasertsit** and **Asst. Prof. Dr. Suratsawadee Kungsanat**, members of my proposal examination committee, for their valuable suggestion, guidance and their kind support.

I take this opportunity to sincerely acknowledge the Department of Chemical Engineering, Faculty of Engineering and their entire teaching and non-teaching staff for providing me all the support to accomplish the tasks related with this thesis. My

sincere gratitude goes to **Ms. Pornpimon Sansuk, Ms. Keerattaya Charoenmark, Mr. Somkid Geenapong, Mr. Tanakorn Kiatkwanboot, Ms. Kanjana Kantakapan, Mr. Narong Apayanugool**) for their continuous support during experimental activities and sampling analysis.

I expand special thanks to my colleagues and friends, Dr. Asadullah, Mr. Syed Haseeb Sultan, Mr. Khurshid Ahmad Baloch, Dr. Faisal Usman, Mr. Zahid Naeem Qaisrani, Dr. Jatuporn Parnthong, Mr. Kyaw Thu, Dr. Issara Sangsat and Dr. Noree Tehlah for their moral support and for stimulating a fun filled environment during stay in Prince of Songkla University.

I gratefully acknowledge the staff and scientist of Scientific Equipment Centre (SEC) and ADCET, PSU, for their sincere support in samples analysis.

I owe a great deal of appreciation and gratitude to National Institute of Coastal Aquaculture (NICA), Songkhla, Thailand for their kind support by providing Marine *Chlorella* Sp. Biomass.

I am very thankful to my seniors, Dr. Supansa Paisan and Mr. Mongkol Tantichantakarun for their support, encouragement and help for biomass collection and processing.

I owe my love and gratitude to my beloved wife **Ms. Sassy Jaffar** and lovely son **Mr. Saim Amin** for their support, care, love and prayers during this entire journey. They played a catalytic role in my life to achieve the desired goals. I highly admire their patience and scarification.

Last but not least, I expand my love and respect to one of the beautiful land in the world “THAILAND” and their friendly nation. Who, welcomed me and my family with open heart, provided me an opportunity for higher studies. I am also enriched with wonderful memories belongs to “HAT YAI”, which is birthplace of my son.

I sincerely thank all committee members of my thesis examination, **Assoc. Prof. Dr. Kamchai Nuithitikul, Assoc. Prof. Dr. Pakamas Chetpattananondh, Assoc. Prof. Dr. Sukritthira Ratanawilai, Assoc. Prof. Dr. Kulchanat Prasertsit** and **Asst. Prof. Dr. Suratsawadee Kungsanat** for their support and invaluable comments on my research. Also, I would like to acknowledge the financial support of Ph.D. scholarship, Prince of Songkla University.

Muhammad Amin

CONTENTS

	Page
ABSTRACT	v
ACKNOWLEDGEMENT	viii
CONTENTS	x
LIST OF FIGURES	xiv
LIST OF TABLES	xvii
ACRONYMS	xix
LIST OF PUBLICATIONS	xxi
1 Introduction	1
1.1 Importance of algal biomass	1
1.2 Algal biomass harvesting and cultivation	3
1.3 Extraction of algae	4
1.4 Crude algal extract	4
1.5 Potential applications of algal residue	6
1.6 Literature information	7
2 Problem statement	9
2.1 Objectives and scope	10
2.2 Expected benefits	11
2.3 Significant results and discussion	13
3 Assesment of drying techniques effects on biochemical quality of marine <i>Chlorella</i> sp. biomass and their extracts	21
3.1 Introduction	23
3.2 Materials and methods	25
3.2.1 Chemicals	25
3.2.2 Strain cultivation, harvesting and wet paste preparation	25
3.2.3 SD, OD and FD processes	26
3.2.4 Ultrasonic extraction	27
3.2.5 Analytical approach	27
3.3 Results and Discussion	28
3.3.1 Analysis of OD, SD and FD biomass and their composition	28
3.3.2 UE of lipid from OD, SD and FD biomass: yield and composition	29

3.3.3	Drying effects on biochemical composition of crude lipid	30
3.3.4	Free fatty acid (FFA) and chlorophylls	31
3.3.5	Analysis of fatty acids composition	32
3.3.6	Selection criteria	33
4	Enhanced lipid recovery from marine <i>Chlorella</i> sp. by ultrasonication with an integrated process approach for wet and dry biomass	48
4.1	Introduction	50
4.2	Material and method	52
4.2.1	Materials	52
4.2.2	Microalgae culture, harvesting and preparation	52
4.2.3	Ultrasonic extraction	53
4.2.4	UE-Solvent recovery system analysis	54
4.2.5	Analytical procedures	55
4.2.6	Energy Analysis	56
4.3	Results and Discussion	56
4.3.1	Wet route extraction: process condition analysis	56
4.3.1.1	Model fitting and optimization	57
4.3.1.2	Effect of storage on wet paste extraction	58
4.3.2	Dry route extraction: process condition analysis	59
4.3.2.1	Model fitting and optimization	59
4.3.3	Comparison between wet and dry route	59
4.3.4	Effect of solvent type, biomass/solvent and extraction system	60
4.3.4.1	Effect of biomass to solvent ratio	60
4.3.4.2	Effect of solvent system	61
4.3.4.3	UE-solvent recovery system analysis (1-1, 2-1 and 2-2 cycle)	61
4.3.5	Biomass and lipid characterization	62
4.3.6	Energy consumption	63
5	Application of extracted marine <i>Chlorella</i> sp. residue for bio-oil production as the biomass feedstock and microwave absorber	84
5.1	Introduction	86
5.2	Material and methodology	88
5.2.1	Feedstock preparation	88

5.2.2	Characteristics of material	89
5.2.3	Microwave pyrolysis	90
5.2.4	GC-MS analysis of bio-oil	92
5.3	Results and discussion	92
5.3.1	Proximate and ultimate analysis	92
5.3.2	FTIR analysis	94
5.3.3	Thermogravemetric analysis of EMCR	95
5.3.4	Microwave pyrolysis optimization	95
5.3.5	GC-MS analysis of bio-oil	98
6	Biochar production from extracted marine <i>Chlorella</i> sp. residue with ultrasonication adsorption for high efficiency of heavy metals removal	117
6.1	Introduction	120
6.2	Materials and methods	122
6.2.1	Chemicals	122
6.2.2	Microalgal biomass and its residue preparation	122
6.2.3	Biochar preparation	122
6.2.4	Biochar characterization	123
6.2.5	Adsorption experiment	123
6.2.6	Adsorption isotherm and kinetic study	124
6.3	Results and discussion	126
6.3.1	Characterization and yield of BC-450	126
6.3.2	Effects of adsorption parameters	129
6.3.2.1	Effect of initial pH solution	129
6.3.2.2	Effect of contact time	130
6.3.2.3	Effect of adsorbent dose	131
6.3.2.4	Effect of initial metal concentration	131
6.3.3	Adsorption isotherm	131
6.3.4	Adsorption kinetics	132
7	Algal waste recycling for biochar production at different temperatures: Physiochemical characterization and application for RYD 145 removal	154
7.1	Introduction	156
7.2	Materials and method	158

7.2.1	Materials	158
7.2.2	Feedstock preparation	158
7.2.3	Biochar preparation	158
7.2.4	Biochar characterization	159
7.2.5	Adsorbate preparation	159
7.2.6	Adsorption experiment	159
7.2.7	Adsorption isotherm and kinetic study	160
7.3	Results and discussion	161
7.3.1	Elemental composition of EMCRSW derived biochar	161
7.3.2	Surface properties of biochar	163
7.3.3	BC-550 performace for UA of RYD 145	164
7.3.3.1	Effect of contact time	164
7.3.3.2	Effect of pH	164
7.3.3.3	Effect of adsorbent dose	164
7.3.3.4	Effect of initial dye concentration	165
7.3.3.5	Effect of ultrasound frequency	165
7.3.4	Adsorption isotherm and kinetics	165
8	Extarction and Quantification of chlorophyll from microalgae <i>Chlorella</i> sp.	180
8.1	Introduction	181
8.2	Material and method	182
8.2.1	Materials and chemicals	182
8.2.2	Biomass harvesting and post processing	183
8.2.3	Analysis	184
8.3	Results and discussion	185
8.3.1	Wet paste biomass compositional analysis	185
8.3.2	Ultrasonic extraction and optimization	186
8.3.3	Dilution factor of methanol/hexane extract in different solvents	187
	VITAE	191

LIST OF FIGURES

		Page
Figure.1.1	<i>Chlorella</i> sp.	3
Figure 1.2	General lipid classification	6
Figure. 2.1	Overall processing scheme	12
Figure. 3.1	A schematic diagram of experimental and analysis work from marine <i>Chlorella</i> sp. cultivation and biomass preparation to lipid extraction.	40
Figure. 3.2	A schematic diagram of mini homemade solar dryer	41
Figure. 3.3	Pictorial view of marine <i>Chlorella</i> sp. biomass (a) Sun dried, (b) Oven dried, (c) Freeze-drying and, and extracted crude lipids	42
Figure. 3.4	Absorption spectra of chlorophylls presented in crude lipid extract of sun dry, oven dry and freeze-dried biomass of marine <i>Chlorella</i> sp. using UV spectrophotometer.	43
Figure. 3.5	Impact of drying techniques on the lipid yield of marine <i>Chlorella</i> sp. biomass	44
Figure. 4.1	Experimental process schematic diagram	73
Figure. 4.2	Extraction and solvent recovery systems,1-1, 2-1 and 2-2-cycle	74
Figure. 4.3	3-D surface plots presenting the effect of temperature and time on lipid yield of (a) wet-route UE and (b) dry-route UE	75
Figure. 4.4	Impact on lipid yield of (a) biomass to solvent ratio, (b) solvent system, (c) extraction and solvent recovery cycle and (d) solvent ratio	76
Figure. 4.5	SEM images (Left: 2000 X, 20.0 kV and 20 μ m; Right: 10,000 X, 20.0 kV and 5 μ m) of freeze-dried biomass before and after ultrasonication at the optimum conditions.	77

Figure. 4.6	GC-FID profile of the extracted lipids from freeze-dried biomass at 35°C for 90 min. using methanol/hexane 2/1 (v/v) with B/S 1/20 (g/ml) by the 2-1-cycle scheme	78
Figure. 5.1	Overall processing scheme of experimental investigation.	106
Figure. 5.2	Microwave pyrolysis system.	107
Figure. 5.3	FTIR profiles of (a) marine <i>Chlorella</i> sp., (b) EMCR and (c) biochar and (d) TG and DTG profiles of EMCR	108
Figure. 5.4	3-D response surface for bio-oil yield showing the effects of (a) time and temperature, (b) temperature and MA loading and (c) MA loading and time.	109
Figure. 5.5	Biochars obtained by MWP at the optimum condition and conventional pyrolysis at 450 °C for 60 min	110
Figure 6.1	Process schematic diagram of algal biomass cultivation to biochar preparation and application.	141
Figure 6.2	Removal efficiency of Cr(VI), Zn(II) and Ni(II) by BC-450 with conventional adsorption and ultrasonic adsorption to study effect of (a) initial pH (b)contact time (c) adsorbent dose and (d) initial heavy metal concentration	142
Figure 6.3	Adsorption isotherms of heavy metals on BC-450 with conventional adsorption (CA) and ultrasonic adsorption (UA): (a) Cr(VI)-CA, (b) Zn(II), (c) Ni(II), (d) Cr(VI)-UA, (e) Zn(II)-UA and (f) Ni(II)-UA	143
Figure 6.4	The pseudo second order (PSO) kinetic plots for adsorption of heavy metals on BC-450: (a) Cr(VI)-CA, (b) Zn(II), (c) Ni(II), (d) Cr(VI)-UA, (e) Zn(II)-UA and (f) Ni(II)-UA	144
Figure. S1	FTIR spectra of BC-450	151
Figure. S2	N ₂ adsorption/desorption isotherms of BC-450	152

Figure. S3	SEM images of (a) EMCR, (b) BC-450, (c) BC-450 after UA of Ni(II) and (d) BC-450 after CA of Ni(II)	153
Figure.7.1	Overall processing scheme of biochar production from EMCRSW and its application for RYD 145 adsorption by ultrasonication	172
Figure. 7.2	FTIR profiles of EMCRSW biochar at different temperatures	173
Figure 7.3	Removal efficiency of RYD-145 by BC-550 with ultrasonic adsorption to study effect of: (a) contact time (b) adsorbent dosage (c) initial concentration and (d) ultrasonic frequency	174
Figure. 7.4	Adsorption isotherm	175
Figure 8.1	Marine <i>Chlorella</i> sp. cultivated in 20 m ³ open pond system	182
Figure. 8.2	Fresh wet algae paste after vacuum filtration	183
Figure 8.3	Surface and contour plots of fitted response for total chlorophyll yield ($\mu\text{g/ml}$).	188

LIST OF TABLES

		Page
Table 1.1	Oil production from different crops per area	2
Table 1.2	Oil contents of different microalgae	2
Table 1.3	Composition (% wt.) of different microalgae species	3
Table 1.4	A comprehensive literature on lipid extraction using different	7
Table 1.5	Algal and lignocellulosic biochars applications as an adsorbent	8
Table 3.1	Biochemical composition of marine <i>Chlorella</i> sp. biomass dried using different drying techniques	45
Table 3.2	Biochemical constituents, FFA and chlorophyll of SD, OD and FD extract	46
Table 3.3	FAME's of lipid extracted from SD, OD and FD biomass	47
Table 4.1	The experimental and model predicted responses for the UE of fresh wet paste and freeze-dried biomass	79
Table 4.2	Analysis of variance (ANOVA) for UE of fresh wet paste and freeze-dried biomass	80
Table 4.3	Regression coefficients of the models for UE of fresh wet paste and freeze-dried biomass	81
Table 4.4	Fatty Acid Methyl Esters of marine <i>Chlorella</i> sp extracted lipid	82
Table 4.5	Energy consumption of processes at lab-scale for wet and dry routes	83
Table 5.1	The experimental and predicted bio-oil yields from microwave pyrolysis of EMCR at various RSM based on CCD conditions.	111
Table 5.2	Proximate and ultimate analysis of marine <i>Chlorella</i> , EMCR, biochar and other algal biomass and residues from literature.	112
Table 5.3	Analysis of variance (ANOVA) and regression coefficients for bio-oil production from EMCR.	113
Table 5.4	Chemical composition of bio-oil from GC-MS analysis.	114
Table 6.1	Characterization of EMCR, BC-450 and other biochars	

	from literature.	145
Table 6.2	Comparison of yield, surface area and maximum adsorption capacity of BC-450 with other biochars from literature	146
Table 6.3	Adsorption isotherm parameters	147
Table 6.4	The pseudo-first-order (PFO) and pseudo-second-order (PSO) kinetic parameters for heavy metal adsorption on BC-450	148
Table 7.1	Adsorbate characteristics	176
Table 7.2	Comparison of pH, and composition of EMCRSW derived biochars with other studies	177
Table 7.3	Comparison of yield and surface area of EMCRSW derived biochars with other biochars and materials from literature	178
Table 7.4	Adsorption isotherm parameters	179
Table 8.1	Full factorial design runs with actual and model predicted response	187
Table 8.2	Regression analysis	188

ACRONYMS

ANOVA	Analysis of Variance
AAS	Atomic Absorption Spectrophotometry
AOAC	Association of Official Analytical Chemistry
ASTM	American Society for Testing Materials
B&D	Bligh and Dyer
B/S	Biomass to solvent ratio
BET	Brunauer-Emmett-Teller
BC	Biochar
CCD	Central Composite Design
CR(VI)	Chromium (VI)
C_i	Initial concentration (mg/L)
C_e	Final concentration (mg/L)
CV	Coefficient of Variance
CA	Conventional adsorption
DF	Degree of Freedom
EMCR	Extracted marine <i>Chlorella</i> Residue
EMCRSW	Extracted marine <i>Chlorella</i> Residue Solid Waste
E	Energy
EDX	Energy Dispersive X-ray
EN	European
FAME	Fatty Acid Methyl Esters
FD	Freeze-Drying
FFD	Full Factorial Design
FP	Fresh Paste
FFA	Free Fatty Acids
FC	Fixed Carbon
FTIR	Fourier Transformed Infrared Spectrophotometer
FW	Fresh Water
GC-FID	Gas Chromatograph-Flame Ionization Detector
GC-MS	Gas Chromatograph-Mass Spectrometry
HHV	Higher Heating Value

h	hour
IL	Ionic Liquid
kCal	kilo calories
K _f	Freundlich Constant
LY	Lipid Yield
MA	Microwave Absorber
MWP	Microwave Pyrolysis
MJ	Megajoule
MAPE	Mean Absolute Percent Error
min	minute
MS	Mean Square
NIST	National Institute of Standard and Technology
NICA	National Institute of Coastal Aquaculture
n.d	not detected
OD	Oven Drying
NL's	Neutral Lipids
Pa	Pascal
PSO	Pseudo Second Order
PFO	Pseudo First Order
RSM	Response Surface Methodology
SW	Saline Water
SD	Sun Drying
SEM	Scanning Electron Microscopy
SWP	Stored Wet Paste
TAG	Triglycerides
TGA	Thermogravimetric Analysis
T	Temperature
UA	Ultrasonic Adsorption
UE	Ultrasonic Extraction
VM	Volatile Matters

LIST OF PUBLICATIONS

- I M. Amin, P. Chetpattananondh “Assessment of drying techniques effects on biochemical quality of marine *Chlorella* sp. biomass and their extracts” (Under process)
- II M. Amin, P. Chetpattananondh “Enhanced lipid recovery from marine *Chlorella* sp. by ultrasonication with an integrated process approach for wet and dry biomass” *Bioenergy Research*, 2019, 1-15.
- III M. Amin, P. Chetpattananondh, S. Ratanawilai “Application of extracted marine *Chlorella* sp. residue for bio-oil production as the biomass feedstock and microwave absorber” *Energy Conversion and Management*, 195 (2019):819-829.
- IV M. Amin, P. Chetpattananondh “Biochar from extracted marine *Chlorella* sp. residue for high efficiency adsorption with ultrasonication to remove Cr (VI), Zn (II) and Ni (II)” *Bioresource Technology*, 289 (2019) 121578.
- V M. Amin, P. Chetpattananondh “Algal waste recycling for biochar production at different temperatures: physiochemical characterization and application for yellow dye removal” (Under process).
- VI M Amin, P Chetpattananondh, M N Khan, F Mushtaq and S K Sami “Extraction and Quantification of Chlorophyll from Microalgae *Chlorella* sp.” *IOP Conf. Series: Material Science and Engineering* 414 (2018) 0120025.
- VII Petty Patent: Process of biochar production from extracted microalage (Under process: No. 1903001414)


Paper-II Acceptance Letter
Journal Bioenergy Research

Find messages, documents, photos or people

← Back ↶ ↷ ➔

📁 Archive 📁 Move

• [Fwd: Decision on your manuscript #BERE-D-18-00366R1]

 • **pakamas.p@psu.ac.th** <pakamas.p@psu.ac.th>
To: engr_amin63@yahoo.com

----- Original Message -----
Subject: Decision on your manuscript #BERE-D-18-00366R1
From: "BioEnergy Research" <em@editorialmanager.com>
Date: Wed, May 15, 2019 9:29 pm
To: "Pakamas Chetpattananondh" <pakamas.p@psu.ac.th>

Dear Dr Chetpattananondh:

I am pleased to inform you that your manuscript, "Enhanced lipid recovery from marine *Chlorella* sp. by ultrasonication with an integrated process approach for wet and dry biomass" has been accepted for publication in BioEnergy Research. I appreciate your diligence in making the suggested corrections. Once again my apologies for the time it took to get the manuscript through the review process, but this will hopefully satisfy the student's degree requirements.

For queries regarding your accepted paper, please contact Ms. Aila Asejo (Aila.Asejo@springer.com). Please remember to always include your manuscript number, #BERE-D-18-00366R1, whenever inquiring about your manuscript. Thank you and congratulations!

Sincerely,

Wilfred Vermerris, PhD
Co-Editor-in-Chief, BioEnergy Research

Paper-III Acceptance Letter
Journal Energy Conversion and Management

Date: May 20, 2019
To: "Pakamas Chetpattananondh" pakamas.p@psu.ac.th,pum08@yahoo.com
From: "Energy Conversion and Management" eesserver@eesmail.elsevier.com
Reply To: "Energy Conversion and Management" ecm-els@elsevier.com
Subject: Acceptance of Paper No. ECM-D-19-01986R1 submitted to Energy Conversion & Management

Manuscript No.: ECM-D-19-01986R1
Title: Application of extracted marine Chlorella sp. residue for bio-oil production as the biomass feedstock and microwave absorber
Article Type: Original research paper
Corresponding Author: Professor Pakamas Chetpattananondh
All Authors: Muhammad Amin; Pakamas Chetpattananondh; Sukritthira Ratanawilai
Submit Date: Mar 28, 2019

Dear Professor Chetpattananondh,

I am pleased to confirm that your paper Application of extracted marine Chlorella sp. residue for bio-oil production as the biomass feedstock and microwave absorber has been accepted for publication in Energy Conversion and Management + OA Mirror

Your accepted manuscript will now be transferred to our production department and work will begin on creation of the proof. If we need any additional information to create the proof, we will let you know. If not, you will be contacted again in the next few days with a request to approve the proof and to complete a number of online forms that are required for publication.

I would like to inform you that, if your institution is a subscriber to Energy Conversion and Management, you may have full text access to the journal online at no additional cost to the print subscription through ScienceDirect Web Editions (<http://www.sciencedirect.com/web-editions>). Such access is limited to the last twelve months. For information on the status of accepted papers, after Elsevier has sent you proofs of the paper, please consult our Online Article Status Information System (OASIS) on the Internet at <http://www.elsevier.com/locate/authors/>.

Thank you for this contribution to Energy Conversion and Management. I hope your present research is progressing well, and I look forward to reading future contributions to Energy Conversion and Management from you and your colleagues. I would appreciate your recommendation to your other colleagues that they consider submitting their manuscripts to Energy Conversion and Management for review and publication.

With kind regards,
Keat Teong Lee
Editor
Energy Conversion and Management + OA Mirror

Paper-IV Acceptance Letter
Journal Bioresource Technology

View Letter

Close

Date: May 27, 2019
To: "Pakamas Chetpattananondh" pakamas.p@psu.ac.th,pum08@yahoo.com
cc: ;engr_amin63@yahoo.com
From: "Bioresource Technology" eesserver@eesmail.elsevier.com
Reply To: "Bioresource Technology" bite@elsevier.com
Subject: Your Submission BITE-D-19-02527R1

Ms. Ref. No.: BITE-D-19-02527R1
Title: Biochar from extracted marine Chlorella sp. residue for high efficiency adsorption with ultrasonication to remove Cr(VI), Zn(II) and Ni(II)
Bioresource Technology

Dear Professor Pakamas Chetpattananondh,

I am pleased to inform you that your manuscript "Biochar from extracted marine Chlorella sp. residue for high efficiency adsorption with ultrasonication to remove Cr(VI), Zn(II) and Ni(II)" has been accepted for publication in Bioresource Technology.

Thank you for submitting your work to Bioresource Technology.

Yours sincerely,

HUU HAO NGO, Ph.D
Editor
Bioresource Technology

For further assistance, please visit our customer support site at <http://help.elsevier.com/app/answers/list/p/7923>. Here you can search for solutions on a range of topics, find answers to frequently asked questions and learn more about EES via interactive tutorials. You will also find our 24/7 support contact details should you need any further assistance from one of our customer support representatives.

Petty Patent

แบบ สป/สผ/อสป/001-ก
หน้า 1 ของจำนวน 2 หน้า

สำหรับเจ้าหน้าที่		
 คำขอรับสิทธิบัตร/อนุสิทธิบัตร <input type="checkbox"/> การประดิษฐ์ <input type="checkbox"/> การออกแบบผลิตภัณฑ์ <input checked="" type="checkbox"/> อนุสิทธิบัตร ข้าพเจ้าผู้ลงลายมือชื่อในคำขอรับสิทธิบัตร/อนุสิทธิบัตรนี้ ขอรับสิทธิบัตร/อนุสิทธิบัตร ตามพระราชบัญญัติสิทธิบัตร พ.ศ. 2522 แก้ไขเพิ่มเติมโดยพระราชบัญญัติสิทธิบัตร (ฉบับที่ 2) พ.ศ. 2535 และ พระราชบัญญัติสิทธิบัตร (ฉบับที่ 3) พ.ศ. 2542	วันรับคำขอ ๓๑ พ.ค. ๒๕๖๒	เลขที่คำขอ 1903001A11
	วันยื่นคำขอ 31 พ.ค. 2562	1903001A11
	สัญลักษณ์จำแนกการประดิษฐ์ระหว่างประเทศ	
	ใช้กับแบบผลิตภัณฑ์ ประเภทผลิตภัณฑ์	
	วันประกาศโฆษณา	เลขที่ประกาศโฆษณา
วันออกสิทธิบัตร/อนุสิทธิบัตร	เลขที่สิทธิบัตร/อนุสิทธิบัตร	
ลายมือชื่อเจ้าหน้าที่		
1. ชื่อที่แสดงถึงการประดิษฐ์/การออกแบบผลิตภัณฑ์ กรรมวิธีการผลิตผ่านชีวภาพจากสารละลายขนาดเล็กที่ผ่านการสกัด		
2. คำขอรับสิทธิบัตรการออกแบบผลิตภัณฑ์นี้เป็นคำขอสำหรับแบบผลิตภัณฑ์อย่างเดียวกันและเป็นคำขอลำดับที่ ในจำนวน _____ คำขอ ที่ยื่นในคราวเดียวกัน		
3. ผู้ขอรับสิทธิบัตร/อนุสิทธิบัตร <input type="checkbox"/> บุคคลธรรมดา <input type="checkbox"/> นิติบุคคล <input checked="" type="checkbox"/> หน่วยงานรัฐ <input type="checkbox"/> มูลนิธิ <input type="checkbox"/> อื่นๆ ชื่อ มหาวิทยาลัยสงขลานครินทร์ ที่อยู่ 15 ถนนกาญจนาภิเษย ตำบล/แขวง คอหงส์ อำเภอ/เขต หาดใหญ่ จังหวัด สงขลา รหัสไปรษณีย์ 90110 ประเทศ ไทย อีเมล sawrarod49@gmail.com		3.1 สัญชาติ ไทย 3.2 โทรศัพท์ 0-7428-9337 3.3 โทรสาร 0-7428-9339
<input type="checkbox"/> เลขประจำตัวประชาชน <input type="checkbox"/> เลขทะเบียนนิติบุคคล <input checked="" type="checkbox"/> เลขประจำตัวผู้เสียภาษีอากร ในกรณีที่มีการมา สื่อสารกับท่าน ท่านสะดวกใช้ทาง <input type="checkbox"/> อีเมลผู้ขอ <input checked="" type="checkbox"/> อีเมลตัวแทน		0 9 9 4 0 0 0 5 8 0 8 6 0 <input type="checkbox"/> เติมเต็ม (ตั้งแบบ)
4. สิทธิในการขอรับสิทธิบัตร/อนุสิทธิบัตร <input type="checkbox"/> ผู้ประดิษฐ์/ผู้ออกแบบ <input checked="" type="checkbox"/> ผู้รับโอน <input type="checkbox"/> ผู้ขอรับสิทธิโดยเหตุอื่น		
5. ตัวแทน (ถ้ามี)		5.1 ตัวแทนเลขที่ 2440

CHAPTER 1

1 INTRODUCTION

1.1 Importance of algal biomass

Energy scarcity has been recognized as a global challenge for decades [1-2]. Rapid depletion of 1st generation energy reserves, increased energy demand, high oil prices and environmental issues are main cause for the energy issue [3]. To overcome these challenges, biomass feedstocks from agricultural crops and their residue i.e. palm oil, soybean and sunflower received high attention in last few years [4]. However, food insecurity, land and fresh water requirements are major barriers to their potential application as a biodiesel feedstock [5-6]. The ideal biomass candidate is one which gives a high yield per unit area, incurs low production costs, causes less contamination and consumes less nutrients [7-8].

Algal biomass, known as the 3rd generation bioenergy feedstock has been emerged as a promising source. Maximum biomass and oil yield per unit area is prominent feature of algal biomass over terrestrial crops (Table 1.1). Algal biomass rapidly grow enabled by high photosynthetic efficiency as compared to lignocellulosic biomass [9-11]. Algal biomass could be cultivated in fresh, saline and wastewater for bioenergy production under controlled condition [12-14]. Algae is not directly associated as a food source and have the potential to meet the global energy demand without affecting the food industry [15]. Macro or micro algae contains 20-50% (wt. dry basis) lipids and found the only source of renewable energy that is capable of meeting the global requirement for transport fuels [16]. In industrial aspects, microalgae also have the potential to be used as a feedstock for many practical and potential metabolic products, such as a food supplements, pharmaceutical substances, lipids, polymers, toxins, pigments, enzymes, biomass, and green energy[17-18].

To date, many macro and micro algal strains have been introduced and investigated for their potential in food and energy sector. Table 1.2 presents some species with their oil contents [7]. The composition of algal specie may vary with respect to location, growth condition, environment and nutrients supply, even same class of macroalgae exhibit different composition as shown in Table 1.3 [19,7].

Chlorella sp. is one of most prominent type of microalgae which has been emerged as a promising source for biodiesel and other byproducts. The word *Chlorella* derived from Greek, Chlors means “Green” and ella meaning minute. Sunlight, carbon dioxide and water are main source of reproduction for *Chlorella* sp. Marine *Chlorella* sp. is single cell organism having spherical shape with diameter of 2-10 μm (Figure. 1) and oil content of 28-32 %. It also contains photosynthetic pigments such as chlorophyll, carotenoids, lutein etc.[7, 20].

Table 1.1 Oil Production from different crops per area [20]

Crop	Cultivation area (m-ha)	Oil yield (L/ha)
Corn	1540	172
Soybean	594	446
Canola	223	1190
Jatropha	140	1892
Coconut	99	2689
Palm oil	45	5950
Microalgae (70% oil yield)	2	136,900
Microalgae (30% oil yield)	4.5	58,700

Table 1.2 Oil contents of different microlagae [20]

Microalgae	Oil contents (%wt. dry basis)
<i>Botryococcus braunii</i>	25-75
<i>Chlorella</i> sp.	28-32
<i>Nannochloris</i> sp.	20-35
<i>Nannochloropsis</i> sp.	31-68
<i>Nitzschia</i> sp.	45-47
<i>Cryptocodinium cohnii</i>	20
<i>Cylindrotheca</i> sp.	16-37
<i>Dunaliella primolecta</i>	23



Figure. 1.1 *Chlorella* sp. [21]

Table 1.3 Composition (% wt.) of different microalgae species [7]

	Strain	Protein	Carbohydrates	Lipids	Nucleic acid
1	<i>Scenedesmus obliquus</i>	50-56	10-17	12-14	3-6
2	<i>Scenedesmus quadricauda</i>	47	-	1.9	-
3	<i>Scenedesmus dimorphus</i>	8-18	21-52	16-40	-
	<i>Chlamydomonas</i>				
4	<i>rheinhardii</i>	48	17	21	-
5	<i>Chlorella vulgaris</i>	51-58	12-17	14-22	4-5
6	<i>Chlorella pyrenoidosa</i>	57	26	2	-
7	<i>Spirogyra</i> sp.	6-20	33-64	11-21	-
8	<i>Dunaliella bioculata</i>	49	4	8	-
9	<i>Dunaliella salina</i>	57	32	6	-
10	<i>Euglena gracilis</i>	39-61	14-18	14-20	-
11	<i>Prymnesium parvum</i>	28-45	25-33	22-38	1-2
12	<i>Tetraselmis maculata</i>	52	15	3	-
13	<i>Porphyridium cruentum</i>	28-39	40-57	9-14	-
14	<i>Spirulina platensis</i>	46-63	8-14	4-9	2-5
15	<i>Spirulina maxima</i>	60-71	13-16	6-7	3-4.5
16	<i>Synechococcus</i> sp.	63	15	11	5
17	<i>Anabaena cylindrica</i>	43-56	25-30	4-7	-
18	<i>Chlorella</i> sp.	68	61	33	-

There are various steps involved in energy derivation from microalgal biomass such as cultivation, harvesting, dewatering, drying, lipid extraction and conversion into biodiesel.

1.2 Algal biomass cultivation, harvesting and dewatering

Commonly known cultivation methods are open pond and photo bioreactor [7]. The open pond cultivation is easy and yields higher biomass. However, it is completely weather dependent process. Harvesting of algae includes departing from the growing media, water removal and associated contaminant removal to obtain the desired

product. Harvesting technique depends on the type of specie. Higher water content of algae must be soaked for better operation. The most common harvesting processes are flocculation, micro-screening and centrifugation, flocculation or by froth flotation. Selected process must be economical [22].

Post harvested microalgae contains $90\pm 5\%$ moisture. This high level moisture could deteriorate the biomass quality and needs to be reduced by some suitable technique i.e. dryings. The moisture in dried product below 10% is safe level, and enhances the viability for lipid extraction. However, the biomass composition may be changed subjected to enzymatic/non-enzymatic processes during drying. Drying is one of the most essential and challenging process in commercial production of microalgae that accounts for almost 30% of the total processing cost. There are various drying methods such as natural sun drying, oven drying, freeze drying, spray drying, drum drying and fluidized bed drying [23-27].

1.3 Extraction of algae

The algal biomass cell needs to be disrupted for lipid extraction. There are generally two methods (a) Mechanical; ultrasonic, expression/expeller (b) Chemical; solvent extraction, Soxhlet. Algae vary in their physical states and composition, different press methods (screw, expeller, piston, etc.) can be applied for specific strain. In commercial applications expeller press combined with solvent is used as well by manufacturer for maximum product yield. Soxhlet extraction using hexane and other solvent is widely used technique but it is time consuming process and extraction efficiency is low as well. Ultrasonication belongs to sonochemistry, can enhance extraction process at good rate. By using an ultrasonic reactor or bath, ultrasonic waves are responsible to generate cavitation in a mixture. In result of cavitation, bubbles movement near the cell walls tend to create shock waves and liquid jets to break cell and release desired contents into the solvent [28-29]. Ultrasonication is preferred technique over other techniques due to some features such as easy use, inexpensive, better control, quick and environmentally friendly [14].

1.4 Crude algal extract

The extract of microalgae mainly composes of lipids and some impurities. Lipids are fat and oil which are insoluble in water but soluble in organic compounds. The chemical structure of these compounds consists of hydrogen, carbon, and oxygen.

They are rich in energy and play key role as biological functions in the body: provide structure to cell membranes, energy storage, and to act as signal transfer agent. These lipids may be structural polar lipids mainly composed of poly unsaturated fatty acid or storage and non-polar mainly in TAG form contain saturated and some unsaturated fatty acids. Storage lipids are then converted into biofuel. Crude algae oil is processed to separate oil from impurities (by products) mainly pigments by suitable technique. The composition of obtained crude algal extract depends on algae strain, cultivation conditions and extraction process.

Algae has been reported as a good alternative for the lipid production. Different species of microalgae can be used to produce specific type of lipids and fatty acids by manipulating physio-chemo character of their culture medium. Algae can accumulate considerable amounts of lipids 20–50% wt. on dry basis. The accumulation of lipids is mainly due to use of sugar at a rapid rate than the rate of cell generation, leads converting excess sugar contents into lipids [30]. Classification of lipids is given in Figure 2.

Chlorophyll is greenish pigment found in almost all leafy plants, microalgae and cyanobacteria. It is main source for photosynthesis action in the presence of sunlight (oilgee.com). Chlorophyll molecules are configured in and around the photosystems in the thylakoid membranes of chloroplasts. The main function of chlorophyll is to absorb sunlight, which is key requirement for substance to carry out photosynthetic process. Chlorophyll is more in leafy plants & vegetables as compare to fruits. For example, in spinach, it can be as high as 1% (dry base). *Chlorella* is also known as ‘Emerald food’ because it contains high amount of chlorophyll than other substances. *Chlorella* have five times greater pigments than *Spirulina*. The chlorophyll content of *Chlorella* is about 7% of the biomass. (oilgae.com). There are mainly two types of chlorophyll, chlorophyll a and b [31].

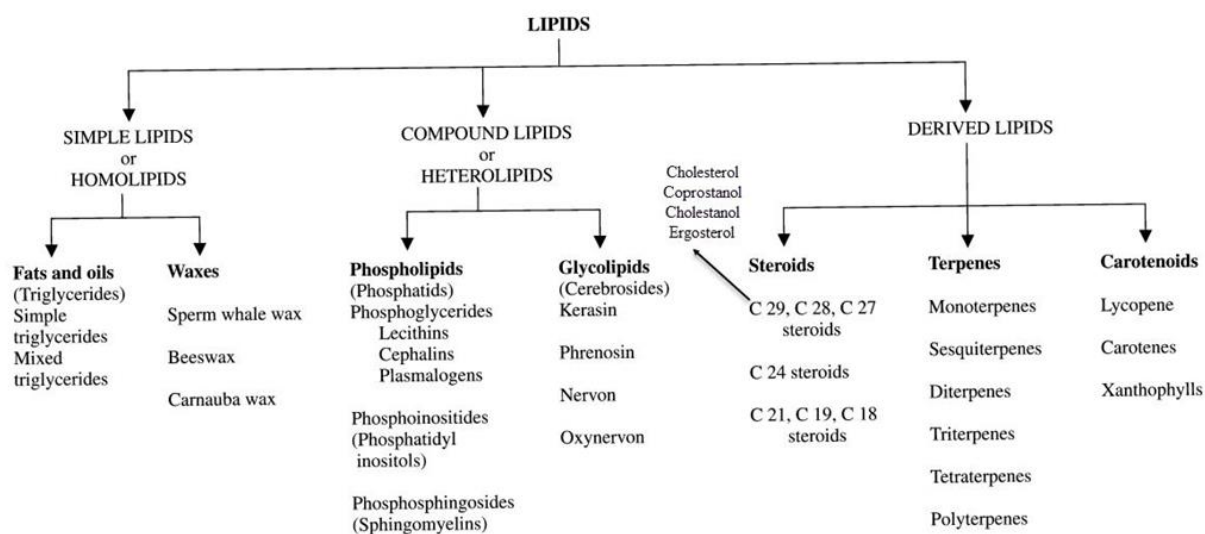


Figure 1.2. General lipid classification

The most popular found content in plants is chlorophyll a, which absorbs light with wavelengths of 430 nm (blue) and 662 nm (red). We see green part in plants, algae due to its strong green color reflection. It has a hydrophobic phytol chain that can be embed in a lipid membrane. The other structure known as a tetrapyrrolic ring present outside of the membrane, responsible to absorbs the energy from light. The metal Mg, at the middle of the structure can possess variable oxidation states, able it to accept and donate electron readily per situation. It is of flexible nature, necessary for molecule function chlorophyll a, due to its stable nature is favorite coloring agent [31]. Chlorophyll a and b are abundant in *Chlorella* and *Spirulina*. It has a similar structure as of chlorophyll a. The light absorbance range is 453 nm and 642-652 nm maximum. It is less in quantity than chlorophyll a. In this pigment methyl group of pigment, a replace by formyl group. Its color is green/yellow. It supports to enhance range of light that a plant can use for energy.

1.5 Potential applications of extracted residue

The residue after lipid extraction is generally known as de-oiled biomass. Biodiesel production from microalgae at large scale would generate a substantial amount of this de-oiled biomass, which requires a careful handling management [32-33]. This algal residue could be used as precursor for valuable products in livestock, chemical and environmental sectors [7,34]. The utilization of extracted residue is environmentally beneficial and could improve the economy of algal industry.

1.6 Literature information

A comprehensive literature information for algal extraction and application of algal residue is presented in Table 1.4 and 1.5, respectively.

Table 1.4. A comprehensive literature information on lipid extraction using different methods

Algal specie	Extraction condition	Lipid yield (%)	References
BG-medium mixed algae	Ultrasonic; Methanol/Chloroform/water (1/1/0.5 v/v/v)	45	[35]
<i>Chlorella</i> sp.	Ultrasonic; 15 min; chloroform/methanol (2/1 ml v/v)	40	[36]
<i>N. Salina</i>	Modified Bligh and Dyer	32	[37]
<i>C. Marina</i>	Modified Bligh and Dyer	20%	
<i>Scenedesmus</i> sp.	Ultrasonication; 2 min; chloroform/methanol (1/1 v/v)	19.85	[38]
<i>Nannochloropsis</i> sp.	Ultrasonication; 5 min; chloroform/methanol (2/1 ml v/v)	34	[39]
	Ultrasonication; 5 min; hexane/methanol (3/2 ml v/v)	22	
<i>Chlorella vulgris</i>	1. Ultrasonication; 40 min; chloroform/methanol (1/1 ml v/v)	52	[16]
	2. Ultrasonication; 60 min Hexane/isopropanol (1/0.6 ml v/v)	2.2	
	3. Soxhlet; 8 h	1.8	
	4. ultrasonication; 30 min; dichloromethane/ methanol (1/0.5 ml v/v)	10.9	
	5. Ultrasonication; 30 min; chloroform/methanol (1/0.5 ml v/v)	16.1	
<i>Chlorella</i> sp.	Ultrasonication; 2 h; methanol/hexane (1/2 v/v)	20	[12]
<i>Chlorella</i> sp. (FACHB-1748)	Soxhlet; chloroform/methanol (1/0.5 ml v/v)	28-43	[40]

Table 1.5 Algal and lignocellulosic biochars applications as an adsorbent

Materials	Condition	Yield (%)	S _{BET} (m ² /g)	q _{max} (mg/g)	Ref.
<i>Chlorella</i> residue BC	800 °C, 30 min	23	310	-	[41]
Extracted algal BC	800 °C, 90 min	22	133	345.1-CR dye	[42]
<i>S.platensis</i> BC	450 °C, 120 min	-	167	51.28-CR dye	[43]
Magnetic algal HBC	500 °C, 120 min	-	63	19.13-Zn(II)	[44]
<i>S. japonica</i> BC	700 °C, 120 min	25	1.3	84.3-Zn	[45]
<i>Eucheum sp.</i> BC	450 °C, 60 min	57	34	-	[46]
Corn straw BC	600 °C, 120 min	-	13.08	11-Zn	[47]
Empty fruit bunch BC	600 °C, 128 min	25	421	15.18-Zn (II)	[48]

CHAPTER 2

2 PROBLEM STATEMENT

The marine *Chlorella* sp. was studied in this study because of its availability and production feasibility at large scale. The selected strain has been already investigated for lipids with high saturated fatty acids contents, which are suitable for biodiesel production. There are many steps involved in bioenergy production from algal strain i.e. cultivation, harvesting, lipid extraction, transesterification, purification and lipid extracted residue management. Post harvesting and downstream processing for lipid extraction has been recognized as an energy intensive processes. So far, lipid extraction process remains of major interest. However, biomass preparation and development of biomass selection criteria is still needs to be explored. Furthermore, many techniques and process strategies have been developed aiming with maximum lipid recovery such as soxhlet extraction, solvent extraction, bead beating, pressing, ultrasonication and microwave. Ultrasonication is proven technology for efficient extraction of lipid from algal biomass. However, it still needs an improvement to establish an optimized condition especially for solvent selectivity, biomass to solvent ratio and development of extraction process and solvent recovery systems.

Likewise, other strains, *Chlorella* based algal biodiesel industry is facing commercialization challenge due to high processing cost associated to lipid extraction and biodiesel production. Hence, sustainable pathway by recovering maximum products from algal biomass is needed. In perspectives of biodiesel production from microalgae at larger scale, a huge amount of extracted biomass known as algal residue will be generated. Utilization of this algal residue to derive valuable products is environmentally beneficial and could offset the algal biodiesel cost. This residue has been proposed or used as cattle feedstock and bioenergy production i.e. bioethanol, biogas. However, it could also be utilized as biofuel and biochar production. Many studies focused on bio-oil and biochar production from raw algae, while some on extracted residue as well. However, biochar production from extracted marine *Chlorella* sp. residue (EMCR) and its potential applications for heavy metals and yellow dye-145 treatment by ultrasonication has not been reported. Moreover, EMCR potential for bio-oil production by microwave pyrolysis using EMCR derived biochar as microwave absorber needs to be explored as well.

2.1 Objectives and scope

In the light of above discussion and relevant potential research gaps, this study aimed to investigate the potential of marine *Chlorella* sp. biomass, extraction and potential applications of the extracted residue. The experiments were divided into three sections. The overall concept of this study is presented in Figure. 2.1

- **Section-I. Effect of drying methods for biomass preparation.**

Marine *Chlorella* sp. biomass cultivated in 25 m³ open pond was harvested by flocculation after 7 days, washed to remove contamination and vacuum filtered to prepare wet paste. This paste (90% moisture) was divided into five parts to be processed for; (I) fresh paste-FP, (II) stored wet paste-SWP, (III) sun drying-SD, (IV) oven drying-OD, and (V) freeze drying (FD). Which were examined for their biochemical constituents and later on processed for lipid extraction (section-II).

- **Section-II. Optimization of extraction by ultrasonication.**

Effects of various extraction factors including temperature (30-40 °C), time (60-120 min), biomass to solvent ratio (1/10-1/25 g/ml), solvent to solvent ratio (ml/ml), extraction cycles and solvent type on lipid yield (LY) were investigated. This section emphasis on development of optimized processing condition for crude lipid extraction by ultrasonication. It is worth noted that development of extraction cycles and solvent recovery system is an emerging idea of this study. Initially, FD biomass was selected to develop an optimized condition. Then, FP, SWP, OD and SD biomasses were extracted at found optimized condition. Further, the biomass selection criteria were developed based on extracted lipids composition, lipid yield and processing energy consumption (MJ/kg of lipid).

- **Section-III. Assessment of extracted marine *Chlorella* sp. residue (EMCR) potential for the recovery of energetic and non-energetic products with their applications.**

EMCR was recycled for (i) biochar production with its application for heavy metals and yellow dye-145 abatement and (ii) bio-oil production via microwave pyrolysis assisted with EMCR derived biochar as a microwave absorber (MA).

2.2 Expected benefits

- To have knowledge on drying techniques effects on biomass quality
- Gain knowledge on optimum conditions for lipid and pigment extraction from *chlorella* sp. by ultrasonic technique
- Gain more value-added products from *Chlorella* sp.
- Can promote the green alternative energy production

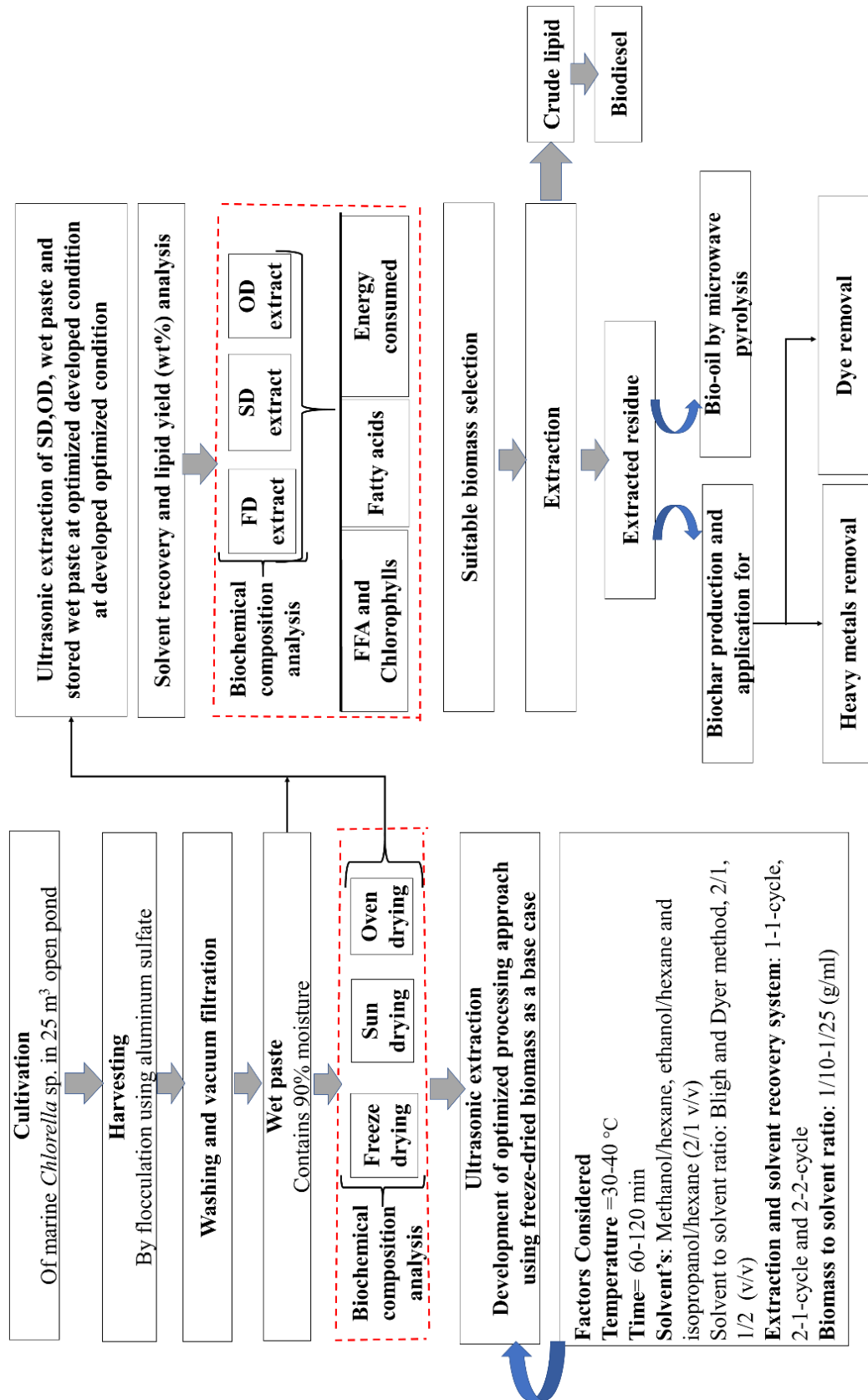


Figure. 2.1 Overall processing scheme

2.3 Significant results and discussion

Section-I

Briefly, the biomass of marine *Chlorella* sp. was obtained from National Institute of Coastal Aquaculture (NICA) located in Songkhla province (latitude: 7.178861° N, 100.624561° E), Thailand. The biomass was cultivated in 25 m³ open pond using CO (NH₂)₂ and 16-16-16 fertilizer (16% nitrogen, 16% phosphorus, and 16% potassium) as a growth media and harvested after 7 days. The harvesting was done by flocculation using aluminum sulfate as a flocculating agent. The slurry was pumped from pond, filled in containers and immediately transferred to working station and kept at 2°C. The slurry was washed three times with deionized water to detach the suspended particles and reduce the salinity. The cleaned algal slurry was dewatered using vacuum filtration and thick wet paste was collected. The moisture contents of paste were approximately 90% (wet basis).

Post harvested microalgae contains 90±5% moisture. This high level moisture could deteriorate the biomass quality and needs to be reduced by some suitable technique i.e. dryings. The moisture in dried product below 10% is safe level, and enhance the viability for lipid extraction [27]. This safe moisture level could be only achieving by drying i.e. sun drying, oven drying, freeze drying, spray drying, drum drying and fluidized bed drying. However, the biomass composition may be changed subjected to enzymatic/non-enzymatic processes during drying [49]. Wet paste of marine *Chlorella* sp. was dried using SD, OD, FD and their biochemical quality were evaluated. FD biomass was a rich green fine powder containing 10.8% crude lipid, which was 8.06%, 5.47% higher than SD and OD, respectively [more information is in Paper I]. Freeze drying was a gentle process, which conserved nutrients of biomass. The protein and carbohydrate contents were nearly similar, while energy contents (kcal) in FD biomass were higher than other OD and SD. The total drying time was accounted as 72 h, 40 h and 24 h for SD, OD and FD, respectively. Obviously, the energy consumption to prepare SD biomass was lowest (14.07 MJ/kg), followed by OD and FD with 590 MJ/kg and 1094 MJ/kg, respectively. However, sun drying requires large area to dry wet algal biomass and long exposure to solar radiation causes the chlorophyll degradation.

Section-II

The optimum ultrasonic extraction condition is very essential with respect to lipid extraction yield. Firstly, freeze-dried biomass was selected to develop an optimum processing condition due to its good storage capability. Then, at found optimized condition lipid extraction yield for wet paste, stored wet paste, SD and OD were performed. The variables considered were shown in Fig.3. The 2-1-cycle using methanol/hexane (2/1 v/v) with biomass to solvent ratio of 1/20 g/ml yielded 31% lipid yield at 35 °C and 90 min was an optimal condition. The lipid yield from fresh wet paste and stored wet paste were significantly lower than FD in 1-1-cycle [Paper II]. Moreover, due to degradation of biomass wet paste was not further considered. While, OD and SD biomass gave 27 and 22% lipid yield, respectively [Paper I]. The quality of SD, OD and FD extracts were determined by their biochemical composition. The SD extract composed highest crude lipid (53%) followed by FD (46%) and OD (34%).

The protein contents in all extracts of dried biomass were also similar and found between 5.8-7.13%. It meant that a huge portion of protein remained unconverted in residual biomass, which could be recycled as a valuable product. The free fatty acids in algal extract were more than 20%, which are very high from standard level of 4%. Which further explains that alkali catalyst is not suitable for marine *Chlorella* sp. lipid transesterification. The chlorophylls in FD extract were high, which is obviously due to good quality of biomass as FD promotes to preserve all the nutrients of the cell. The energy consumption was observed as 2570, 4172 and 5300 MJ/kg lipid for SD, OD and FD, respectively.

The energy consumption for FD biomass processing is 51 and 21.2% higher than SD and OD, respectively. But lipid yield of FD is 29% and 13% higher than SD and OD, respectively. Guldhe et. al [39] studied the sun, oven and freeze drying of *Scenedesmus* sp. and reported the process energy consumption in following order: sun drying < oven drying < freeze-drying. While, their study also revealed that drying technique have no significant impact on the lipid yield. Moreover, the total fatty acid contents were not affected by drying technique, but it was 4% higher in FD extract than OD and SD. The major fatty acids were C:16.0 and C16:1, which are suitable feedstock for biodiesel production. The detail of energy calculation procedure could be seen in Paper II. FD required more energy consumption process, but the product quality and

storage ability was better than OD and SD. Moreover, recovery of chlorophylls and other byproducts can offset this drawback. Based on high lipid yield, excellent biomass quality and long term storage capability, the FD biomass was selected for further processing in this study.

Section-III

The extracted marine *Chlorella* sp. residue (EMCR) was recycled with aim for maximum byproducts recovery and to manage the generated solid waste. The EMCR was pyrolyzed to derive biochar at different temperatures named as BC-450, BC-550 and BC-650. The surface areas of the produced biochars were found high as compared to other algal and some lignocellulosic biomass. The surface increased from 266 m²/g to 351 m²/g as temperature increased from 450°C - 550 °C and then decreased. This could be attributed to condensation of volatiles during pyrolysis process. The surface of biochars was negatively charged and contained OH functional groups, which play an important role in removal of heavy metals and dyes. BC-450 and BC-550 due to high surface area were further investigated for heavy metals and yellow dye-145 removal, respectively [Paper IV and Paper V]. BC-450 showed high efficiency for CR(VI), Zn(II) and Ni(II) with ultrasonication adsorption. It is worth noted that heavy metals removal using ultrasonic adsorption and conventional adsorption using BC-450 was first time evaluated as per best our knowledge. The ultrasonic adsorption performance was 1.1-1.3 times better than conventional adsorption [Paper IV]. The adsorption process was monolayer and well satisfied by pseudo second order model. It was believed that as BC-450 performance was excellent so BC-550 with high surface area would gave similar result. Because dyes and heavy metals are common industrial problem. So BC-550 performance was evaluated for yellow dye-145 adsorption by ultrasonication. Remarkable results with high adsorption (99%) within 1 min processing time were achieved [Paper IV].

The potential of EMCR as bio-oil was assessed by microwave pyrolysis process using BC-450 as microwave absorber [Paper-III]. The bio-oil was produced by microwave pyrolysis (MWP) with investigation of temperature (350-450 °C), time (20-40 min) and MA loading (10-30 wt.%) at fixed microwave power of 850 W. The pyrolysis condition was optimized to obtain maximum bio-oil yield using the Response Surface Methodology (RSM) based on Central Composite Design (CCD). The

optimum condition was 350 °C, 15% MA loading and 40 min, which yielded 46% bio-oil. The composition of bio-oil obtained at the optimized condition was characterized by GC-MS. The compounds are classified in the groups of amines/amides/indoles (30.37%), phenols (17.64%), esters (17.62%), acids (12.18%), furans and aromatics (5.56%), alcohols (6.07%), ketones/aldehydes/ethers (2.88%), sugars (2.30%), alkenes (0.5%) and others (4.88%). The high proportion of nitrogenated hydrocarbons confirmed that bio-oil from EMCR consisted of high nitrogen compounds, which was generally reported in bio-oil derived from algae. The nitrogen is from unconverted proteins in algal biomass. The bio-oil with high nitrogen is not good for fuel application as nitrogen oxides and soot can be generated from the combustion leading to air pollution. The solution is to remove proteins from EMCR prior to pyrolysis. These proteins can be high valuable products.

The effects of processing condition on chlorophyll recovery during lipid extraction was optimized [Paper VI]. The highest amount of chlorophylls was recovered at low temperature (30 °C) and longer extraction time (120 min). The dilution factor (1/20 ml/ml) was found appropriate to get clear peaks during UV spectrophotometry analysis. It was found that dissolving the extract in similar solvent as used for extraction is much better choice for results accuracy [Paper VI].

References

- [1] K. Azizi, M. Keshavarz Moraveji, and H. Abedini Najafabadi, "A review on bio-fuel production from microalgal biomass by using pyrolysis method," *Renewable and Sustainable Energy Reviews*. 2018.
- [2] Y. I. Mandik, B. Cheirsilp, P. Boonsawang, and P. Prasertsan, "Optimization of flocculation efficiency of lipid-rich marine *Chlorella* sp. biomass and evaluation of its composition in different cultivation modes," *Bioresour. Technol.*, vol. 182, pp. 89–97, 2015.
- [3] S. V. Vassilev and C. G. Vassileva, "Composition, properties and challenges of algae biomass for biofuel application: An overview," *Fuel*, vol. 181. pp. 1–33, 2016.
- [4] F. Diana da Silva Araújo, I. C. Araújo, I. C. G. Costa, C. V. Ô. Rodarte de Moura, M. H. Chaves, and E. C. E. Araújo, "Study of degumming process and evaluation of oxidative stability of methyl and ethyl biodiesel of *Jatropha curcas* L. oil from three different Brazilian states," *Renew. Energy*, 2014.
- [5] S. N. Naik, V. V. Goud, P. K. Rout, and A. K. Dalai, "Production of first and

- second generation biofuels: A comprehensive review,” *Renewable and Sustainable Energy Reviews*. 2010.
- [6] P. S. Nigam and A. Singh, “Production of liquid biofuels from renewable resources,” *Progress in Energy and Combustion Science*. 2011.
- [7] Y. Chisti, “Biodiesel from microalgae beats bioethanol,” *Trends Biotechnol.*, vol. 26, no. 3, pp. 126–131, 2008.
- [8] I. A. Nascimento *et al.*, “Screening Microalgae Strains for Biodiesel Production: Lipid Productivity and Estimation of Fuel Quality Based on Fatty Acids Profiles as Selective Criteria,” *Bioenergy Res.*, 2013.
- [9] L. Raslavičius, V. G. Semenov, N. I. Chernova, A. Keršys, and A. K. Kopeyka, “Producing transportation fuels from algae: In search of synergy,” *Renewable and Sustainable Energy Reviews*. 2014.
- [10] M. Saber, B. Nakhshiniev, and K. Yoshikawa, “A review of production and upgrading of algal bio-oil,” *Renewable and Sustainable Energy Reviews*. 2016.
- [11] L. Rodolfi *et al.*, “Microalgae for oil: Strain selection, induction of lipid synthesis and outdoor mass cultivation in a low-cost photobioreactor,” *Biotechnol. Bioeng.*, 2009.
- [12] S. Paisan, P. Chetpattananondh, and S. Chongkhong, “Assessment of water degumming and acid degumming of mixed algal oil,” *J. Environ. Chem. Eng.*, vol. 5, no. 5, pp. 5115–5123, 2017.
- [13] N. Sanyano, P. Chetpattananondh, and S. Chongkhong, “Coagulation-flocculation of marine *Chlorella* sp. for biodiesel production,” *Bioresour. Technol.*, vol. 147, pp. 471–476, 2013.
- [14] A. R. Byreddy, A. Gupta, C. J. Barrow, and M. Puri, “Comparison of cell disruption methods for improving lipid extraction from thraustochytrid strains,” *Mar. Drugs*, vol. 13, no. 8, pp. 5111–5127, 2015.
- [15] K. Y. Show, D. J. Lee, J. H. Tay, T. M. Lee, and J. S. Chang, “Microalgal drying and cell disruption - Recent advances,” *Bioresour. Technol.*, vol. 184, pp. 258–266, 2015.
- [16] G. S. Araujo *et al.*, “Extraction of lipids from microalgae by ultrasound application: Prospection of the optimal extraction method,” *Ultrason. Sonochem.*, vol. 20, no. 1, pp. 95–98, 2013.
- [17] T. Suganya, M. Varman, H. H. Masjuki, and S. Renganathan, “Macroalgae and microalgae as a potential source for commercial applications along with biofuels production: A biorefinery approach,” *Renewable and Sustainable Energy Reviews*. 2016.
- [18] R. Harun, M. Singh, G. M. Forde, and M. K. Danquah, “Bioprocess engineering of microalgae to produce a variety of consumer products,” *Renew. Sustain. Energy Rev.*, vol. 14, no. 3, pp. 1037–1047, 2010.
- [19] B. K. Upreti, B. Venkatesagowda, and S. K. Rakshit, “Current Prospects on Production of Microbial Lipid and Other Value-Added Products Using Crude

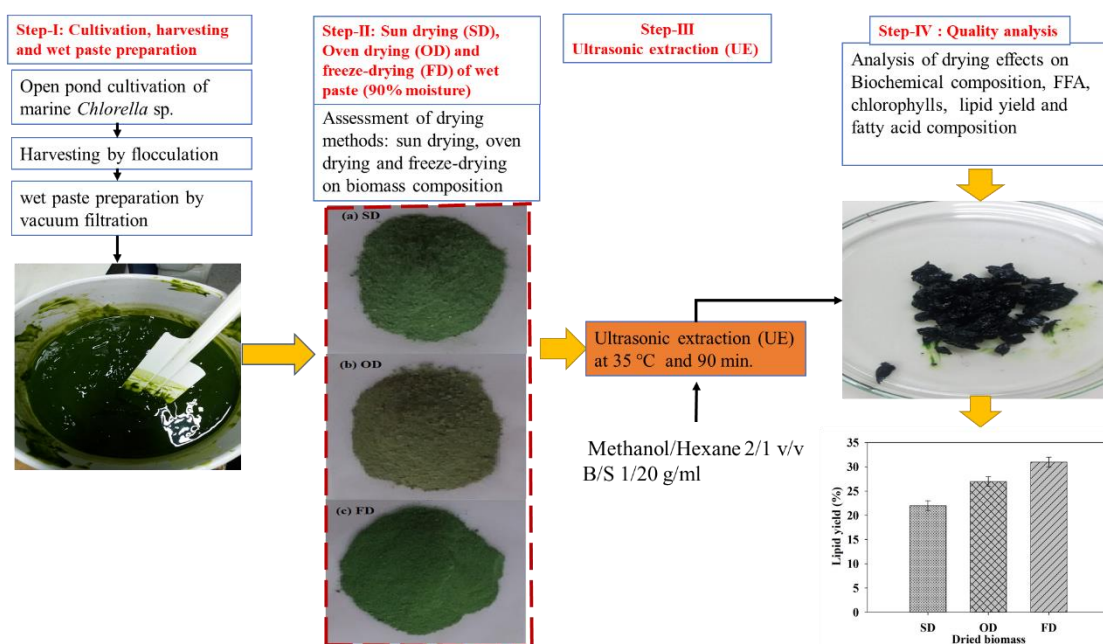
- Glycerol Obtained from Biodiesel Industries,” *Bioenergy Research*. 2017.
- [20] Y. Chisti, “Biodiesel for microalgae,” *Biotechnol. Adv.*, vol. 25, pp. 294–306, 2007.
- [21] P. Gupta, D. Sinha, and R. Bandopadhyay, “Isolation and screening of marine microalgae *Chlorella* sp. _pr1 for anticancer activity,” *Int. J. Pharm. Pharm. Sci.*, 2014.
- [22] T. M. Mata, A. A. Martins, and N. S. Caetano, “Microalgae for biodiesel production and other applications: A review,” *Renew. Sustain. Energy Rev.*, vol. 14, no. 1, pp. 217–232, 2010.
- [23] S. K. Bagchi, P. S. Rao, and N. Mallick, “Development of an oven drying protocol to improve biodiesel production for an indigenous chlorophycean microalga *Scenedesmus* sp.,” *Bioresour. Technol.*, vol. 180, pp. 207–213, 2015.
- [24] N. V. S. N. M. Konda, S. Singh, B. A. Simmons, and D. Klein-Marcuschamer, “An Investigation on the Economic Feasibility of Macroalgae as a Potential Feedstock for Biorefineries,” *Bioenergy Res.*, 2015.
- [25] M. K. Lam and K. T. Lee, “Microalgae biofuels: A critical review of issues, problems and the way forward,” *Biotechnology Advances*. 2012.
- [26] S. Pang and A. S. Mujumdar, “Drying of Woody Biomass for Bioenergy: Drying Technologies and Optimization for an Integrated Bioenergy Plant,” *Dry. Technol.*, vol. 28, no. 5, pp. 690–701, 2010.
- [27] H. Hosseinizand, S. Sokhansanj, and C. J. Lim, “Studying the drying mechanism of microalgae *Chlorella vulgaris* and the optimum drying temperature to preserve quality characteristics,” *Drying Technology*, pp. 1–12, 2017.
- [28] M. Wang, W. Yuan, X. Jiang, Y. Jing, and Z. Wang, “Disruption of microalgal cells using high-frequency focused ultrasound,” *Bioresour. Technol.*, vol. 153, pp. 315–321, 2014.
- [29] J. R. McMillan, I. A. Watson, M. Ali, and W. Jaafar, “Evaluation and comparison of algal cell disruption methods: Microwave, waterbath, blender, ultrasonic and laser treatment,” *Appl. Energy*, vol. 103, pp. 128–134, 2013.
- [30] G. S. Araujo *et al.*, “Extraction of lipids from microalgae by ultrasound application: Prospection of the optimal extraction method,” *Ultrason. Sonochem.*, vol. 20, no. 1, pp. 95–98, 2013.
- [31] H. Of and M. Microalgae, *No Title*. .
- [32] D. Su *et al.*, “Ultrasonic bleaching of rapeseed oil: Effects of bleaching conditions and underlying mechanisms,” *J. Food Eng.*, vol. 117, no. 1, pp. 8–13, 2013.
- [33] Y. M. Chang, W. T. Tsai, M. H. Li, and S. H. Chang, “Preparation and characterization of porous carbon material from post-extracted algal residue by a thermogravimetric system,” *Algal Res.*, vol. 9, pp. 8–13, 2015.
- [34] N. Rashid, M. S. U. Rehman, and J. I. Han, “Recycling and reuse of spent microalgal biomass for sustainable biofuels,” *Biochem. Eng. J.*, vol. 75, pp. 101–

- 107, 2013.
- [35] U. D. Keris-Sen, U. Sen, G. Soydemir, and M. D. Gurol, "An investigation of ultrasound effect on microalgal cell integrity and lipid extraction efficiency," *Bioresour. Technol.*, vol. 152, pp. 407–413, 2014.
- [36] P. Prabakaran and A. D. Ravindran, "A comparative study on effective cell disruption methods for lipid extraction from microalgae," *Lett. Appl. Microbiol.*, vol. 53, no. 2, pp. 150–154, 2011.
- [37] A. Muthukumar, S. Elayaraja, T. T. Ajithkumar, S. Kumaresan, and T. Balasubramanian, "Biodiesel Production from Marine Microalgae *Chlorella Marina* and *Nannochloropsis Salina*," *J. Pet. Technol. Altern. Fuels*, 2012.
- [38] A. Guldhe, B. Singh, I. Rawat, K. Ramluckan, and F. Bux, "Efficacy of drying and cell disruption techniques on lipid recovery from microalgae for biodiesel production," *Fuel*, vol. 128, no. July, pp. 46–52, 2014.
- [39] R. K. Balasubramanian, T. T. Yen Doan, and J. P. Obbard, "Factors affecting cellular lipid extraction from marine microalgae," *Chem. Eng. J.*, vol. 215–216, pp. 929–936, 2013.
- [40] X. Zhou, L. Xia, H. Ge, D. Zhang, and C. Hu, "Feasibility of biodiesel production by microalgae *Chlorella* sp. (FACHB-1748) under outdoor conditions," *Bioresour. Technol.*, vol. 138, pp. 131–135, 2013.
- [41] Y. M. Chang, W. T. Tsai, and M. H. Li, "Characterization of activated carbon prepared from chlorella-based algal residue," *Bioresour. Technol.*, vol. 184, pp. 344–348, 2014.
- [42] Y. di Chen, Y. C. Lin, S. H. Ho, Y. Zhou, and N. qi Ren, "Highly efficient adsorption of dyes by biochar derived from pigments-extracted macroalgae pyrolyzed at different temperature," *Bioresour. Technol.*, vol. 259, pp. 104–110, 2018.
- [43] P. Nautiyal, K. A. Subramanian, and M. G. Dastidar, "Adsorptive removal of dye using biochar derived from residual algae after in-situ transesterification: Alternate use of waste of biodiesel industry," *J. Environ. Manage.*, vol. 182, pp. 187–197, 2016.
- [44] E. B. Son, K. M. Poo, J. S. Chang, and K. J. Chae, "Heavy metal removal from aqueous solutions using engineered magnetic biochars derived from waste marine macro-algal biomass," *Sci. Total Environ.*, vol. 615, pp. 161–168, 2018.
- [45] K. M. Poo, E. B. Son, J. S. Chang, X. Ren, Y. J. Choi, and K. J. Chae, "Biochars derived from wasted marine macro-algae (*Saccharina japonica* and *Sargassum fusiforme*) and their potential for heavy metal removal in aqueous solution," *J. Environ. Manage.*, vol. 206, pp. 364–372, 2018.
- [46] D. A. Roberts, N. A. Paul, S. A. Dworjanyn, M. I. Bird, and R. De Nys, "Biochar from commercially cultivated seaweed for soil amelioration," *Sci. Rep.*, vol. 5, pp. 1–6, 2015.
- [47] X. Chen *et al.*, "Adsorption of copper and zinc by biochars produced from

- pyrolysis of hardwood and corn straw in aqueous solution,” *Bioresour. Technol.*, vol. 102, no. 19, pp. 8877–8884, 2011.
- [48] S. A. Zamani, R. Yunus, A. W. Samsuri, M. A. M. Salleh, and B. Asady, “Removal of Zinc from Aqueous Solution by Optimized Oil Palm Empty Fruit Bunches Biochar as Low Cost Adsorbent,” *Bioinorg. Chem. Appl.*, vol. 2017, pp. 1–9, 2017.
- [49] C. L. Chen, J. S. Chang, and D. J. Lee, “Dewatering and Drying Methods for Microalgae,” *Dry. Technol.*, vol. 33, no. 4, pp. 443–454, 2015.

CHAPTER 3

Assessment of drying techniques on biochemical quality of marine *Chlorella* sp. biomass and their extracts



Highlights

- Marine *Chlorella* sp. wet paste was dried using sun, oven and freeze drying
- FD biomass gave 4% and 9% high lipid yield than OD and SD, respectively
- 34.1% protein in extract of SD biomass was highest, while 65.9% remained unconverted
- The effect of drying method on fatty acid composition was not significant
- C16:0, C:16.1 and C18:1 were major FAMES as desired for biodiesel production

Assessment of drying techniques on biochemical quality of marine *Chlorella* sp. biomass and their extracts

Muhammad Amin^{1,2}, Pakamas Chetpattananondh^{1*}

¹Department of Chemical Engineering Faculty of Engineering, Prince of Songkla University, 90110, Hat Yai, Songkhla, Thailand

²Department of Chemical Engineering, Balochistan University of Information Technology, Engineering and Management Sciences, 87300, Quetta, Pakistan.

Corresponding author email: pakamas.p@psu.ac.th (Pakamas Chetpattananondh)

Abstract

Harvested algal biomass perish quickly due to microbial action in the presence of water and needs to be dried. The drying technique could affect the bio compositional quality of biomass and extract. In this study, harvested marine *Chlorella* sp. was dried using sun drying (SD), oven drying (OD) and freeze-drying (FD) followed by lipid extraction. The drying effects on biochemical constituents of the dried biomass and their extract, lipid yield, fatty acids, free fatty acids (FFA) and chlorophyll contents were studied. Fatty acids methyl esters were determined by GC-FID. Total time taken by SD, OD and FD were 72 h, 40 h and 24 h, respectively. Final moisture in dried biomass was below 10%, while ash and protein contents were of 38±1% and 20.91±1%, respectively. FD biomass contained 275 calories and were the highest. The FD biomass showed the highest lipid extraction yield with 31% (wt% dry basis) followed by OD (27%) and SD (22%), respectively. The SD extract containing 53% crude lipid was 8% and 19% higher than those of FD and OD. The chlorophyll-a (136 µg/ml) in FD was greater than OD and SD extract. The main fatty acids in crude lipids were C16:0, C16:1 and C18:1 and did not affected by drying method. These fatty acid are highly suitable for biodiesel production.

Key words: *Chlorella* sp.; sun drying; oven drying; freeze drying; quality

3.1 Introduction

Marine *Chlorella sp.* is green strain has shown a great potential as bioenergy feedstock [1-3]. It has several advantages over terrestrial crops such as rapid growth rate, minimal arable land and fresh water requirement, high photosynthetic efficiency, no food security, higher CO₂ sequestration, growth in waste water and maximum production yield [4-7]. However, cost effectiveness due to high energy required for the processing is still a major challenge for the algal industry [8]. These processes include cultivation, harvesting, dewatering, drying, lipid extraction and conversion into biodiesel [2, 9].

Post harvested microalgae contains 90±5% moisture. This high level moisture could deteriorate the biomass quality and needs to be reduced by some suitable technique i.e. dryings. The moisture in dried product below 10% is safe level, and enhance the viability for lipid extraction [10]. However, the biomass composition may be changed subjected to enzymatic/non-enzymatic processes during drying [4, 11, 12]. Drying is one of the most essential and challenging process in commercial production of microalgae that accounts for almost 30% of the total processing cost [13] There are various drying methods such as natural sun drying, oven drying, freeze drying, spray drying, drum drying and fluidized bed drying [14].

Sun drying is perhaps the most common and inexpensive technique used to preserve the contents of agricultural products. Open sun drying is widely used an ancient way, where crops are spread over floors and directly receive short wavelength radiations to carry away the moisture. However, direct and long exposure of biomass surface to solar radiation reduces the quality and limit its application [15-16]. To control and improve the crop quality, open sun drying was modified into solar energy drying i.e. solar cabinet greenhouse drying. The cabinet greenhouse drying is inexpensive, simple and a direct type passive solar system. Glass or polythene sheets are main materials used as roof and walls of such dryer [17]. The blackened surface and sides of sample holding trays enhance the solar heat absorption. The short wavelength solar radiation passes through the walls and roof of dryer, and get absorbed by the sample. Which tends to warm up the sample in tray and removal of moisture takes place either by natural or forced convection mode. In natural convection drying mode the fresh air

entered at base of system and warm moist air leaves from upper section. In this type of system, heated air is circulated through the crop by buoyancy forces [18].

The hot air oven drying is also well known in foodstuffs drying [19]. Where hot air circulation transfers the heat into the sample through its surface and carry away the moisture by latent heat of vaporization. The pressure difference between sample surface and inner layer could also be the mechanism for moisture removal. The performance efficiency and quality of dried product depends on oven temperature. The wet algal biomass must be dried between 60-80 °C [10].

Freeze drying or lyophilisation technique operated under vacuum is gentle process with capability to preserve all the cell constituents [20-21]. While, Mata et al.[22] reported that freeze drying is energy intensive process and not a suitable choice for algal biofuels. However, it remained an attractive choice of many other studies reported in literature. Hot air oven drying is an alternative way for moisture reduction of algal biomass. Wong and Cheung et al. [23] reported that extraction capacity and quality of protein from oven dried was better than freeze-dried biomass. Bagchi et al. [11] obtained 93% lipid recovery from oven dried *Scenedesmus* sp. biomass. However, Guldhe et al. [14] reported 29% lipid yield from freeze-dried biomass followed by oven dried (28.63%) and sun dried (28.33%). Another study reported that oven dried *Chlorella vulgaris* gave an 21.95% lipid yield, which is 1.97% higher than FD biomass [8]. Ansari et al. [24] presented a significantly high lipid yield (18.45%) from FD as compared to OD and SD biomass. Hosseinizand et al. [13] suggested that drying at medium temperature (60-80°C) is best choice to preserve *Chlorella vulgaris* constituents. However, their study also revealed that FD biomass used as a base case had higher lipid contents than OD but protein and carbohydrate contents were almost similar. While, Balasubramaniam et al. [25] did not found any significant effect of drying technique on lipid extraction yield. In this study, marine *Chlorella* sp. was dried using sun drying, oven drying and freeze drying. Several studies have been conducted on algal biomass drying and extraction by various means focusing on lipid yield and fatty acid contents. However, the effect of drying techniques on biochemical quality of marine *Chlorella* sp. biomass and their extract has limited information.

Thus, this study aimed to investigate the drying of marine *Chlorella* sp by natural sun drying (SD), oven drying (OD) and freeze-drying (FD) and their effects on (1) biochemical composition of the biomass (3) lipid yield and their biochemical composition (4) FFA and chlorophyll contents and (5) fatty acid composition. A schematic diagram of experimental and analysis work from marine *Chlorella* sp. cultivation and biomass preparation to lipid extraction of this work is presented in Fig. 3.1.

3.2 Materials and methodology

3.2.1 Chemicals

The methanol and n-hexane used were commercial grade (purity>95%) and were purchased from RCI Labscan Ltd., while, $Al_2(SO_4)_3$ to be used as flocculating agent was purchased from Siam Chemicals Co. Ltd. Thailand.

3.2.2 Strain cultivation, harvesting and wet paste preparation

The green strain marine *Chlorella* sp. was cultivated in a 25 m³ open pond at the National Institute of Coastal Aquaculture (NICA) located in Songkhla (latitude: 7.178861° N, 100.624561° E), Thailand. The fertilizer $CO(NH_2)_2$ and 16-16-16 (16% nitrogen, 16% phosphorus, and 16% potassium) was used as a growth media. The cultivation processing was carried at a temperature of 25-30 °C under sunlight using saline water for 7 days. The biomass was harvested by flocculation using Aluminum sulfate as a flocculation agent. The diluted microalgae slurry was pumped out from the pond, filtered to detach the growth media and placed in containers followed by immediate storage at 4 °C to prevent from degradation. Being nature of saline, the microalgal slurry was washed three times with deionized water to neutralize its pH and to remove any contaminants present. The washed slurry was then dewatered to increase the biomass concentration by vacuum filtration using Whatman no. 4 filter paper and a vacuum pump (GENVAC Agilent Technologies, PVL 35, 930 Watt). 1.5 kg thick wet paste (90% moisture) obtained after dewatering was collected and equally divided for SD, OD and FD processing.

3.2.3 SD, OD and FD process

- *SD process*

500 g wet paste was sun dried using mini homemade natural convection greenhouse dryer as presented in Fig. 3.2. The tray surface was made black for maximal absorption of solar heat. The dryer was provided with two holes at top and bottom of tray for air inlet and exit, respectively. A thin layer of wet paste was spread in tray sample area and dryer was covered with transparent polythene sheet. The surface temperature of sample monitored by infrared device and weight of sample measured by balance were recorded after 1 h interval. When the end moisture of sample reached below 10%, the experiment was suspended and dried sample was collected carefully. The experiment was started at 9:00 A.M-5:00 P.M from 18-20 February, 2019 and it took approximately 72 h to get the final desired moisture. The surface color of SD biomass was light green as shown in Fig. 3.3 (a).

- *OD process*

Thin layered wet paste (500 g) was spread uniformly in tray and placed in hot air oven at 80 °C. This temperature selection is based on preliminary evaluation as well as the best condition reported in literature. The weight of sample was recorded after every 1 h. The experiment was suspended as the final moisture reached below 10% and the sample was collected. It took about 40 h to achieve the safe moisture level. The OD biomass presented in Fig. 3.3 (b) was found less greenish than SD. It was pulverized, kept in zip lock bags and stored at 4 °C.

- *FD process*

To freeze dry, the 500 g wet paste was frozen overnight at -16 °C and lyophilized using a freeze dryer (Dura-Dry MP, FTS systems, USA, 4400 Watt) at -50 °C under vacuum (12.66 Pa) for 24 hours, at the Scientific Equipment Center, Prince of Songkla University, Thailand. The freeze-dried powder shown in Fig. 3.3 (c) was well structured and seems rich with chlorophyll as compared to SD and OD biomass. The final moisture was recorded as 5%. It was pulverized using a mortar and pestle and stored at 4 °C prior to further processing. The FD biomass was smooth, homogeneous and greener than OD and SD.

3.2.4 Ultrasonic extraction (UE)

SD, OD and FD biomass were subjected to lipid extraction by ultrasonication. The optimum ultrasonic extraction condition was established as 35 °C and 90 min. with biomass to solvent ratio of 1/20 g/ml in our previous study. The reason for extracting the biomass at above condition was based on best result achieved in preliminary evaluation. Thirty gram (% dry basis) of each dried biomass sample was mixed with 600 ml methanol and hexane (2:1 v/v) in a 1000 ml Duran bottle sealed with aluminum foil. The samples were sonicated at the desired conditions using an ultrasonic bath (CP 2600 Crest Power sonic, USA, 45 kHz, 300 Watt). The UE process was repeated twice. The supernatant was recovered by vacuum filtration using Whatman no. 4 filter and subjected to rotary evaporation at 45 °C (Heidolph Laborota 4000, USA, 1400 Watt) for solvent recovery. The lipid yield of each dried biomass was recorded gravimetrically. A vacuum pressure of 33.7 kPa was applied initially and then gradually decreased to 7.2 kPa for hexane, methanol and water recovery. The extract obtained from each dried biomass were greenish black and solid at room temperature as illustrated Fig.3.3 (d). The extracted lipids were stored at -20 °C prior to further processing.

3.2.5 Analytical approaches

Biochemical compositional of the SD, OD and FD biomass and their crude lipids were determined by following the standard analytical procedures defined by the Association of Official Analytical Chemists (AOAC). Where, protein, ash and moisture contents were found by AOAC 991.20, 942.05 and 934.01, respectively. The conversion factor 6.25 was employed for the protein calculation. While crude lipid contents were determined by AOAC (Bligh and Dyer method). The carbohydrate and energy contents (calories) of dried materials and extracted lipids were determined by eq. (3.1) and (3.2), respectively. while free fatty acids (FFA) in extracted lipids were determined by eq. (3.3)

$$\text{Total carbohydrate (\%)} = 100 - (\text{Moisture} + \text{Ash} + \text{Protein} + \text{Fat}) \quad (3.1)$$

$$\text{Total energy (kcal)} = (\text{Protein} \times 4) + (\text{Fat} \times 9) + (\text{Carbohydrate} \times 4) \quad (3.2)$$

$$\text{FFA (\%)} = 27 \times \text{NaOH conc. (\%)} \times \text{Volume of titrant (ml)} / \text{Sample wt. (g)} \quad (3.3)$$

The chlorophylls in the extract were analyzed using a UV spectrophotometer (Agilent 8453, USA); Approximately 1 g of extracted crude lipid dissolved in 10 ml methanol was centrifuged at 3,000 rpm for 5 minutes to remove any suspended particles. The supernatant was further diluted using methanol and an absorbance reading was taken against a methanol blank. The chlorophyll concentration was calculated by Eq. (3.4)

$$\begin{aligned} \text{Ch - a} &= 16.72A_{665.2} - 9.16A_{652.4} \\ \text{Ch - b} &= 34.09A_{652.4} - 15.28A_{665.2} \end{aligned} \quad (3.4)$$

The fatty acid composition of the lipids was analyzed by gas chromatograph-flame ionization detector, GC-FID (Hewlett Packard 6890, USA) equipped with a 30 m CP 9080 capillary column, of internal diameter 0.32 mm and film thickness 0.25 μm . The fatty acid methyl esters were prepared and analyzed by following the European standard Norm EN 14013, protocol.

3.3 Results and Discussion

3.3.1 Analysis of OD, SD, FD biomass yield and their biochemical composition

Marine *Chlorella* sp. wet paste (90% moisture) was dried using SD, OD and FD. 500 g of wet paste used in each drying technique yielded approximately 50 g dried biomass with final moisture lower than 10%. Which is generally considered as safe level to preserve the quality of biomass [10]. The drying effects on biochemical composition of biomass were evaluated and presented in Table 3.1. The crude lipid contents of algal biomass are major precursor for food and biodiesel industry. FD biomass contains highest crude lipid as compared to OD and SD. It showed that drying technique significantly influenced the crude lipid (%) of biomass, where 8.06% and 5.47% loss accounted for SD and OD biomass, respectively. It is possible and could be interlinked with mechanism of drying process. The heat treatment effects the properties of biomass [4], as observed for OD and SD. Whereas, FD is gentle process operated under vacuum and having the capability to preserve all nutrients of cell.

However, the protein and ash contents of different dried products were almost similar and found between 20%-22% and 37.5%-39%, respectively. The protein contents generally remained unaffected but the fat amount of shrimp was remarkably influenced by drying method [26]. High ash contents were recognized for all dried products of marine *Chlorella* sp. Algae generally have higher ash than terrestrial

biomass as they have different composition, organic structure and rapid metabolism which take up much more nutrients during cultivations. The ash contents are in the range of 0.1-46.3% (mean 6.8%) for terrestrial biomass and 13.1-42.8% (mean 26.6%) for algae [27]. The carbohydrates of FD biomass were observed 6.2-6.8% lower than OD and SD biomass. Dineshkumar et al. [28] study presented that *Chlorella vulgaris* dried at 80 °C contained 34.56, 41.09 and 28.20 (mg/g) protein, carbohydrates and lipids, respectively. While, another study on drying of *Chlorella* reported that FD biomass contains 10.63% total lipids, 12% protein and 26% carbohydrate [13]. Phukan et al reported 9% carbohydrate, 43% protein and 28% lipids in *Chlorella* sp. Reddy et al. [29] stated that *Chlorella* sp. contains 10.7% lipid, 44.6% protein and 42.8% carbohydrate.

The biochemical composition of algal biomass depends on the specie characteristics, cultivation environment, growth medium, post harvesting processing, and other complex factors. Which could be different, even composition of same class of algal specie could vary due to different culturing condition. The FD biomass containing 271 kcal were of the highest amount among the dried products. This could be correlated to the high amount of crude lipid presence in FD, which was used in correlation (Eq.3.2) for energy evaluation. The biochemical constituents i.e. energy, protein and carbohydrates of SD, OD and FD biomass of this study are in reasonable range which shows their potential as a suitable feedstock for energy and food industry.

3.3.2 UE of lipid from OD, SD and FD biomass: yield and biochemical composition

The marine *Chlorella* sp. biomass of SD, OD and FD were extracted by ultrasonication at predefined conditions to observe the drying effect on lipid yield. The FD biomass yielded 31% which is 4% and 9% higher than OD and SD biomass respectively as presented in Fig. 3.5. The high lipid yield of FD biomass could be possibly correlated to its high crude lipid contents (Table 3.1). Which is further described as that maximum possible crude lipid was extracted with respect to their availability in the biomass. As FD biomass contains more crude lipid than other ones, which on complete extraction provided higher extraction yield. Furthermore, it may be associated to the nature and structure of FD biomass cells. These findings are in

compliance with Guldhe et al. [15] study. Which presented the highest extracted lipid yield of 29.5% from FD *Scenedesmus* sp. by microwave disruption followed by OD and SD with 28.65% and 28.33% lipid yield. While, with ultrasonic it was 19.85%, 18.8% and 18.9% for FD, OD and SD, respectively. There is negligible difference in lipid yield among dried biomass either extracted by microwave or ultrasonication. While, Balasubramanian et al. [22], obtained $22\pm 1\%$ lipid yield from SD, OD and FD biomass of *Nannochloropsis* sp. and reported insignificant effect of drying techniques on lipid yield. Although the lipid yield (22%) of SD biomass is attractive but considerably lower than FD and OD biomass in this study. Which is possible due to difference in biomass characteristics, intensity of solar radiations with respect to geographic location and environmental condition. The direct contact of sun radiation with algal biomass causes the chlorophyll destruction and alters the surface color and texture of product. The high intensity solar radiations directed at biomass surface are uncontrollable and major cause of system overheating. This overheating/heat treatment effects the properties of dried biomass [4, 30].

3.3.3 Drying effects on biochemical composition of crude lipids

Effect of different drying method on biochemical composition, FFA and chlorophyll contents of SD, OD and FD biomass extract was evaluated as presented in Table 3.2. The moisture and ash contents are between 10-11% for respective products and remained unaffected. The protein content in SD, OD and FD extract were found as 7.13%, 6.05% and 5.87%. A smaller but negligible difference for amount of protein among extracts showed that it was not influenced significantly by drying method and extraction technique. It is worth noted that only 34.1%, 28.93%, and 26.62% protein contents extracted, while 65.9%, 71% and 73.3% remains unconverted and present in extracted residue of SD, OD and FD, respectively. This extracted residue is generally regarded as waste of algal industry but presence of high amount of unchanged protein is making it a valuable feedstock. In perspectives of microalgae processing at larger scale, a huge amount of this extracted residue will be generated. Its utilization to derive valuable products is environmentally beneficial and could improve the economy of algal industry. The protein rich extracted residue of SD, OD and FD could be used in livestock, biofuel and environmental sector [5,31]. The protein in residue must be

extracted prior to be used as a bio-oil feedstock. Otherwise, its cracking will enrich the bio-oil with nitrogenous compounds during pyrolysis process. The bio-oil with high nitrogen is not good for fuel application as nitrogen oxides and soot can be generated from the combustion leading to air pollution [32-33].

The crude lipid contents were major constituent of extracted SD, OD and FD biomass. This crude lipid is in the form of stored energy i.e. triglycerides is a biodiesel feedstock. The crude lipid in the extract of SD biomass was 53%, which is 7.2%, 19.2% higher than FD and OD extract, respectively. It is possibly owing to the nature of extraction process, solvent interaction capability with cell surface and drying technique. The mean deviation of crude lipid contents among FD and SD extracts is minimum but of OD is too high. The energy contents of SD and FD extracts are nearly similar but of higher than OD. Hence, SD and FD could be better feedstock than OD for bioenergy and food sector.

3.3.4 Free fatty acids (FFAs) and chlorophylls

The cellular lipid can be degraded into organic or free fatty acids. Their determination is essential prior to transesterification process. Which is generally performed with low cost homogeneous alkali catalyst in case of FFA lower than 4% [23]. The free fatty acids (% FFA) in SD, OD and FD extracts were determined (Table 3.2). Overall, the extract of all dried biomass showed FFA contents between 20-30%, which is significantly higher than standard level. The FFA contents of SD extract were highest followed by OD, FD. These results are in compliance with study of Balasubramanian et al. [23], where they reported similar trend in FFA content of lipids extracted from *Nannochloropsis* sp. dried using sun drying, oven drying and freeze drying. The heat treatment of biomass for long period of time i.e. 72 h, is negatively correlated with FFA. This long exposure time likely increased the chances of triglycerides oxidation and resulted in high FFA contents. The presence of chlorophyll in algal biomass serve as a sensitizer to promote and enhance the photo-oxidation of lipids [23, 33]. Moreover, the free fatty acid in algal biomass extract can reach as high as 84%. The high levels of FFA are unlikely to have been present in the algae during growth since they would have had a cytotoxic effect on the cells [34]. So, due to high

FFA contents extracts of dried biomass in current study, the acid esterification would be suitable choice.

The concentrations of total Chlorophyll (a and b) were 204.57, 159.66 and 137.24 $\mu\text{g/ml}$ in FD, OD and SD, extracts respectively in this study. The lower concentration of chlorophylls in SD and OD is owing to the heating effect in drying process. The high amount of chlorophylls gave a dark green color to the extract and puts an obstacle for phase separation after transesterification. The uv spectrophotometry profiles of chlorophylls is presented in Fig. 3.4. These chlorophylls can lower the quality of the biodiesel which could be separated from extract by adding acid to form a solid precipitate or three-phase partitioning system [35-37]. Due to non-toxic, non-carcinogenic nature, antioxidative and immune-boosting features the Chlorophylls have various applications in food, cosmetic, diagnostic, and pharmaceutical industries [38]. Therefore, the extraction of SD, OD and FD *Chlorella* sp. could also produce a high amount of chlorophylls and their separation by suitable technique needs to be investigated.

3.3.5 Analysis of fatty acid composition

The SD, OD and FD extract of marine *Chlorella* sp. were investigated for fatty acid profiling by GC-FID. The fatty acid contents are presented in Table 3.3. Palmitic acid (C16:0; saturated) and palmitoleic acid (C16:1; monounsaturated) were dominant fatty acids despite using different drying techniques contributing from 26.52-26.71% and 20.15-22.46%, respectively. The saturated and unsaturated amount of fatty acids were 36.06%, 35.97%, 36.73% and 26.64%, 26.51%, 29.31% in SD, OD and FD, respectively. The saturated fatty acids are considerably dominant over unsaturated fatty acids. The fatty acid composition has a great influence over fuel characteristics and its combustion properties. A high saturated fatty acids are desired for good quality of biodiesel and its long term storage, while high unsaturated fatty acids gave better cold flow properties for its use in cold countries. In this way the oxidation stability and cold flow property are in inversely related [15]. The high proportion of saturated contents in the lipids from *Chlorella* sp. has been reported as indicating its usefulness as a good quality fuel agent. Biodiesel from palm oil which has a high saturated fatty acid content gives excellent combustion properties, such as a high cetane number and a high calorific value, even in cold conditions because of its high kinematic viscosity [39]. Biodiesel

produced from triglycerides with a high level of monounsaturated fatty acids, e.g. rapeseed oil or olive pomace oil, presents the optimal characteristics in regard to chemical and physical properties [40]. Although, saturated fatty acids could be separated by winterization process but this additional step will significantly affect the biodiesel cost. The mixture of saturated and unsaturated fatty acids in lipids is highly desirable to strike a balance between oxidation stability and cold flow property. The linolenic acid exceeding from 12% (C18:3) may have adverse effect on the oxidation stability of fuel and causes the rancidity [41]. It is worth noted that crude lipid of SD, OD and FD of marine *Chlorella* sp. contain 0% C18:3. Which ensuring that biodiesel from marine *Chlorella* sp. is of good quality.

3.4 Selection criteria

The analysis for the selection criteria of biomass based on their characterization for suitable application is necessary and presented here. Three different techniques for drying of marine *Chlorella* sp. were performed and their effects on biochemical quality of biomass and their extracts was studied with perspectives of bioenergy feedstock. The quality and composition of FD biomass was observed much better than OD and SD. Obviously, sun drying is cost and energy effective process, but it is uncontrollable and require longer time and larger area. While, FD and OD are energy intensive process and their application at large scale are still under consideration. Regardless, of high energy consumption, FD is still an attractive choice for pharmaceutical and food industry, while it could be upgraded for biodiesel industry as well in future. Biochemical composition of FD and SD was found much better than OD, but the yield of SD was significantly low. The energy contents of FD biomass and its extract were prominent. Fatty acid profiling showed that SD, OD and FD are all suitable as biodiesel feedstock but FD showed highest total fatty acids. Which were mainly belongs to saturated class. FD products shown consistency in terms of biochemical composition throughout during processing as compared to OD and SD. Hence, FD application at larger scale application for biodiesel industry needs to be investigated.

Conclusion

Wet paste of marine *Chlorella* sp. was dried using sun drying, oven drying and freeze-drying. The drying technique affected the biochemical composition of biomass and their crude lipid extract. FD biomass showed better consistency throughout the processing and also gave the high CL yield. FFA in CL of all dried biomass were higher than allowable limit and suggesting the acid transesterification. The fatty acid composition was nearly similar for all dried biomass with major contribution of C16:0 and C16:1. The saturated fatty acids were dominant over unsaturated fatty acids. Which are suitable for biodiesel feedstock. The concentration of C18:3 was 0% indicating the better oxidation capacity of lipids. FD biomass and products consistency throughout but it consumes high energy. Its application in food and pharmaceutical are promising. The FD would be of great choice, if large scale and energy optimized equipment developed for algal industry. Unless otherwise, SD is better choice due to low energy cost and better biochemical composition.

Acknowledgment

This research was financially supported by Thailand's Education Hub for Southern Region of ASEAN Countries (TEH-AC, 56/2016) granted by the Graduate School, Prince of Songkla University (PSU), Hat Yai, Songkhla, Thailand. We are grateful to the Department of Chemical Engineering, Faculty of Engineering, PSU for providing all facilities and supporting staff to accomplish this work.

References

- [1] H. Hosseinizand, S. Sokhansanj, C.J. Lim, Co-pelletization of microalgae *Chlorella vulgaris* and pine sawdust to produce solid fuels, *Fuel Process. Technol.* (2018). doi:10.1016/j.fuproc.2018.04.015.
- [2] M.M. Phukan, R.S. Chutia, B.K. Konwar, R. Kataki, Microalgae *Chlorella* as a potential bio-energy feedstock, *Appl. Energy.* 88 (2011) 3307–3312. doi:10.1016/j.apenergy.2010.11.026.
- [3] K.Y. Show, D.J. Lee, J.H. Tay, T.M. Lee, J.S. Chang, Microalgal drying and cell disruption - Recent advances, *Bioresour. Technol.* 184 (2015) 258–266. doi:10.1016/j.biortech.2014.10.139.

- [4] Y. Chisti, Biodiesel for microalgae, *Biotechnol. Adv.* 25 (2007) 294–306. doi:10.1016/j.biotechadv.2007.02.001.
- [5] P. Nautiyal, K.A. Subramanian, M.G. Dastidar, Production and characterization of biodiesel from algae, *Fuel Process. Technol.* 120 (2014) 79–88. doi:10.1016/j.fuproc.2013.12.003.
- [6] T.M. Mata, A.A. Martins, N.S. Caetano, Microalgae for biodiesel production and other applications: A review, *Renew. Sustain. Energy Rev.* 14 (2010) 217–232. doi:10.1016/j.rser.2009.07.020.
- [7] N. Sanyano, P. Chetpattananondh, S. Chongkhong, Coagulation-flocculation of marine *Chlorella* sp. for biodiesel production, *Bioresour. Technol.* 147 (2013) 471–476. doi:10.1016/j.biortech.2013.08.080.
- [8] S.K. Bagchi, P.S. Rao, N. Mallick, Development of an oven drying protocol to improve biodiesel production for an indigenous chlorophycean microalga *Scenedesmus* sp., *Bioresour. Technol.* 180 (2015) 207–213. doi:10.1016/j.biortech.2014.12.092.
- [9] K.Y. Show, D.J. Lee, A.S. Mujumdar, Advances and Challenges on Algae Harvesting and Drying, *Dry. Technol.* (2015). doi:10.1080/07373937.2014.948554.
- [10] H. Hosseinizand, S. Sokhansanj, C.J. Lim, Studying the drying mechanism of microalgae *Chlorella vulgaris* and the optimum drying temperature to preserve quality characteristics, *Dry. Technol.* (2017) 1–12. doi:10.1080/07373937.2017.1369986.
- [11] C.L. Chen, J.S. Chang, D.J. Lee, Dewatering and Drying Methods for Microalgae, *Dry. Technol.* 33 (2015) 443–454. doi:10.1080/07373937.2014.997881.
- [12] A. Guldhe, B. Singh, I. Rawat, K. Ramluckan, F. Bux, Efficacy of drying and cell disruption techniques on lipid recovery from microalgae for biodiesel production, *Fuel*. 128 (2014) 46–52. doi:10.1016/j.fuel.2014.02.059.

- [13] P. Chen, M. Min, Y. Chen, L. Wang, Y. Li, Q. Chen, C. Wang, Y. Wan, X. Wang, Y. Cheng, S. Deng, K. Hennessy, X. Lin, Y. Liu, Y. Wang, B. Martinez, R. Ruan, Review of the biological and engineering aspects of algae to fuels approach, *Int. J. Agric. Biol. Eng.* 2 (2009) 1–30. doi:10.3965/j.issn.1934-6344.2009.04.001-030.
- [14] L. Brennan, P. Owende, Biofuels from microalgae-A review of technologies for production, processing, and extractions of biofuels and co-products, *Renew. Sustain. Energy Rev.* 14 (2010) 557–577. doi:10.1016/j.rser.2009.10.009.
- [15] S. Karaaslan, O. Uysal, F.O. Uysal, K. Ekinici, B.S. Kumbul, Mathematical Modelling of Drying of *Chlorella* sp., *Neochloris conjuncta* and *Botryococcus braunii* at different drying conditions, *Eur. J. Sustain. Dev.* (2018). doi:10.14207/ejsd.2016.v5n4p421.
- [16] G.L. Visavale, Principles, Classification and Selection of Solar Dryers, in: *Sol. Dry. Fundam. Appl. Innov.*, 2012.
- [17] O. Prakash, A. Kumar, Solar greenhouse drying: A review, *Renew. Sustain. Energy Rev.* (2014). doi:10.1016/j.rser.2013.08.084.
- [18] P.S. Chauhan, A. Kumar, Performance analysis of greenhouse dryer by using insulated north-wall under natural convection mode, *Energy Reports.* (2016). doi:10.1016/j.egyr.2016.05.004.
- [19] E.K. Akpınar, Drying of mint leaves in a solar dryer and under open sun: Modelling, performance analyses, *Energy Convers. Manag.* (2010). doi:10.1016/j.enconman.2010.05.005.
- [20] R. Halim, M.K. Danquah, P.A. Webley, Extraction of oil from microalgae for biodiesel production: A review, *Biotechnol. Adv.* (2012). doi:10.1016/j.biotechadv.2012.01.001.
- [21] N. Mallick, S.K. Bagchi, S. Koley, A.K. Singh, Progress and challenges in microalgal biodiesel production, *Front. Microbiol.* (2016). doi:10.3389/fmicb.2016.01019.

- [22] T.M. Mata, A.A. Martins, N.S. Caetano, Microalgae for biodiesel production and other applications: A review, *Renew. Sustain. Energy Rev.* 14 (2010) 217–232. doi:10.1016/j.rser.2009.07.020.
- [23] K. Wong, P. Chikeung Cheung, Influence of drying treatment on three *Sargassum* species 2. Protein extractability, in vitro protein digestibility and amino acid profile of protein concentrates, *J. Appl. Phycol.* (2001). doi:10.1023/A:1008188830177.
- [24] F.A. Ansari, S.K. Gupta, M. Nasr, I. Rawat, F. Bux, Evaluation of various cell drying and disruption techniques for sustainable metabolite extractions from microalgae grown in wastewater: A multivariate approach, *J. Clean. Prod.* (2018). doi:10.1016/j.jclepro.2018.02.098.
- [25] R.K. Balasubramanian, T.T. Yen Doan, J.P. Obbard, Factors affecting cellular lipid extraction from marine microalgae, *Chem. Eng. J.* 215–216 (2013) 929–936. doi:10.1016/j.cej.2012.11.063.
- [26] P.T. Akonor, H. Ofori, N.T. Dziedzoave, N.K. Kortei, Drying Characteristics and Physical and Nutritional Properties of Shrimp Meat as Affected by Different Traditional Drying Techniques, *Int. J. Food Sci.* (2016). doi:10.1155/2016/7879097.
- [27] S. V. Vassilev, C.G. Vassileva, Composition, properties and challenges of algae biomass for biofuel application: An overview, *Fuel.* 181 (2016) 1–33. doi:10.1016/j.fuel.2016.04.106.
- [28] S. kumar P, Cultivation and Chemical Composition of Microalgae *Chlorella vulgaris* and its Antibacterial Activity against Human Pathogens, *J. Aquac. Mar. Biol.* 5 (2017). doi:10.15406/jamb.2017.05.00119.
- [29] H.K. Reddy, T. Muppaneni, S. Ponnusamy, N. Sudasinghe, A. Pegallapati, T. Selvaratnam, M. Seger, B. Dungan, N. Nirmalakhandan, T. Schaub, F.O. Holguin, P. Lammers, W. Voorhies, S. Deng, Temperature effect on hydrothermal liquefaction of *Nannochloropsis gaditana* and *Chlorella* sp., *Appl. Energy.* 165 (2016) 943–951. doi:10.1016/j.apenergy.2015.11.067.

- [30] L. Bennamoun, M.T. Afzal, A. Léonard, Drying of alga as a source of bioenergy feedstock and food supplement - A review, *Renew. Sustain. Energy Rev.* (2015). doi:10.1016/j.rser.2015.04.196.
- [31] N. Rashid, M.S.U. Rehman, J.I. Han, Recycling and reuse of spent microalgal biomass for sustainable biofuels, *Biochem. Eng. J.* 75 (2013) 101–107. doi:10.1016/j.bej.2013.04.001.
- [32] M. Francavilla, P. Kamaterou, S. Intini, M. Monteleone, A. Zabaniotou, Cascading microalgae biorefinery: Fast pyrolysis of *Dunaliella tertiolecta* lipid extracted-residue, *Algal Res.* (2015). doi:10.1016/j.algal.2015.06.017.
- [33] A. Aboulkas, H. Hammani, M. El Achaby, E. Bilal, A. Barakat, K. El harfi, Valorization of algal waste via pyrolysis in a fixed-bed reactor: Production and characterization of bio-oil and bio-char, *Bioresour. Technol.* (2017). doi:10.1016/j.biortech.2017.06.098.
- [34] L. Chen, T. Liu, W. Zhang, X. Chen, J. Wang, Biodiesel production from algae oil high in free fatty acids by two-step catalytic conversion, *Bioresour. Technol.* (2012). doi:10.1016/j.biortech.2012.02.033.
- [35] B.R. Moser, Biodiesel production, properties, and feedstocks, *Vitr. Cell. Dev. Biol. - Plant.* (2009). doi:10.1007/s11627-009-9204-z.
- [36] A. Sathish, R.C. Sims, Biodiesel from mixed culture algae via a wet lipid extraction procedure, *Bioresour. Technol.* 118 (2012) 643–647. doi:10.1016/j.biortech.2012.05.118.
- [37] W. Zhao, M. Duan, X. Zhang, T. Tan, A mild extraction and separation procedure of polysaccharide, lipid, chlorophyll and protein from *Chlorella* spp., *Renew. Energy.* 118 (2018) 701–708. doi:10.1016/j.renene.2017.11.046.
- [38] H. Chakdar, S. Pabbi, Algal Pigments for Human Health and Cosmeceuticals, in: *Algal Green Chem. Recent Prog. Biotechnol.*, 2017. doi:10.1016/B978-0-444-63784-0.00009-6.
- [39] M.D. Redel-Macías, S. Pinzi, M.F. Ruz, A.J. Cubero-Atienza, M.P. Dorado,

Biodiesel from saturated and monounsaturated fatty acid methyl esters and their influence over noise and air pollution, *Fuel*. (2012).
doi:10.1016/j.fuel.2012.01.070.

- [40] S. Pinzi, D. Leiva, G. Arzamendi, L.M. Gandia, M.P. Dorado, Multiple response optimization of vegetable oils fatty acid composition to improve biodiesel physical properties, *Bioresour. Technol.* 102 (2011) 7280–7288.
doi:10.1016/j.biortech.2011.05.005.
- [41] B. Singh, A. Guldhe, I. Rawat, F. Bux, Towards a sustainable approach for development of biodiesel from plant and microalgae, *Renew. Sustain. Energy Rev.* (2014). doi:10.1016/j.rser.2013.08.067.

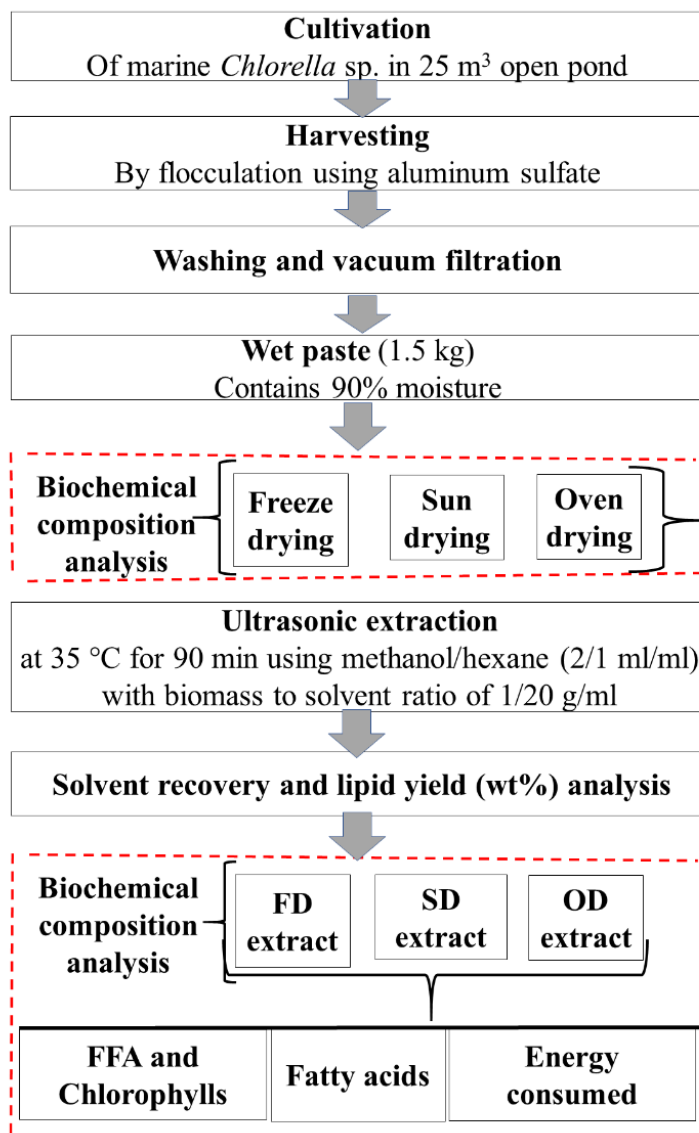


Figure 3.1. A schematic diagram of experimental and analysis work from marine *Chlorella* sp. cultivation and biomass preparation to lipid extraction.

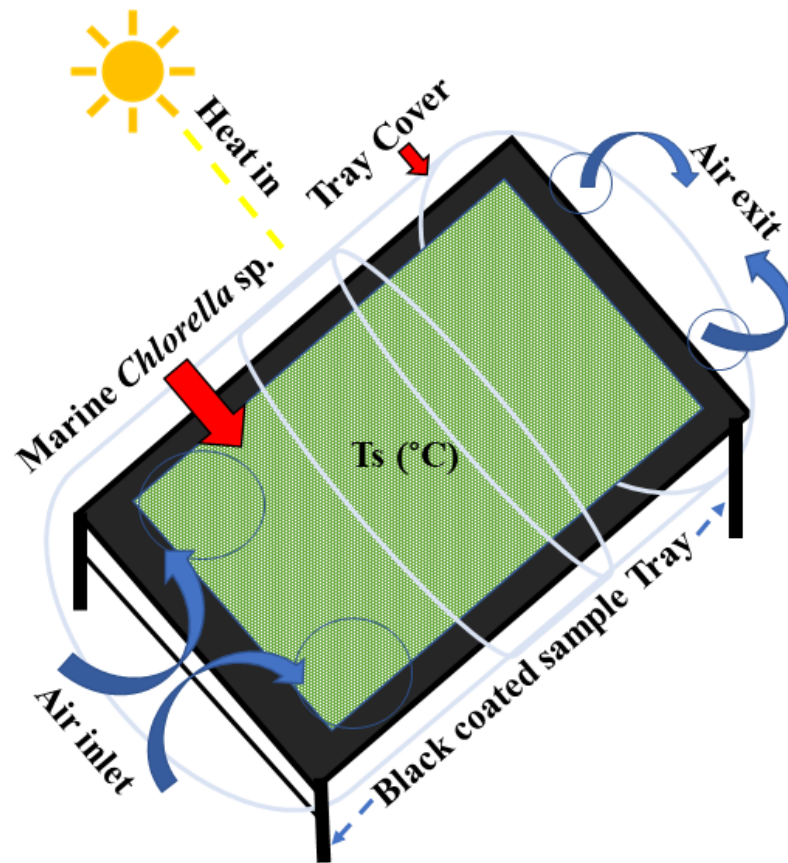


Figure 3.2. A schematic diagram of mini homemade solar dryer

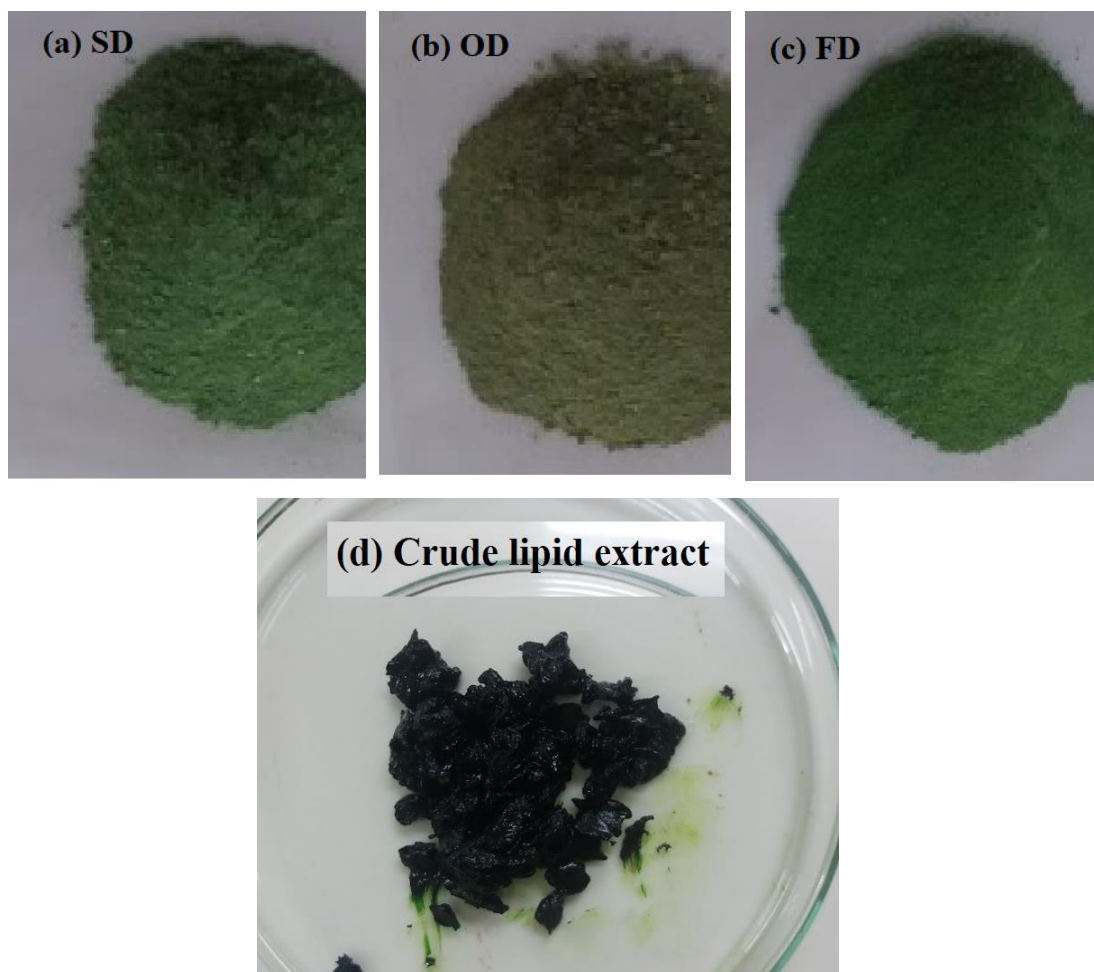


Figure 3.3. Pictorial view of marine *Chlorella* sp. biomass (a) Sun dried, (b) Oven dried, (c) Freeze-drying and, and extracted crude lipids

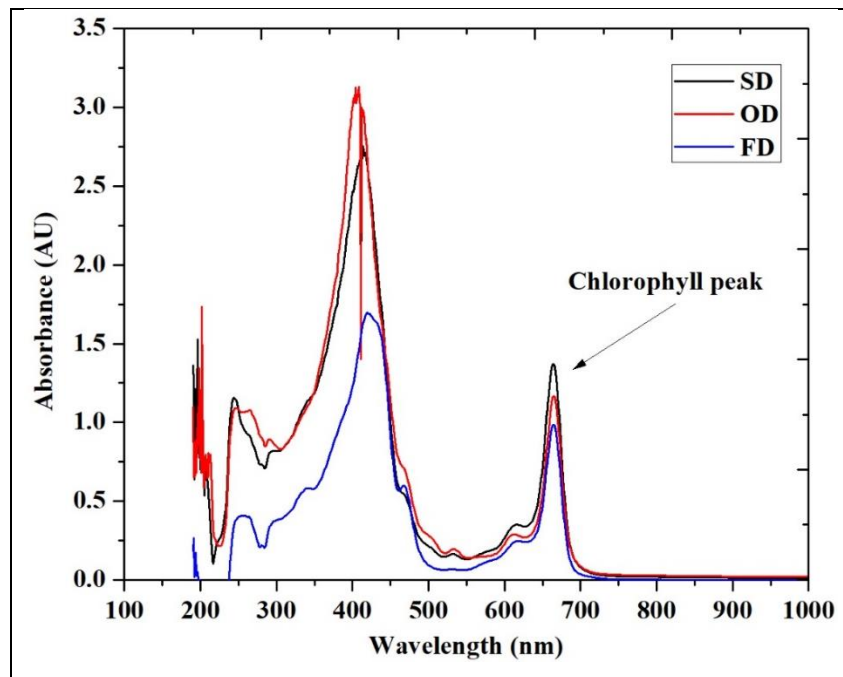


Figure 3.4. Absorption spectra of chlorophylls presented in crude lipid extract of sun dry, oven dry and freeze-dried biomass of marine *Chlorella* sp. using UV spectrophotometer.

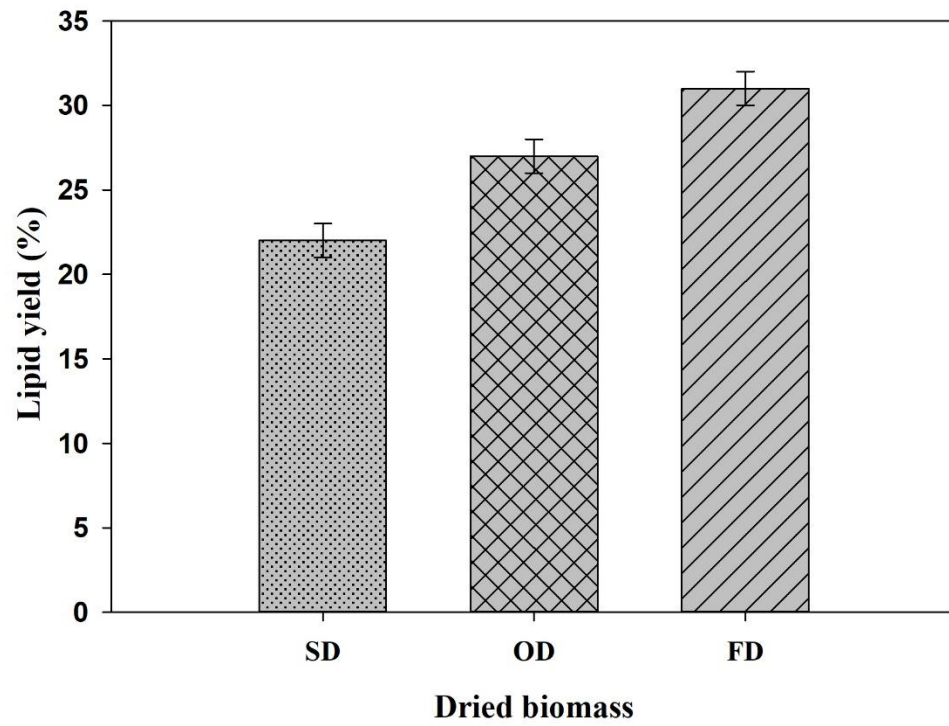


Figure 3.5. Impact of drying techniques on the lipid yield of marine *Chlorella* sp. biomass

Table 3.1 Biochemical composition of marine *Chlorella* sp. biomass dried using different drying techniques

Constituents	Marine <i>Chlorella</i> sp. biomass		
	Sun dried	Oven dried	Freeze dried
Moisture (%)	9.0±1	8.05±1	8.1±1
Protein (%)	20.91±0.05	20.91±0.05	22.1±0.06
Crude lipid (%)	2.64±0.01	5.23±0.01	10.7±0.01
Carbohydrates (%)	28.45±0.5	27.81±0.5	21.60±0.5
Ash (%)	39.0±1	38±1	37.5±1
Energy (kcal/100g)	221.20	241.95	271.10

Table 3.2 Biochemical constituents, FFA and chlorophyll of SD, OD and FD extract

Constituents	Crude lipid extract		
	Sun dried	Oven dried	Freeze dried
Moisture (%)	9.4±1	8.1±1	6.3±1
Protein (%)	7.13±0.05	6.05±0.05	5.87±0.06
Crude lipid (%)	53.2±0.01	34.0±0.01	46.0±0.01
Lipid (%)	11.70	9.18	14.26
Carbohydrates (%)	19.87±0.5	41.65±0.5	32.13±0.5
Ash (%)	11.2±1	10.0±1	10.1±1
Energy (kcal/100 gm)	585	499	566
FFA (%)	29.6	24.3	20.1
Chlorophyll-a (µg/ml)	102.6	122.31	136.71
Chlorophyll-b (µg/ml)	34.64	37.35	67.86

Table 3.3 Fatty acid methyl esters of lipid extracted from sun, oven and freeze-dried biomass

Fatty acid methyl esters (Area %)												
	C8:0	C10:0	C12:0	C13:0	C14:0	C15:0	C16:0	C16:1	C17:0	C18:0	C18:1	C18:2
SD	0.09	0.51	0.54	1.15	5.58	0.38	26.52	20.15	0.35	0.94	4.51	1.98
OD	0.08	0.52	0.58	1.39	5.90	0.38	25.84	20.89	0.35	0.93	3.83	1.79
FD	0.11	0.49	0.62	1.16	5.93	0.40	26.71	22.46	0.39	0.92	4.98	1.87

CHAPTER 4

Enhanced lipid recovery from marine *Chlorella* sp. by ultrasonication with an integrated process approach for wet and dry biomass

Submitted by

Muhammad Amin, Pakamas Chetpattananondh

Department of Chemical Engineering, Faculty of Engineering, Prince of Songkla University, 90112, Hat Yai, Thailand

Corresponding author email: pakamas.p@psu.ac.th

Acknowledgements

This research was financially supported by Thailand's Education Hub for Southern Region of ASEAN Countries (TEH-AC, 56/2016) granted by the Graduate School, Prince of Songkla University (PSU), Hat Yai, Songkhla, Thailand. We are grateful to the Department of Chemical Engineering, Faculty of Engineering, PSU for providing all facilities and supporting staff to accomplish this work. We are really thankful to Research and Development Office (RDO), PSU for their support in English language editing and proofreading.

Enhanced lipid recovery from marine *Chlorella* sp. by ultrasonication with an integrated process approach for wet and dry biomass

Abstract

Lipid extraction from microalgal biomass faces some challenges such as the selection of a suitable biomass type and its quality, lipid yield (LY) and process energy consumption. This study aimed to develop optimized processing conditions using response surface methodology, for the ultrasonic extraction (UE) of lipids from wet and dried marine *Chlorella* sp. Integrated process approaches with different extraction and solvent recovery steps were developed for the evaluation of the lipid recovery and process energy consumption. The effects of other processing factors, such as the biomass to solvent ratio, solvent type and solvent to solvent ratio were investigated. The biomass and lipids extracted were characterized by Scanning Electron Microscopy-Energy Dispersive-X-ray (SEM-EDX) and Gas Chromatography-Flame Ionization Detector (GC-FID) analysis, respectively. With single extraction and single solvent recovery (1-1-cycle) process the LYs from fresh and stored paste were 11.7% and 6%, respectively, while freeze-dried biomass produced an 18.5% LY. The energy consumption was 6,000 MJ/kg lipid for the wet route and 8,200 MJ/kg lipid for the dry route in the 1-1-cycle process. Dried biomass was selected for further investigation due to its longer storage-period capability and higher LY. The LY of the 2-1-cycle process using methanol/hexane (2/1 v/v) with a biomass to solvent ratio 1/20 g/ml was 31% and considered as a base case scenario of this study, which is 40.3% and 9.7% greater than those of the 1-1-cycle and 2-2-cycle, respectively. The lipids obtained from the 2-1 cycle at the optimum condition were mainly saturated fatty acids which is suitable for a biodiesel feedstock.

Keywords: *Chlorella* sp.; ultrasonic extraction; energy consumption; lipids; biomass

4.1 Introduction

Microalgae are considered to be a third generation biofuel resource [1], as they contain a higher oil content in shorter period cultivation than other feedstocks and have no competition with agricultural food and feed production [2, 3]. The ideal biomass candidate is one which gives a high yield per unit area, incurs low production costs, causes less contamination and consumes less nutrients. Algae produce the maximum biomass yield per unit area compared to terrestrial crops [2, 4, 5], due to rapid growth enabled by high photosynthetic efficiency [6]. Algal biomass could be cultivated in fresh, saline and waste water [7, 8] for bioenergy production under controlled condition [9, 10].

Chlorella sp. is single-celled strain of green algae with a diameter of 2-10 μm and an oil content of 28-32 % [2, 11]. It contains about 20% lipid, 45% protein and 20% carbohydrate [12, 13]. The composition of biomass and lipid yield (LY) vary with respect to location, growth conditions, nutrients and environmental impact [14, 15]. Even within the same class of microalgae the characteristics vary due to different culture conditions [16]. Nevertheless, *Chlorella* has shown considerable potential for biodiesel production [17, 18].

Microalgal biomass has a high moisture content, ~90 % [19, 20]. After harvesting, wet biomass should be dehydrated quickly to obtain a high quality biomass for application in downstream processes [21, 22]. It has been reported that a final moisture content of 10% in biomass is sufficient to preserve its quality in most applications [23, 24]. Drying of algal biomass has variously been conducted by sun drying, solar heat drying, freeze drying, spray drying, oven drying, etc. [25]. Freeze-dried biomass has been extensively used in research and has produced good yields and quality products. However, the drying process has been reported as being time consuming and accounts for 50-70 % of the total process cost [26, 27].

Direct extraction of lipids from wet biomass has gained serious attention in recent years as a way of overcoming the economic challenges associated with dried biomass extraction. Dong et al. [28] suggested that direct wet extraction of lipids faces major challenges such as low solvent diffusion and emulsion formation leading to the poor extraction of lipids. The release of lipids from the cell by breaking the cell wall is an important process in terms of product quantity and economic viability. The selection

of the cell disruption method along with the selection of the solvent is essential for the maximum product recovery. The thick wall of the microalgae cell is the main constraint to extracting a high LY by conventional methods [29]. Several disruption techniques have been investigated, such as bead beating, grinding, sonication, microwave treatment and osmotic shock [30]. Sonication ruptures the cell wall by the generation of a cavitation effect due to shock waves and the collapsing of bubbles is a highly efficient, low cost and environmentally friendly method which requires less time than other methods to conduct [31, 32]. Therefore, ultrasonication was chosen as the extraction technique in the study reported.

Extraction and solvent recovery are critical stages in biodiesel production from microalgae. Conventionally, a single extraction and a single solvent recovery process (1-1-cycle) has been reported for lipid production using different techniques from algal biomass [33, 34]. Only a small number of studies have considered double extraction and single solvent recovery to maximize the recovery of product [10, 35]. However, those studies did not evaluate the quantity of product recovered at each stage nor the energy consumption. Due to lack of knowledge in this area the current study was initiated to thoroughly investigate three different process schemes: the 1-1-cycle (single extraction and single solvent recovery), the 2-1-cycle (double extraction and single solvent recovery) and the 2-2-cycle (double extraction and double solvent recovery).

Many studies have successfully converted wet and dried biomass into bioenergy using various extraction methods. The wet and dry routes both have advantages and disadvantages. However, some important factors still need to be explored, such as the effect of the extraction conditions on the LY for wet and dried biomass, the effect of biomass storage on LY and the energy consumed in wet and dry processes. The objectives of this study were to investigate (1) the impact of biomass type: fresh, stored wet-paste and freeze-dried biomass on LY, (2) the optimum ultrasonic extraction (UE), the conditions for the wet route and the dry route, (3) the effect of the biomass to solvent ratio, solvent type and solvent to solvent ratio (4) the extraction and solvent recovery system (1-1, 2-1 and 2-2-cycles), (5) biomass and lipid characterization and (6) the energy consumption for wet and dry processes. A schematic diagram of this work is presented in Fig. 4.1.

Firstly, the optimum UE condition was determined for the wet route (both fresh wet paste and stored wet paste). Secondly, the dry-route UE process was evaluated and optimized. The wet and dry routes were then compared in terms of their optimum process conditions, their LY and their energy consumption. The optimum biomass type was selected for further investigation and the impact of the type of organic solvent used, the biomass to solvent and solvent to solvent ratios and the extraction-solvent recovery process were evaluated.

4.2 Materials and methodology

4.2.1 Materials

The methanol, ethanol, n-hexane and isopropanol used were commercial grade (purity>95%) and were purchased from RCI Labscan Ltd., while aluminum sulphate was purchased from Siam Chemicals Co. Ltd. Thailand.

4.2.2 Microalgae culture, harvesting and sample preparation

Marine *Chlorella* sp. was obtained from the National Institute of Coastal Aquaculture (NICA) located in Songkhla (latitude: 7.178861° N, 100.624561° E), Thailand and was cultivated in a 25 m³ (6x3x1.4 m) aerated open pond. The growth medium used was composed of CO (NH₂)₂ and 16-16-16 fertilizer (16% nitrogen, 16% phosphorus, and 16% potassium). Culture was carried out in ambient conditions at a temperature of 25-28 °C using natural resources (sunlight and marine water). The biomass was harvested in its peak growth phase (cell density = 0.5g/l) after one week of cultivation. The energy consumption for water circulation in the pond was determined to be 0.15 MJ/day. Aluminum sulfate [18] was added as a flocculation agent and ample time was allowed for the biomass flocs to settle following which the surface water was decanted. The diluted microalgae slurry was pumped out from the pond using a Tornado 0.1 kW submersible pump for 3 minutes. It was filtered via cheesecloth and placed in containers. The containers were immediately transferred to the work station and stored at 4 °C. The pH of the slurry was recorded as 7.8. The microalgal slurry was washed three times with deionized water to remove any water-soluble contaminants present. The contamination-free slurry was then dewatered to increase the biomass concentration by vacuum filtration using Whatman no. 4 filter paper and a vacuum pump (PVL 35, 930 Watt; PVR, Valmadrera, Italy) for 4 hours. The slurry was gently

stirred using a spoon to prevent the clogging of the filter paper during dewatering, but care was taken to prevent damage to the filter paper.

The thick wet paste (90% moisture) obtained after dewatering was collected in pre-weighed zip lock airtight bags and kept at 4 °C prior to further processing. The wet paste was divided as per the requirements of the experiment into fresh paste and stored wet paste for the wet route UE and freeze-dried paste for the dry route UE. To freeze dry the wet paste a sample was frozen overnight at -16 °C and lyophilized using a freeze dryer (Dura-Dry MP, FTS systems, 4400 Watt; Stone Ridge, New York, USA) at -50 °C under vacuum (12.66 Pa) for 24 hours, at the Scientific Equipment Center (SEC), Prince of Songkla University, Thailand. The freeze-dried powder was pulverized using a mortar and stored at 4 °C.

4.2.3 Ultrasonication extraction

The UE process was performed for the fresh wet paste and the freeze-dried biomass. The biomass sample of 10 g (dry basis) was mixed with 100 ml methanol and hexane (2:1 v/v) in a 250 ml Duran bottle sealed with aluminum foil. The samples were extracted using an ultrasonic bath (CP 2600 Crest Power sonic 45 kHz, 300 Watt; Trenton, New Jersey, USA). The supernatant was recovered by vacuum filtration using Whatman no. 4 filter paper in 4 for the wet and 3 minutes for the dry route, then transferred to a pre-weighed boiling flask for solvent recovery. The residual biomass was kept in zip-lock bags for further use. The supernatant was evaporated using a vacuum rotary evaporator (Heidolph Laborota 4000, 1400 Watt; Schwabach, Bavaria, Germany). The water bath and condenser temperatures were maintained at 45 °C and 10 °C, respectively while maintaining the flask rotation at 70 rpm. A vacuum pressure of 33.7 kPa was applied initially and then gradually decreased to 7.2 kPa for hexane, methanol and water recovery. Solvent recovery was accomplished in 70 minutes for the wet and 25 minutes for the dry route. The lipids were recovered from the flask using a spatula, then redissolved in 10 ml hexane and stored at -20 °C. After solvent recovery, the LY was determined gravimetrically using Eq. (4.1).

$$\text{Lipid yield} = \frac{\text{weight of lipid (g)}}{\text{weight of biomass (g)}} \times 100 \quad (4.1)$$

Response surface methodology based on a full factorial design (FFD) with three replications was applied to obtain the optimum conditions for wet and dry UE.

Temperature (30, 35 and 40 °C) and time (60, 90 and 120 min) were the two factors evaluated at 3 levels (3^2) with the LY as the response. The factors were designated as X_1 (temperature) and X_2 (time) and were coded into -1 (low), 0 (center) and +1 (high) to estimate the goodness of fit of the coefficients and values calculated. The relationship between the actual and coded values was calculated using Eq. (4.2).

$$X_i = \frac{x_i - x_o}{\Delta x} \quad (4.2)$$

where X_i is the coded value of the independent variable; x_i is the original factor; x_o is the base value at the center point and Δx is the step change between low and high level. Analysis of variance (ANOVA) and analysis by multiple regression and optimization was performed using the Statistica version 10.0 . The experimental data were fitted according to Eq. (4.3), which is the general form of the proposed model.

$$y = \beta_o + \sum_{i=1}^k \beta_i X_i + \sum_{i=1}^k \beta_{ii} X_i^2 + \sum_{i>j}^k \beta_{ij} X_i X_j + \varepsilon \quad (4.3)$$

where y is the response and β_o , β_i , β_{ii} β_{ij} are the linear, quadratic and interaction terms of the model. The response was further transformed into a dimensionless “desirability” scale covering values 0-1 (or 0-100 %), in which 0 showed a completely undesirable experimental design and 1 (100 %) indicated a fully desirable design [36].

4.2.4 UE-solvent recovery system analysis

As explained in the Introduction, a single extraction-single solvent recovery process (1-1-cycle) has been the conventional method used for lipid extraction from algal biomass. However, in the present study, two further processing schemes, double extraction and single solvent recovery (2-1-cycle) and double extraction and double solvent recovery (2-2-cycle) were developed for evaluation as shown in Fig. 4.2. In the 2-1-cycle, after the 1st UE was performed the supernatant was collected and the residual biomass was re-extracted also using ultrasonication (2nd UE). The supernatants of the 1st and 2nd extraction were then combined for a single evaporation step (solvent recovery). In the 2-2-cycle the 1st UE was performed followed by the 1st solvent recovery and the residual biomass was then subjected to the 2nd UE followed by a 2nd evaporated for solvent recovery.

4.2.5 Analytical procedures

The compositional analysis of the biomass and crude lipids was carried out using the standard procedures of the Association of Official Analytical Chemists (AOAC). The amount of protein was determined based on AOAC 991.20 using the Kjeldahl method, in which a conversion factor of 6.25 was employed for the calculation [37]. The crude lipid content was determined by the AOAC 920.39 method [10]. The ash content (burned at 550-600 °C) was analyzed by the AOAC 942.05 method. The crude fiber content was tested using an ANKOM²⁰⁰ fiber analyzer, while the carbohydrate and energy contents were determined by calculation using Eq. (4.4) and (4.5), respectively. The initial moisture content of the wet biomass was examined by the standard procedure of AOAC 934.01. The characterization of the algal biomass before and after UE was performed by Scanning Electron Microscopy-Energy Dispersive-X-ray (SEM-EDX) spectroscopy (Quanta 400, FEI, Brno, Czech Republic) analyzer at the Scientific Equipment Center, Prince of Songkla University. The samples for SEM-EDX analysis were prepared by gold-coating using argon gas (68.9 kPa) in sputter coater (SPI module, West Chester, Pennsylvania, USA).

$$\text{Total carbohydrate} = 100 - (\text{Moisture} + \text{Ash} + \text{Protein} + \text{Lipid}) \quad (4.4)$$

$$\text{Total energy} = (\text{Protein} \times 4) + (\text{Lipid} \times 9) + (\text{Carbohydrate} \times 4) \quad (4.5)$$

The chlorophyll concentration in the extract was analyzed using a UV spectrophotometer (Agilent 8453, Santa Clara, California, USA); 5 g lipid was dissolved in 30 ml methanol as a stock solution and centrifuged at 3,000 rpm for 5 minutes to remove any suspended particles. 1 ml of the supernatant was diluted with 20 ml methanol and an absorbance reading was taken against a methanol blank. The chlorophyll concentration was calculated by Eq. (4.6) [38].

$$\begin{aligned} \text{Ch - a} &= 16.72A_{665.2} - 9.16A_{652.4} \\ \text{Ch - b} &= 34.09A_{652.4} - 15.28A_{665.2} \end{aligned} \quad (4.6)$$

The fatty acid methyl esters were prepared by saponification 200 mg of crude lipid with 1 mL of KOH-CH₃OH for 30 min. at 100°C in a screw cap tube. Then, 400 µl of HCl /Methanol (4/1 v/v) was added to the mixture obtained from the saponification reaction and heated at 100°C for 30 min. Reaction mixture was cooled and washed with 2 ml of water. After that, it was extracted with 6 ml of petroleum ether.

The organic layer was collected, dried with N₂ and the resulted FAMEs were dissolved in heptane. The fatty acid composition of the lipids was analyzed by Gas Chromatography-Flame Ionization Detector (GC-FID) (Agilent 7890, Santa Clara, California, USA) equipped with a 30 m select biodiesel CP 9080 capillary column with internal diameter 0.32 mm and film thickness 0.25 μm. The split ratio was 50:1 and the detector temperature was 290 °C. The oven temperature program commenced at 210 °C for 12 minutes, and was increased at 20 °C/min up to 250 °C and kept at that temperature for 8 minutes. Helium was used as the carrier gas with a flow rate of 1 mL/min.

4.2.6 Energy analysis

The energy consumption from the cultivation to extraction and solvent recovery stages was determined for both the wet and dry routes. The energy consumed in each process was calculated by applying Eq. (4.7), where E is energy in MJ, P is the power of the equipment and t is the operational time in hours [35, 39]. The power (P, Watt) consumed by the equipment at each stage was determined by measuring the voltage and current supply ($P = V \times I$) using a Kew snap current meter.

$$E = P \times t \quad (4.7)$$

4.3 Results and discussion

4.3.1 Wet route extraction: Process condition analysis

The moisture content of the wet fresh paste of marine *Chlorella* sp. used in this study was determined to be 90%. UE of the fresh paste was performed at the designated conditions and the results are presented in Table 4.1. The reproducibility of the method was assessed by performing each run in triplicate. The maximum LY of 12.10% dry basis was observed at 35 °C and 60 min. using methanol/hexane (2/1 v/v) with a biomass to solvent ratio of 1/10 (g/ml). Zheng et al. [40] extracted lipids from wet *Chlorella vulgaris* by various techniques including ultrasonication at 600 W for 20 minutes using 1/1 v/v chloroform/methanol and obtained a 15% LY (dry basis). They observed that ultrasound extraction is competitive with the other disruption methods tested, viz, microwave treatment, grinding, lysosome and bead beating. Balasubramanian et al. [41] obtained a 13 % LY from wet paste (85% moisture contents) from marine *Nannochloropsis* sp. using an accelerated solvent extraction

technique at 100 °C, 1200 kPa for 30 minutes and suggested that a high moisture content has a negative effect on the LY. The presence of water is a major hindrance to completely extracting the lipid content [42]. In all the reports discussed and also including the current study, variation in the LY is fully attributable to the use of different technologies, microalgal species and experimental conditions.

The results in Table 4.1 show that the LY increased significantly when the temperature was increased from 30°C to 35°C and declined thereafter. The increasing LY with the temperature rising to 35°C is possibly due to the rapid disruption of the microalgal cell wall and an increase in solvent accessibility (i.e., a high mass transfer rate to carry away the lipids). A mild temperature during ultrasonication is favorable because it reduces the vapor pressure inside the cavitation bubbles providing faster bubble collapse and greater shear [43]. The reduction in LY with temperatures higher than 35 °C is attributable to lower shear stress generation and solvent penetration. The maximum LY was obtained with a time of 60 min. Extraction times longer than 60 min. resulted in lower LYs at every temperature. This is because the solvent became saturated with product at 60 minutes and the LY therefore showed no further improvement.

4.3.1.1 Model fitting and optimization

The actual and predicted responses of the 3² full factorial experiment (in triplicate: 27 runs) are given in Table 4.1 and the results from the ANOVA are presented in Table 2. The R² value of 0.97 shows that the model accounts for most of the observed variance. The adjusted R² and predicted R² were also both close to this R² value. The coefficient of variance (4.17%) represents the reliability of the experiment. Both the temperature and time as well as their interactions had significant impacts on the LY as can be observed from the p-values, whereby values ≤ 0.05 are considered to represent statistically significant factors (Table 4.3). The equation developed for the LY prediction of the wet-route UE is shown as Eq. (4.8).

$$LY = 10.14 - 0.52X_1 - 1.18X_2 - 3.37X_1^2 + 0.29X_2^2 - 0.30X_1X_2 \quad (4.8)$$

A 3-D response surface plot was generated to better visualize the process variable effects and is shown in Fig. 4.3a. Process optimization with the objective of LY maximization was performed. The maximum actual LY was 12.10 % at the

optimum conditions of 35°C and 60 min., while the model predicted 11.62% with 94 % desirability. Below or above the optimal point the desirability value decreased. This optimum condition of the model was validated by conducting three more experiments and the average value obtained was 11.70 % with a deviation of +0.08 %.

4.3.1.2 Effect of storage on wet paste extraction

It has been previously stated that after harvesting, wet paste microalgal biomass should be processed quickly to prevent degradation [9, 43], which appears to be correct as was observed in the current study. While the factors relevant were taken to be the specific storage conditions and age of the wet paste, there is a lack of information available relating to exactly what factors need to be taken into account. Samples of the fresh wet paste produced from marine *Chlorella* sp. were stored for 1 week at 4 °C to evaluate the storage effect on the LY. Following extraction with UE it was found that at the optimum conditions earlier established for fresh paste (35°C and 60 minutes), the stored wet paste provided a significantly lower response with only a 6% lipid yield, representing an approximately 50% reduction compared to the fresh biomass. Chen et al. [44] investigated the effect of storage conditions using a wet paste from *Scenedesmus* sp. kept for 1 day at different temperatures (4°C, 20°C, 37°C, -20°C and -80°C) and reported no significant effect on the total LY, however they found a considerable difference in lipid composition. The free fatty acid increased to 62% for the wet paste kept at 4°C for 4 days owing to the degradation of triacylglyceride, which has a negative effect in biodiesel production.

The UE of freeze-dried biomass was then investigated to compare with those results and the findings are described in the following section.

4.3.2 Dry-route extraction: Process condition analysis

Freeze-dried or lyophilized biomass has been used in many previous studies and has been reported as representing a suitable raw material. The UE of the freeze-dried sample (8% moisture content) was carried out in similar way to that of the fresh wet paste with some modification. The experiments were initially performed with a 2-1-cycle and the optimum conditions were determined. Then, at the optimum conditions, 1-1-cycle UE was conducted and the outcome was compared with the UE of fresh paste in terms of conditions and yield. The LY was determined to increase as

the temperature increased from 30 to 35°C and time from 60 to 90 minutes, and that at temperatures and times above those ranges the LY declined.

4.3.2.1 Model fitting and optimization

The actual vs predicted LYs from the UE of freeze-dried biomass are in good agreement as shown by the low residual values in Table 4.1. Furthermore, all the statistical data presented in Table 4.2 were found to be in good agreement and the model explains 97% of the total variation. A second order polynomial was fitted to the data and the coefficients given in Table 4.3 were developed to express the model equation, Eq. (4.9) for the LY of dry-route UE.

$$LY = 26.64 + 0.71X_1 - 0.83X_2 - 1.69X_1^2 - 4.11X_2^2 - 0.51X_1X_2 \quad (4.9)$$

The 3-D surface plot shown in Fig. 4.3b clearly shows the effect of both factors on LY. Regression analysis indicated that the optimum conditions were 35°C and 90 minutes. At these optimum conditions the actual LY was 28% while the model predicted 26.64% with 85% desirability. The optimum conditions of the model were assessed by conducting three more experiments and the average value obtained was 26.73% with a deviation of +0.08%. Dry-route extraction was performed at the optimized conditions (35°C and 90 minutes) using the 1-1-cycle process to achieve a fair comparison with the wet route extraction. The dry route 1-1-cycle process produced LY of an 18.5%.

4.3.3 Comparison between wet and dry UE

Both wet and dry UE produced their maximum LY at a temperature of 35°C. although with different extraction times, 60 minutes for fresh wet paste and 90 minutes for freeze-dried biomass. The freeze-dried biomass produced an 18.5% LY, which was 6.6% more than that from the fresh wet paste and 12.6% above that from the stored wet paste. The presence of water in wet biomass forms a film impeding the solvent from reaching the lipids, which limits the efficiency of lipid extraction [42]. In a previous study, the moisture content of the biomass of *Nannochloropsis* sp. had a significant negative effect on the LY extracted by methanol/hexane (2/3 v/v) [41]. Water molecules surrounding the hydrophilic outer layer of the cell wall resist the penetration of the non-polar solvent into the cell, so that lipid extraction is impeded. The difference in the mean LY from the biomass with 4.5 and 20.6% moisture content was not, however,

statistically significant. The use of a microalgal biomass with a 20% moisture content for extraction considerably reduces the energy requirement for drying. Therefore, because of the better LY achieved from the freeze-dried biomass and the fact that freeze dried biomass can be stored without diminishing the LY, the dry route was selected for further investigation.

4.3.4 Effect of solvent type, biomass/solvent ratio and extraction system

4.3.4.1 Effect of biomass to solvent ratio

As described in section 3.2, the temperature and time were optimized using methanol/hexane (2/1 v/v) with a biomass-to-solvent (B/S) ratio of 1/10 g/ml. Therefore, B/S ratios of 1/15, 1/20 and 1/25 g/ml were further investigated, and the results are presented in Fig 4.4a. The LY increased with decreases in the B/S ratio and reached a maximum (31%) at 1/20 g/ml, after which it decreased sharply. Wu et al. [45] extracted *Chlorella* sp. with incubation at 60°C and stirring for 3 hours using a methanol/ethyl acetate solvent with B/S ratios of 1/5 – 1/25 and reported that the LY increased with decreases in the B/S ratio, and the ratio 1/15 (w/v) was recommended from an economic point of view. In another study, wet *Chlorella vulgaris* was extracted using a magnetic stirrer at ambient temperature with ionic liquid (IL) mixed with methanol. The product recovery increased as B/S ratios decreased from 1/1 and 1/5 to 1/10 g/ml, but reduced at 1/15 g/ml because of emulsion formation [46]. An increased solvent quantity stimulates mass transfer efficiency, resulting in a higher lipid extraction yield. However, the application of excess amounts of solvent limits mass transfer and is not cost-effective since the separation of lipids from the solvent is an energy intensive process.

4.3.4.2 Effect of solvent system

The combination of a polar and non-polar solvent at the proper ratio is necessary to obtain the maximum LY. Because only the neutral lipids (NLs), triacylglycerol, monoglyceride and diglyceride are normally used in biodiesel production, determining which solvent system produced the highest NLs was also a target of this study. Lipid extraction of microalgae by solvents is highly dependent on the penetrability of the microalgae cell membrane and the solubility of lipids in organic solvents. At the optimized levels of the three factors (temperature: 35°C, time: 90 minutes, B/S ratio: 1/20 g/ml) different solvent mixtures, ethanol/hexane and

isopropanol/hexane (2/1 v/v) were studied to compare with the results from the use of methanol/hexane (2/1 v/v) and it was determined that the methanol/hexane solvent system was superior with a 31% LY. Ethanol/hexane and isopropanol/hexane yielded 18 and 14%, respectively, as shown in Fig.4.4b. In a previous study, methanol produced the highest total LY among the five solvents evaluated (hexane, ethyl acetate, chloroform, ethanol and methanol) for the extraction of *Chlorella* spp. with a high NL-recovery ratio and only ethyl acetate gave a slightly higher yield of NLs [45]. Therefore, the optimum solvent system of methanol/hexane (2/1 v/v) applied in this study broadly agrees with those findings.

4.3.4.3 UE-Solvent recovery system analysis (1-1-cycle, 2-1-cycle and 2-2-cycle)

The effect of the extraction and solvent recovery system: 1-1-cycle, 2-1-cycle and 2-2-cycle on LY is presented in Fig.4.4c. At the optimum conditions (methanol/hexane 2/1 v/v, 35°C, 90 minutes, 1/20 g/ml) the conventional 1-1-cycle yielded 18.5% total lipids. The Bligh and Dyer method [47] and modified forms of this method using chloroform/methanol have been extensively applied for lipid extraction from biomass. The application of the modified Bligh and Dyer method using chloroform/methanol/water (1/1/0.9 v/v/v) and sonication at 35°C for 90 minutes gave a greater LY than the 1-1-cycle extraction system as can be seen in Fig. 4.4d. However, chloroform is an extremely hazardous substance and its use on a large-scale is precluded due to its environmental and health risks [45]. Therefore, the methanol/hexane solvent system, which is less toxic, was further investigated. The solvent system ratio of methanol/hexane 2/1 v/v was reciprocated to 1/2 v/v and the observed LY was 14%, which is 4.5% lower. The reason for this could be that methanol is better able to penetrate the microalgal cell membrane and therefore extracted more lipids than h-hexane, as discussed earlier [45].

The lipid yield of the 2-1-cycle using methanol/hexane (2/1 v/v) with a biomass to solvent ratio 1/20 g/ml was 31%. This is in agreement with literature for LY of *Chlorella* sp. [2, 12]. Whereas the 1-1-cycle and 2-2-cycle resulted in LYs of 18.5 and 28%, respectively. Due to high LY of the 2-1-cycle process, it was considered as a base case scenario. The LYs of 1-1-cycle and 2-2-cycle processes were almost 40.3% and 9.7% lower than the base case value. The efficiency of the 1-1-cycle process was the lowest. The lipid loss in the 2-2-cycle process compared to the 2-1-cycle process

occurred during the solvent recovery step. Hence, the 2-1-cycle was found to be the most efficient method and is recommended based on the results of this study as the most suitable extraction and solvent recovery process to obtain the maximum LY.

4.3.5 Biomass and lipid characterization

The characteristics of the biomass before and after UE were analyzed by SEM-EDX and surface images are presented in Fig. 4.5. It can be observed that before extraction the surface of the biomass was smooth, but that there were small holes after extraction. This confirms the ultrasonication effect on the algal cell wall, which makes it permeable and enables the solvent to extract its components. The EDX analysis showed that before UE, carbon (39.2%) and oxygen (40.7%) were the major constituents, which is similar to the findings of Hosseinizand et al. [24]. The other elements present in the biomass were Al (9.8 %), Mg (2.6 %), Cl (2.5 %), Na (1.5 %), S (1.3 %), and P (1.2 %). After extraction the biomass contained less carbon (34%) but more oxygen (45 %), while the contents of the other element remained almost the same.

The composition of the freeze-dried algal biomass before UE was analyzed in terms of its moisture, protein, crude lipid, ash, crude fiber, carbohydrate, and energy contents, which were determined to be 8%, 22.1%, 10.7%, 38.4%, 29.1%, 20.8% and 214.48 kcal, respectively. Hosseinizand et al. [24] reported that *Chlorella* contains 10.63% total lipids, 12% protein and 26.1% carbohydrate, while Phukan et al. [12] reported 9% carbohydrate, 43% protein and 28% lipids in *Chlorella* sp. Another study reported 10.7% lipid, 44.6% protein and 42.8% carbohydrate in *Chlorella* [48]. The algal biomass composition depends on the cultivation conditions and other complex factors and varies even within the same algal species. The extract from freeze-dried biomass in this work was similarly characterized and determined to contain protein, crude lipid, moisture, ash, total carbohydrate and energy of 5.2%, 42.7%, 35.2%, 10.3%, 6.7% and 431.7 kcal, respectively. Crude lipid formed the largest portion of the extract. Because of the composition of the biomass of *Chlorella* sp., consisting of carbohydrates, lipids, proteins and special other substances, the strain has the potential for use as a raw material for processing in biorefineries.

The concentrations of Chlorophyll a and b were 8.25 and 7.0 µg/ml, respectively in this study. The high amount of chlorophylls made the crude extract dark green in color, which would be a disadvantage in biodiesel production, since chlorophylls can

lower the quality of the biodiesel [49]. However, these chlorophylls can be separated from lipids by adding acid to form a solid precipitate [50] or three-phase partitioning (TPP) [51]. Chlorophylls have various applications in food, cosmetic, diagnostic, and pharmaceutical industries because of their non-toxic, non-carcinogenic nature and health-improving effects, such as their antioxidative and immune-boosting properties [52]. Therefore, the extraction of *Chlorella* sp. with the proposed conditions and system could also produce a high amount of chlorophylls along with a substantial LY. The separation and purification processes to extract chlorophylls should be further investigated.

A GC-FID profile of the extracted lipids is presented in Fig. 4.6 and major fatty acids found in the freeze-dried extract are shown in Table 4. Palmitic acid (C-16), which is a saturated fatty acid and palmitoleic acid (C-16:1), which is a monounsaturated fatty acid were the two major fatty acid constituents found. A greater amount of saturated fatty acids (34 %) were obtained over unsaturated fatty acids (23 %). The high proportion of saturated contents in the lipids from *Chlorella* sp. has been reported as indicating its usefulness as a good quality fuel agent. Biodiesel from palm oil which has a high saturated fatty acid content gives excellent combustion properties, such as a high cetane number and a high calorific value, even in cold conditions because of its high kinematic viscosity [53]. Biodiesel produced from triglycerides with a high level of monounsaturated fatty acids, e.g. rapeseed oil or olive pomace oil, presents the optimal characteristics in regard to chemical and physical properties [54]. In addition, from the analysis of exhaust and noise emissions of a three-cylinder direct-injection diesel engine operated with palm oil methyl esters (PME) and olive pomace oil methyl esters (OPME), PME blends showed the best performance. Therefore, suitable lipids for use as biodiesel feedstock should contain higher amounts of saturated fatty acids.

4.3.6 Energy consumption

The energy consumption was considered from pond cultivation through the lipid-extraction processes on an actual performance basis based on the cultivation in 25 m³ open pond, which yielded 20 kg wet biomass or 2.0 kg dry biomass. The results from the energy consumption analysis of the different processes are summarized in Table 4.5. For the 1-1-cycle process the energy consumption for wet-route extraction and dry-route extraction were 731 and 1,482 MJ/kg of dried biomass, respectively. In

wet-route extraction, the solvent recovery was found to be the biggest consumer of energy followed by UE. In dry-route extraction the energy consumed in freeze drying was highest followed by that for solvent recovery and UE. Ferreira et al. [55] reported a UE yield of 21% from the dried biomass of *Chlorella vulgaris* and the energy consumption including extraction and solvent recovery was 140 MJ/kg of dried biomass, which was 760 MJ/kg of lipids. In another study, 4 g of *Chlorella* sp. was disrupted by ultrasonication at 490 W for 6 minutes and the energy consumed was 44 MJ/kg dry biomass [29]. Halim et al. [56] disrupted *Chlorococcum* sp. by ultrasonication and reported an energy consumption for cell disruption of 132 MJ/kg dry biomass, whereas Adam et al. [57] reported the energy consumption for the UE of *Nannochloropsis* sp. as 360 MJ/kg of dried biomass. Hence, the calculated energy consumption for UE of 108 MJ/kg of dried biomass (wet route) and 162 MJ/kg dry biomass (dry route) fall within the range of values reported in the literature.

Although total energy consumed in dry-route extraction per dried biomass was more than double that for wet-route extraction, the total energy consumption per kg lipid was only 37% greater because of the higher LY obtained. Wet-route extraction is widely considered as being the cheaper process, but its economic viability is questionable in terms of biomass storage, product quality and quantity. As previously discussed a major problem with wet extraction is biomass storage and the storage cost for wet-route extraction should also be taken into account in any comparison with the cost of dry-route extraction, including the drying cost. In this study freeze drying was utilized, which represented the greatest use of energy among the dry route processes. While the use of freeze drying in lipid extraction for the food, cosmetic, diagnostic, and pharmaceutical industries is still recommended, for the extraction of lipids for biodiesel production, other drying methods should be considered.

For dry-route extraction the total energy consumption of the 2-1 and 2-2-cycle systems was 5,300 and 6,600 MJ/kg of lipids, resulting in LYs of 31 and 28%, respectively. The energy consumption per kg of lipids of the 2-2 process was higher than that of the 2-1 process and this was a result of lipid loss during the solvent recovery process. The product yield obtained using the 2-1-cycle system was 1.7 times higher than that of the 1-1 system, which entailed a lower energy consumption per kg of lipids. Hence, lipid extraction from freeze dried biomass using the 2-1-cycle is proposed as

being the most efficient process in terms of its product yield and energy consumption. The process recommended in the current study produced a remarkable performance. Its application in large-scale production is also feasible because industrial scale equipment is available, and implementation would likely result in lower costs and greater energy efficiency [57].

Conclusion

Fresh paste was suitable for lipid extraction with a 12% LY and the lowest energy consumption of the methods evaluated in this study, but the need to store biomass is a major disadvantage, as a 50% reduction in the total LY of wet paste was observed when the biomass was stored for one week. Freeze-dried biomass produced a higher LY than wet paste in the 1-1-cycle, but more energy was expended with the freeze-drying step. The difference in energy consumption between the wet and dry routes may, however, not be significant if the energy consumed for the storage of wet paste is taken into account. Freeze-dried biomass was preferable due to its ability to be stored for longer periods and its greater LY. The lipid yield achieved with the 2-1-cycle was 40.3% and 9.7% higher than the 1-1-cycle and 2-2-cycle, respectively. The 2-1-cycle UE using methanol/hexane (2/1 v/v) with a biomass to solvent ratio of 1/20 g/ml at 35 °C and 90 minutes with freeze-dried biomass are therefore proposed as being the optimum extraction conditions.

References

1. Dragone G, Fernandes B, Vicente A, Teixeira J (2010) Third generation biofuels from microalgae. *Curr Res Technol Educ Top Appl Microbiol Microb Biotechnol* 1355–1366 . doi: 10.1016/j.apenergy.2011.03.012
2. Chisti Y (2008) Biodiesel from microalgae beats bioethanol. *Trends Biotechnol* 26:126–131 . doi: 10.1016/j.tibtech.2007.12.002
3. Liu AY, Chen W, Zheng LL, Song LR (2011) Identification of high-lipid producers for biodiesel production from forty-three green algal isolates in China. *Prog Nat Sci Mater Int* 21:269–276 . doi: 10.1016/S1002-0071(12)60057-4
4. Nascimento IA, Marques SSI, Cabanelas ITD, et al (2013) Screening

- Microalgae Strains for Biodiesel Production: Lipid Productivity and Estimation of Fuel Quality Based on Fatty Acids Profiles as Selective Criteria. *Bioenergy Res.* doi: 10.1007/s12155-012-9222-2
5. Nascimento IA, Marques SSI, Cabanelas ITD, et al (2014) Microalgae Versus Land Crops as Feedstock for Biodiesel: Productivity, Quality, and Standard Compliance. *Bioenergy Res.* doi: 10.1007/s12155-014-9440-x
 6. Hussain J, Liu Y, Lopes WA, et al (2015) Effects of Different Biomass Drying and Lipid Extraction Methods on Algal Lipid Yield, Fatty Acid Profile, and Biodiesel Quality. *Appl Biochem Biotechnol* 175:3048–3057 . doi: 10.1007/s12010-015-1486-5
 7. Schenk PM, Thomas-Hall SR, Stephens E, et al (2008) Second Generation Biofuels: High-Efficiency Microalgae for Biodiesel Production. *BioEnergy Res.* doi: 10.1007/s12155-008-9008-8
 8. Quinn JC, Catton K, Wagner N, Bradley TH (2012) Current Large-Scale US Biofuel Potential from Microalgae Cultivated in Photobioreactors. *Bioenergy Res.* doi: 10.1007/s12155-011-9165-z
 9. Mata TM, Martins AA, Caetano NS (2010) Microalgae for biodiesel production and other applications: A review. *Renew Sustain Energy Rev* 14:217–232 . doi: 10.1016/j.rser.2009.07.020
 10. Mandik YI, Cheirsilp B, Boonsawang P, Prasertsan P (2015) Optimization of flocculation efficiency of lipid-rich marine *Chlorella* sp. biomass and evaluation of its composition in different cultivation modes. *Bioresour Technol* 182:89–97 . doi: 10.1016/j.biortech.2015.01.125
 11. Kelaiya S V, Chauhan PM, Akbari SH (2015) Fuel Property of Biodiesel Made from Microalgae (*Chlorella* sp.). *Curr World Environ* 10:912–919
 12. Phukan MM, Chutia RS, Konwar BK, Kataki R (2011) Microalgae *Chlorella* as a potential bio-energy feedstock. *Appl Energy* 88:3307–3312. doi: 10.1016/j.apenergy.2010.11.026

13. Kay RA, Barton LL (1991) Microalgae as Food and Supplement. *Crit Rev Food Sci Nutr* 30:555–573 . doi: 10.1080/10408399109527556
14. Paisan S, Chetpattananondh P, Chongkhong S (2017) Assessment of water degumming and acid degumming of mixed algal oil. *J Environ Chem Eng* 5:5115–5123 . doi: 10.1016/j.jece.2017.09.045
15. Uprety BK, Venkatesagowda B, Rakshit SK (2017) Current Prospects on Production of Microbial Lipid and Other Value-Added Products Using Crude Glycerol Obtained from Biodiesel Industries. *Bioenergy Res.*
16. Li YG, Xu L, Huang YM, et al (2011) Microalgal biodiesel in China: Opportunities and challenges. *Appl Energy*. doi: 10.1016/j.apenergy.2010.12.067
17. Sharma KK, Li Y, Schenk PM (2015) Rapid Lipid Induction in *Chlorella* sp. by UV-C Radiation. *Bioenergy Res.* doi: 10.1007/s12155-015-9633-y
18. Sanyano N, Chetpattananondh P, Chongkhong S (2013) Coagulation-flocculation of marine *Chlorella* sp. for biodiesel production. *Bioresour Technol* 147:471–476 . doi: 10.1016/j.biortech.2013.08.080
19. Bagchi SK, Rao PS, Mallick N (2015) Development of an oven drying protocol to improve biodiesel production for an indigenous chlorophycean microalga *Scenedesmus* sp. *Bioresour Technol* 180:207–213 . doi: 10.1016/j.biortech.2014.12.092
20. Konda NVSNM, Singh S, Simmons BA, Klein-Marcuschamer D (2015) An Investigation on the Economic Feasibility of Macroalgae as a Potential Feedstock for Biorefineries. *Bioenergy Res.* doi: 10.1007/s12155-015-9594-1
21. Lam MK, Lee KT (2012) Microalgae biofuels: A critical review of issues, problems and the way forward. *Biotechnol. Adv.*
22. Pang S, Mujumdar AS (2010) Drying of Woody Biomass for Bioenergy: Drying Technologies and Optimization for an Integrated Bioenergy Plant. *Dry*

- Technol 28:690–701 . doi: 10.1080/07373931003799236
23. Villagracia ARC, Mayol AP, Ubando AT, et al (2016) Microwave drying characteristics of microalgae (*Chlorella vulgaris*) for biofuel production. Clean Technol Environ Policy 18:2441–2451 . doi: 10.1007/s10098-016-1169-0
 24. Hosseinizand H, Sokhansanj S, Lim CJ (2017) Studying the drying mechanism of microalgae *Chlorella vulgaris* and the optimum drying temperature to preserve quality characteristics. Dry. Technol. 1–12
 25. Show KY, Lee DJ, Tay JH, et al (2015) Microalgal drying and cell disruption - Recent advances. Bioresour Technol 184:258–266 . doi: 10.1016/j.biortech.2014.10.139
 26. Chen P, Min M, Chen Y, et al (2009) Review of the biological and engineering aspects of algae to fuels approach. Int. J. Agric. Biol. Eng. 2:1–30
 27. Kadam KL (2002) Environmental implications of power generation via coal-microalgae cofiring. Energy 27:905–922 . doi: 10.1016/S0360-5442(02)00025-7
 28. Dong T, Knoshaug EP, Pienkos PT, Laurens LML (2016) Lipid recovery from wet *Oleaginous* microbial biomass for biofuel production: A critical review. Appl. Energy
 29. Martinez-Guerra E, Gude VG, Mondala A, et al (2014) Microwave and ultrasound enhanced extractive-transesterification of algal lipids. Appl Energy 129:354–363 . doi: 10.1016/j.apenergy.2014.04.112
 30. Lee JY, Yoo C, Jun SY, et al (2010) Comparison of several methods for effective lipid extraction from microalgae. Bioresour Technol 101:S75–S77 . doi: 10.1016/j.biortech.2009.03.058
 31. Prabakaran P, Ravindran AD (2011) A comparative study on effective cell disruption methods for lipid extraction from microalgae. Lett Appl Microbiol 53:150–154

32. Gerde JA, Montalbo-Lombay M, Yao L, et al (2012) Evaluation of microalgae cell disruption by ultrasonic treatment. *Bioresour Technol* 125:175–181 . doi: 10.1016/j.biortech.2012.08.110
33. Yang F, Xiang W, Sun X, et al (2014) A novel lipid extraction method from wet microalga *Picochlorum* sp. at room temperature. *Mar Drugs* 12:1258–1270 . doi: 10.3390/md12031258
34. Araujo GS, Matos LJBL, Fernandes JO, et al (2013) Extraction of lipids from microalgae by ultrasound application: Prospection of the optimal extraction method. *Ultrason Sonochem* 20:95–98 . doi: 10.1016/j.ultsonch.2012.07.027
35. Guldhe A, Singh B, Rawat I, et al (2014) Efficacy of drying and cell disruption techniques on lipid recovery from microalgae for biodiesel production. *Fuel* 128:46–52 . doi: 10.1016/j.fuel.2014.02.059
36. Mushtaq M, Sultana B, Bhatti HN, Asghar M (2015) RSM based optimized enzyme-assisted extraction of antioxidant phenolics from underutilized watermelon (*Citrullus lanatus* Thunb.) rind. *J Food Sci Technol*. doi: 10.1007/s13197-014-1562-9
37. Sweeney RA, Rexroad PR (1986) Comparison of LECO FP-228 “nitrogen determinator” with AOAC copper catalyst Kjeldahl method for crude protein. *J Assoc Off Anal Chem* 70:1028–30
38. Sumanta N, Haque CI, Nishika J, Suprakash R (2014) Spectrophotometric Analysis of Chlorophylls and Carotenoids from Commonly Grown Fern Species by Using Various Extracting Solvents. *Res J Chem Sci Res J Chem Sci* 4:2231–606
39. Ali M, Watson I a. (2015) Microwave treatment of wet algal paste for enhanced solvent extraction of lipids for biodiesel production. *Renew Energy* 76:470–477 . doi: 10.1016/j.renene.2014.11.024
40. Zheng H, Yin J, Gao Z, et al (2011) Disruption of *Chlorella vulgaris* cells for the release of biodiesel-producing lipids: A comparison of grinding,

- ultrasonication, bead milling, enzymatic lysis, and microwaves. *Appl Biochem Biotechnol* 164:1215–1224 . doi: 10.1007/s12010-011-9207-1
41. Balasubramanian RK, Yen Doan TT, Obbard JP (2013) Factors affecting cellular lipid extraction from marine microalgae. *Chem Eng J* 215–216:929–936 . doi: 10.1016/j.cej.2012.11.063
 42. Taher H, Al-Zuhair S, Al-Marzouqi AH, et al (2014) Effective extraction of microalgae lipids from wet biomass for biodiesel production. *Biomass and Bioenergy* 66:159–167 . doi: 10.1016/j.biombioe.2014.02.034
 43. Lee AK, Lewis DM, Ashman PJ (2012) Disruption of microalgal cells for the extraction of lipids for biofuels: Processes and specific energy requirements. *Biomass and Bioenergy* 46:89–101 . doi: 10.1016/j.biombioe.2012.06.034
 44. Chen L, Liu T, Zhang W, et al (2012) Biodiesel production from algae oil high in free fatty acids by two-step catalytic conversion. *Bioresour Technol*. doi: 10.1016/j.biortech.2012.02.033
 45. Wu J, Alam MA, Pan Y, et al (2017) Enhanced extraction of lipids from microalgae with eco-friendly mixture of methanol and ethyl acetate for biodiesel production. *J Taiwan Inst Chem Eng* 71:323–329 . doi: 10.1016/j.jtice.2016.12.039
 46. Orr VCA, Plechkova N V., Seddon KR, Rehm L (2016) Disruption and Wet Extraction of the Microalgae *Chlorella vulgaris* Using Room-Temperature Ionic Liquids. *ACS Sustain Chem Eng* 4:591–600 . doi: 10.1021/acssuschemeng.5b00967
 47. Bligh EG, Dyer WJ (1959) A RAPID METHOD OF TOTAL LIPID EXTRACTION AND PURIFICATION. *Can J Biochem Physiol* 37:911–917 . doi: 10.1139/o59-099
 48. Reddy HK, Muppaneni T, Ponnusamy S, et al (2016) Temperature effect on hydrothermal liquefaction of *Nannochloropsis gaditana* and *Chlorella* sp. *Appl Energy*. doi: 10.1016/j.apenergy.2015.11.067

49. Moser BR (2009) Biodiesel production, properties, and feedstocks. *Vitr Cell Dev Biol - Plant*. doi: 10.1007/s11627-009-9204-z
50. Sathish A, Sims RC (2012) Biodiesel from mixed culture algae via a wet lipid extraction procedure. *Bioresour Technol* 118:643–647 . doi: 10.1016/j.biortech.2012.05.118
51. Zhao W, Duan M, Zhang X, Tan T (2018) A mild extraction and separation procedure of polysaccharide, lipid, chlorophyll and protein from *Chlorella* spp. *Renew Energy*. doi: 10.1016/j.renene.2017.11.046
52. Chakdar H, Pabbi S (2017) Algal Pigments for Human Health and Cosmeceuticals. In: *Algal Green Chemistry: Recent Progress in Biotechnology*
53. Redel-Macías MD, Pinzi S, Ruz MF, et al (2012) Biodiesel from saturated and monounsaturated fatty acid methyl esters and their influence over noise and air pollution. *Fuel*. doi: 10.1016/j.fuel.2012.01.070
54. Pinzi S, Leiva D, Arzamendi G, et al (2011) Multiple response optimization of vegetable oils fatty acid composition to improve biodiesel physical properties. *Bioresour Technol*. doi: 10.1016/j.biortech.2011.05.005
55. Ferreira AF, Dias APS, Silva CM, Costa M (2016) Effect of low frequency ultrasound on microalgae solvent extraction: Analysis of products, energy consumption and emissions. *Algal Res* 14:9–16 . doi: 10.1016/j.algal.2015.12.015
56. Halim R, Harun R, Danquah MK, Webley PA (2012) Microalgal cell disruption for biofuel development. *Appl Energy* 91:116–121 . doi: 10.1016/j.apenergy.2011.08.048
57. Adam F, Abert-Vian M, Peltier G, Chemat F (2012) “Solvent-free” ultrasound-assisted extraction of lipids from fresh microalgae cells: A green, clean and scalable process. *Bioresour Technol* 114:457–465 . doi: 10.1016/j.biortech.2012.02.096

Figure Captions

Figure. 4.1 Experimental process schematic diagram

Figure. 4.2 Extraction and solvent recovery systems, 1-1-cycle, 2-1-cycle and 2-2-cycle

Figure. 4.3 3-D surface plots presenting the effect of temperature and time on lipid yield of (a) wet-route UE and (b) dry-route UE

Figure. 4.4 Impact on lipid yield of (a) biomass to solvent ratio, (b) solvent system, (c) extraction and solvent recovery cycle scheme, and (d) solvent ratio

Figure. 4.5 SEM images (Left: 2000 X, 20.0 kV and 20 μm ; Right: 10,000 X, 20.0 kV and 5 μm) of freeze-dried biomass before and after ultrasonication at the optimum conditions.

Figure. 4.6 GC-FID profile of the extracted lipids from freeze-dried biomass at 35°C for 90 min. using methanol/hexane 2/1 (v/v) with B/S 1/20 (g/ml) by the 2-1-cycle scheme

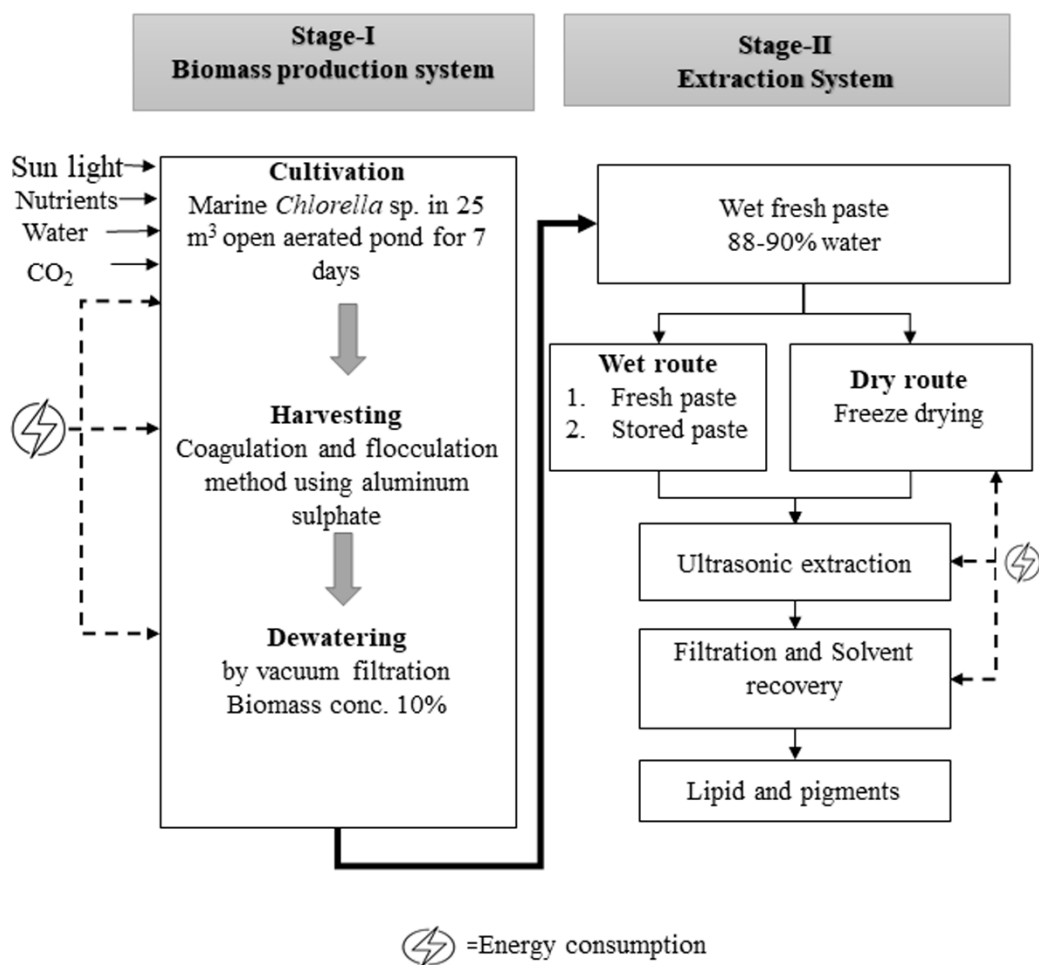


Figure 4.1 Experimental process schematic diagram

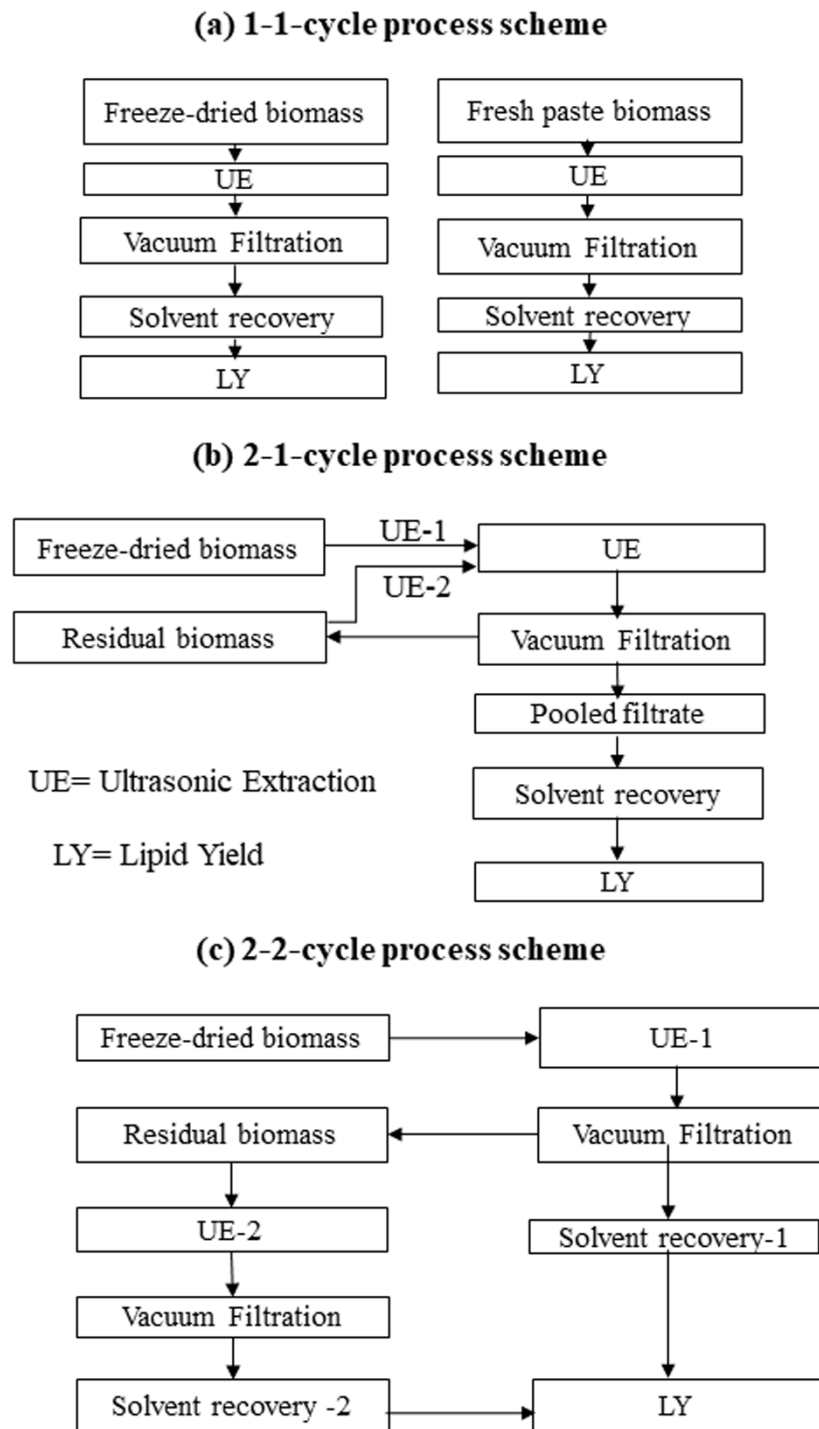


Figure 4.2 Extraction and solvent recovery systems, 1-1-cycle, 2-1-cycle and 2-2-cycle

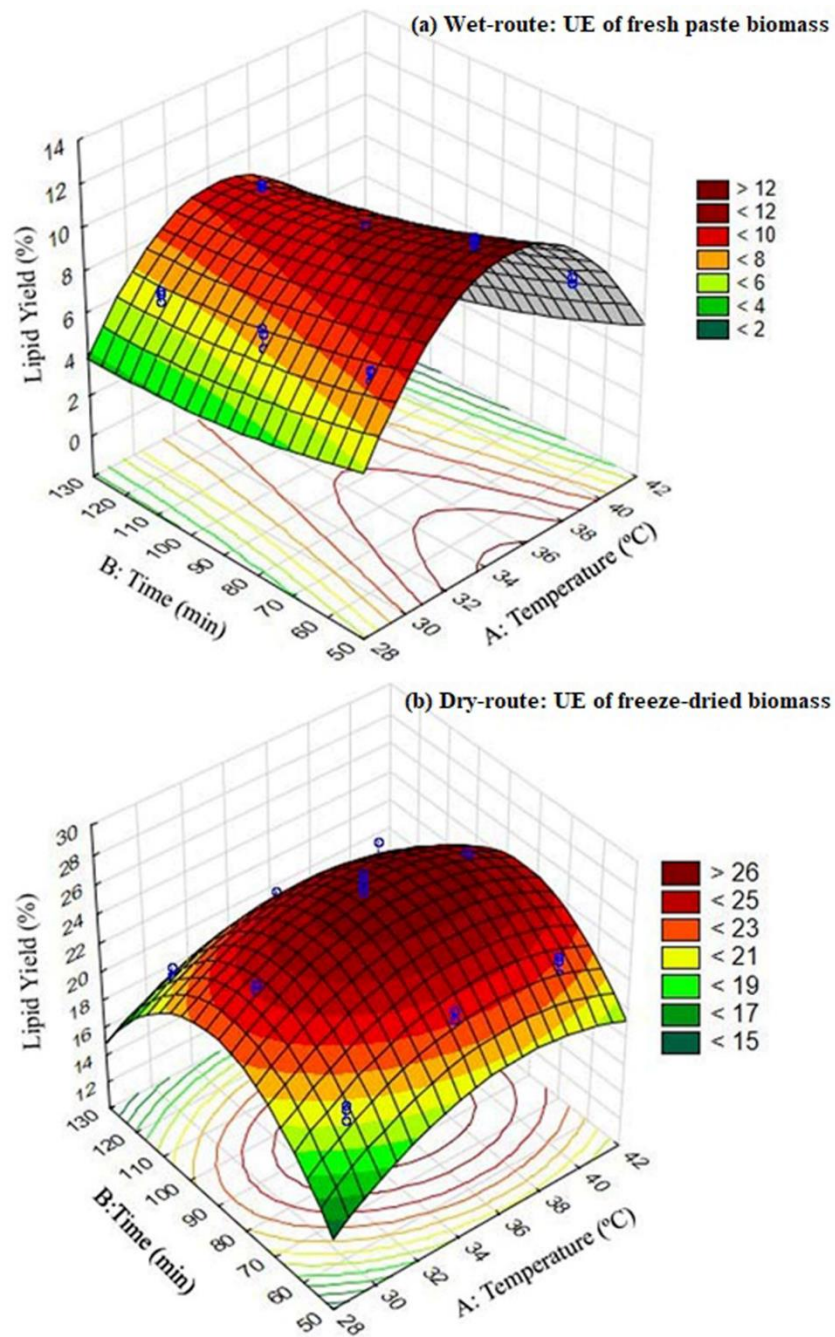


Figure 4.3 3-D surface plots presenting the effect of temperature and time on lipid yield of (a) wet-route UE and (b) dry-route UE

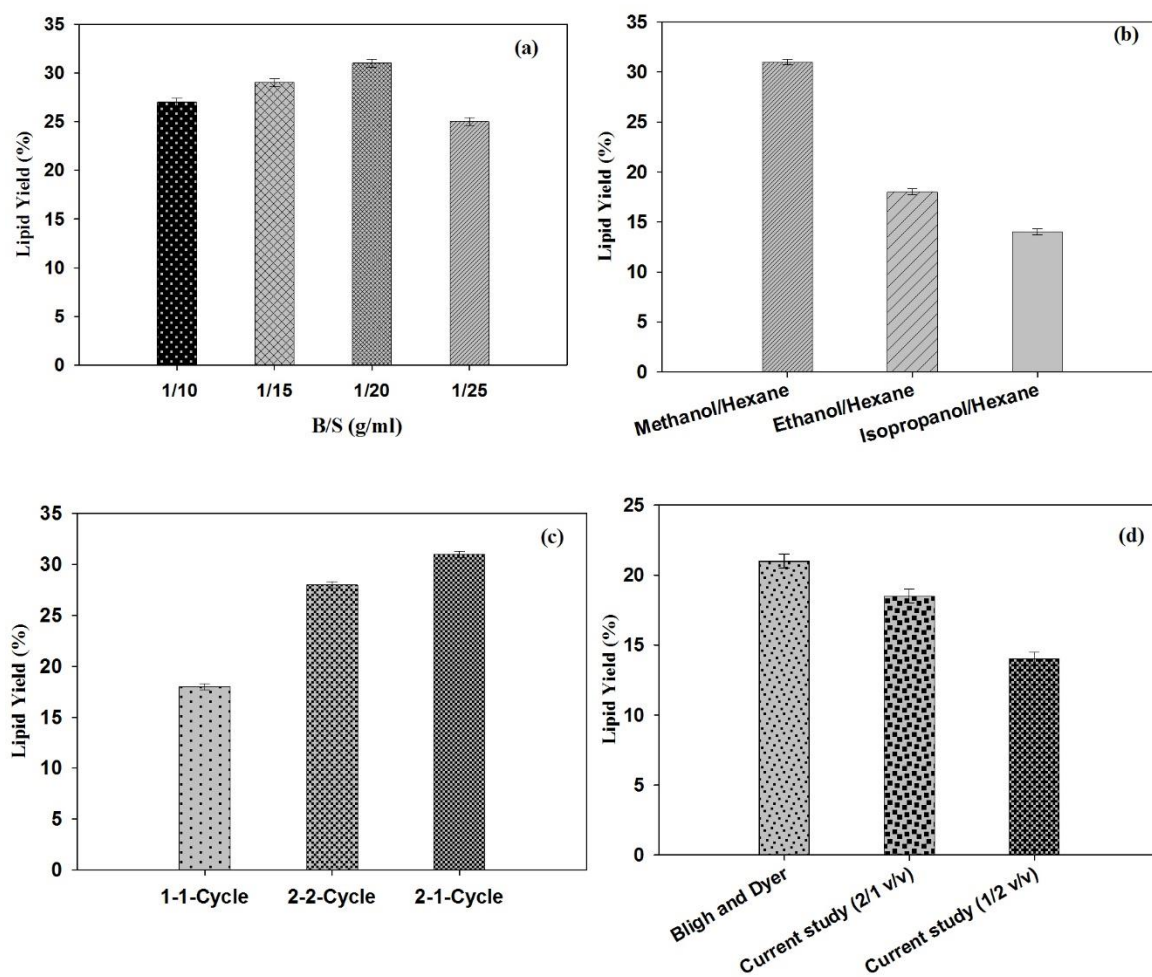
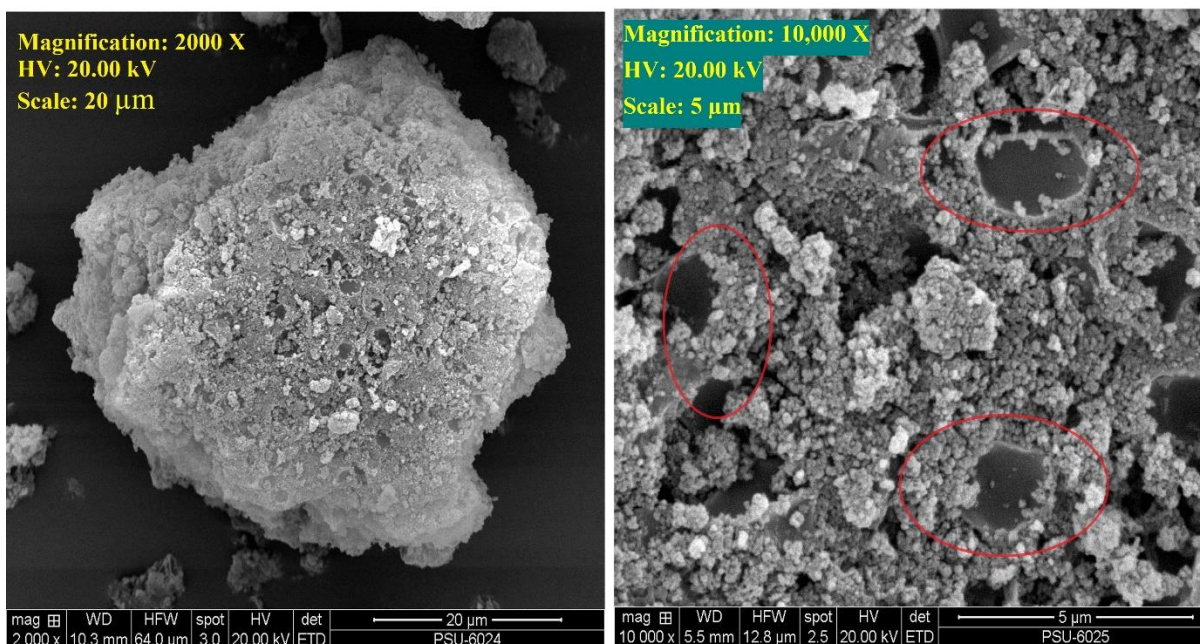


Figure 4.4 Impact on lipid yield of (a) biomass to solvent ratio, (b) solvent system, (c) extraction and solvent recovery cycle scheme, and (d) solvent ratio

Before Ultrasonic Effect



After Ultrasonic Effect

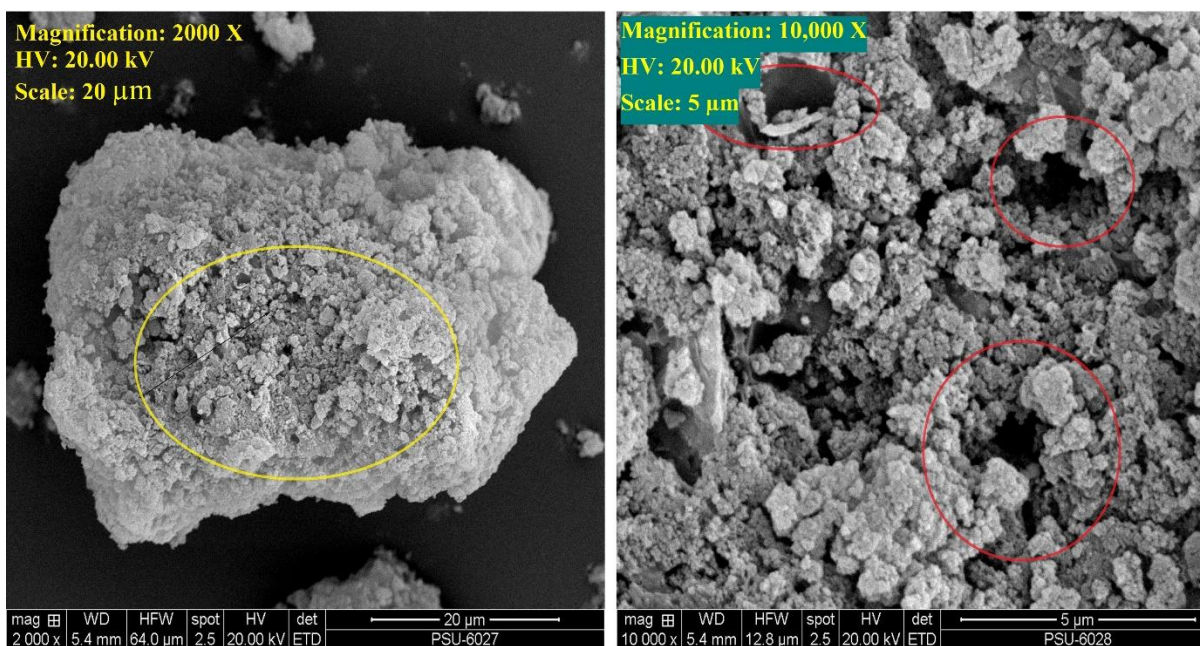


Figure 4.5 SEM images (Left: 2000 X, 20.0 kV and 20 μ m; Right: 10,000 X, 20.0 kV and 5 μ m) of freeze-dried biomass before and after ultrasonication at the optimum conditions.

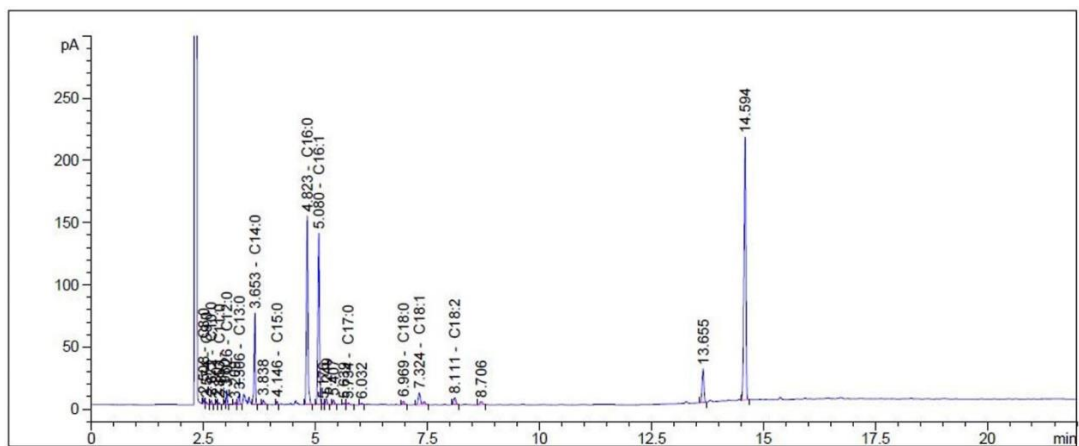


Figure 4.6 GC-FID profile of the extracted lipids from freeze-dried biomass at 35°C for 90 min. using methanol/hexane 2/1 (v/v) with B/S 1/20 (g/ml) by the 2-1-cycle scheme

Table 4.1 The experimental and model predicted responses for the UE of fresh wet paste and freeze-dried biomass

R ^a	Run	Factors		Fresh paste extraction			Freeze-dried extraction		
		Temperature (X ₁)	Time (X ₂)	Observed	Predicted	Residual	Observed	Predicted	Residual
R-1	1	30 (-1)	60 (-1)	8.50	8.48	0.02	20.00	20.43	-0.43
	2	30 (-1)	90 (0)	7.80	7.30	0.50	23.80	24.22	-0.42
	3	30 (-1)	120 (1)	6.80	6.71	0.09	20.50	19.80	0.70
	4	35 (0)	60 (-1)	11.50	11.62	-0.12	22.60	23.36	-0.76
	5	35 (0)	90 (0)	9.70	10.14	-0.44	27.30	26.64	0.66
	6	35 (0)	120 (1)	8.90	9.25	-0.35	21.50	21.69	-0.19
	7	40 (1)	60 (-1)	8.20	8.02	0.18	23.20	22.90	0.30
	8	40 (1)	90 (0)	6.00	6.24	-0.24	25.00	25.66	-0.66
	9	40 (1)	120 (1)	5.20	5.05	0.15	22.00	20.20	1.80
R-2	10	30 (-1)	60 (-1)	8.60	8.48	0.12	20.80	20.43	0.37
	11	30 (-1)	90 (0)	6.90	7.30	-0.40	23.30	24.22	-0.92
	12	30 (-1)	120 (1)	6.40	6.71	-0.31	19.90	19.80	0.10
	13	35 (0)	60 (-1)	12.10	11.62	0.48	23.60	23.36	0.24
	14	35 (0)	90 (0)	9.80	10.14	-0.34	28.00	26.64	1.36
	15	35 (0)	120 (1)	9.50	9.25	0.25	20.20	21.69	-1.49
	16	40 (1)	60 (-1)	7.90	8.02	-0.12	22.30	22.90	-0.60
	17	40 (1)	90 (0)	6.70	6.24	0.46	25.40	25.66	-0.26
	18	40 (1)	120 (1)	5.00	5.05	-0.05	20.00	20.20	-0.20
R-3	19	30 (-1)	60 (-1)	8.10	8.48	-0.38	21.10	20.43	0.67
	20	30 (-1)	90 (0)	7.50	7.30	0.20	24.20	24.22	-0.02
	21	30 (-1)	120 (1)	6.90	6.71	0.19	19.80	19.80	-0.00
	22	35 (0)	60 (-1)	11.90	11.62	0.28	23.00	23.36	-0.36
	23	35 (0)	90 (0)	10.10	10.14	-0.04	26.80	26.64	0.16
	24	35 (0)	120 (1)	9.60	9.25	0.35	22.10	21.69	0.41
	25	40 (1)	60 (-1)	7.60	8.02	-0.42	23.50	22.90	0.60
	26	40 (1)	90 (0)	6.60	6.24	0.36	25.80	25.66	0.14
	27	40 (1)	120 (1)	4.80	5.05	-0.25	19.10	20.20	-1.10

^a Replicates

Table 4.2 Analysis of variance (ANOVA) for UE of fresh wet paste and freeze-dried biomass

Source	Wet Route UE						Dry Route UE					
	SS	DF	MS	F	p	**	SS	DF	MS	F	p	**
Temperature (X_1)	5.0	1	5.0	50	0.00001	Yes	9.2	1	9.2	16.7	0.0006	Yes
Time (X_2)	25.2	1	25.2	251	0.0000	Yes	12.5	1	12.5	22.5	0.00015	Yes
X_1^2	68.2	1	68.2	679	0.0000	Yes	17.2	1	17.2	31.1	0.00002	Yes
X_2^2	0.5	1	0.5	5.1	0.035	Yes	101.4	1	101.4	183.1	0.0000	Yes
X_1X_2	1.0	1	1.0	10.7	0.004	Yes	3.2	1	3.2	5.7	0.027	Yes
Model	100	5	20	200	0.0001	Yes	143.5	5	28.7	52.1	0.0001	Yes
Lack of fit	0.6	3	0.2	1.9	0.15	NO	3.68	3	1.2	2.2	0.12	NO
Pure error	1.8	18	0.10				9.96	18	0.55			
Total	102	26					157	26				
	R²	R²	R²	SD	C.V %		R²	R²	R²	SD	C.V %	
	Adjusted	Predicted					Adjusted	Predicted				
	0.97	0.97	0.96	0.34	4.17		0.91	0.90	0.85	0.81	3.54	

** : Significance; SS=Sum of Square; MS=Mean Square; DF=Degree of Freedom; SD=Standard deviation; CV=Coefficient of variation

Table 4.3 Regression coefficients of the models for UE of fresh wet paste and freeze-dried biomass

		Fresh paste extraction		Freeze-dried extraction	
Coefficients		Value	p-value	Value	p-value
b ₀	Intercept	10.14	0.000001	26.64	0.00001
b ₁	X ₁	-0.52	0.000001	0.71	0.0007
b ₂	X ₂	-1.18	0.00000	-0.83	0.00015
b ₃	X ₁ ²	-3.37	0.00000	-1.69	0.000002
b ₄	X ₂ ²	0.29	0.035	-4.11	0.0000
b ₅	X ₁ X ₂	-0.30	0.004	-0.51	0.027

Table 4.4 Fatty Acid Methyl Esters of marine *Chlorella* sp extracted lipid

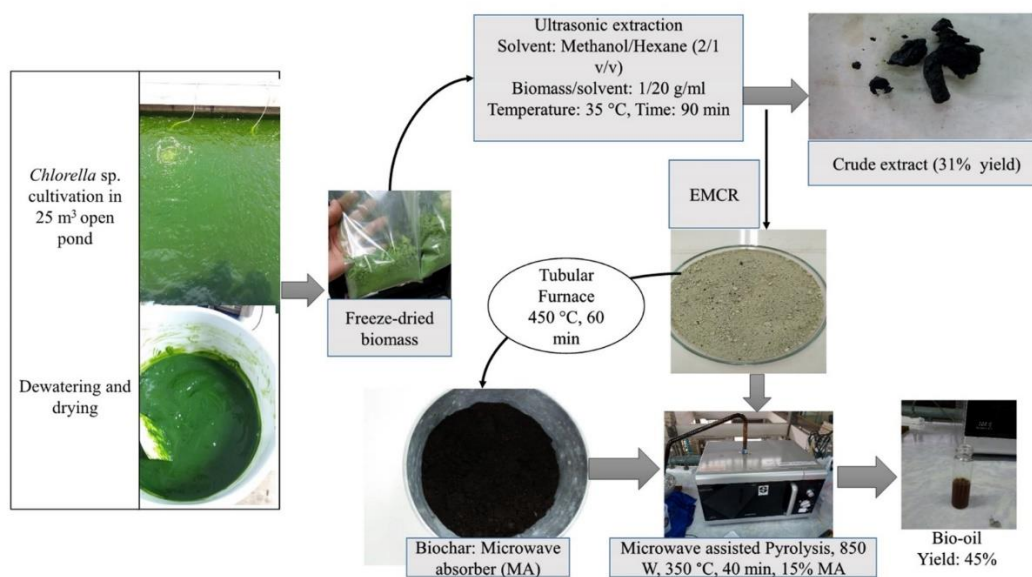
No	Fatty Acid Methyl Esters		Area %
1	Caprylic acid	C8:0	0.45
2	Nonanoic acid	C9:0	0.22
3	Capric acid	C10:0	0.42
4	Undecanoic acid	C11:0	0.14
5	Lauric acid	C12:0	1.07
6	Tridecanoic acid	C13:0	0.98
7	Myristic acid	C14:0	8.36
8	Pentadecanoic acid	C15:0	0.32
9	Palmitic acid	C16:0	21.43
10	Palmitoleic acid	C16:1	19.10
11	Heptadecanoic acid	C17:0	0.26
12	Stearic acid	C18:0	0.53
13	Oleic acid	C18:1	2.35
14	Linoleic acid	C18:2	1.27
15	Linolenic acid	C18:3	n.d
16	Arachidic acid	C20:0	n.d
17	Eicosenoic acid	C20:1	n.d
18	Behenic acid	C22:0	n.d
19	Erucic acid	C22:1	n.d
20	Lignoceric acid	C24:0	n.d
21	Selacholeic acid	C24:1	n.d [#]

[#] n.d = not detected

Table 4.5 Energy consumption of processes at lab-scale for wet and dry routes

Processes	Wet Route		Dry Route	
	(MJ)		(MJ)	
	1-1-Cycle	1-1-Cycle	2-1-Cycle	2-2-Cycle
Cultivation	1.05	1.05	1.05	1.05
Harvesting	0.02	0.02	0.02	0.02
Dewatering	13	13	13	13
Freeze drying	-	1,080	1,080	1,080
Ultrasonic extraction	108	162	324	324
Filtration	21	16.70	16.70	33.4
Solvent recovery	588	210	210	420
Total energy consumption	731	1,482	1,645	1,870
(MJ/kg dry biomass)				
Lipid (g)/kg biomass (% dry basis)	120	180	310	280
Lipid (g)/g biomass (% dry basis)	0.12	0.18	0.31	0.28
Energy consumed (MJ/kg lipid)	6,000	8,200	5,300	6,600

CHAPTER 5

Application of extracted marine *Chlorella* sp. residue for bio-oil production as the biomass feedstock and microwave absorber

Highlights

- EMCR was subjected to pyrolysis for biochar and bio-oil production
- EMCR derived biochar has high surface area due to ultrasonication extraction effect
- EMCR derived biochar was the first time introduced as a microwave absorber
- RSM based on CCD was used to optimize the condition for maximum bio-oil yield
- Bio-oil is suitable to be synthesized for valuable chemicals rather than as a fuel

Application of extracted marine *Chlorella* sp. residue for bio-oil production as the biomass feedstock and microwave absorber

Muhammad Amin, Pakamas Chetpattananondh^{*}, Sukritthira Ratanawilai

Department of Chemical Engineering Faculty of Engineering, Prince of Songkla University, 90110, Hat Yai, Songkhla, Thailand.

^{*}Corresponding author email: pakamas.p@psu.ac.th (Pakamas Chetpattananondh)

Abstract

The extracted marine *Chlorella* sp. residue (EMCR) was used as a feedstock for biochar and bio-oil production. The biochar was prepared by slow pyrolysis at 450 °C for 60 min in a tube furnace and employed as a microwave absorber (MA). The bio-oil was produced by microwave pyrolysis (MWP) with investigation of temperature (350-450 °C), time (20-40 min) and MA loading (10-30 wt.%) at fixed microwave power of 850 W. The pyrolysis condition was optimized to obtain maximum bio-oil yield using the Response Surface Methodology (RSM) based on Central Composite Design (CCD). The optimum condition was 350 °C, 15% MA loading and 40 min, which yielded 46% bio-oil. Characterization of *Chlorella* sp. biomass, EMCR, biochar and bio-oil was performed by proximate and ultimate analysis, FTIR, TGA and GC-MS. The higher heating values of biomass, EMCR and biochar were 22.43, 15.49 and 10.79 MJ/kg, respectively. The results showed a high feasibility of applying EMCR as the feedstock for biochar and bio-oil production. The EMCR derived biochar presented great efficiency as the MA with high surface area of 266 m²/g. The bio-oil consisted of a mixture of chemicals, which requires further processes before using in many applications.

Keywords: *Chlorella* residue; Microwave pyrolysis; Microwave absorber; Bio-oil; Biochar

5.1 Introduction

Algal biomass is known to be the third generation and promising bioenergy feedstock due to its higher oil production capacity among other crops [1], which makes them highly attractive and sustainable choice [2-4]. Marine *Chlorella* sp. has shown its potential for biodiesel production. However, the biodiesel production from this strain

and other algal species is still facing commercialization challenge due to high processing cost [4-5]. In perspectives of biodiesel production from microalgae at larger scale, a huge amount of extracted biomass known as algal residue will be generated. Utilization of this algal residue to derive valuable products is environmentally beneficial and could offset the algal biodiesel cost [6-9].

The algal waste can be converted into valuable products by thermochemical or biochemical process. However, thermochemical is better choice due to its capability to recover energy and chemical value of any kind of biomass [10]. Pyrolysis, a thermochemical process is of great interest now a day since the product quality and selectivity for suitable end use could be easily controlled by regulating the process parameters [11-12]. The most common techniques are fixed bed pyrolysis and microwave pyrolysis (MWP). Later one has gained more focus in recent years due to fast, even and selective heating, easy control, low temperature and energy efficient characteristics [13-15]. In microwave pyrolysis process, biomass is thermally degraded at moderate temperature 300-600 °C in oxygen depleted environment to obtain bio-oil, gas and char. The proportion of these pyrolytic products are strongly dependent on feedstock type and operating conditions [16-18]. Bio-oil is considered to be very promising source for fuel, power, heat and intermediate valuable chemicals [18-19]. It is a complex mixture of organic compounds, mainly composed of phenols, acids, esters, aromatics etc. while, the percent share of these compounds varies among the biomass type and pyrolysis operating conditions. Generally, bio-oil is produced from lignocellulosic materials and algal biomass is shown its potential for bio-oil production. However, the bio-oil composition of both feedstocks are not similar due to their different composition. The lignocellulosic biomass is mainly composed of cellulose, hemicellulose and lignin while algal biomass is normally composed of proteins, carbohydrates and lipids without lignin [20].

There is limited information for bio-oil production from algal biomass, especially from algal residue. Ferrera et al. studied the microwave pyrolysis operated at 750 °C for 60 min by using 6 g of *Gelidium* residue and obtained 35 wt.% bio-oil yield, which mainly composed of pyrroles, phenols and benzene compounds [21]. Another study reported 29 wt.% yield of bio-oil containing carbonyls, nitrogenous and

hydrocarbon compounds from lipid extracted *Tribonema minus* at 450 °C pyrolyzed for 60 min [17]. The study of Wang et al. achieved 53 wt.% bio-oil from defatted *Chlorella vulgaris*, which was thermally degraded at 500 °C in fluidized bed reactor [22]. As extracted biomass of some algal species were applied as the bio-oil feedstocks, so potential of extracted marine *Chlorella* sp. residue (EMCR) is investigated in this study.

Some biomass feedstocks are low energy absorber and could not achieve the desired temperature subjected to sufficient amount of microwave energy. Microwave absorbers (MA) have tendency to convert the received microwave energy into thermal energy and transfer it to biomass. Generally, the solid carbon based materials are good choice to be introduced as MA with biomass to attain the desired process condition [14,23,24]. Ferrera et al. [21] reported that algal meals were highly transparent to microwave energy and thus needed to be mixed with suitable MA. In their study, 6 g of char from wasted *Gelidium* was intimately mixed with biomass, which yielded 35 wt.% oil. Mushtaq et al. [13] studied 35-75 wt.% of coconut activated carbon as the MA for pyrolysis of palm shell waste and reported 45 wt.% MA loading as an optimum to obtain 32% bio-oil yield. They also suggested that uniform distribution of microwave absorber over biomass surface improved the product yield and process performance. Moreover, MA were developed from other biomaterials [13,14,25]. In this work bio-char is developed from EMCR and applied as the MA for the first time.

This study is therefore aimed to (1) study the characterization of *Chlorella* sp. biomass, EMCR, and EMCR derived biochar, (2) apply EMCR as biomass feedstock and EMCR derived biochar as microwave absorber for bio-oil production by microwave pyrolysis, (3) optimize the operating variables including temperature, time and MA loading to obtain maximum bio-oil yield using RSM-CCD and (4) study the chemical composition of bio-oil.

5.2 Materials and methodology

5.2.1 Feedstock preparation

The biomass of marine *Chlorella* sp. was acquired from National Institute of Coastal Aquaculture (NICA) located in Songkhla province (latitude: 7.178861° N, 100.624561° E), Thailand. Briefly, microalgal biomass was cultivated in 25 m³ open pond using CO (NH₂)₂ and 16-16-16 fertilizer (16% nitrogen, 16% phosphorus, and 16% potassium). It was harvested by flocculation using aluminum sulfate as a

flocculent agent, vacuum filtered using GENVAC Agilent Technologies pump (PVL 35, 930 Watt) and freeze-dried using Dura-Dry MP (FTS systems, USA, 4400 Watt). The Freeze-dried algal biomass was extracted using methanol/hexane (2/1 v/v) at 35 °C for 90 min by ultrasonication using an ultrasonic bath (CP 2600 Crest Power sonic, USA, 45 kHz, 300 Watt), which yielded 31% (dry wt.) crude extract. The ultrasonic extraction is a proven highly efficient algal extraction technique. The ultrasound cracks the cell wall by the generation of a cavitation effect due to shock waves and the collapsing of bubbles enhances the extraction process. The extraction using ultrasonic bath provided higher lipid yield in shorter extraction time compared to the conventional extraction with Soxhlet apparatus from previous study. The extracted algal residue was collected, washed with deionized water water to normalize the pH and vacuum filtered. The filtered EMCR was dried in hot air oven at 105 °C for 24 hours, placed in desiccator and its weight was recorded until constant. Approximately 500 g of EMCR was obtained. It was kept in air tight bags and stored at room temperature.

A portion of prepared EMCR (100 g) was used to produce biochar via slow pyrolysis (10 °C /min) in a laboratory scale stainless steel tube furnace under N₂ flushed environment at 450 °C for 60 min. The raw biochar was collected from furnace chamber after attaining the room temperature, cleaned with DI water and oven dried at 105 °C for 3 hours. The prepared biochar was sieved to a particle size of 0.4 mm, kept in zip lock bags, stored at room temperature and applied as a microwave absorber. The overall processing scheme of experimental investigation is illustrated in Fig. 5.1.

5.2.2 Characterization of materials

Proximate analysis of marine *Chlorella* sp., EMCR and biochar was performed based on ASTM E871 for moisture content, ASTM E872-82 for volatile matter, and ASTM D1102-84 for ash [26]. Briefly, the moisture content was determined by weight loss at 105 °C for 4 h. The volatile matter was discarded in an electric furnace operated at 900 °C for 7 minutes with an inert atmosphere. The ash was then evaluated as percentage of residual mass after heating in the furnace at 815 °C for 1 h in the presence of oxygen. The fixed carbon was determined by difference method as shown in Eq. (5.1).

$$\text{Fixed carbon} = 100 - \text{moisture} - \text{ash} - \text{volatile matters} \quad (5.1)$$

Analysis of C, H, N and S was carried out by dynamic flash combustion technique using CHNS/O analyzer (Flash 2000, Thermo Scientific, Italy) where O content was calculated by difference on an ash free dry basis. The surface functional groups of *Chlorella* sp., EMCR and biochar were identified using pellet KBr technique by Fourier Transformed Infrared Spectrometer (FTIR, VERTEX 70, Bruker, Germany) recorded within 400-4000 cm^{-1} wavenumber. Thermo-decomposition of organic matter under pyrolysis of EMCR was characterized by heating 5 mg sample from 25 to 1000 °C at 10 °C/min using thermogravimetric analysis (TGA) by simultaneous Thermal Analyzer, STA8000, perkin Elmer, USA. A pore volume, pore diameter and surface area of biochar were determined by degassing the sample for 6 hours and using static volumetric N_2 gas adsorption technique via BET technique using ASAP2460 Surface area and porosity analyzer, Micromeritics, USA.

5.2.3 Microwave pyrolysis

The microwave pyrolysis experiments were conducted in modified TDS SAMSUNG microwave oven rated with maximum output power capacity of 1,000 W operated at 2.54 GHz. The microwave pyrolysis (MWP) unit is consisted of a modified microwave oven, quartz glass, two 250-ml flasks for bio-oil and trap collection, vacuum system, water cooling circulation system, glass condensers, ice bath, and biomass holder as presented in Fig. 5.2. Infrared optical pyrometer was used to measure the temperature of biomass, while the bio-oil temperature was monitored by inserting the thermometer at one neck of the flask. The vacuum system was used to drive off the volatiles through condensing unit. N_2 is generally used as a carrier gas in a pyrolysis system, but Beneroso et al. [27] stated that use of carrier gas has no significant influence on the product yield and composition. In this study applying vacuum without feeding N_2 gas is feasible and economic. Tap water (5-7 °C) was constantly counter currently circulated in condensers and iced bath was provided around the collecting flasks to keep the bio-oil temperature about 2-5 °C.

10 g of EMCR was placed in biomass holder, followed by uniform distribution of appropriate quantity of biochar as the microwave absorber over the biomass surface. Biomass holding plate was placed in the microwave oven and glass tubes were assembled. These glass tubes were covered with aluminum foil to prevent the heat losses. Microwave oven, water circulation and vacuum system were turned on and

microwave power was set at a desired level. The rise in temperature was monitored with 1-minute interval until reaching the desired temperature. The biomass was annealed for specified duration at the desired temperature according to the experimental design conditions. When the experiment was completed the system was switched off and cooled down for 2-3 hours. The bio-oil sample was collected and its yield was determined gravimetrically.

The microwave power was fixed at 850 W as it is sufficient for complete pyrolysis from the preliminary experiments. The effect of studied parameters including temperature, time and MA loading on bio-oil yield was investigated. Response Surface Methodology (RSM) based on Central Composite Design (CCD) was used to evaluate the effect and optimized the bio-oil yield. The second order quadratic polynomial model was developed to study the response variable and its validation. The experimental runs could be calculated according to Eq. (5.2), while distance (α) between center point and axial point could be calculated using Eq. (5.3).

$$N=2k+2^k+M \quad (5.2)$$

$$\alpha=(2k)^{0.25} \quad (5.3)$$

Where N is number of experimental runs, k is numbers of factors to be evaluated and M is number of center points to be included.

The effect of three parameters including temperature (350-450 °C), time (20-40 minutes) and MA loading (10-30 wt.%) on bio-oil yield was designed at five levels. The factors were designated as X_1 (temperature), X_2 (time), and X_3 (MA loading) and levels were coded into star low ($-\alpha$), low (-1), center (0), high (+1), and star high ($+\alpha$). For three variables ($k=3$) and 6 center point tests the total number of 20 runs were required to be executed with axial point distance of 1.68. The experimental conditions presented in Table 5.1 are grouped into two blocks. Block-1 has total 9 runs (6 factorials and 3 center points), while block-2 is handling an 11 runs in total (8 axial points and 3 center points). The experimental data of CCD were fitted to a second-order polynomial model as shown in Eq. (5.4) to correlate the relationship between the influencing variables and the response variable.

$$Y = \beta_o + \sum_{i=1}^k B_i X_i + \sum_{i=1}^k B_{ii} X_i^2 + \sum_{i>j}^k B_{ij} X_i X_j \quad (5.4)$$

Where Y is the response and β_0 , β_i , β_{ii} , and β_{ij} are the linear, quadratic and interaction terms of the model. The response was further transformed into a dimensionless “desirability” scale covering values 0-1 (or 0-100 %), in which 0 shows a completely undesirable experimental design and 1 indicates a fully desirable design.

STATISTICA version 10.0 was performed by a standard least square method for experimental design and regression model analysis of bio-oil yield. The CCD-RSM model results were analyzed statistically and graphically. The good fitness of the predicted model was determined by the coefficient of determination R^2 value. Data were analyzed by the analysis of variance (ANOVA) and the p-value lower than 0.05 was considered significant.

5.2.4 GC-MS analysis of bio-oil

The chemical composition of EMCR derived bio-oil was analyzed using Agilent Technologies CP-9205 gas chromatograph (GC) with VF-WAX MS capillary column (30 m \times 250 μ m \times 0.25 μ m). GC oven temperature was raised from 70 to 250 °C at the rate of 5 °C/min and held constant for 10 minutes at the final temperature. 1 μ l of bio-oil sample and 3 ml/min helium used as a carrier gas were injected into the column. The GC was interconnected with a mass selective detector spectroscopy system (MSD 5977, Agilent Technologies, USA), which was operated in normal data acquisition scan mode. The mass spectroscopy was conducted in full scanning range (50-550) at emission current of 34.5 μ A, while ionization energy was recorded as 70 eV. The peak identification for chemical compound was performed using the National Institute of Standards and Technology (NIST) library with Agilent Chemstation software [13].

5.3 Results and Discussion

5.3.1 Proximate and ultimate analysis

Table 5.2 illustrates the proximate and ultimate analysis of marine *Chlorella* sp., EMCR and biochar. The moisture contents of the three samples were observed below 10 wt.%, which is considered good for safe storage. The volatile matter (VM), fixed carbon (FC) and ash are crucial in fuel characterization. A high content of VM promotes combustible gasses and bio-oil generation during thermal conversion. FC is necessary for conversion of biomass into liquid fuels. A high ash amount may induce problems in thermal conversion from fouling of slag formation [28]. The fixed carbon

of marine *Chlorella* sp. in this study is lower than many biomass fuels reported in Table 2 and study of De Jong and Van Ommen [29] with FC = 14.5-87.7%, but still higher than greenhouse residue (FC = 5.5%), meat and bone meal (FC = 12.4%), and sewage sludge (FC = 4.7%). High ash content is recognized for marine *Chlorella* sp. Algae generally have much higher ash than terrestrial biomass as they have different composition, organic structure and rapid metabolism which take up much more nutrients during cultivations. The ash contents are in the range of 0.1-46.3% (mean 6.8%) for terrestrial biomass and 13.1-42.8% (mean 26.6%) for algae [30]. After extraction (presented as EMCR) and slow pyrolysis (presented as biochar) the reduction of volatile matters and fixed carbon contents were observed, while the ash contents were increased. Liu et al. [31] also reported that after partial oil extraction the residual biomass of *Hapalosiphon* sp. and *Botryococcus braunii* had lower FC and higher ash than the original biomass, while VM was the same for *Hapalosiphon* sp. and a little bit lower for residual biomass of *B. Braunii*.

Ultimate analysis is performed to understand the beneficial effects of using the microalgae as a biofuel feedstock. In addition, the gross calorific value of the biofuel can be calculated from the elemental contents of carbon, hydrogen, and oxygen. The marine *Chlorella* sp. consists of 40.74% carbon, 11.11% hydrogen, 5.74% nitrogen, 1.66% sulfur and 40.75% oxygen. The C, H, N contents in EMCR and biochar are lower, while oxygen is higher than their precursor. The decreasing of elemental carbon from raw material through its derivative is due to lipid extraction. Francavilla et al. [32] studied pyrolysis of *Dunaliella tertiolecta* and its residue and reported reduction of carbon in residue and biochar because of lipid extraction. The algal biomass and its derivative have lower carbon than lignocellulosic biomass due to higher ash and nitrogen contents [33]. The high nitrogen in algal biomass is from the cultivation condition, while in the extracted residue is from unconverted protein [34]. The CHNS contents of different algal species including their residues and biochar from the literature are also given in Table 2. The C, H and N were observed in the range of 11-60-68.5%, 0.70-9.70% and 1.32-12.85%, respectively. The CHN contents of marine *Chlorella* sp., EMCR and biochar are in these ranges, while hydrogen is slightly higher attributed to different processing conditions. The higher heating values (HHVs, MJ/kg) of marine *Chlorella* sp., EMCR, and biochar were 22.43, 15.49 and 10.79 MJ/kg,

respectively. The HHV of marine *Chlorella* sp. is greater than many algal species and similar to *C. vulgaris* and *Chlorella* reported by other works. In addition, the HHVs of EMCR and biochar are comparable to some residues and biochar from the literature, however lower than those from *C. vulgaris* and *Chlorella* sp. The HHV is strongly influenced by the elemental composition and respective H/C and O/C ratios. The HHV increases with increasing of H/C or decreasing of O/C [32,34].

The surface area, pore volume and pore diameter of biochar were 266 m²/g, 0.61 m³/g and 92.85 Å, respectively. The surface area of biochar prepared in this work is higher than the biochar prepared by other algal species and carbonaceous materials [35,36,37,38]. The high surface area obtained in this work is attributed to combined effects of ultrasonication (during cell wall disruption for lipid extraction) and pyrolysis (EMCR to biochar) processes. Salema and Ani [39] worked on MW pyrolysis of oil palm biomass using palm shell char as microwave absorber. They reported that BET surface area (150 m²/g) of the char played an important role in absorbing the microwave energy.

5.3.2 FTIR analysis

The FTIR spectra of marine *Chlorella*, EMCR and biochar are shown in Fig. 5.3 (a-c). The identification of peaks is based on Coates [40]. It could be observed that some peaks of raw biomass were disappeared in the EMCR and biochar due to lipid extraction and pyrolysis, respectively. Mayur et al. [8] stated that the CH₂ stretching vibrations in the region 3100-2800 cm⁻¹ signified the presence of lipids and the region 1800-800 cm⁻¹ is corresponded to proteins and carbohydrates. The increase of the bands at 3100-2800 cm⁻¹ and 1800-800 cm⁻¹ observed in EMCR compared to *Chlorella* sp. confirmed the leaching of lipids, proteins and carbohydrates from extraction process. The peaks disappeared in the biochar were due to the release of volatiles because of high temperature applied in pyrolysis. This is in agreement with decreasing of VM of biochar in the proximate analysis. The three biomass consisted of high O-functional groups while N-functional groups were reduced in biochar. The N containing functional groups were due to the presence of unconverted proteins, which further accumulate as N compounds (amine, amides and nitriles) on decomposition in pyrolysis process [34]. High O and N functional groups presented in the biomass if still exist in bio-oil will

lower its quality for fuel application. The aromatic ring stretch is particularly presented in *Chlorella* sp. (1459 cm^{-1}) and biochar (1461 cm^{-1}). The peaks 1411 cm^{-1} in *Chlorella* sp. and 1407.8 cm^{-1} in EMCR are assigned to vinyl C-H of alkene group or phenol or tertiary alcohol. The peak at 1250 cm^{-1} in *Chlorella* sp. is aromatic primary amine (CN stretch), while the peak at 1238 cm^{-1} in EMCR is aromatic ethers (Aryl-O stretch). The peaks around $1093\text{-}1058\text{ cm}^{-1}$ are due to C-O stretching vibration of alkyl substituted ether. The two peaks at 875 and 839 cm^{-1} in *Chlorella* sp. could be 1-4 substitution of C-H aromatic ring group or nitrate ions, while the peak at 693 cm^{-1} is due to thiol C-S stretch. The peaks in the range $500\text{-}600\text{ cm}^{-1}$ are associated with aliphatic iodo compounds (C-I stretch).

5.3.3 Thermogravimetric analysis of EMCR

The thermal decomposition behavior of EMCR under pyrolysis was studied using TGA to measure the mass loss as a function of temperature and presented as TG plot in Fig. 5.3 (d). Its derivative with respect to temperature was derived from the derivative of thermogravimetric (DTG) plot. The TG profile of EMCR presented the three stages including dehydration, devolatilization, and solid decomposition during pyrolysis. The first weight loss for moisture content was shown at the temperatures $25\text{-}150\text{ }^{\circ}\text{C}$. The decomposition was mainly occurred in the second stage ($150\text{-}500\text{ }^{\circ}\text{C}$) and referred to as the zone of active pyrolysis. It was associated with the thermal degradation of volatile components with a maximum weight loss between temperatures 340 and $360\text{ }^{\circ}\text{C}$. The minimal weight loss at a slow rate was observed at the last stage from around $600\text{-}900\text{ }^{\circ}\text{C}$. The peak in DTG plot appeared around $340\text{ }^{\circ}\text{C}$ with its peak shoulder lasts around $410\text{ }^{\circ}\text{C}$, indicating that the greatest volatile matter was released and maximum bio-oil yield was gain. As the Microwave Thermal Analyzer is not available the TGA data were used as a guideline for microwave pyrolysis temperature. Therefore, the pyrolysis of EMCR was designed to carry out in the temperature range $350\text{-}450\text{ }^{\circ}\text{C}$. In addition, the decomposition of EMCR is comparable to many biomass sources reported by Chaiwong et al. [41] as the temperature at the maximum bio-oil yield is similar ($346\text{ }^{\circ}\text{C}$ for corncob and $377\text{ }^{\circ}\text{C}$ for palm shell).

5.3.4 Microwave pyrolysis optimization

The bio-oil production by microwave pyrolysis of EMCR with biochar derived from EMCR as the microwave absorber was optimized using RSM with CCD approach.

The actual values and the predicted values of the RSM model are given in Table 1. The R^2 value of 0.96 is satisfied for a good relationship between the actual and the model data. The different of adjusted R^2 and predicted R^2 is less than 0.2, which is in reasonable agreement [15]. The Coefficient of Variation (C.V.) of 5.0%, which is lower than 10% is a good indicator for reproducibility of the investigated model. The non-significant Lack of fit F-value as shown in Table 5.3 from ANOVA confirms the reliable and accurate of the proposed model. The high F-value of 37.43 represents that the model is significant. The variables in terms of linear and quadratic relationships are significant with p-value less than 0.05. The interactive relationship between variables is significant for temperature and time only. The equation developed for the bio-oil yield prediction is shown as Eq. (5.5) where X_1 , X_2 and X_3 are the coded values.

$$\begin{aligned} \text{Bio-oil yield (wt.\%)} = & 40.99 - 6.34X_1 + 1.19X_2 - 3.19X_3 - 3.36X_1^2 - 1.98X_2^2 \\ & - 3.10X_3^2 - 1.60X_1X_2 + 0.55X_1X_3 - 1.22X_2X_3 \end{aligned} \quad (5.5)$$

The 3-D response surface plots were generated to better visualize the process variable effects on bio-oil yield and are shown in Fig. 5.4. It can be seen that temperature, time and MA loading have effects on bio-oil yield. With 15% MA loading (Fig. 5.4a) the bio-oil increased with temperature from 300 to 350 °C and time from 10 to 40 min. Fig. 5.4b presents the combined effects of temperature and MA loading for fixed time at 40 min and Fig. 5.4c shows the combine effects of MA loading and time for fixed temperature at 350 °C. The increase of bio-oil yield with increasing temperature is owing to the devolatilization, depolymerisation, and decarboxylation. Moreover, they were explained as: (1) more energy was involved in the chemical reactions with increment of pyrolysis temperature and (2) more strong organic bonds in the biomass were cracked and more volatiles were liberated to construct condensable gases for bio-oil components [42]. However, when the pyrolysis temperature was above 350°C the bio-oil yield decreased as greater temperature preferred the development of non-condensable combustible gases more than liquid products.

The maximum bio-oil yield was observed at 350 °C, 15% MA loading and 40 min. The critical parameters suggested by the model were also the same. The greatest effects on bio-oil yield is from linear and quadratic terms of temperature with lowest p-

values (Table 5.3). In addition, the temperature 350 °C is in agreement with the TGA peak of EMCR. The production of bio-oil was then performed at this optimum condition. The average maximum actual bio-oil yield was 46%, while the predicted value was 45.8% with 95 % desirability. Below or above the optimal point the desirability value decreased. Several studies investigated the impact of pyrolysis conditions on bio-oil yields for different biomaterials and suggested different optimum conditions. Compared with the conventional heating pyrolysis, microwave pyrolysis causes the feedstock to decompose at lower temperatures resulting in more bio-oil yield. Optimum pyrolysis temperatures are in the range of 350 [43] – 800 [42] °C depended on the biomass and parameters used. The pyrolysis time is also important parameter. Long time provided a complete pyrolysis and more volatiles were released from the biomass to form bio-oil components. On the other hand, pyrolysis for too long decreased the bio-oil yield because the condensable vapors (bio-oil components) were disintegrated by secondary reactions to create non-condensable combustible gases (syngas components) in the high pyrolysis temperatures. The wide range pyrolysis times from 6 [42] to 60 [17] min were reported. The pyrolysis time of 40 minute in this study is in agreement with the MWP of oil palm shell waste biomass with coconut activated carbon (CAC) as the microwave absorber, which yielded 31.70 % bio-oil at the optimum condition of 490 W, 45.05% CAC loading and 4.9 l/min of N₂ [13]. The optimal temperature of 350 °C in this study is lower than report of Du et al. [44] for MWP of *Chlorella* sp. at the optimum condition of 750 W, 570 °C, 20 min, 20% activated carbon as the MA and 0.5 l/min of N₂ to obtain 28.6% bio-oil yield.

The MA loading played an important role to optimize the bio-oil yield. From our further experiments addition of MA reduced the time required to achieve the final pyrolysis temperature. With 15% MA loading at the optimum condition the final temperature of 350 °C was obtained within 15 min, whereas more than 30 min was required without MA. In addition, the bio-oil yield by performing pyrolysis at the optimum condition without MA was about 5% lower than applying 15% MA. Decrease of bio-oil yield with MA loading higher than 15% could be attribution of low energy transfer into biomass layer due to hindrance by increasing MA thickness. This resistance leaded to incomplete thermal degradation of biomass and resulted in low bio-oil yield. Mushtaq et al. [13] studied the effect of MA (activated carbon) on bio-oil

yield and found that non uniform distribution of MA caused uneven heat distribution and high absorber loading could possibly hinder the heat transfer rate. Therefore, minimum MA loading should be determined as thick absorber layer is not an economical choice.

The moisture content in a biomass could increase its microwave absorbance leading to higher bio-oil yield. However, the bio-oil would contain high aqueous fraction. The positive effects of moisture content on the pyrolysis is confined due to its evaporation during the process. A feedstock with low moisture content is then favored for MWP [42]. EMCR as the pyrolysis feedstock in this study consisted of 7% moisture content, which is considered low enough to obtain good bio-oil yield. The ash content of a biomass also has impacts on the MWP as the ash components (Al_2O_3 , CaO , Fe_2O_3 , K_2O , MgO , MnO , MnO_2 , Na_2O , TiO_2 , etc.) are normally good microwave absorbents promoting the heating rates and maximum pyrolysis temperatures accompanied by high bio-oil yield [45]. The biochar applied as the MA in this study had 56% ash content, which is good for MWP. Nonetheless, since the ash components cannot be transformed to bio-oil, too high ash content in biomass may decrease the overall bio-oil yield [42]. The ash content of 43% in EMCR used as the biomass feedstock seems all right for MWP.

Moreover, the MWP also produced biochar with 42% yield at the optimum condition. However, the biochar derived from MWP contained higher ash content (66%) resulted to lower amount of carbon compared to the biochar derived from the conventional pyrolysis (prepared by slow pyrolysis at 450 °C and a heating rate of 10 °C/min for 60 min in a tube furnace under N_2 flushed environment, which yield 45% biochar). This can be obvious seen from Fig. 5.5. Therefore, the biochar derived from the conventional pyrolysis is considered more suitable to be used as the microwave absorber.

5.3.5 GC-MS analysis of bio-oil

The composition of bio-oil obtained at the optimized condition was characterized by GC-MS and is listed in Table 5.4. The compounds are classified in the groups of amines/amides/indoles (30.37%), phenols (17.64%), esters (17.62%), acids (12.18%), furans and aromatics (5.56%), alcohols (6.07%), ketones/aldehydes/ethers (2.88%), sugars (2.30%), alkenes (0.5%) and others (4.88%). The high proportion of

nitrogenated hydrocarbons confirmed that bio-oil from EMCR consisted of high nitrogen compounds, which was generally reported in bio-oil derived from algae. The nitrogen is from proteins in algal biomass. The bio-oil with high nitrogen is not good for fuel application as nitrogen oxides and soot can be generated from the combustion leading to air pollution. The solution is to remove proteins from EMCR prior to pyrolysis. These proteins can be high valuable products for food and pharma applications.

Esters were also found with both methyl and ethyl esters and little portion of alkenes were incorporated. The bio-oil derived from EMCR composed of large amount of organic compounds including phenols, acids, aldehydes and ketones, which is not suitable for fuel application without upgrading. The requirement of upgrading is also widely stated for the bio-oils from other feedstocks. However, bio-oil can also be a highly valuable feedstock for the production of green chemicals, which are able to replace the conventional fuel based products [46]. Phenols, which were high in the produced bio-oil can be extracted with liquid-liquid extraction and used as raw materials for developing bio-based antioxidants, resin and additives [47]. Acids presented in the bio-oil can be converted to esters. It is feasible to produce specialty chemicals by extraction or reactions of bio-oil, e.g., surfactants, biodegradable polymers, preservatives, liquid smoke, resin precursors, adhesives, additives in fertilising and pharmaceutical industries, flavouring agents in food industries, etc [48]. The bio-oil quality upgrading and economic analysis are required for further investigation.

Conclusion

The HHV of marine *Chlorella* sp. is greater than many algal species, while the HHVs of EMCR and biochar are comparable to some residues and biochars from the literature. The surface area of EMCR derived biochar is 266 m²/g, which is high compared to biochars from many feedstocks. This high surface area is due to combined effects of ultrasonication extraction and pyrolysis processes. The biochar was applied as the microwave absorber (MA) in the microwave pyrolysis of EMCR. Addition of MA reduced the time required to achieve the final pyrolysis temperature and provided higher bio-oil yield. The high ash content (56%) in the biochar is considered good for

microwave absorbent. Maximum bio-oil yield was obtained at 850 W, 350 °C, 15% microwave absorber loading, and 40 minutes. The bio-oil composed of a complex mixture of amines, amides, indoles, phenols, esters, acids, furans, aromatics, alcohol, ketone, aldehydes, ethers, sugar, and alkenes. The high nitrogen in bio-oil could be reduced by protein extraction from EMCR before pyrolysis. The bio-oil is required to be upgraded before using in fuel applications. In addition, various valuable chemicals could be derived to be used in many industries. Therefore, the application of marine *Chlorella* sp. is widely extended in this study. The biomass can be extracted for lipids, pigments and other compounds and its residue (EMCR) showed a great potential for conversion to both biochar and bio-oil. These integrated processes are greatly beneficial with management and economic of a large-scale algal biofuel industry.

Acknowledgment

The National Institute of Coastal Aquaculture (Thailand) is gratefully acknowledged for providing marine *Chlorella* sp. This research was financially supported via Grant no. ENG580582M by Prince of Songkla University and Thailand's Education Hub for Southern Region of ASEAN Countries (TEH-AC, 56/2016) granted by the Graduate School, Prince of Songkla University (PSU), Hat Yai, Songkhla, Thailand. We are thankful to Department of Chemical Engineering, Faculty of Engineering, PSU for providing all facilities and supporting staffs to accomplish this work.

References

- [1] Chen L, Yu Z, Fang S, Dai M, Ma X. Co-pyrolysis kinetics and behaviors of kitchen waste and *Chlorella vulgaris* using thermogravimetric analyzer and fixed bed reactor. *Energy Convers Manag* 2018. doi:10.1016/j.enconman.2018.03.042.
- [2] Chisti Y. Biodiesel from microalgae beats bioethanol. *Trends Biotechnol* 2008;26:126–31. doi:10.1016/j.tibtech.2007.12.002.
- [3] Paisan S, Chetpattananondh P, Chongkhong S. Assessment of water degumming and acid degumming of mixed algal oil. *J Environ Chem Eng* 2017;5:5115–23. doi:10.1016/j.jece.2017.09.045.
- [4] Sanyano N, Chetpattananondh P, Chongkhong S. Coagulation-flocculation of

- marine *Chlorella* sp. for biodiesel production. *Bioresour Technol* 2013;147:471–6. doi:10.1016/j.biortech.2013.08.080.
- [5] Phukan MM, Chutia RS, Konwar BK, Kataki R. Microalgae *Chlorella* as a potential bio-energy feedstock. *Appl Energy* 2011;88:3307–12. doi:10.1016/j.apenergy.2010.11.026.
- [6] Rashid N, Ur Rehman MS, Sadiq M, Mahmood T, Han JI. Current status, issues and developments in microalgae derived biodiesel production. *Renew Sustain Energy Rev* 2014;40:760–78. doi:10.1016/j.rser.2014.07.104.
- [7] Bui HH, Tran KQ, Chen WH. Pyrolysis of microalgae residues - A Kinetic study. *Bioresour Technol* 2015. doi:10.1016/j.biortech.2015.08.069.
- [8] Maurya R, Paliwal C, Ghosh T, Pancha I, Chokshi K, Mitra M, et al. Applications of de-oiled microalgal biomass towards development of sustainable biorefinery. *Bioresour Technol* 2016. doi:10.1016/j.biortech.2016.04.115.
- [9] Gao MT, Shimamura T, Ishida N, Takahashi H. Investigation of utilization of the algal biomass residue after oil extraction to lower the total production cost of biodiesel. *J Biosci Bioeng* 2012. doi:10.1016/j.jbiosc.2012.04.002.
- [10] Guo F, Wang X, Yang X. Potential pyrolysis pathway assessment for microalgae-based aviation fuel based on energy conversion efficiency and life cycle. *Energy Convers Manag* 2017. doi:10.1016/j.enconman.2016.11.020.
- [11] Chutia RS, Kataki R, Bhaskar T. Characterization of liquid and solid product from pyrolysis of *Pongamia glabra* deoiled cake. *Bioresour Technol* 2014. doi:10.1016/j.biortech.2014.03.118.
- [12] Bordoloi N, Narzari R, Sut D, Saikia R, Chutia RS, Kataki R. Characterization of bio-oil and its sub-fractions from pyrolysis of *Scenedesmus dimorphus*. *Renew Energy* 2016. doi:10.1016/j.renene.2016.03.081.
- [13] Mushtaq F, Abdullah TAT, Mat R, Ani FN. Optimization and characterization of bio-oil produced by microwave assisted pyrolysis of oil palm shell waste biomass with microwave absorber. *Bioresour Technol* 2015. doi:10.1016/j.biortech.2015.02.055.
- [14] Mushtaq F, Mat R, Ani FN. A review on microwave assisted pyrolysis of coal and biomass for fuel production. *Renew Sustain Energy Rev* 2014.

- doi:10.1016/j.rser.2014.07.073.
- [15] Arafat Hossain M, Ganesan P, Jewaratnam J, Chinna K. Optimization of process parameters for microwave pyrolysis of oil palm fiber (OPF) for hydrogen and biochar production. *Energy Convers Manag* 2017. doi:10.1016/j.enconman.2016.10.046.
- [16] Maguyon MCC, Capareda SC. Evaluating the effects of temperature on pressurized pyrolysis of *Nannochloropsis oculata* based on products yields and characteristics. *Energy Convers Manag* 2013. doi:10.1016/j.enconman.2013.08.033.
- [17] Ji X, Liu B, Chen G, Ma W. The pyrolysis of lipid-extracted residue of *Tribonema minus* in a fixed-bed reactor. *J Anal Appl Pyrolysis* 2015. doi:10.1016/j.jaap.2015.09.006.
- [18] Aboulkas A, Hammani H, El Achaby M, Bilal E, Barakat A, El harfi K. Valorization of algal waste via pyrolysis in a fixed-bed reactor: Production and characterization of bio-oil and bio-char. *Bioresour Technol* 2017. doi:10.1016/j.biortech.2017.06.098.
- [19] Wang S, Wang Q, Jiang X, Han X, Ji H. Compositional analysis of bio-oil derived from pyrolysis of seaweed. *Energy Convers Manag* 2013. doi:10.1016/j.enconman.2013.01.014.
- [20] Casoni AI, Zunino J, Piccolo MC, Volpe MA. Valorization of *Rhizoclonium* sp. algae via pyrolysis and catalytic pyrolysis. *Bioresour Technol* 2016. doi:10.1016/j.biortech.2016.05.066.
- [21] Ferrera-Lorenzo N, Fuente E, Bermúdez JM, Suárez-Ruiz I, Ruiz B, Bermudez JM, et al. Conventional and microwave pyrolysis of a macroalgae waste from the Agar–Agar industry. Prospects for bio-fuel production. *Bioresour Technol* 2014. doi:http://dx.doi.org/10.1016/j.biortech.2013.10.047.
- [22] Wang K, Brown RC, Homsy S, Martinez L, Sidhu SS. Fast pyrolysis of microalgae remnants in a fluidized bed reactor for bio-oil and biochar production. *Bioresour Technol* 2013;127:494–9. doi:10.1016/j.biortech.2012.08.016.
- [23] Wang N, Tahmasebi A, Yu J, Xu J, Huang F, Mamaeva A. A Comparative study of microwave-induced pyrolysis of lignocellulosic and algal biomass.

- Bioresour Technol 2015. doi:10.1016/j.biortech.2015.04.038.
- [24] Bu Q, Lei H, Ren S, Wang L, Zhang Q, Tang J, et al. Production of phenols and biofuels by catalytic microwave pyrolysis of lignocellulosic biomass. Bioresour Technol 2012. doi:10.1016/j.biortech.2011.12.125.
- [25] Mushtaq F, Mat R, Ani FN. Fuel production from microwave assisted pyrolysis of coal with carbon surfaces. Energy Convers Manag 2016. doi:10.1016/j.enconman.2015.12.008.
- [26] Bae YJ, Ryu C, Jeon JK, Park J, Suh DJ, Suh YW, et al. The characteristics of bio-oil produced from the pyrolysis of three marine macroalgae. Bioresour Technol 2011. doi:10.1016/j.biortech.2010.11.023.
- [27] Beneroso D, Bermúdez JM, Arenillas A, Menéndez JA. Influence of carrier gas on microwave-induced pyrolysis. J Anal Appl Pyrolysis 2015. doi:10.1016/j.jaap.2014.12.005.
- [28] Haugstad BH. Fuel characterization and process analysis of hydrothermal liquefaction of algae. 2017.
- [29] De Jong W, Van Ommen JR. Biomass as a sustainable energy source for the future: Fundamentals of conversion processes. 2014. doi:10.1002/9781118916643.
- [30] Vassilev S V., Vassileva CG. Composition, properties and challenges of algae biomass for biofuel application: An overview. Fuel 2016. doi:10.1016/j.fuel.2016.04.106.
- [31] Liu YQ, Lim LRX, Wang J, Yan R, Mahakhant A. Investigation on pyrolysis of microalgae *Botryococcus braunii* and *Hapalosiphon* sp. Ind Eng Chem Res 2012. doi:10.1021/ie202799e.
- [32] Francavilla M, Kamaterou P, Intini S, Monteleone M, Zabaniotou A. Cascading microalgae biorefinery: Fast pyrolysis of *Dunaliella tertiolecta* lipid extracted-residue. Algal Res 2015. doi:10.1016/j.algal.2015.06.017.
- [33] Bird MI, Wurster CM, de Paula Silva PH, Bass AM, de Nys R. Algal biochar - production and properties. Bioresour Technol 2011. doi:10.1016/j.biortech.2010.07.106.
- [34] Kim SS, Ly HV, Kim J, Lee EY, Woo HC. Pyrolysis of microalgae residual biomass derived from *Dunaliella tertiolecta* after lipid extraction and

- carbohydrate saccharification. Chem Eng J 2015.
doi:10.1016/j.cej.2014.11.045.
- [35] Han Y, Cao X, Ouyang X, Sohi SP, Chen J. Adsorption kinetics of magnetic biochar derived from peanut hull on removal of Cr (VI) from aqueous solution: Effects of production conditions and particle size. Chemosphere 2016.
doi:10.1016/j.chemosphere.2015.11.050.
- [36] Roberts DA, Paul NA, Dworjanyn SA, Bird MI, De Nys R. Biochar from commercially cultivated seaweed for soil amelioration. Sci Rep 2015.
doi:10.1038/srep09665.
- [37] Chen Y di, Lin YC, Ho SH, Zhou Y, Ren N qi. Highly efficient adsorption of dyes by biochar derived from pigments-extracted macroalgae pyrolyzed at different temperature. Bioresour Technol 2018.
doi:10.1016/j.biortech.2018.02.094.
- [38] Nautiyal P, Subramanian KA, Dastidar MG. Adsorptive removal of dye using biochar derived from residual algae after in-situ transesterification: Alternate use of waste of biodiesel industry. J Environ Manage 2016.
doi:10.1016/j.jenvman.2016.07.063.
- [39] Salema AA, Ani FN. Pyrolysis of oil palm biomass using palm shell char as microwave absorber. J Oil Palm Res 2008;24:1497–512.
- [40] Coates J. Interpretation of infrared spectra, A practical approach. Encycl Anal Chem 2006:10815–37. doi:10.1002/9780470027318.a5606.
- [41] Chaiwong K, Kiatsiriroat T, Vorayos N, Thararax C. Study of bio-oil and bio-char production from algae by slow pyrolysis. Biomass and Bioenergy 2013.
doi:10.1016/j.biombioe.2013.05.035.
- [42] Zhang Y, Chen P, Zhou N, Anderson E, Fan L, Li B, et al. Microwave-assisted pyrolysis of biomass for bio-oil production. Pyrolysis, 2017.
doi:10.5772/67442.
- [43] Ly HV, Kim SS, Choi JH, Woo HC, Kim J. Fast pyrolysis of *Saccharina japonica* alga in a fixed-bed reactor for bio-oil production. Energy Convers Manag 2016. doi:10.1016/j.enconman.2016.06.019.
- [44] Du Z, Li Y, Wang X, Wan Y, Chen Q, Wang C, et al. Microwave-assisted pyrolysis of microalgae for biofuel production. Bioresour Technol 2011.

- doi:10.1016/j.biortech.2011.01.055.
- [45] Suriapparao D V., Pradeep N, Vinu R. Bio-oil production from *Prosopis juliflora* via microwave pyrolysis. *Energy and Fuels* 2015. doi:10.1021/acs.energyfuels.5b00357.
- [46] Cherubini F. The biorefinery concept: Using biomass instead of oil for producing energy and chemicals. *Energy Convers Manag* 2010. doi:10.1016/j.enconman.2010.01.015.
- [47] Shah Z, CV R, AC M, DS R. Separation of Phenol from Bio-oil Produced from Pyrolysis of Agricultural Wastes. *Mod Chem Appl* 2017. doi:10.4172/2329-6798.1000199.
- [48] Xiu S, Shahbazi A. Bio-oil production and upgrading research: A review. *Renew Sustain Energy Rev* 2012. doi:10.1016/j.rser.2012.04.028.
- [49] Kanyaporn C, Tanongkiat K, Nat V, Churat T. Biochar production from freshwater algae by slow pyrolysis. *Maejo Int J Sci Technol* 2012;6:186–95.
- [50] Watanabe H, Li D, Nakagawa Y, Tomishige K, Kaya K, Watanabe MM. Characterization of oil-extracted residue biomass of *Botryococcus braunii* as a biofuel feedstock and its pyrolytic behavior. *Appl Energy* 2014. doi:10.1016/j.apenergy.2014.07.037.
- [51] Chang YM, Tsai WT, Li MH. Chemical characterization of char derived from slow pyrolysis of microalgal residue. *J Anal Appl Pyrolysis* 2015;111:88–93. doi:10.1016/j.jaap.2014.12.004.
- [52] Bird MI, Wurster CM, de Paula Silva PH, Paul NA, de Nys R. Algal biochar: Effects and applications. *GCB Bioenergy* 2012;4:61–9. doi:10.1111/j.1757-1707.2011.01109.x.

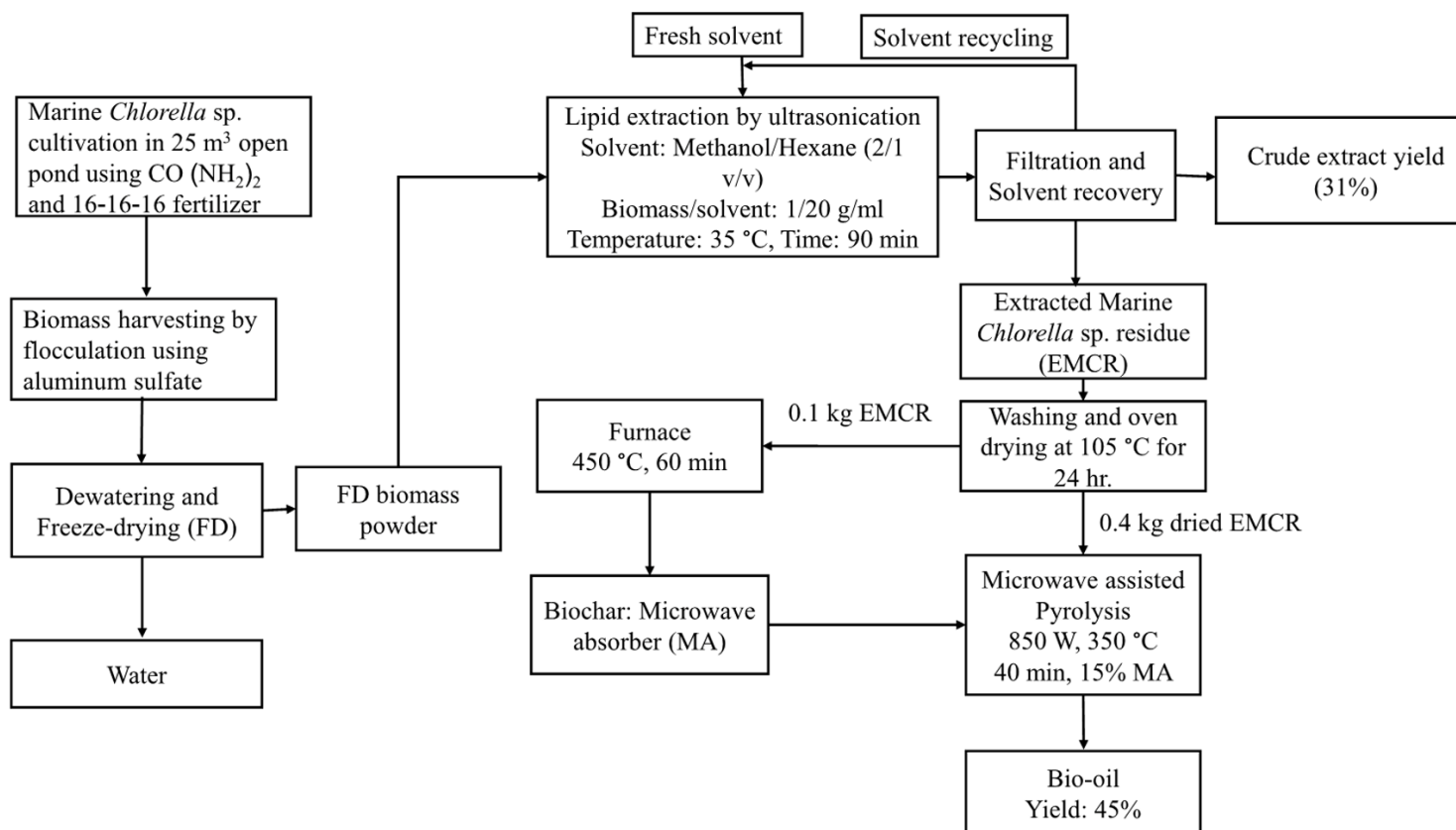


Fig. 5.1. Overall processing scheme of experimental investigation.

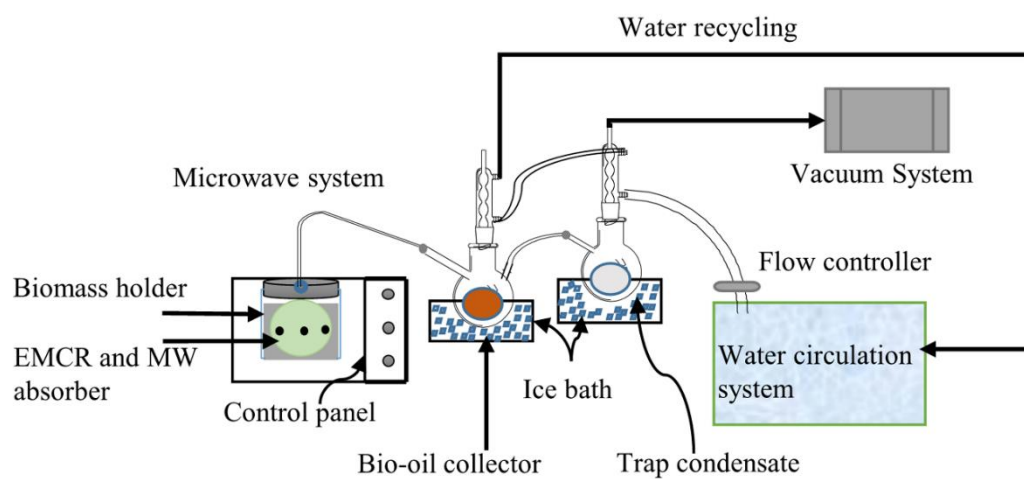


Fig. 5.2. Microwave pyrolysis system.

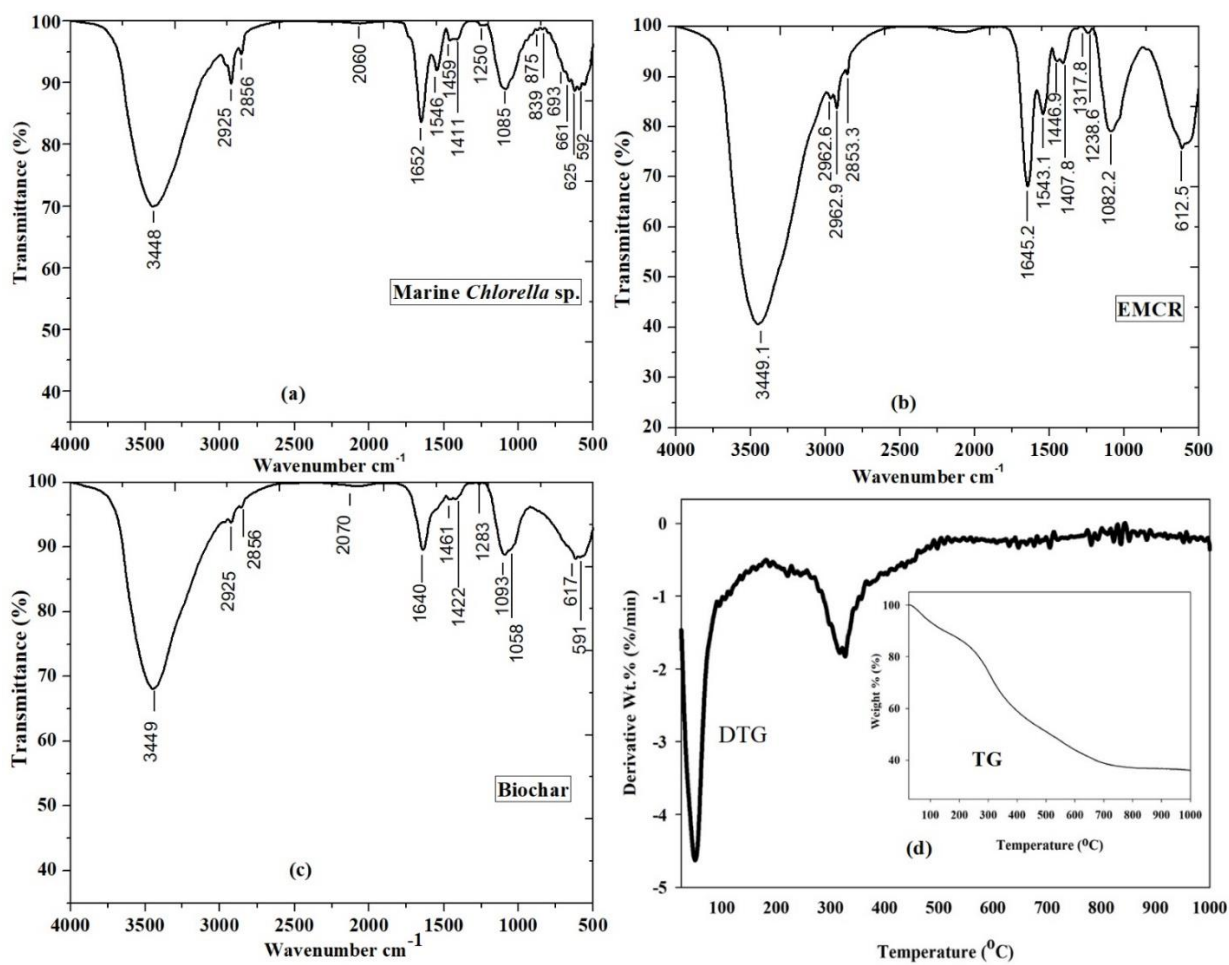


Fig. 5.3. FTIR profiles of (a) marine *Chlorella* sp., (b) EMCR and (c) biochar and (d) TG and DTG profiles of EMCR.

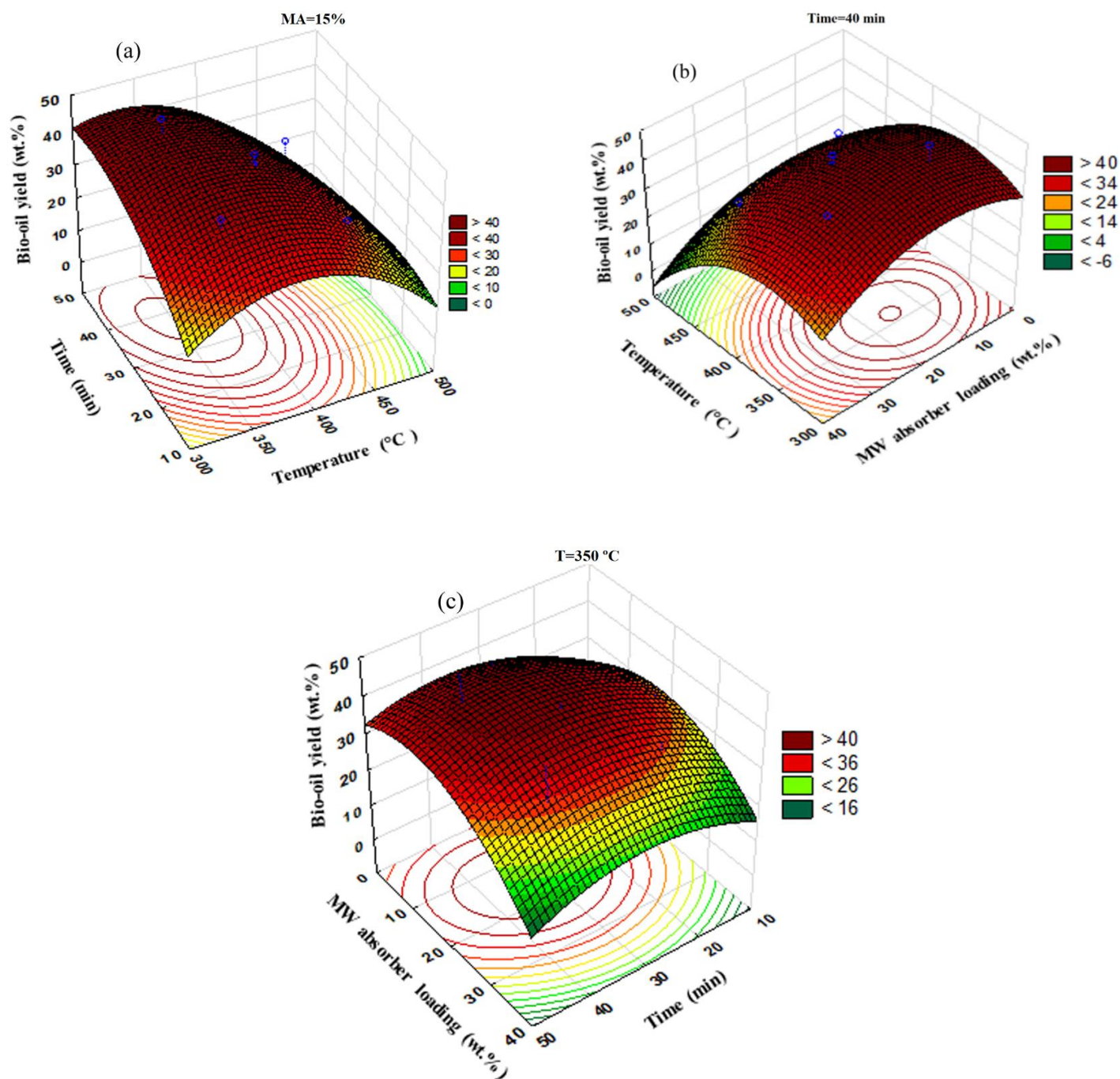


Fig. 5.4. 3-D response surface for bio-oil yield showing the effects of (a) time and temperature, (b) temperature and MA loading and (c) MA loading and time.

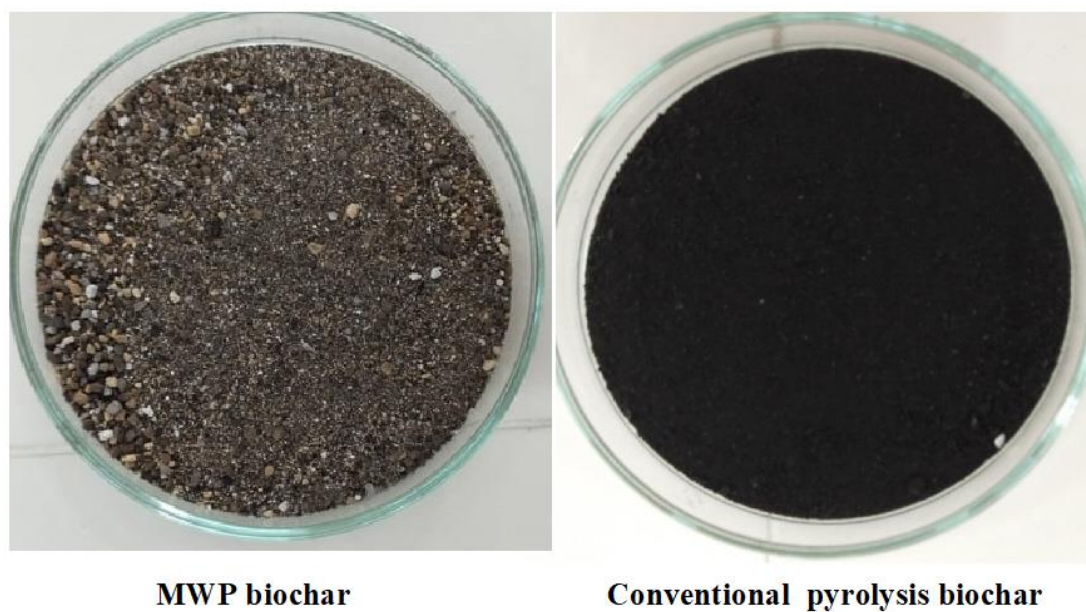


Fig. 5.5. Biochars obtained by MWP at the optimum condition and conventional pyrolysis at 450 °C for 60 min under nitrogen flushed environment.

Table 5.1

The experimental and predicted bio-oil yields from microwave pyrolysis of EMCR at various RSM based on CCD conditions.

Run	Factors						Block	Observed Response	Predicted response	Residual
	Temperature (°C)		Time (min)		MA (%)			Bio-oil yield (%)	Bio-oil yield (%)	
1	350	-1	20	-1	10	-1	1	41.0	38.6	2.4
2	350	-1	20	-1	30	1	1	35.0	33.5	1.5
3	350	-1	40	1	10	-1	1	48.0	46.6	1.4
4	350	-1	40	1	30	1	1	37.0	36.7	0.3
5	450	1	20	-1	10	-1	1	29.5	28.0	1.5
6	450	1	20	-1	30	1	1	25.6	25.2	0.4
7	450	1	40	1	10	-1	1	30.0	29.6	0.4
8	450	1	40	1	30	1	1	21.3	21.9	-0.6
9	400	0	30	0	20	0	1	41.4	40.9	0.5
10	400	0	30	0	20	0	1	40.6	40.9	-0.3
11	400	0	30	0	20	0	1	40.3	40.9	-0.6
12	315.91	- α	30	0	20	0	2	40.0	42.1	-2.1
13	484.09	+ α	30	0	20	0	2	21.0	20.8	0.2
14	400	0	13.18	- α	20	0	2	31.0	33.3	-2.3
15	400	0	46.82	+ α	20	0	2	38.2	37.3	0.9
16	400	0	30	0	3.18	- α	2	35.4	37.5	-2.1
17	400	0	30	0	36.82	+ α	2	26.8	26.8	-0.0
18	400	0	30	0	20	0	2	43.3	40.9	2.4
19	400	0	30	0	20	0	2	40.1	40.9	-0.8
20	400	0	30	0	20	0	2	40.3	40.9	-0.6

Table 5.2

Proximate and ultimate analysis of marine *Chlorella*, EMCR, biochar and other algal biomass and residues from literature.

	Proximate Contents				Ultimate analysis (ash free dry basis)									Ref
	Moisture	VM	FC	Ash	C	H	N	S	O	H/C	O/C	C/N	HHV*	
<i>Spirogyra</i> sp.	8.45	71.52	15.29	13.19	39.26	6.11	6.65	0.57	47.41	1.86	0.90	6.88	13.55	[49]
<i>Cladophora</i> sp.	5	63.8	35.17	1.03	28.78	4.02	3.06	5.29	58.85	1.67	1.53	10.97	4.93	[22]
<i>C. vulguris</i>	6.18	70.94	12.39	16.67	51	8.12	7.96	-	33	1.91	0.48	7.47	23.01	[22]
<i>Chlorella</i> sp.	3.20	-	-	5.4	53.5	7.6	10	-	28.9	1.70	0.40	6.24	23.84	[50]
<i>C. vulguris</i>	6.26	76.13	6.11	11.5	47.32	6.9	8.48	0.85	36.45	1.74	0.57	6.51	19.38	[23]
<i>C. vulguris</i> residue	4.39	76.01	15.27	8.72	49.34	7.53	10.72	-	32.41	1.83	0.49	5.36	21.7	[22]
<i>Chlorella</i> residue	-	-	-	4.8	50.46	7.54	10.48	-	31.52	1.79	0.46	5.61	22.26	[51]
<i>Rhizoclonium</i> sp.	11.20	75.50	16.5	8	38.1	5.9	4.2	-	51.80	1.85	1.01	10.58	12.06	[20]
<i>T. minus</i> residue	3.42	67.80	21.06	11.14	32.27	5.09	4.03	-	58.61	1.89	1.36	9.34	7.69	[17]
Algal waste	5.04	68.91	12.09	19	35.27	4.71	4.44	0.73	54.85	1.60	1.16	9.26	8.83	[18]
<i>D. tertiolecta</i> residue	9.38	62.64	18.23	19.13	44.78	6.78	8.4	-	40.04	1.81	0.67	6.21	17.7	[34]
FW algal biochar	-	-	-	74.4	11.6	0.7	1.32	-	11.70	0.72	0.75	10.25	2.82	[52]
SW algal biochar	-	-	-	59.4	17.4	1.77	3.27	-	18.10	1.22	0.78	6.2	5.17	[52]
<i>D. tertiolecta</i>	4.20	79.50	11.80	8.60	52.6	6.92	8.01	0.64	31.87	1.57	0.45	7.66	22.02	[32]
<i>D. tertiolecta</i> residue	9.80	87.10	11.80	8.40	42.9	7.09	5.45	0.87	43.69	1.98	0.76	9.18	16.86	[32]
<i>B. braunii</i>	3.40	-	-	2.50	68.5	9.70	3.0	-	18	1.69	0.19	26.63	33.91	[50]
<i>B. braunii</i> residue	4.80	-	-	3.30	61.5	8.80	5.3	-	22.40	1.71	0.27	13.53	29.45	[50]
Marine <i>Chlorella</i> sp.	8.0	45	14	41	41	11	6	1.6	40.50	3.21	0.74	7.97	22.43	
EMCR	7.0	47	10	43	30.2	10.2	5.6	1.7	52.30	4.05	1.29	6.29	15.49	This
Biochar	5.0	39	4	56	24.5	9.3	3.6	2.1	60.50	4.55	1.85	7.93	10.79	study

VM = volatile matters; FC = Fixed carbon; *HHV (MJ/kg) = Higher heating value = $0.3383 C + 1.442(H - O/8)$; FW = Fresh water and SW = Saline water

Table 5.3
 Analysis of variance (ANOVA) and regression coefficients for bio-oil production
 from EMCR.

Source	SS	DF	MS	F	p	Significant
Model	1048	9	116	37.43	<0.0001	Yes
Block	0.4	1	0.4	3.62	0.12	No
Temperature (X_1)	548.16	1	548.16	177	0.00006	Yes
Time (X_2)	19.08	1	19.08	6.13	0.030	Yes
MW absorber (X_3)	139.82	1	139.82	45	0.00088	Yes
X_1^2	161.65	1	161.65	52	0.0006	Yes
X_2^2	53.04	1	53.04	17.05	0.0054	Yes
X_3^2	140.26	1	140.26	45.01	0.00087	Yes
X_1X_2	20.48	1	20.48	6.58	0.027	Yes
X_1X_3	2.42	1	2.42	0.78	0.3070	NO
X_2X_3	12.01	1	12.01	3.86	0.06	NO
Lack of fit	20.92	5	4.19	2.37	0.21	NO
Pure error	7.07	4	1.77			
Total	1076	19				

SS = Sum of Square; MS = Mean Square; DF = Degree of Freedom

Table 5.4

Chemical composition of bio-oil obtained from GC-MS analysis.

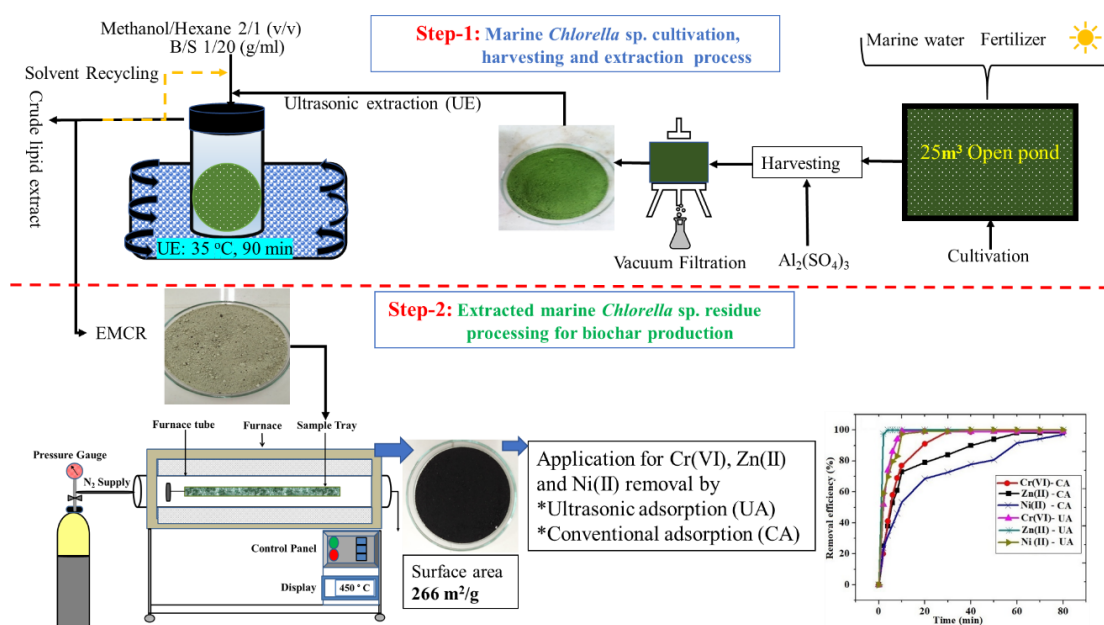
Group	Compound Name	Formula	RT/min	% Area
Amine/amide/indoles (Nitrogenated compounds) (30.37%)	2-Butanone, 4-(dimethylamino)-	C ₆ H ₁₃ NO	2.43	0.30
	Pyridine	C ₅ H ₅ N	5.83	3.83
	Pyrazine	C ₄ H ₄ N ₂	6.30	0.11
	2-Pyridineacetic acid	C ₇ H ₇ NO ₂	6.38	0.09
	1H-Imidazole, 1-ethenyl-	C ₅ H ₆ N ₂	7.31	1.23
	3-methyl-pyridine	C ₆ H ₇ N	7.90	0.97
	2-methyl-pyridine	C ₆ H ₇ N	8.06	0.25
	Dimethyl Pyrazine	C ₆ H ₈ N ₂	8.60	0.14
	Pyridine, 2,3-dimethyl-	C ₇ H ₉ N	9.27	0.07
	Pyrimidine, 2-(1-bromo-1-methylethyl)-	C ₇ H ₉ BrN ₂	15.78	0.22
	3-Pyridinecarbonitrile	C ₆ H ₄ N ₂	18.08	0.64
	Propanamide, 2-methyl-	C ₄ H ₉ NO	19.17	0.17
	Propanamide	C ₃ H ₇ NO	19.27	0.53
	Pyridine, 1-acetyl-1,2,3,4-tetrahydro-	C ₇ H ₁₁ NO	19.42	0.89
	2-Pyrimidinamine	C ₄ H ₅ N ₃	20.69	0.55
	2-Pyridinamine	C ₅ H ₆ N ₂	21.19	0.58
	Butanamide, 3-methyl-	C ₅ H ₁₁ NO	21.50	0.71
	Ethanone, 1-(1H-pyrrol-2-yl)-	C ₆ H ₇ NO	22.69	0.57
	2-Pyrrolidinone	C ₄ H ₇ NO	23.92	0.52
	Pentanamide, 4-methyl-	C ₆ H ₁₃ NO	24.39	0.32
	3-Pyridinol	C ₅ H ₅ NO	30.76	1.19
	1H-Pyrrole-2-carbonitrile	C ₅ H ₄ N ₂	32.21	0.78
	1H-indole	C ₈ H ₇ N	31.24	1.74
	Benzeneacetamide	C ₈ H ₉ NO	35.51	0.19
	Pyrrole-2-carboxamide	C ₅ H ₆ N ₂ O	37.78	0.69
	Niacinamide	C ₆ H ₆ N ₂ O	39.21	1.75
	1H-Imidazo[1,5-a] azepine-3,8(2H,5H)-dione, tetrahydro-1,1-dimethyl-	C ₁₀ H ₁₆ N ₂ O ₂	39.61	0.15
	(1H)-pyrrole	C ₄ H ₅ N	12.82	0.32
	Pyrimidine, 2-methyl-	C ₅ H ₆ N ₂	7.52	2.65
	(S)-1-(2-Pyridyl)-2-methylpropylamine	C ₉ H ₁₄ N ₂	8.95	0.22
	Formamide, N,N-dimethyl-	C ₃ H ₇ NO	8.77	0.6
	Methanamine, N,N-dimethyl-	C ₃ H ₉ N	2.11	0.27
	Acetonitrile, (dimethylamino)-	C ₄ H ₈ N ₂	6.73	1.07
	2,4-Imidazolidinedione, 5-methyl-	C ₄ H ₆ N ₂ O ₂	42.39	2.51
	5-Isopropyl-2,4-imidazolidinedione	C ₆ H ₁₀ N ₂ O ₂	42.87	1.53
	5-Ethylhydantoin	C ₅ H ₈ N ₂ O ₂	43.28	1.20
	Benzonitrile, 4-amino-	C ₇ H ₆ N ₂	30.66	0.17
	benzene-propane-nitrile	C ₉ H ₉ N	24.02	0.65

Furans and aromatics (5.56%)	2-furan-carboxaldehyde	C ₅ H ₄ O ₂	11.66	0.19	
	Ethanone, 1-(2-furyl)-	C ₆ H ₆ O ₂	12.60	0.43	
	2-Furancarboxaldehyde, 5-methyl-	C ₆ H ₆ O ₂	14.17	1.78	
	2-Furanmethanol	C ₅ H ₆ O ₂	16.10	1.64	
	Benzonitrile	C ₇ H ₅ N	14.89	0.31	
	Benzeneacetonitrile	C ₈ H ₇ N	21.82	0.57	
	Isoquinoline	C ₉ H ₇ N	21.96	0.42	
	Quinazoline	C ₈ H ₆ N ₂	23.20	0.22	
	Phenols (17.64%)	Phenol, 2-methoxy-	C ₇ H ₈ O ₂	20.42	1.86
		Creosol	C ₈ H ₁₀ O ₂	22.37	1.17
Phenol		C ₆ H ₆ O	23.38	9.35	
Guaiacol, 4-ethyl-		C ₉ H ₁₂ O ₂	23.82	1.00	
p-Cresol		C ₇ H ₈ O	24.99	2.37	
Phenol, 2-methoxy-4-(2-propenyl)-, acetate		C ₁₂ H ₁₄ O ₃	26.39	0.37	
m-ethyl-phenol		C ₈ H ₁₀ O	26.56	1.35	
Phenol, 2,4-dimethyl-		C ₈ H ₁₀ O	27.40	0.17	
Acids (12.18%)		Acetic acid	C ₂ H ₄ O ₂	11.44	7.50
		Propanoic acid	C ₃ H ₆ O ₂	13.45	2.00
	Butanoic acid, 2-methyl-	C ₅ H ₁₀ O ₂	16.40	1.37	
	Benzoic acid	C ₇ H ₆ O ₂	31.17	1.16	
	2-Butenoic acid	C ₄ H ₆ O ₂	18.70	0.15	
Esters (17.62%)	Octadecanoic acid, ethyl ester	C ₂₀ H ₄₀ O ₂	31.42	0.45	
	Ethanedioic acid, dimethyl ester	C ₄ H ₆ O ₄	18.32	1.20	
	2-Pyridinepropanoic acid, .beta.-oxo-, ethyl ester	C ₁₀ H ₁₁ NO ₃	19.05	0.15	
	Hexadecanoic acid, methyl ester	C ₁₇ H ₃₄ O ₂	27.26	10	
	Hexadecanoic acid, ethyl ester	C ₁₈ H ₃₆ O ₂	27.92	4.39	
	Diethyl 2-(m-methoxybenzyl)malonate	C ₁₅ H ₂₂ O ₅	10.23	0.11	
	Methyl stearate	C ₁₉ H ₃₈ O ₈	30.84	1.32	
	Ketones/aldehydes /ethers (2.88%)	2-Cyclopenten-1-one, 2-methyl-	C ₆ H ₈ O	9.51	0.27
2-Cyclopenten-1-one, 3-methyl-		C ₆ H ₈ O	12.96	0.72	
Hex-3-en-2,5-dione		C ₆ H ₈ O ₂	15.01	0.08	
3-methyl-2-butenyl phenacyl ether[(prenyloxy)aceto-phenone]		C ₁₃ H ₁₆ O ₂	15.91	0.30	
2-Cyclopentene-1-ethanol acetate		C ₉ H ₁₄ O ₂	21.33	0.08	
1H-Pyrrole-2-carboxaldehyde		C ₅ H ₅ NO	23.76	0.23	
2,5-Hexanedione		C ₆ H ₁₀ O ₂	25.81	0.55	
Methyl 3-(nitrooxy)-2-methyl-4-oxo-4-phenylbutanoate		C ₁₂ H ₁₃ NO ₆	35.05	0.39	
Acetophenone, 2'-hydroxy-5'-methoxy-4'-methyl-		C ₁₀ H ₁₂ O ₃	35.24	0.14	
1,3-Dioxolane, 2,2-dimethyl-		C ₅ H ₁₀ O ₂	10.39	0.12	

Sugars (2.30%)	1,4:3,6-Dianhydro-.alpha.-d-glucopyranose	C ₆ H ₈ O ₄	30.45	2.00
	2,6-Anhydro-.beta.,D-fuctofuranose	C ₆ H ₁₀ O ₅	33.27	0.30
Alkenes (0.5%)	2-Butene, 2-methyl-	C ₅ H ₁₀	11.82	0.20
	1-Octyne	C ₈ H ₁₄	21.65	0.30
Alcohols (6.07%)	1-Butanol	C ₄ H ₁₀ O	5.12	0.66
	1-Methoxy-4 (tetrahydropyranyloxy) hydroquinone	C ₁₂ H ₁₆ O ₃	15.10	0.14
	2-Pentanol	C ₅ H ₁₂ O	21.05	0.33
	Benzeneethanol	C ₈ H ₁₀ O	21.45	0.34
	Benzenemethanol	C ₇ H ₈ O	24.84	2.76
	Ethanone, 1-(4-hydroxy-3 methoxyphenyl)-	C ₉ H ₁₀ O ₃	34.29	0.67
	erythro-2-ethyl-3-ethoxybutan-1-ol	C ₈ H ₁₈ O ₂	15.53	1.00
	1-Butyne, 3-methoxy-3-methyl-	C ₆ H ₁₀ O	37.72	0.17
Others				4.88
Total				100

CHAPTER 6

Biochar from extracted marine *Chlorella* sp. residue with ultrasonic adsorption for high efficiency of Cr(VI), Zn(II) and Ni(II) removal



Highlights

- Development of biochar (BC-450) from extracted marine *Chlorella* sp. residue
- BC-450 had high surface area (266 m²/g) due to ultrasonic extraction and pyrolysis
- BC-450 presented great potential for Cr(VI), Zn(II) and Ni(II) adsorptive removal
- Adsorption process was enhanced using ultrasonication technique
- Effects of adsorption parameters were evaluated to optimize the removal efficiency

Biochar from extracted marine *Chlorella* sp. residue with ultrasonication adsorption for high efficiency of Cr(VI), Zn(II) and Ni(II) removal

Muhammad Amin, Pakamas Chetpattananondh*
Department of Chemical Engineering
Faculty of Engineering, Prince of Songkla University, 90110, Hat Yai, Songkhla,
Thailand.

*Corresponding author email: pakamas.p@psu.ac.th (Pakamas Chetpattananondh)

Abstract

The biochar BC-450 derived from the extracted marine *Chlorella* sp. residue (EMCR) had high surface area (266 m²/g) with rich of ash and O-functional groups. Its characteristic is suitable for heavy metal adsorption application. Effects of adsorption parameters were investigated to optimize the removal efficiency of Cr(VI), Zn(II) and Ni(II) from aqueous solution by conventional adsorption (CA) and ultrasonication adsorption (UA). The adsorption mechanism was well described by Langmuir isotherm and pseudo-second-order model. The equilibrium times were 10, 8, 15 and 40, 60, 80 minutes for removal of Cr(VI), Zn(II) and Ni(II) with UA and CA, respectively. The maximum adsorption capacities of Cr(VI), Zn(II) and Ni(II) for CA and UA were 15.94, 17.62 and 24.76 mg/g and 18.86, 21.31 and 27.45 mg/g, respectively. UA presented 1.1-1.3 times greater removal efficiencies than CA in much shorter time. The EMCR is promising feedstock for production of low cost and high efficient adsorbent.

Keywords: Algal residue; Adsorbent; Heavy metals; Ultrasonic; Conventional shaker

6.1 Introduction

Chlorella sp. has shown a great potential for biodiesel production (Phukan et al., 2011; Sanyano et al., 2013). However, it is not commercialized yet due to high processing cost. The production of biodiesel from algal biomass could be more economic by recovery of other precious substances and turn them into valuable products (Neto et al., 2013). The residue after lipid extraction is generally known as de-oiled biomass. Biodiesel production from microalgae at large scale would generate a substantial amount of this de-oiled biomass, which requires a careful handling management (Maurya et al., 2016; Chang et al., 2015). This algal residue could be used as precursor for valuable products in livestock, chemical and environmental sector (Yusuf, 2007; Rashid et al., 2013). Production of biochar from residue and its application as an adsorbent to treat the polluted effluents is one of considerable pathways (Bird et al., 2011; Rashid et al., 2013).

Biochar is a black carbon with high porosity obtained from any kind of carbonaceous biomass and organic waste residues via thermochemical process at 300-800 °C under limited oxygen supply (Rangabhashiyam and Balasubramanian, 2019; Inyang et al., 2016; Ye et al., 2017). The biochar characteristics from different materials varies subjected to processing conditions (Li et al., 2018). Slow pyrolysis (10 °C/min) at 450-500 °C for 60 min is feasible choice to obtain high yield and good quality biochar (Chang et al., 2015; Yu et al., 2017;). Microalgal biochar containing less carbon, high nitrogen, high ash and mineral contents is different in nature from the biochar produced from lignocellulosic biomass. The biochar with large nitrogen and ash could elevate the quality and productivity of soils (Torri et al., 2011). The algal biochar with low in carbon but high in nitrogen, phosphorus, and other nutrients could be applied as a powerful carbon sequestration and soil improvement (Bird et al., 2011). High ash in algal biochar may improve adsorption of dye (Chen et al., 2018). The algal biochar is considered as low cost adsorbent with high adsorption capacity, highly porous structure, special surface chemical behavior and high thermal stability (Chen et al., 2018).

Presence of heavy metals beyond the set limits defined by Environmental Protection Agency (EPA) is harmful to environment and must be removed by suitable process. (Rangabhashiyam and Balasubramanian, 2018; Ye et al., 2019; Sharma and

Srivastava, 2011). Adsorption process using biochar is one of the effective technique (Li et al., 2018). Zheng et al. (2017) reported that biochar from *Chlorella* sp. had higher potential to remove p-nitro phenols (PNP) from wastewater than powder activated carbon. About 82.6% congo red dye was removed using the biochar derived from residual biomass of *Spirulina platensis* (Nautiyal et al., 2016). The pigments extracted macroalgae derived biochar (MDBC) could remove 90% dye from wastewater (Chen et al., 2018). The biochars from extracted biomass of different macro and micro algae species have been prepared and characterized in the literature but their applications for heavy metal adsorption have been not yet published.

Traditionally, batch-adsorption experiments are performed to study the adsorption capacity of the adsorbent using shaker equipment. Ultrasonication is widely combined with extraction, reaction, oxidation, and desorption. However, there have been limited published reports on ultrasonication adsorption and the results are still contradictory. Ultrasonic waves can enhance mass transport phenomena and improve the adsorption rate by the generation of a cavitation effect to form cavitation bubbles, which violently collapse on or near the sorbent surface and direct microjets of liquid toward it. In addition, shock waves have the potential of creating microscopic turbulence within interfacial films surrounding nearby solid particles, also referred as microstreaming (Nouri and Hamdaoui, 2007). Adsorption of p-chlorophenol onto granular activated carbon was lower with presence of ultrasound, whereas desorption was enhanced by increasing ultrasound intensity (Hamdaoui et al., 2003). Similarly, adsorption of Geniposide on Resin 1300 was lower in the presence of ultrasonication (Ji et al., 2006). On the other hand, the ultrasonic irradiation significantly accelerated the removal efficiency of cadmium from aqueous phase by wheat bran (Nouri and Hamdaoui, 2007). Sharifpour et al. (2018) investigated the ultrasonic-assisted removal of dye-safranin O using ZnO nanorod-loaded activated carbon and found that Langmuir isotherm was well fitted with adsorption equilibrium data and the maximum monolayer capacity was found to be 32.06 mg/g. The application of ultrasonication for adsorption of Cr(VI), Zn(II), and Ni(II) has not yet been reported.

Assessment of extracted marine *Chlorella* sp. residue)EMCR(derived biochar for adsorption of heavy metals enhancing by ultrasonication is presented in this study for the first time. In addition, this work aimed to (1) evaluate the EMCR derived biochar

for its potential as a low cost adsorbent, (2) study the biochar properties for its applications, (3) investigate the adsorption parameters to optimize removal efficiency and (4) study the mechanisms of heavy metal adsorption using sorption kinetics and isotherms for both conventional adsorption and ultrasonic adsorption. The knowledge of this work can be a source of information regarding algal biomass residue applications to be beneficial for biofuel industry and environmental concerns.

6.2 Materials and methodology

6.2.1 Chemicals

Heavy metal salts of $K_2Cr_2O_7$, $Zn(NO_3)_2$, and $NiSO_4 \cdot 6H_2O$ were purchased from Sigma-Aldrich and Loba Chemie, respectively. While NaOH and HNO_3 were purchased from Ajax Finechem, Thailand. Aluminum sulfate was purchased from ACI Labscon Ltd. Thailand. All chemicals used were analytical grade.

6.2.2 Microalgal biomass and its residue preparation

A marine *Chlorella* sp. cultivated in 25 m³ open pond was obtained from National Institute of Coastal Aquaculture (NICA) located in Songkhla (latitude: 7.178861° N, 100.624561° E). It was harvested by flocculation using aluminum sulfate as a flocculent agent, vacuum filtered employed GENVAC Agilent Technologies, PVL 35 at 930 Watt and freeze-dried with Dura-Dry MP, FTS systems, USA at 4400 Watt. The Freeze-dried algal biomass was extracted using (2/1 v/v) methanol/hexane at 35 °C for 90 min by ultrasonication with an ultrasonic bath (CP 2600 Crest Power sonic, USA, 45 kHz, 300 Watt), which yielded 31 wt% (dry basis). The EMCR was collected, washed with DI water and vacuum filtered. The EMCR was dried in hot air oven at 105 °C for 24 hours, placed in desiccator and its weight was recorded immediately. Then it was kept in air tight bags and stored at room temperature. The overall process scheme is presented in Fig. 6.1.

6.2.3 Biochar preparation

Two hundred gram EMCR was fed into a 75×15 cm stainless steel tube furnace under 100 ml/min N₂ flushed for 20 min and pyrolyzed at 450 °C with a heating rate of 10 °C /min for 60 min. The pyrolysis was fixed at the stated condition as it gave high yield of biochar and good characteristics of biochar for adsorption from preliminary study. The sample was collected from furnace chamber after attaining room temperature. It was cleaned with deionized water and oven dried for 3 h at 105 °C. The

yield of dried biochar was recorded gravimetrically. The prepared biochar was named as “BC-450” and kept in zip lock bags at room temperature.

6.2.4 Biochar characterization

Biochar pH was measured in a 1:10 suspension of biochar in de-ionized water (Chen et al., 2018). A proximate analysis of the BC-450 was performed using ASTM methods E871, E872-82 and D-1102-84 for moisture, volatile matter and ash content, respectively. While the fixed carbon was determined by difference method. The elemental characterization for C, H, N and S was analyzed by dynamic flash combustion technique using CHNS/O analyzer (Flash 2000, Thermo Scientific, Italy), whereas O content was calculated by difference. The surface functional groups in the range of 400-4000 cm^{-1} were confirmed using pellet KBr technique by Fourier transformed infrared spectrometer (FTIR, VERTEX 70, Bruker, Germany). A BC-450 sample was degassed for 6 hours and its surface area was determined by nitrogen adsorption via BET method using ASAP2460 Surface area and porosity analyzer, Micromeritics, USA. Zeta potential of BC-450 dispersed in deionized water was measured by zeta potential analyzer (ZetaPALS, Brookhaven, USA). The surface morphologies of EMCR, BC-450 before and after adsorption were observed by scanning electron microscopy (SEM) using Quanta 400 SEM, FEI, Brno, Czech Republic at 20,000 x magnification. The specimen for SEM analysis was dried and prepared by gold-coating using argon gas (68.9 kPa) in the sputter coater (SPI module, West Chester, Pennsylvania, USA).

6.2.5 Adsorption experiment

BC-450 performance as an adsorbent was assessed for Cr(VI), Zn(II) and Ni(II) removal from aqueous solution by conventional adsorption (CA) using Daihan WIS-20 shaking incubator at 150 rpm compared with ultrasonic adsorption (UA) using CP 2600 Crest Power sonic, USA at 45 kHz and 300 W at room temperature. The temperature of UA was controlled by circulating cooled water in the chamber. The effects of process variables including contact time (2-90 min), adsorbent loading (0.1-0.9 g/L), initial solution pH (3-9) and initial concentration of heavy metal (50-400 mg/L) were investigated by varying one variable and fixing the others. The initial solution pH was adjusted by 1 M NaOH or 1 M HNO₃. The stock solutions (1,000 mg/L) of Cr(VI), Zn(II) and Ni(II) were prepared by dissolving 2.82, 2.89 and 2.63 g

of respective heavy metal salts in 1 L deionized water. These stock solutions were further diluted as per requirement. An aliquot of 50 mg/L sample of each heavy metal solution was prepared from stock solution followed by addition of 0.5 g adsorbent as an initial assessment. These samples were placed in 250 ml Duran bottles to perform the adsorption test. After the adsorption was finished the samples were taken out and filtered through 0.45 μm , 13 mm Nylon syringe filter of SimplePure. The concentration of Cr(VI), Zn(II) or Ni(II) in solution after adsorption was measured as its total concentration using atomic absorption spectrophotometer (AAS, Perkin-Elmer, USA).

6.2.6 Adsorption isotherm and kinetic study

The heavy metal adsorption can be calculated from Eq. (6.1) and percentage of removal is calculated from Eq. (6.2).

$$q_e = \frac{(C_i - C_e) \times V}{m_a} \quad (6.1)$$

$$\text{Removal (\%)} = \frac{(C_i - C_e)}{C_i} \times 100 \quad (6.2)$$

Where q_e (mg/g) is quantity of adsorbed heavy metal by biochar, V (mL) is volume of solution, m_a (g) is mass of adsorbent, C_i (mg/L) is initial concentration of heavy metal and C_e (mg/L) is equilibrium concentration of heavy metal.

The adsorption isotherm is needed to study the relationship between adsorbent and adsorbate. Many isotherms have been proposed and there are limitations of each isotherm. Adsorption of heavy metals on BC-450 was studied by two parameter isotherms including Langmuir, Freundlich and Temkin and three parameter isotherms including Redlich-Peterson and Toth isotherms using the nonlinear forms to reduce many errors from the transformations to linear forms (Shahmohammadi-Kalalagh and Babazadeh, 2014). Langmuir isotherm is based on assumption that the adsorbent has a homogeneous monolayer surface and energetically equivalent sites for adsorbate interaction (Chen et al., 2018). The adsorbate molecules do not deposit on the other already adsorbed molecules of adsorbate, but only on the free surface of adsorbent. The Langmuir isotherm is given by Eq. (6.3).

$$q_e = \frac{q_m C_e K}{1 + C_e K} \quad (6.3)$$

Where q_e (mg/g) is heavy metal adsorbed per mass of adsorbent, q_m (mg/g) is maximum adsorption capacity of BC-450, C_e (mg/L) is equilibrium concentration and K (L/mg) is Langmuir constant.

Freundlich isotherm is an empirical model without any theoretical basis. The model is applicable to adsorption processes that occur on heterogeneous surfaces (Tohdee et al., 2018). The Freundlich isotherm is expressed by Eq. (6.4).

$$q_e = K_f C_e^{1/n} \quad (6.4)$$

Where K (mg/g) and $1/n$ are Freundlich constants related to adsorption capacity and sorption intensity, respectively.

Temkin isotherm assumes that the adsorption heat of all molecules reduces linearly with increasing of adsorbent surface coverage. The adsorption is characterized by a uniform distribution of binding energies up to the maximum value (Piccin et al., 2011). This model is given by Eq. (6.5).

$$q_e = \frac{RT}{b_t} \ln(A C_e) \quad (6.5)$$

Where A (L/g) is Temkin isotherm equilibrium binding constant, b_t (J/mol) is Temkin isotherm constant related to the heat of sorption, R is the gas constant (8,314 J/mol. K) and T is the absolute temperature (K).

A three parameter Redlich-Peterson isotherm as shown in Eq. (6.6) is associated to combined the features of Langmuir and Freundlich models.

$$q_e = \frac{A C_e}{1 + B C_e^g} \quad (6.6)$$

Where A (L/g) and B (L/mg)^g are model parameters and their ratio presents the adsorption capacity, while g is an exponent with value from 0-1. The equation becomes Langmuir model when g approaches unity. With high concentration of C_e , the model transforms into Freundlich.

Another three parameter isotherm, Toth is a modified form of Langmuir, which was proposed to minimize the error in model fitting. The model is expressed as Eq. (6.7).

$$q_e = \frac{q_r C_e}{(1/K_t + C_e^m)^{1/m}} \quad (6.7)$$

Where q_t (mg/g) is model adsorption capacity, K_t is model constant and m is Toth model exponent. When $m = 1$, the equation reduces to Langmuir isotherm, which implies the homogeneous adsorption process. If m deviates from unity the heterogeneous adsorption occurs.

The model fitting quality is evaluated by mean absolute percentage error (MAPE) using Eq. (6.8).

$$\text{MAPE (\%)} = \sum_{i=1}^k \left| \frac{[q_{\text{experimental}} - q_{\text{predicted}}] / q_{\text{experimental}}}{N} \right| \times 100 \quad (6.8)$$

Where q (mg/g) is experimental and predicted maximum adsorption capacity and N is number of data points.

Adsorption kinetics determine the rate of adsorption, which are influenced by the surface complexity of the adsorbent, solute concentration, pH, temperature and flow. The mostly used adsorption kinetic models, pseudo-first-order (PFO) proposed by Lagergren and pseudo-second-order (PSO) proposed by Blanchard et al. in nonlinear forms are expressed as Eq. (9) and (10), respectively (Tohdee et al., 2018):

$$\text{PFO} \quad \frac{dq_t}{dt} = k_{P-1}(q_e - q_t) \quad (6.9)$$

$$\text{PSO} \quad \frac{dq_t}{dt} = k_{P-2}(q_e - q_t)^2 \quad (6.10)$$

Where q_e (mg/g) and q_t (mg/g) are BC-450 capacity to adsorb heavy metal at equilibrium and at given time, respectively. k_{P-1} (1/min) and k_{P-2} (g/mg.min) are rate constants for PFO and PSO, respectively while t (min) is time.

6.3 Results and Discussion

6.3.1 Characterization and yield of BC-450

The pH value of BC-450 was 8.3 exhibiting an alkaline nature, which is in agreement with many algal biochars presented in Table 6.1. The impact of pyrolysis temperature on biochar pH has been reported. Pyrolysis above 300 °C causes releasing of alkali salts and increases biochar pH. The pH is constant at a temperature around 600 °C (Chen et al., 2011). The alkaline pH of BC-450 guides that it can be applied to neutralize soil acidity, which is an important factor in metal mobility.

Proximate and ultimate analysis of BC-450 and its precursor (EMCR) was made to understand the fundamental properties and potential applications. The inherent moisture contents in BC-450 and EMCR were below 10 wt.%, which is normally appropriate for materials storage. The BC-450 had 13% higher ash and 9% lower volatile matters than EMCR due to the pyrolysis effect, where condensable matters released at 450 °C and caused volatile reduction. In addition, the ash content increased as some mineral salts and metal elements could not evaporate at this temperature (Gong et al., 2014). The ash contents of algal and lignocellulose biochars presented in Table 6.1 are ranged from 4.67-74.7%. The BC-450 has 17.9%, 16.7% and 2.6% less ash than fresh water algal biochar, *Chaetomorpha indica* biochar and saline water algal biochar, respectively. Fixed carbon in BC-450 was 4.2%, which is 4.8% lower than EMCR. There is an inverse relation between the ash and fixed carbon (Sewu et al., 2017). Generally, high ash is recognized feature of algal biochars compared to lignocellulosic biochars (Bird et al., 2011; Yu et al., 2017). High ash in biochar could help to improve the adsorption process and adsorbent capacity (Chen et al., 2018; Sewu et al., 2017).

The International Biochar Initiative (IBI) has graded biochar into three classes based on carbon content including Class 1 with 60% carbon or more, Class 2 with 30-60% carbon and Class 3 with 10-30% carbon (Mohan et al., 2014). The carbon storage class estimates long-term (i.e., 100 year) soil carbon storage potential of a biochar (https://biochar-international.org/classification_tool_faqs/). From elemental analysis as shown in Table 6.1 the BC-450 with 10.5% carbon lied in class 3. The BC-450 had lower carbon, but higher oxygen and nitrogen than lignocellulosic biochars, which is usually observed for the algal biochars. Although the algal biochars are less able to provide the carbon than lignocellulosic biochars, they can contribute direct nutrient benefits to soil and crop and are notably useful for application on acidic soil (Bird et al., 2011).

The degree of carbonization could be characterized by the molar H/C ratio (Chen et al., 2011). The high value H/C of BC-450 implied that it was weakly carbonized and composed of moderate amounts of aromatization form. The molar O/C ratio is used to express the surface hydrophilicity because it is indicative of polar-group content. The BC-450 had high O/C, which is probably useful for adsorption of heavy metals (Son et al., 2018). In addition, the partly carbonized biochar produced at

temperature lower than 500 °C contains a higher content of dissolved organic carbon and oxygen functional groups with relatively low C/N ratio is more suitable for removal of inorganic pollutants (Oliveira et al., 2017). Functional groups like carboxylic, amino, and hydroxyl groups have a great importance in metal sorption (Li et al., 2017). The FTIR analysis of BC-450 was performed as shown in supplementary information. The broad bands at 3449 cm^{-1} and 2856 or 2925 cm^{-1} were assigned to O-H and C-H stretching, respectively (Son et al., 2018). This confirmed the presence of alcohol and methyl groups of alkenes. While peak at 1640 cm^{-1} was associated carboxylic compounds. The bands at 1422 and 1460 cm^{-1} were features of C=C, while peaks at 1283, 1093 and 1058 were related to C-O stretch due to alcohols, ethers and phenols, respectively. The bands at 617 cm^{-1} and 591 cm^{-1} were assigned to MeX (M: metal, X: halogen) stretching vibrations in both organic and inorganic halogen compounds (Son et al., 2018; Chen et al., 2018). The BC-450 surface produced at 450 °C was rich in O functional groups as evidenced from FTIR data and high O/C content. Furthermore, zeta potential of -11.81 ± 0.25 showed that the BC-450 surface was negative charge. Hence, it can be applied for positive charge heavy metal abatement.

The higher heating value (HHV) of BC-450 was too low for fuel purpose because lipids were already extracted from its precursor. The algal residue biochar with low HHV is able to use for soil amendment but its carbon content is low and needed to be blend with C rich char. Alternatively, it could be effectively applied for heavy metal treatment (Robert et al., 2015) as concentrated in this work. The specific surface area is one of the important property of adsorbent (Zheng et al., 2017). The BC-450 was further analyzed for pore volume and surface area and found as 0.61 cm^3/g and 266 m^2/g , respectively. In addition, N_2 adsorption-desorption isotherms of the BC-450 (provided as E-supplementary data in online version) belong to Type II of International Union of Pure and Applied Chemistry (IUPAC) classification, which is a typical characteristic of macroporus adsorbent (Thommes et al., 2015). The hysteresis loop is type H3, which is for non-rigid aggregates of plate-like particle consisting of macro pores. It has been evidenced that the specific surface area of algal biochar is low (Bird et al., 2011). Poo et al. (2018) reported that the surface area of biochar derived from *S. japonica* was only 1.3 m^2/g , which is much lower than lignocellulosic biomass derived chars. Roberts et al. (2015) stated that the biochar produced from *Eucheuma* sp. had a

significantly high surface area of 30.03–34.82 m²/g compared with the other algal species with surface area in the range of 1.29 to 8.87 m²/g. Obviously, the surface area of BC-450 is much higher than the reported algal biochars and some lignocellulosic biochars but lower than activated carbon presented in Table 6.2. The high surface area of BC-450 was due to ultrasonication effect during extraction, where ultrasonic shock waves ruptured the cell wall of marine *Chlorella* sp. very effectively and produced porous EMCR. Furthermore, the pyrolysis process made the BC-450 to have higher surface area and porosity than EMCR as seen in SEM pictures (provided as E-supplementary data in online version). The high surface area of carbonaceous material is preferred for an excellent adsorption capacity (Chen et al., 2018).

Biochar yield is dependent on pyrolytic conditions, such as temperature, heating rate, time and nitrogen flow rate. Generally, temperature and time are negatively correlated with the biochar yield. The BC-450 was 45% yield obtained at 450 °C, heating rate 10 °C /min, 60 min and N₂ flow rate 100 mL/min. This BC-450 yield is in a reasonable range reported from other studies in Table 6.2. Moreover, Yu et al. (2017) reviewed on recent advances in microalgal biochar and reported 20-63% yield. The high yield of BC-450 is a positive indication of EMCR potential to be recycled as the biochar feedstock.

6.3.2 Effects of adsorption parameters

The performance of BC-450 was assessed for Cr(VI), Zn(II) and Ni(II) removal using conventional adsorption (CA) compared with ultrasonic adsorption (UA). The influence of contact time, adsorbent dose, initial solution pH, and initial concentration of metal was evaluated.

6.3.2.1 Effect of initial solution pH

The initial pH of metal solution is considered as an important factor in adsorption process. BC-450 was assessed for the removal of Cr(VI), Zn(II) and Ni(II) in batch experiments by regulating the initial pH in the range of 2-8 and fixing contact time at 60 min, adsorbent loading 0.5 g/L and initial metal concentration 50 mg/L. The removal efficiency of BC-450 for Cr(VI) was found maximum at pH 2 for both CA and UA as shown in Fig. 6.2 (a). Increasing pH from 2 to 8 decreased Cr(VI) removal rate. Only removal efficiencies of 32 % for CA and 40 % for UA were succeeded at pH 8. The maximum removal of Cr(VI) by polyethyleneimine-sodium xanthogenate (PEX)

was also observed at initial pH of 2 (Wang et al., 2013). This is in agreement with removal of Cr(VI) using Ni/Fe bimetallic nanoparticles (Zhou et al., 2014). There are generally three forms of chromium in aqueous solution including $\text{Cr}_2\text{O}_7^{2-}$, HCrO_4^- and CrO_4^{2-} dependent on pH. The predominant of HCrO_4^- is observed at pH between 2 and 6, while CrO_4^{2-} is attained at pH above 7. In addition, Cr(VI) ions have high redox potential under acidic conditions, and can be reduced to Cr(III) ions. Removal of Cr(VI) using the polyethylenimine modified biochar also depended on solution pH, and a low pH value was favorable (Ma et al., 2014).

On the other hand, the maximum Zn(II) and Ni(II) removal efficiencies were observed at pH 6 and 7, respectively. The maximum adsorption of zinc by activated carbon was reported at pH 5-6 (Kumar et al., 2014). The adsorption of nickel on biochar derived from wheat straw pellets and rice husk was enlarged with high alkaline environment (Shen et al., 2017) The sorption capacity of both Zn(II) and Ni(II) onto BC-450 surged with pH because of increasing surface negative charge enhancing the electrostatic adsorption. Increasing pH was combined with addition of removal rates and gradual decrease of H^+ competitive effects. While in acidic condition the sorption of metal ions was suppressed by the extreme presence of H^+ which compete for available reactive sites. Initial solution pH of 2, 6 and 7 were then selected for adsorption of Cr(VI), Zn(II) and Ni(II), respectively.

6.3.2.2 Effect of contact time

The performance of BC-450 for Cr(VI), Zn(II) and Ni(II) removal was studied at variable time with 0.5 g/L adsorbent dose and 50 mg/L initial metal concentration at the optimized initial solution pH. From Fig. 6.2 (b) it can be seen that the equilibrium times were observed at 10, 8, 15 and 40, 60, 80 minutes for removal of Cr(VI), Zn(II) and Ni(II) with UA and CA, respectively. Not only shorter times, but also higher removal efficiencies were gain by UA. Tohdee et al. (2018) studied adsorption of Zn(II) using bentonite with CA and reported 10 min as equilibrium time. Equilibrium times of 60 and 80 min using modified *Aspergillus flavus* biomass were stated for Zn(II) and Ni(II) removal, respectively (Foroutan et al., 2017). The removal efficiency relation with time could vary due to different characteristics of adsorbents. The adsorption of heavy metals by algal biochar using UA has not been reported. Ultrasound was applied to assist the adsorption of dye-safranin O and the equilibrium time was achieved in 5

min (Sharifpour et al., 2018). The shorter contact time and higher efficiency obtained with UA is highly favorable for practical approach.

6.3.2.3 Effect of adsorbent dose

The adsorbent dose effect on heavy metal removal rate was tested using 50 mg/L initial solution concentration at optimized pH and contact time for each heavy metal. The results for CA and UA are shown in Fig.6.2 (c). The removal rate sharply increased as adsorbent dosage increased from 0.1 to 0.5 g/L, thereafter small increment was observed in both techniques. With 0.5 g/L adsorbent dose the high removal efficiency of more than 95% were observed for all heavy metals. Therefore, the adsorbent dose 0.5 g/L was selected as the optimum value.

6.3.2.4 Effect of initial metal concentration

The effect of initial concentration (50-400 mg/L) was studied with 0.5 g/L adsorbent dose at the optimized pH and contact time of each metal. As seen in Fig.6.2 (d) the overall response trend is similar across all cases in which the removal efficiency declined with increasing of initial metal concentration due to the limitation of adsorbent site availability. The high initial concentration is driving force to eliminate the resistance between solid and liquid phase and increment in concentration is possible factor for enhancing adsorption capacity. While decrease in removal efficiency at high concentration is attributed to saturated surface of adsorbent (Saravanan et al., 2016). The removal efficiencies at 50-200 mg/L initial concentration were observed between 84-99% and 72-95% for UA and CA, respectively. The UA showed higher removal efficiencies compared to CA for all heavy metals.

6.3.3 Adsorption isotherms

The widely used two parameter isotherms: Langmuir, Freundlich and Temkin and three parameter isotherms: Redlich-Peterson and Toth were applied to describe the adsorption process. The identified isotherm parameters and coefficient of determination (R^2) are given in Table 6.3 and the model based responses of q_e vs C_e are shown in Fig. 6.3. For two parameter models Langmuir isotherm with high R^2 and low MAPE was best fitted with the adsorption of Cr(VI), Zn(II) and Ni(II) in both CA and UA. The process is then considered as homogeneous adsorption. The homogeneous adsorption mechanism was confirmed by the three parameter isotherms, Redlich-Peterson (mixed

feature of Langmuir and Freundlich) and Toth (extended form of Langmuir) as g and m constants were approached the unity. The maximum adsorption capacities determined by Langmuir of Cr(VI), Zn(II) and Ni(II) for CA and UA were 15.94, 17.62 and 24.76 mg/g and 18.86, 21.31 and 27.45 mg/g, respectively. The values were closed to the maximum adsorption capacities obtained from the experiments. It can be seen that UA presented 1.1-1.3 times greater removal efficiencies than CA. Furthermore, UA provided much shorter contact time than CA. In addition, it can be seen from SEM pictures that there is more adhering Ni(II) on the surface of the BC-450 after UA than the BC-450 after CA (provided as E-supplementary data in online version). Therefore, the ultrasonic adsorption is recommended for enhancement of adsorption process. The adsorption capacity of BC-450 was compared to other biochar and biomass in the literature as presented in Table 6.2 and the results showed great potential for its adsorption application.

6.3.4 Adsorption kinetics

The pseudo-first-order (PFO) and pseudo-second-order (PSO) were used to characterize mono-nuclear and binuclear adsorption processes, respectively. The model parameters are presented in Table 6.4 and the curve fits are shown in Fig. 6.4. The PSO with R^2 closer to unity than PFO successfully described the binuclear adsorption of Cr(VI), Zn(II) and Ni(II) by BC-450 for both CA and UA. The adsorption of Cu(II) and Zn(II) by algal derived biochar was also better described by PSO than PFO (Chen et al. (2018)). The PSO suggested that the adsorption rate-limiting step may be chemisorption and the adsorption is via surface complexation reactions at specific sorption sites. Additionally, the values of q_e from experiment and calculation were well matched for PSO, confirming the reliability of the model. The higher rate constants of UA than CA confirmed better adsorption performance using ultrasonication.

Conclusion

The developed biochar possessing high surface area, ash content and O-functional groups was successfully demonstrated its application for heavy metal adsorption. The maximum uptake capacity (mg/g) of biochar was highest for Ni(II) and observed as 24.76, 27.45 in CA and UA, respectively. The adsorption mechanism was governed by homogeneous adsorption of Langmuir isotherm and chemisorption of pseudo-second-order model. UA provided much shorter contact time and 1.1-1.3 times

greater removal efficiencies than CA. The recycle of EMCR as the feedstock of biochar production and application as an efficient adsorbent is environmentally friendly approach and beneficial for biofuel and biomaterial industries.

Supplementary material: “E-supplementary data of this work can be found in online version of the paper”

Acknowledgment

This research was financially supported by Thailand’s Education Hub for Southern Region of ASEAN Countries (TEH-AC, 56/2016) granted by the Graduate School, Prince of Songkla University (PSU), Hat Yai, Songkhla, Thailand. We are thankful to Department of Chemical Engineering, Faculty of Engineering, PSU for providing all facilities and supporting staffs to accomplish this work. We are really thankful to Research and Development Office (RDO), PSU for their support in English language editing and proofreading.

References

- [1] Bird, M.I., Wurster, C.M., de Paula Silva, P.H., Bass, A.M., de Nys, R., 2011. Algal biochar - production and properties. *Bioresour. Technol.* 102, 1886–1891. <https://doi.org/10.1016/j.biortech.2010.07.106>
- [2] Bird, M.I., Wurster, C.M., de Paula Silva, P.H., Paul, N.A., de Nys, R., 2012. Algal biochar: Effects and applications. *GCB Bioenergy* 4, 61–69. <https://doi.org/10.1111/j.1757-1707.2011.01109.x>
- [3] Chang, Y.M., Tsai, W.T., Li, M.H., 2015. Chemical characterization of char derived from slow pyrolysis of microalgal residue. *J. Anal. Appl. Pyrolysis* 111, 88–93. <https://doi.org/10.1016/j.jaap.2014.12.004>
- [4] Chang, Y.M., Tsai, W.T., Li, M.H., 2014. Characterization of activated carbon prepared from *Chlorella*-based algal residue. *Bioresour. Technol.* 184, 344–348. <https://doi.org/10.1016/j.biortech.2014.09.131>
- [5] Chen, Y. di, Lin, Y.C., Ho, S.H., Zhou, Y., Ren, N. qi, 2018. Highly efficient adsorption of dyes by biochar derived from pigments-extracted macroalgae pyrolyzed at different temperature. *Bioresour. Technol.* 259, 104–110. <https://doi.org/10.1016/j.biortech.2018.02.094>

- [6] Chen, X., Chen, G., Chen, L., Chen, Y., Lehmann, J., McBride, M.B., Hay, A.G., 2011. Adsorption of copper and zinc by biochars produced from pyrolysis of hardwood and corn straw in aqueous solution. *Bioresour. Technol.* 102, 8877–8884. <https://doi.org/10.1016/j.biortech.2011.06.078>
- [7] Chisti, Y., 2007. Biodiesel for microalgae. *Biotechnol. Adv.* 25, 294–306. <https://doi.org/10.1016/j.biotechadv.2007.02.001>
- [8] Foroutan, R., Esmaceli, H., Rishehri, S.D., Sadeghzadeh, F., Mirahmadi, S., Kosarifard, M., Ramavandi, B., 2017. Zinc, nickel, and cobalt ions removal from aqueous solution and plating plant wastewater by modified *Aspergillus flavus* biomass: A dataset. *Data Br.* 12, 485–492. <https://doi.org/10.1016/j.dib.2017.04.031>
- [9] Gaur, S., Reed, T.B., 1995. An atlas of thermal data for biomass and other fuels, NREL/TP-433-7965.
- [10] Gong, X., Zhang, B., Zhang, Y., Huang, Y., Xu, M., 2014. Investigation on pyrolysis of low lipid microalgae *Chlorella vulgaris* and *Dunaliella salina*. *Energy and Fuels* 28, 95–103. <https://doi.org/10.1021/ef401500z>
- [11] Hamdaoui, O., Naffrechoux, E., Tifouti, L., Pétrier, C., 2003. Effects of ultrasound on adsorption-desorption of p-chlorophenol on granular activated carbon. *Ultrason. Sonochem.* 10, 109–14.
- [12] Han, Y., Cao, X., Ouyang, X., Sohi, S.P., Chen, J., 2016. Adsorption kinetics of magnetic biochar derived from peanut hull on removal of Cr (VI) from aqueous solution: Effects of production conditions and particle size. *Chemosphere* 145, 336–341. <https://doi.org/10.1016/j.chemosphere.2015.11.050>
- [13] https://biochar-international.org/classification_tool/ (accessed 14 April, 2019)
- [14] Inyang, M.I., Gao, B., Yao, Y., Xue, Y., Zimmerman, A., Mosa, A., Pullammanappallil, P., Ok, Y.S., Cao, X., 2016. A review of biochar as a low-cost adsorbent for aqueous heavy metal removal. *Crit. Rev. Environ. Sci. Technol.* 46, 406–433. <https://doi.org/10.1080/10643389.2015.1096880>
- [15] Ji, J. bing, Lu, X. hong, Xu, Z. chao, 2006. Effect of ultrasound on adsorption of Geniposide on polymeric resin. *Ultrason. Sonochem.* 13, 463–470.

- <https://doi.org/10.1016/j.ultsonch.2005.08.004>
- [16] Kumar, P.R., Swathanthr, P.A., Rao, V.V.B., Rao, S.R.M., 2014. Adsorption of Cadmium and Zinc Ions from Aqueous Solution Using Low Cost Adsorbents. *J. Appl. Sci.* 14, 1372–1378. <https://doi.org/10.3923/jas.2014.1372.1378>
- [17] Li, H., Dong, X., da Silva, E.B., de Oliveira, L.M., Chen, Y., Ma, L.Q., 2017. Mechanisms of metal sorption by biochars: Biochar characteristics and modifications. *Chemosphere* 178, 466–478. <https://doi.org/10.1016/j.chemosphere.2017.03.072>
- [18] Li, R., Deng, H., Zhang, X., Wang, J.J., Awasthi, M.K., Wang, Q., Xiao, R., Zhou, B., Du, J., Zhang, Z., 2019. High-efficiency removal of Pb(II) and humate by a CeO₂–MoS₂ hybrid magnetic biochar. *Bioresour. Technol.* 273, 335–340. <https://doi.org/10.1016/j.biortech.2018.10.053>
- [19] Li, R., Wang, J.J., Gaston, L.A., Zhou, B., Li, M., Xiao, R., Wang, Q., Zhang, Z., Huang, Hui, Liang, W., Huang, Heteng, Zhang, X., 2018. An overview of carbothermal synthesis of metal–biochar composites for the removal of oxyanion contaminants from aqueous solution. *Carbon N. Y.* 129, 674–687. <https://doi.org/10.1016/j.carbon.2017.12.070>
- [20] Ma, Y., Liu, W.J., Zhang, N., Li, Y.S., Jiang, H., Sheng, G.P., 2014. Polyethylenimine modified biochar adsorbent for hexavalent chromium removal from the aqueous solution. *Bioresour. Technol.* 169, 403–408. <https://doi.org/10.1016/j.biortech.2014.07.014>
- [21] Maurya, R., Paliwal, C., Ghosh, T., Pancha, I., Chokshi, K., Mitra, M., Ghosh, A., Mishra, S., 2016. Applications of de-oiled microalgal biomass towards development of sustainable biorefinery. *Bioresour. Technol.* 214, 787–796. <https://doi.org/10.1016/j.biortech.2016.04.115>
- [22] Mohan, D., Sarswat, A., Ok, Y.S., Pittman, C.U., 2014. Organic and inorganic contaminants removal from water with biochar, a renewable, low cost and sustainable adsorbent - A critical review. *Bioresour. Technol.* 160, 191–202. <https://doi.org/10.1016/j.biortech.2014.01.120>
- [23] Nautiyal, P., Subramanian, K.A., Dastidar, M.G., 2016. Adsorptive removal of dye using biochar derived from residual algae after in-situ transesterification: Alternate use of waste of biodiesel industry. *J. Environ. Manage.* 182, 187–197.

- <https://doi.org/10.1016/j.jenvman.2016.07.063>
- [24] Neto, A.M.P., Sotana de Souza, R.A., Leon-Nino, A.D., da Costa, J.D. arc A., Tiburcio, R.S., Nunes, T.A., Sellare de Mello, T.C., Kanemoto, F.T., Saldanha-Corrêa, F.M.P., Giancesella, S.M.F., 2013. Improvement in microalgae lipid extraction using a sonication-assisted method. *Renew. Energy* 55, 525–531. <https://doi.org/10.1016/j.renene.2013.01.019>
- [25] Nouri, L., Hamdaoui, O., 2007. Ultrasonication-assisted sorption of cadmium from aqueous phase by wheat bran. *J. Phys. Chem. A* 111, 8456–8463. <https://doi.org/10.1021/jp0721393>
- [26] Oliveira, F.R., Patel, A.K., Jaisi, D.P., Adhikari, S., Lu, H., Khanal, S.K., 2017. Environmental application of biochar: Current status and perspectives. *Bioresour. Technol.* 246, 110–122. <https://doi.org/10.1016/j.biortech.2017.08.122>
- [27] Phukan, M.M., Chutia, R.S., Konwar, B.K., Kataki, R., 2011. Microalgae *Chlorella* as a potential bio-energy feedstock. *Appl. Energy* 88, 3307–3312. <https://doi.org/10.1016/j.apenergy.2010.11.026>
- [28] Piccin, J.S., Dotto, G.L., Pinto, L.A.A., 2011. Adsorption isotherms and thermochemical data of FD and C RED N° 40 Binding by chitosan. *Brazilian J. Chem. Eng.* 28, 295–304. <https://doi.org/10.1590/S0104-66322011000200014>
- [29] Poo, K.M., Son, E.B., Chang, J.S., Ren, X., Choi, Y.J., Chae, K.J., 2018. Biochars derived from wasted marine macro-algae (*Saccharina japonica* and *Sargassum fusiforme*) and their potential for heavy metal removal in aqueous solution. *J. Environ. Manage.* 206, 364–372. <https://doi.org/10.1016/j.jenvman.2017.10.056>
- [30] Radjenovic, A., Medunic, G., 2015. Removal of Cr(VI) from aqueous solution by a commercial carbon black. *Desalin. Water Treat.* 55, 183–192. <https://doi.org/10.1080/19443994.2014.912966>
- [31] Rangabhashiyam, S., Balasubramanian, P., 2018. Characteristics, performances, equilibrium and kinetic modeling aspects of heavy metal removal using algae. *Bioresour. Technol. Reports* 5, 261–279. <https://doi.org/10.1016/j.biteb.2018.07.009>
- [32] Rashid, N., Rehman, M.S.U., Han, J.I., 2013. Recycling and reuse of spent

- microalgal biomass for sustainable biofuels. *Biochem. Eng. J.* 75, 101–107. <https://doi.org/10.1016/j.bej.2013.04.001>
- [33] Roberts, D.A., Paul, N.A., Dworjanyn, S.A., Bird, M.I., De Nys, R., 2015. Biochar from commercially cultivated seaweed for soil amelioration. *Sci. Rep.* 5, 1–6. <https://doi.org/10.1038/srep09665>
- [34] Sanyano, N., Chetpattananondh, P., Chongkhong, S., 2013. Coagulation-flocculation of marine *Chlorella* sp. for biodiesel production. *Bioresour. Technol.* 147, 471–476. <https://doi.org/10.1016/j.biortech.2013.08.080>
- [35] Saravanan, A., Senthil Kumar, P., Preetha, B., 2016. Optimization of process parameters for the removal of chromium(VI) and nickel(II) from aqueous solutions by mixed biosorbents (custard apple seeds and *Aspergillus niger*) using response surface methodology. *Desalin. Water Treat.* 57, 14530–14543. <https://doi.org/10.1080/19443994.2015.1064034>
- [36] Sewu, D.D., Boakye, P., Woo, S.H., 2017. Highly efficient adsorption of cationic dye by biochar produced with Korean cabbage waste. *Bioresour. Technol.* 224, 206–213. <https://doi.org/10.1016/j.biortech.2016.11.009>
- [37] Shahmohammadi-Kalalagh, S., Babazadeh, H., 2014. Isotherms for the sorption of zinc and copper onto kaolinite: Comparison of various error functions. *Int. J. Environ. Sci. Technol.* 11, 111–118. <https://doi.org/10.1007/s13762-013-0260-x>
- [38] Sharifpour, E., Ghaedi, M., Nasiri Azad, F., Dashtian, K., Hadadi, H., Purkait, M.K., 2018. Zinc oxide nanorod-loaded activated carbon for ultrasound-assisted adsorption of safranin O: Central composite design and genetic algorithm optimization. *Appl. Organomet. Chem.* 32, 1–11. <https://doi.org/10.1002/aoc.4099>
- [39] Sharma, Y.C., Srivastava, V., 2011. Comparative Studies of Removal of Cr(VI) and Ni(II) from Aqueous Solutions by Magnetic Nanoparticles. *J. Chem. Eng. Data* 56, 819–825. <https://doi.org/10.1021/je100428z>
- [40] Shen, Z., Zhang, Y., McMillan, O., Jin, F., Al-Tabbaa, A., 2017. Characteristics and mechanisms of nickel adsorption on biochars produced from wheat straw pellets and rice husk. *Environ. Sci. Pollut. Res.* 24, 12809–12819. <https://doi.org/10.1007/s11356-017-8847-2>

- [41] Son, E.B., Poo, K.M., Chang, J.S., Chae, K.J., 2018. Heavy metal removal from aqueous solutions using engineered magnetic biochars derived from waste marine macro-algal biomass. *Sci. Total Environ.* 615, 161–168. <https://doi.org/10.1016/j.scitotenv.2017.09.171>
- [42] Thommes, M., Kaneko, K., Neimark, A. V., Olivier, J.P., Rodriguez-Reinoso, F., Rouquerol, J., Sing, K.S.W., 2015. Physisorption of gases, with special reference to the evaluation of surface area and pore size distribution (IUPAC Technical Report). *Pure Appl. Chem.* 87, 1051–1069. <https://doi.org/10.1515/pac-2014-1117>
- [43] Tohdee, K., Kaewsichan, L., Asadullah, 2018. Enhancement of adsorption efficiency of heavy metal Cu(II) and Zn(II) onto cationic surfactant modified bentonite. *J. Environ. Chem. Eng.* 6, 2821–2828. <https://doi.org/10.1016/j.jece.2018.04.030>
- [44] Torri, C., Samorì, C., Adamiano, A., Fabbri, D., Faraloni, C., Torzillo, G., 2011. Preliminary investigation on the production of fuels and bio-char from *Chlamydomonas reinhardtii* biomass residue after bio-hydrogen production. *Bioresour. Technol.* 102, 8707–8713. <https://doi.org/10.1016/j.biortech.2011.01.064>
- [45] Wang, G., Chang, Q., Zhang, M., Han, X., 2013. Effect of pH on the removal of Cr(III) and Cr(VI) from aqueous solution by modified polyethyleneimine. *React. Funct. Polym.* 73, 1439–1446. <https://doi.org/10.1016/j.reactfunctpolym.2013.07.009>
- [46] Ye, S., Zeng, G., Wu, H., Liang, J., Zhang, C., Dai, J., Xiong, W., Song, B., Wu, S., Yu, J., 2019. The effects of activated biochar addition on remediation efficiency of co-composting with contaminated wetland soil. *Resour. Conserv. Recycl.* 140, 278–285. <https://doi.org/10.1016/j.resconrec.2018.10.004>
- [47] Ye, S., Zeng, G., Wu, H., Zhang, Chang, Dai, J., Liang, J., Yu, J., Ren, X., Yi, H., Cheng, M., Zhang, Chen, 2017. Biological technologies for the remediation of co-contaminated soil. *Crit. Rev. Biotechnol.* 37, 1062–1076. <https://doi.org/10.1080/07388551.2017.1304357>

- [48] Yu, K.L., Lau, B.F., Show, P.L., Ong, H.C., Ling, T.C., Chen, W.H., Ng, E.P., Chang, J.S., 2017. Recent developments on algal biochar production and characterization. *Bioresour. Technol.* 246, 2–11. <https://doi.org/10.1016/j.biortech.2017.08.009>
- [49] Zamani, S.A., Yunus, R., Samsuri, A.W., Salleh, M.A.M., Asady, B., 2017. Removal of Zinc from Aqueous Solution by Optimized Oil Palm Empty Fruit Bunches Biochar as Low Cost Adsorbent. *Bioinorg. Chem. Appl.* 2017, 1–9. <https://doi.org/10.1155/2017/7914714>
- [50] Zheng, H., Guo, W., Li, S., Chen, Y., Wu, Q., Feng, X., Yin, R., Ho, S.H., Ren, N., Chang, J.S., 2017. Adsorption of p-nitrophenols (PNP) on microalgal biochar: Analysis of high adsorption capacity and mechanism. *Bioresour. Technol.* 244, 1456–1464. <https://doi.org/10.1016/j.biortech.2017.05.025>
- [51] Zhou, S., Li, Y., Chen, J., Liu, Z., Wang, Z., Na, P., 2014. Enhanced Cr(VI) removal from aqueous solutions using Ni/Fe bimetallic nanoparticles: Characterization, kinetics and mechanism. *RSC Adv.* 4, 50699–50707. <https://doi.org/10.1039/c4ra08754b>

List of Figures

Figure 6.1 Process schematic diagram of algal biomass cultivation to biochar preparation and application.

Figure 6.2 Removal efficiency of Cr(VI), Zn(II), and Ni(II) by BC-450 with conventional adsorption and ultrasonic adsorption to study effect of **(a)** initial pH **(b)** contact time **(c)** adsorbent dosage and **(d)** initial heavy metal concentration.

Figure 6.3 Adsorption isotherms of heavy metals on BC-450 with conventional adsorption (CA) and ultrasonic adsorption (UA): **(a)** Cr(VI)-CA, **(b)** Zn(II)-CA, **(c)** Ni(II)-CA, **(d)** Cr(VI)-UA, **(e)** Zn(II)-UA and **(f)** Ni(II)-UA.

Figure 6.4 The pseudo second order (PSO) kinetic plots for adsorption of heavy metals on BC-450: **(a)** Cr(VI)-CA, **(b)** Zn(II)-CA, **(c)** Ni(II)-CA, **(d)** Cr(VI)-UA, **(e)** Zn(II)-UA and **(f)** Ni(II)-UA.

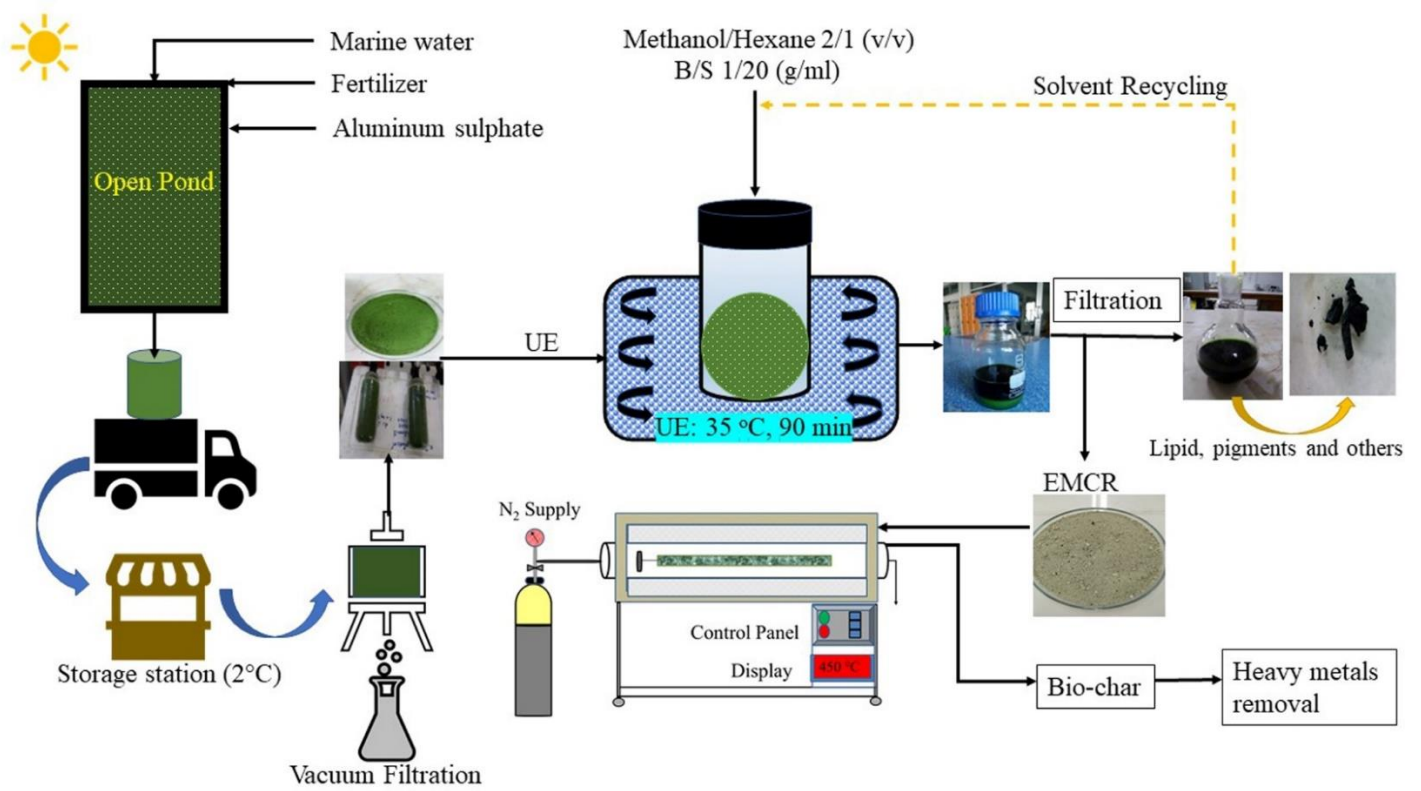


Figure 6.1

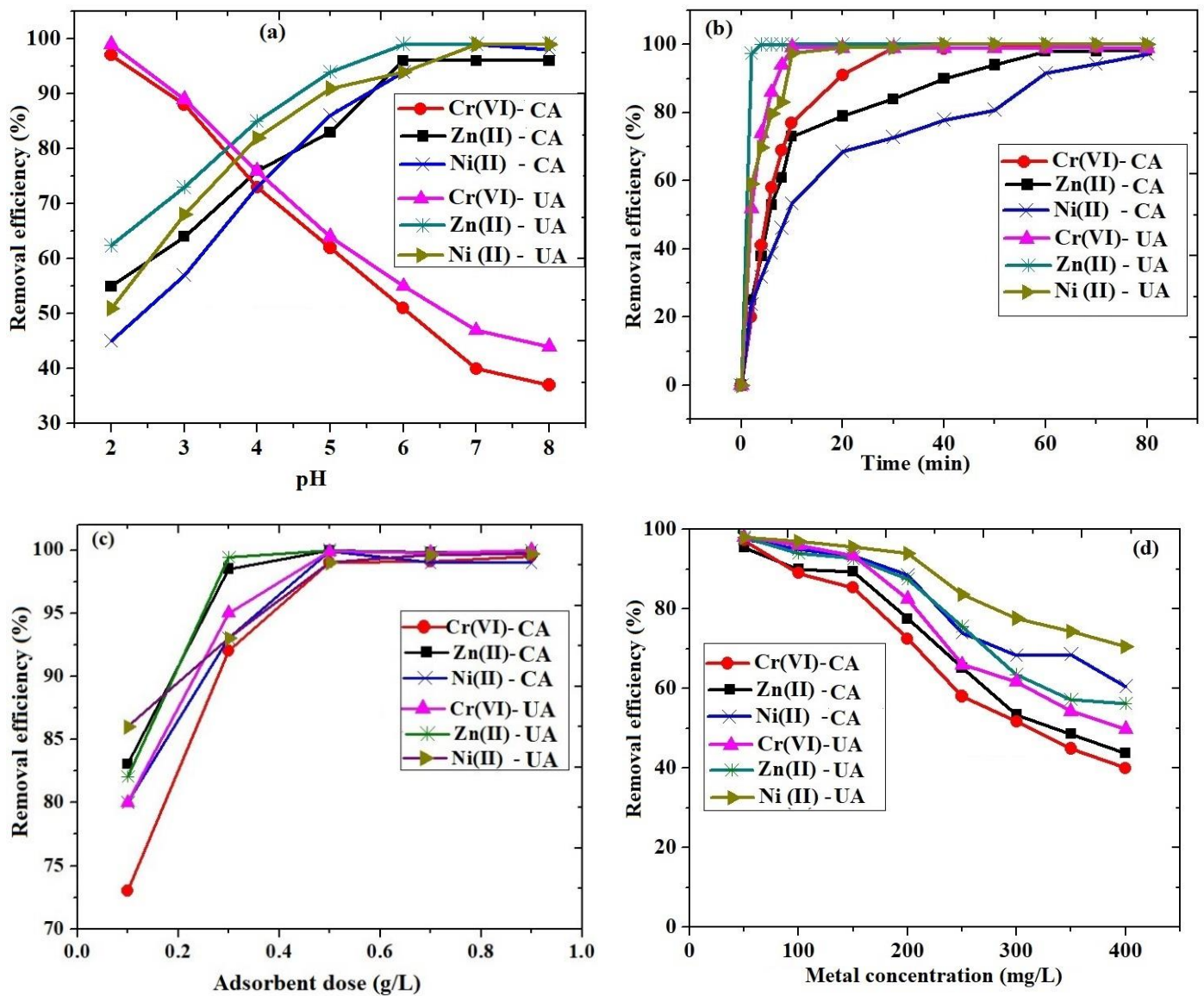


Figure 6.2

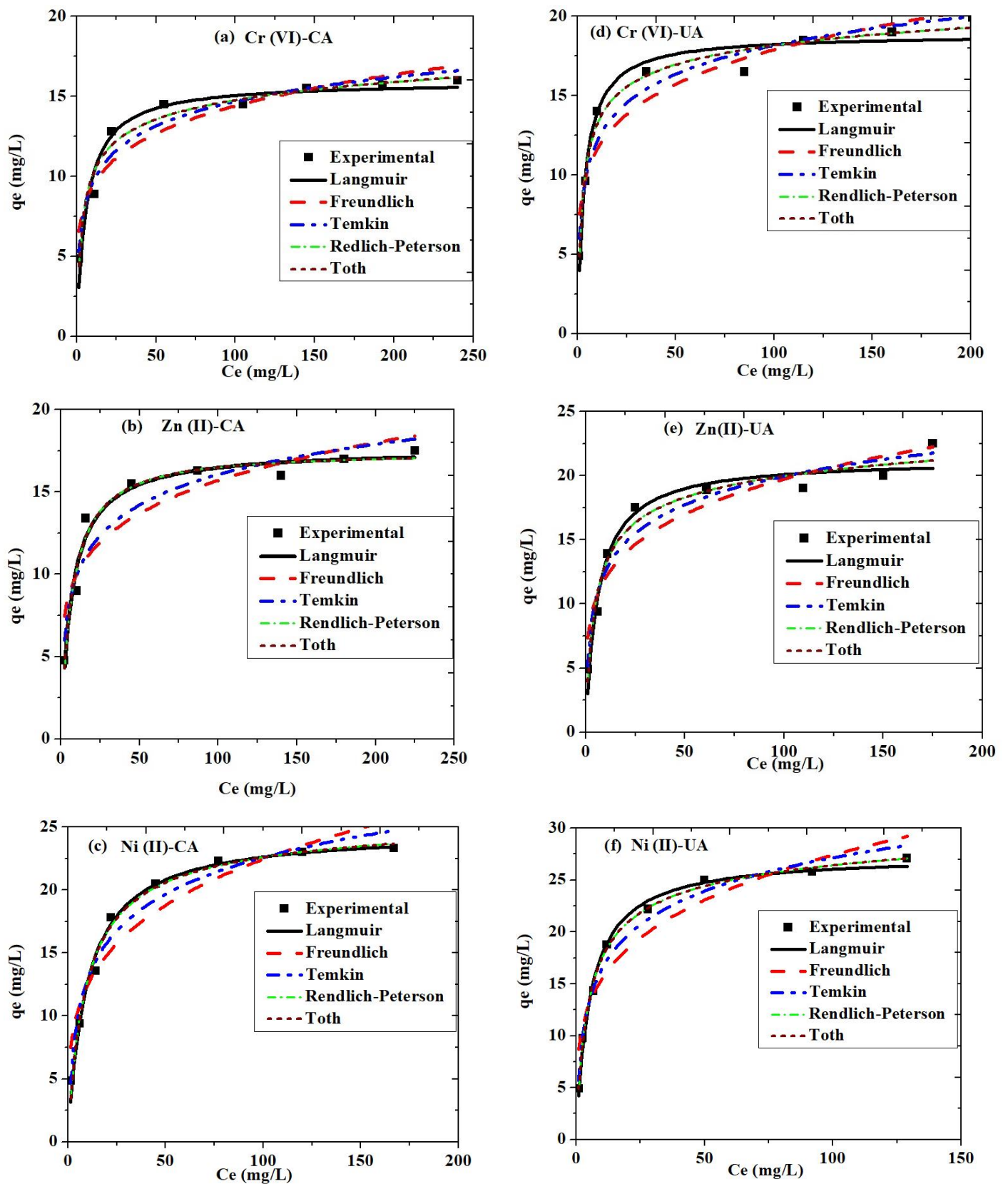


Figure 6.3

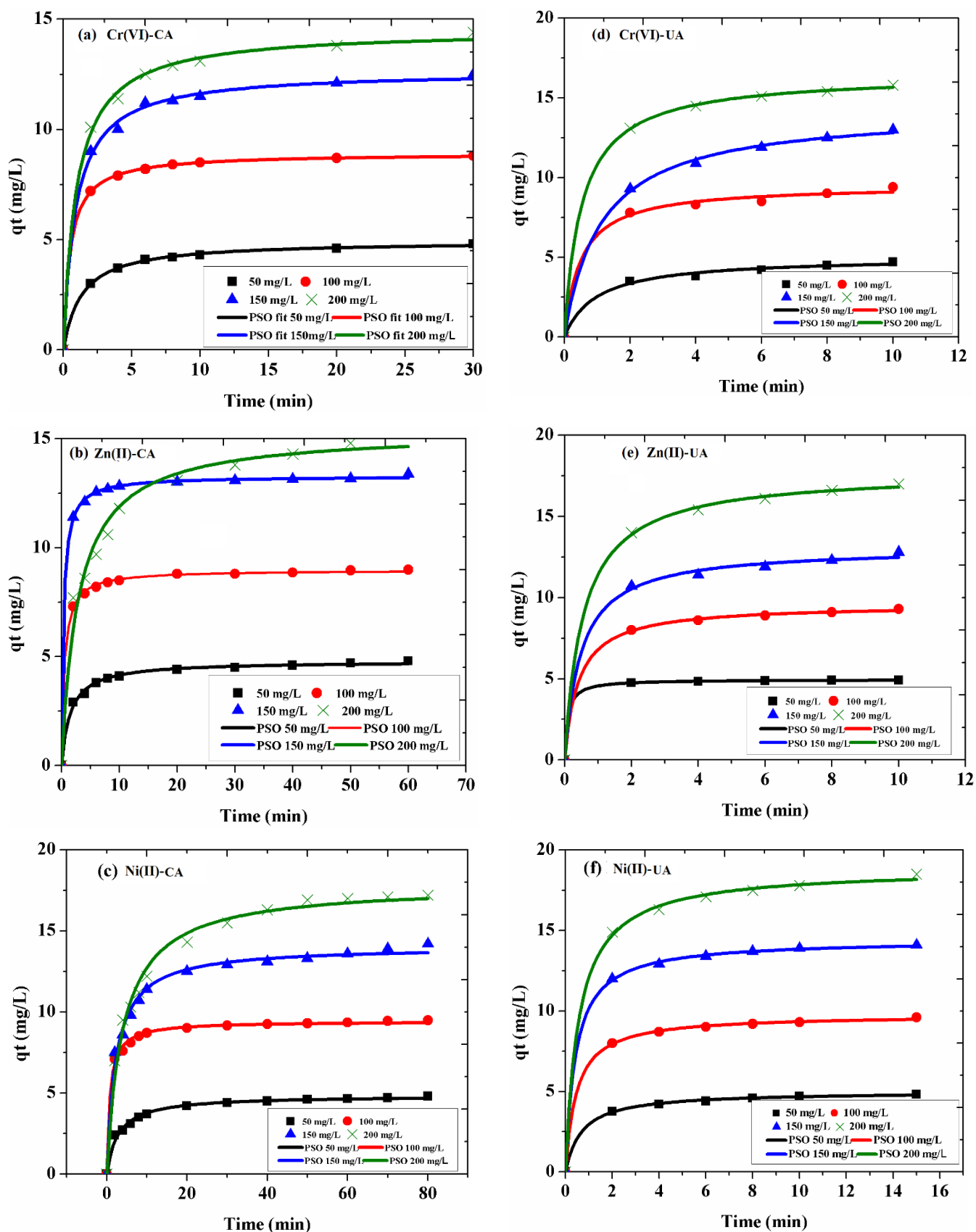


Figure 6.4

Table 6.1

Material	pH	C	H	N	S	O	Ash	H/C	O/C	C/N	HHV [#]	Reference
Wheat straw BC	9.9	68.3	2.1	1.4	-	6.9	21.2	0.36	0.07	49.10	25.2	Shen et al. (2017)
Rice husk BC	9.7	48.6	1.2	1.0	-	2.5	46.9	0.30	0.04	46.73	17.3	Shen et al. (2017)
FW algal BC	8.1	11.6	0.7	1.3	-	11.7	74.7	0.72	0.75	8.78	2.2	Bird et al. (2012)
SW algal BC	6.1	17.4	1.8	3.3	-	18.1	59.4	1.22	0.78	5.32	5.1	Bird et al. (2012)
<i>Gracilaria</i> BC	7.6	30.9	2.2	2.8	4.4	16.5	43.2	0.85	0.40	11.03	15.6	Robert et al. (2015)
<i>Eucheuma</i> BC	8.2	24.5	1.5	0.8	9.3	24.9	39	0.73	0.76	30.62	17.3	Robert et al. (2015)
<i>Saccharina</i> BC	11.2	35	2.4	2.4	1.6	18.4	40.2	0.82	0.39	14.58	14.1	Robert et al. (2015)
<i>C. indica</i> BC	7.8	10.2	0.8	1.1	-	14.4	73.5	0.94	1.05	9.27	1.6	Bird et al. (2011)
<i>Chlorella</i> sp. BC	-	62.2	1.7	6.6	-	11.9	17.4	0.33	0.14	9.36	22.1	Zheng et al. (2017)
Algal residue BC	8.3	40.4	1.9	4.3	-	7.0	46.2	0.57	0.13	9.33	14.7	Chen et al. (2018)
EMCR	7.1	17.2	5.8	3.2	0.9	29.7	43.0	4.05	1.29	5.37	10	This study
BC-450	8.3	10.5	4	1.6	1.0	26.1	56.8	4.57	1.86	6.56	5.6	This study

Characterization of EMCR, BC-450 and other biochars from literature

[#]HHV (MJ/kg) = Higher heating value = $0.35C + 1.18H + 1.10S - 0.02N - 0.10O - 0.02Ash$ (Gaur and Reed, 1995)

BC = Biochar; WH = Water hyacinth; FW = Fresh water; SW = Saline water

Table 6.2

Comparison of yield, surface area and maximum adsorption capacity of BC-450 with other biochars and materials from literature

Materials	Condition	Yield (%)	S _{BET} (m ² /g)	q _{max} (mg/g)	Reference
BC-450	450 °C, 60 min	45	266	15.94-Cr(VI)-CA 17.62-Zn(II)- CA 24.76-Ni(II)- CA	This study
BC-450	450 °C, 60 min	45	266	18.86-Cr(VI)-UA 21.31-Zn(II)- UA 27.45-Ni(II)- UA	This study
<i>Chlorella</i> residue BC	800 °C, 30 min	23	310	-	Chang et al. (2014)
Extracted algal BC	800 °C, 90 min	22	133	345.1-CR dye-CA	Chen et al. (2018)
<i>S.platensis</i> BC	450 °C, 120 min	-	167	51.28-CR dye-CA	Nautiyal et al. (2016)
Magnetic algal HBC	500 °C, 120 min	-	63	19.13-Zn(II)-CA	Son et al. (2018)
<i>S. japonica</i> BC	700 °C, 120 min	25	1.3	84.3-Zn-CA	Poo et al. (2018)
<i>Eucheum sp.</i> BC	450 °C, 60 min	57	34	-	Roberts et al.(2015)
Corn straw BC	600 °C, 120 min	-	13.08	11-Zn-CA	Chen et al. (2011)
Empty fruit bunch BC	600 °C, 128 min	25	421	15.18-Zn (II)-CA	Zamani et. al. (2017)
Peanut hull BC	450 °C, 60 min	-	24.01	77.25-Cr(VI)-CA	Han et al. (2016)
Carbon black	-	-	107	12.71-Cr(VI)-CA	Radjenovic and Medunic (2015)
Magnetic nanoparticles	-	-	86.55	11.53-Ni(II)-CA 3.52-Cr(VI)-CA	Sharma and Srivastava (2011)
Natural bentonite	-	-	44.60	19.76-Zn(II)-CA	Tohdee et al. (2018)

Table 6.3

Adsorption isotherm parameters

Adsorption parameter	Conventional adsorption			Ultrasonic adsorption		
	Zn(II)	Cr(VI)	NI(II)	Zn (II)	Cr(VI)	NI(II)
Experimental q_{\max} (mg/g)	17.50	16.01	23.3	22.51	19.9	27.1
Langmuir						
q_{\max} (mg/g)	17.62	15.94	24.76	21.31	18.86	27.45
K_L	0.14	0.16	0.10	0.16	0.28	0.18
R^2	0.97	0.94	0.99	0.97	0.96	0.99
MAPE (%)	0.0	0.0	0.1	0.11	0.1	0.1
*RMSD	0.25	0.28	0.26	0.4	0.31	0.24
Freundlich						
K_f	6.33	6.17	6.90	7.33	7.59	8.72
N	5.26	5.55	4.01	4.76	5.40	4.16
R^2	0.85	0.90	0.91	0.88	0.90	0.90
MAPE (%)	0.01	0.03	0.15	0.20	0.10	0.10
RMSD	0.57	0.4	0.66	0.6	0.51	0.76
Temkin						
b_T (J/mol)	947.06	1145.5	601.2	784.7	965.1	541.7
A_T (L/mg)	4.10	7.77	2.16	4.99	10.37	3.43
R^2	0.90	0.94	0.96	0.94	0.95	0.97
MAPE (%)	0.04	0.0	0.11	0.14	0.07	0.1
RMSD	0.43	0.3	0.38	0.43	0.35	0.34
Redlich Peterson						
A (L/g)	2.43	5.38	2.90	5.36	8.01	6.40
B (L/mg) ^g	0.13	0.53	0.13	0.37	0.59	0.30
G	1.00	0.91	0.95	0.92	0.93	0.94
R^2	0.97	0.96	0.98	0.96	0.98	0.99
MAPE (%)	0.02	0.07	0.07	0.08	0.05	0.0
RMSD	0.25	0.24	0.25	0.37	0.22	0.37
Toth						
q_t (mg/g)	18.40	14.57	20.67	20.15	15.21	29.10
K_t	0.13	0.18	0.13	0.17	0.35	0.15
m	1.0	0.98	0.96	0.99	0.96	1.0
R^2	0.97	0.95	0.98	0.95	0.98	0.98
MAPE (%)	0.0	0.2	0.0	0.14	0.2	0.25
RMSD	0.25	0.28	0.25	0.4	0.27	0.28

*RMSD= Root mean square deviation

Table 6.4

The pseudo-first-order (PFO) and pseudo-second-order (PSO) kinetic parameters for heavy metal adsorption on BC-450

Metal	C_i (mg/l)	${}^a q_e$ (mg/g)	<u>Pseudo-first-order</u>			<u>Pseudo-second-order</u>			
			K_{P1}	${}^b q_e$ (mg/g)	R^2	K_{P2}	${}^b q_e$ (mg/g)	R^2	
CA	Cr(VI)	50	4.86	0.48	4.48	0.85	0.15	4.90	0.99
		100	8.90	0.89	8.40	0.76	0.23	8.90	0.99
		150	12.80	0.63	11.70	0.74	0.08	12.75	0.99
		200	14.50	0.60	13.30	0.75	0.07	14.51	0.99
	Zn(II)	50	4.70	0.38	4.47	0.78	0.13	4.78	0.98
		100	9.00	0.84	8.60	0.65	0.22	8.99	0.99
		150	13.40	1.00	12.90	0.67	0.21	13.38	0.99
		200	15.50	0.02	14.00	0.81	0.02	15.45	0.97
	Ni(II)	50	4.90	0.22	4.51	0.85	0.07	4.85	0.98
		100	9.40	0.62	9.03	0.61	0.13	9.41	0.97
		150	13.60	0.26	13.17	0.83	0.03	13.63	0.98
		200	17.80	0.17	16.33	0.88	0.01	17.84	0.98
UA	Cr(VI)	50	4.90	0.67	4.44	0.63	0.20	5.00	0.97
		100	9.60	0.99	8.87	0.47	0.21	9.52	0.98
		150	14.00	0.62	12.52	0.86	0.06	14.24	0.99
		200	16.50	0.92	15.34	0.85	0.11	16.48	0.99
	Zn(II)	50	4.90	1.79	4.88	0.73	0.35	4.94	0.99
		100	9.40	1.04	9.03	0.76	0.25	9.57	0.97
		150	13.90	0.99	12.20	0.59	0.15	13.81	0.98
		200	17.50	0.90	16.45	0.80	0.10	17.70	0.99
	Ni (II)	50	4.95	0.78	4.60	0.77	0.29	4.98	0.99
		100	9.75	0.96	9.22	0.75	0.22	9.75	0.99
		150	14.32	1.00	13.68	0.77	0.16	14.32	0.99
		200	18.80	0.87	17.62	0.75	0.09	18.84	0.98

^a Experimental, ^b Calculated

Supplementary Data

Biochar from extracted marine *Chlorella* sp. residue with ultrasonication adsorption for high efficiency of heavy metal removal

Muhammad Amin, Pakamas Chetpattananondh*

Department of Chemical Engineering Faculty of Engineering, Prince of Songkla University, 90110, Hat Yai, Songkhla, Thailand.

*Corresponding author: pakamas.p@psu.ac.th (Pakamas Chetpattananondh)

The supplementary data contains:

- Pages: 6
- Figures: 4

List of Figures

Figure. S1 FTIR spectra of BC-450

Figure. S2 N₂ adsorption/desorption isotherms of BC-450

Figure. S3 SEM images of, (a) EMCR, (b) BC-450, (c) BC-450 after UA of Ni(II) and (d) BC-450 after CA of Ni(II)

Figure. S4 XRD

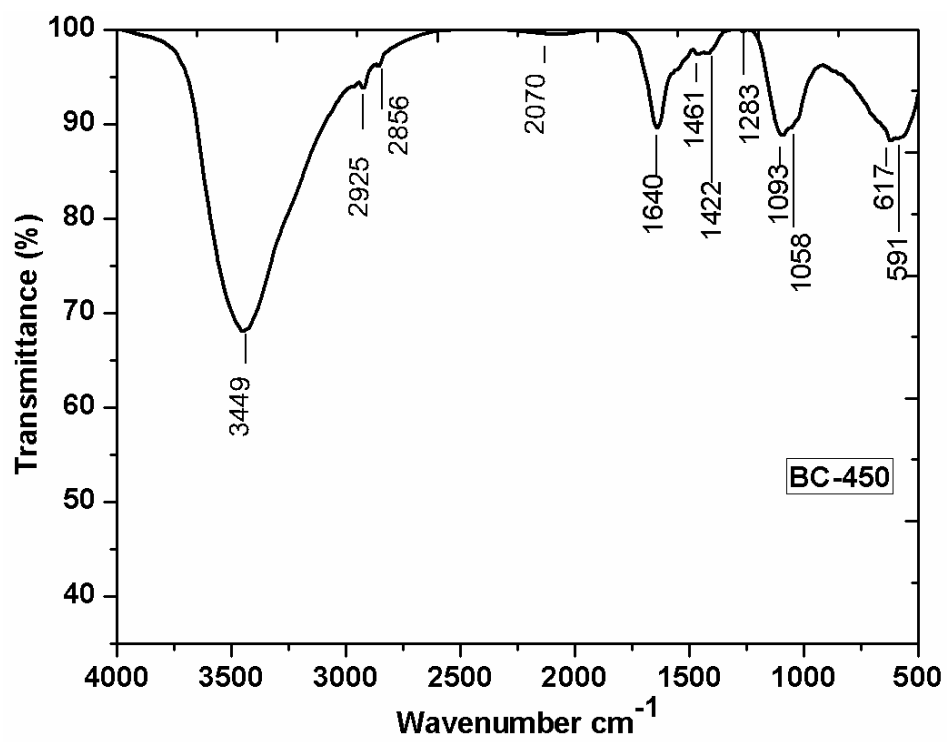


Figure S1 FTIR spectra of BC-450

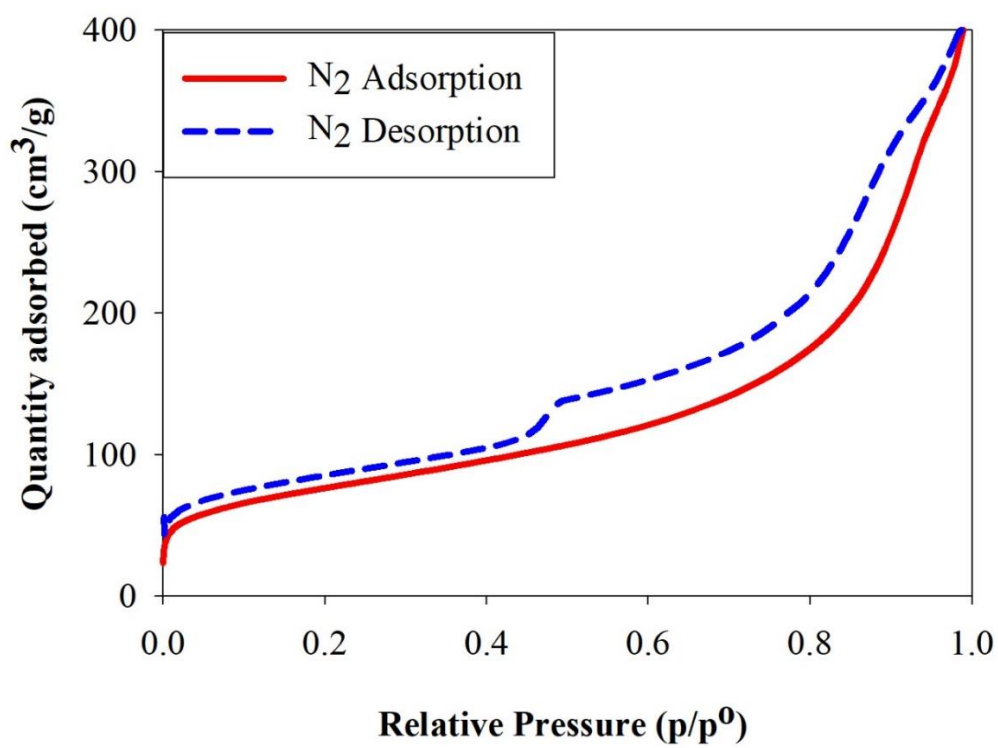


Figure S2. N₂ adsorption/desorption isotherms of BC-450

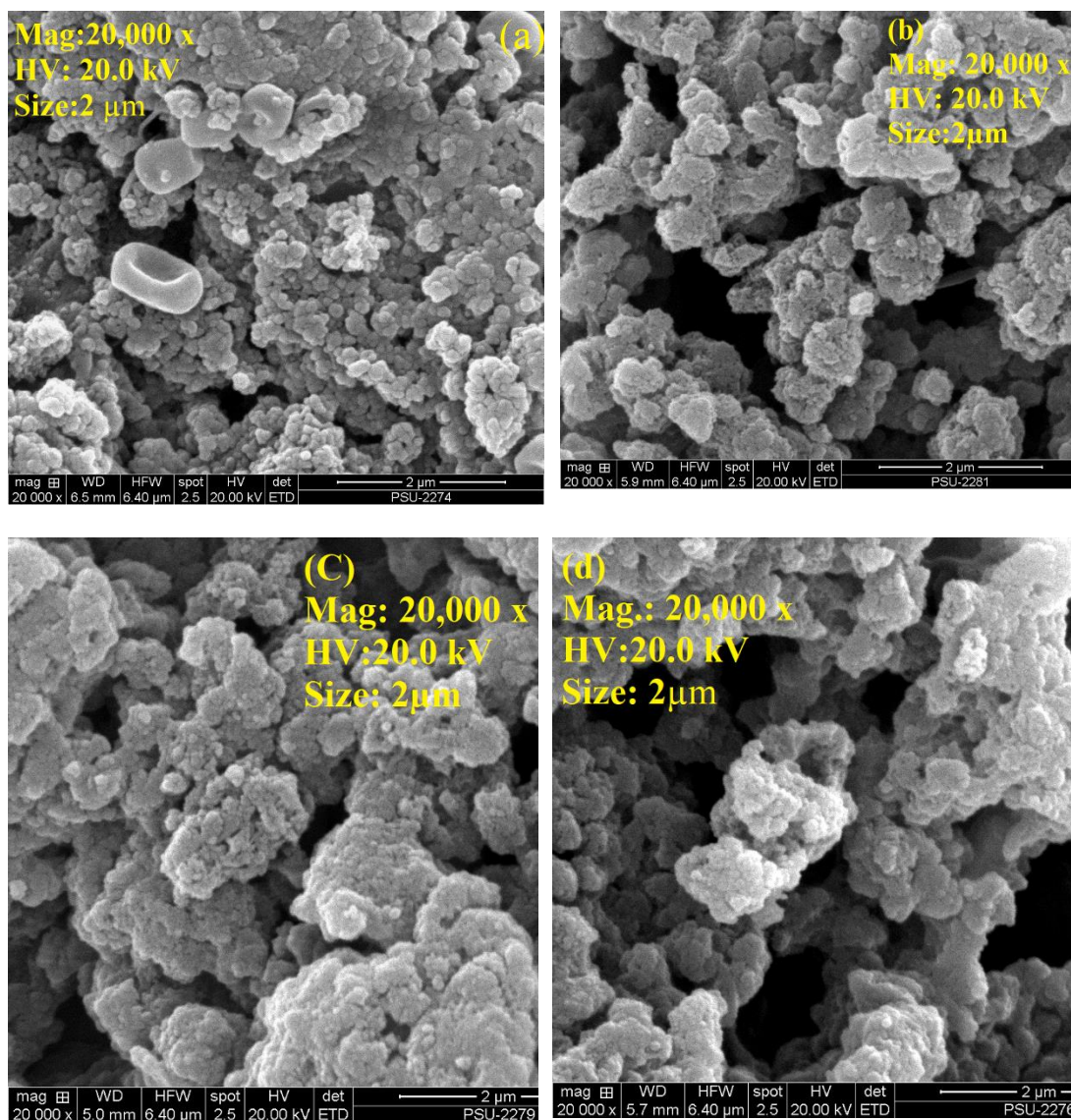
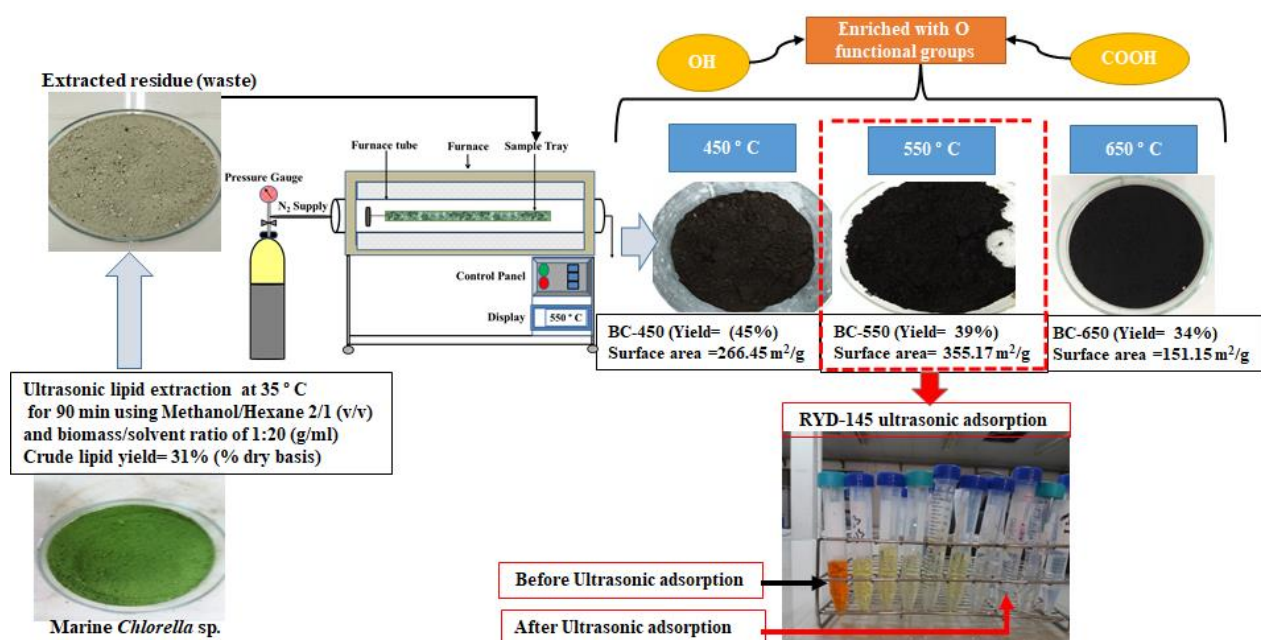


Figure S3 SEM images of, (a) EMCR, (b) BC-450, (c) BC-450 after UA of Ni(II) and (d) BC-450 after CA of Ni(II)

CHAPTER 7

Effects of pyrolysis temperature on extracted marine *Chlorella* solid waste biochar properties and highly efficient ultrasonic adsorption of reactive yellow dye



Highlights

- Recycling of extracted marine *Chlorella* sp. solid waste for biochar production
- Surface area (353.2 m²/g) reduced (151.5 m²/g) as T (°C) rise from 550 °C to 650 °C
- BC-550 surface was negatively charged and O containing functional groups
- Highly efficient adsorption of RYD-145 attained in 1 min. by ultrasonication
- Low frequency ultrasound is better with economic concern

Effects of pyrolysis temperature on extracted marine *Chlorella* solid waste biochar properties and highly efficient ultrasonic adsorption of reactive yellow dye

Muhammad Amin, Pakamas Chetpattananondh*

Department of Chemical Engineering Faculty of Engineering, Prince of Songkla University, 90110, Hat Yai, Songkhla, Thailand.

*Corresponding author email: pakamas.p@psu.ac.th (Pakamas Chetpattananondh)

Abstract

Microalgal biomass extraction for lipid to be used as a primary source for biodiesel, generates a considerable amount of solid waste. Which needs to be managed and could be used to derive valuable byproducts. In this work, extracted marine *Chlorella* sp. solid waste (EMCSW) was recycled to produce biochar (BC) at different temperatures. Physiochemical characterization of resulted biochars were made, and the one with high surface area was selected for reactive yellow dye 145 (RYD-145) treatment by at low and high frequency ultrasonication. The result showed that temperature did not altered the elemental composition significantly and biochars were low in carbon (10 ± 0.8). However, it greatly affected the surface area, which increased from $266\text{ m}^2/\text{g}$ ($450\text{ }^\circ\text{C}$) to $355\text{ m}^2/\text{g}$ ($500\text{ }^\circ\text{C}$) and then decreased to $155\text{ m}^2/\text{g}$ at $650\text{ }^\circ\text{C}$. The high iodine value (129.87 mg/g) of BC-550 among other biochars also supported this trend. The adsorption capacity of BC-550 for RYD-145 was found 40 mg/g under ultrasound treatment for 1 minute. Which could be referred as very effective and quick processing approach. Langmuir and second order kinetic models well described the adsorption mechanism with high correlation coefficient ($R^2=0.99$). Overall, EMCSW recycling to derive efficient adsorbent with high surface area is one of the feasible pathway. Which could substantially improve the environment and economic situation of algal industry.

Keywords: *Chlorella* sp.; solid waste; biochar; ultrasonic; dye adsorption

7.1 Introduction

Domestic and industrial waste water effluents containing toxic pollutants are of major concern for scientific society. The removal of these effluents toxic is essential with environmental perspectives to save this earth [1-2]. Nowadays, modern world industries use a versatile natural or synthetic dyes for better appearance and composition of their final products to attract the customers [3]. The synthetic dyes have found extensive applications in textiles, plastics, paper, leather, clothing, footwear, cosmetics, food processing and minerals industries [2]. Approximately, only textile industry discharges 100 tonnes of different dyes into waste streams [4]. Reactive yellow dye (RYD-145) having sulfate groups of ethyl sulfone and monochlorotriazine belongs to azo structure (double bond of nitrogen) group is widely used for cotton dyeing in textile industry [5]. Such kind of dyes are toxic, less biodegradable and are of dangerous class, which must be removed before effluent discharge [6-7]. The Environmental Protection Agency (EPA) and other environmental regulating organizations have imposed serious regulations to limit the dye consumption and their concentration in discharged effluent [8]. The RYD (145) laden polluted streams can be treated by number of processes namely adsorption, filtration, coagulation, chemical precipitation, nanofiltration, electrochemical, ozonation etc.[9] The adsorption process for dyes is of great interest due to its simple, low cost, stable and highly efficient nature [10]. Biochar has received significant attention as an adsorbent in last few years due to its high efficiency performance for waste water treatment. It is a black solid carbonaceous product obtained by pyrolysis of biomass under controlled condition at 300-800 °C [11-12]. The characteristics of biochar may vary due to difference in the composition of biomass and operating condition [13]. However, slow pyrolysis has been recognized to produce good quality biochar [14]. So far, many adsorbents from various sources i.e. orange peel [15], hazelnut shell [16], Chitosan [17], agricultural residues [18], rice husk [19], tea leaves [20], durian peel [21], bamboo [22], silkworm cocoon [23], watermelon [2] and activated carbon [24] have been developed to treat the waste water. While, research is still going on to find substances for low cost and highly efficient adsorbent.

Micro algae i.e. marine *Chlorella* sp. are promising feedstock of biodiesel and food industry because of their high pigment and lipid content [25-26]. The algal biomass has received attention over terrestrial crops due to high oil contents [27-28]. However, the

high costs of algal biomass preparation associated to cultivation and drying make the downstream process of biodiesel production quite expensive [29]. The production of biodiesel from algal biomass could be more economic by recovery of other precious substances and turn them into valuable products [30]. The residue after lipid extraction is a solid waste and known as extracted or de-oiled biomass. Biodiesel plant of algae at large scale would generate a huge amount of this extracted biomass, which requires a careful handling management [31,14]. This extracted biomass could be used as feedstock for valuable byproducts in livestock, chemical and environmental sector [32-33]. Therefore, the recycling of extracted biomass does not only improve the economy of the *Chlorella* based algal industry but also provides a solution for solid waste management [5]. Post extracted algal biomass contains substantial amount of protein and polysaccharides which can be converted to make biochar to be used as an adsorbent for pollutant removal [25, 30]. Chen et al. [26] has reported the biochar from pigments extracted macroalgae with adsorption capacity of 5306.2 mg/g, 1222.5 mg/g and 345.2 mg/g for malachite, crystal violet and congo red dyes, respectively. 90 mg/l uptake capacity for congo red dye could be attained by adsorption using extracted *Spirulina platensis* derived biochar [29]. While Benkaddour et al. [2] obtained 115 mg/g of reactive yellow dye adsorption on treated watermelon seeds. Biochar from *Gelidiella acerosa* biomass adsorbed 512.5 mg/g methylene blue dye at 30 °C [34]. Zheng et al. [35] reported that biochar from *Chlorella* sp. had higher potential to remove p-nitrophenols (PNP) from waste wastewater than powder activated carbon. The wasted algal biochar could remove 98% of heavy metals from aqueous solution [36]. The biochar preparation at different temperature. The high energy waves of ultrasonic can positively support the mass transport phenomena and enhance the adsorption rate by the generation of a cavitation impact to create the cavitation bubbles, which rapidly collapse near the adsorbent surface and direct microjets of liquid toward it. In addition, shock waves have the potential of creating microscopic turbulence within interfacial films surrounding nearby solid particles, also referred as microstreaming [37]. There is limited information on extracted marine *Chlorella* sp. biochar, its characterization and specifically its application for reactive yellow dye 145 removal by at low and high frequency ultrasonication and is presented in this study for the first time.

This work aimed to (1) investigate the effect of pyrolysis temperature (450 °C-650°C) on the yield, elemental composition and surface functional properties of biochar derived from extracted marine *Chlorella* sp. solid waste (2) evaluate the potential of biochar for RYD-145 adsorption by ultrasonication (3) evaluate the adsorption parameters for optimized removal efficiency and (4) understand the mechanisms of dye adsorption using adsorption kinetics and isotherms

7.2 Materials and methodology

7.2.1 Materials

The reactive yellow dye 145 (RYD 145) used as an adsorbate was of commercial grade and kindly provided by KPT corporation Co. Ltd. Thailand. While NaOH and HNO₃ were purchased from Ajax Finechem, Thailand.

7.2.2 Feedstock preparation

A marine *Chlorella* sp. was cultivated in 25 m³ open pond and was obtained from National Institute of Coastal Aquaculture (NICA) located in Songkhla. it was lyophilized with Dura-Dry MP, FTS systems, USA at 4400 Watt. and extracted by (2/1 v/v) methanol/hexane at 35 °C for 90 min by ultrasonication with an ultrasonic bath (CP 2600 Crest Power sonic, USA, 45 kHz, 300 Watt). The extraction was performed twice. Sufficient quantity of EMCSW was collected. It was washed with DI water, vacuum filtered and dried in hot air oven at 105 °C for 24 hours. The weight of dried product was recorded (300 g) and kept in air tight bags. It was equally divided into three parts for biochar production in next stage. Fig. 7.1 present the overall processing scheme of this work.

7.2.3 Biochar preparation

A hundred gram of EMCSW was used to prepare biochar at 450 °C, 550 °C and 650 °C in each. It was subjected into stainless steel furnace for biochar preparation at set temperature. The furnace chamber was flushed with 100 ml/min N₂ for 20 min. The heating rate was set at 10 °C /min and sample was annealed for 60 min. The raw biochar was collected from furnace chamber as process finished and system cooled down. Biochar was washed with water and oven dried for 3 h at 105 °C. The biochar yield was recorded gravimetrically. The prepared biochars were named as “BC-450, BC-550 and BC-650” and were kept at ambient temperature.

7.2.4 Biochar characterization

Biochars pH was determined in a 1/10 suspension of biochar in DI water (Chen et al., 2018). The elemental properties of biochars was done by proximate analysis using ASTM methods E871, E872-82 and D-1102-84 for moisture, volatile matter and ash content, respectively. While the fixed carbon was calculated by difference. The C, H, N and S was determined by dynamic flash combustion technique using CHNS/O analyzer (Flash 2000, Thermo Scientific, Italy), whereas O content was determined by difference. The surface properties of biochars such as functional groups in the range of 400-4000 cm^{-1} were evaluated using pellet KBr technique by Fourier transformed infrared spectrometer (FTIR, VERTEX 70, Bruker, Germany). The sample was degassed for 6 hours followed by surface area approximation by nitrogen adsorption via BET method using ASAP2460 Surface area and porosity analyzer, Micromeritics, USA. The surface charge property such as zeta potential of biochar samples was determined by dispersing the sample in deionized water and analysis by zeta potential analyzer (ZetaPALS, Brookhaven, USA). The surface structure was observed by scanning electron microscopy (SEM) using Quanta 400 SEM, FEI, Brno, Czech Republic at 20,000 x magnification. The sample to obtain SEM figures was dried and prepared by gold-coating using argon gas (68.9 kPa) in the sputter coater (SPI module, West Chester, Pennsylvania, USA).

7.2.5 Adsorbate preparation

The main features of adsorbate are given in Table 7.1 [2]. Stock solution with 1000 mg/l concentration was prepared by dissolving Specific amount of RYD 145 in double distilled water. Further series of dilutions were made of it for adsorption study.

7.2.6 Adsorption experiment

The potential of high surface area biochar was assessed for RYD 145 removal from aqueous solution by ultrasonic adsorption using CP 2600 Crest Power sonic, USA at ambient temperature. Cool water was circulated during operation to maintain the desired temperature. The effects of processing factors including time (0 sec-2 min), BC dose (0.1-0.5 g/L), pH (3-9), concentration of dye (50-300 mg/L) and ultrasonic frequency (low and high) were studied by varying one factor and fixing the others. The pH of solution was adjusted by 1 M NaOH or 1 M HNO₃. 50 mg/L sample was prepared from RYD 145 stock solution. Initially, 0.3 g BC was used as an adsorbent. The sample

was filled in 250 ml Duran glass bottles and placed in ultrasonic bath at pre-defined conditions. After the adsorption was finished the samples were taken out and filtered through 0.45 μm , 13 mm Nylon syringe filter of CHROM@SEP. The concentration of remaining RYD 145 in solution after adsorption was measured by UV spectrophotometer (HP Agilent 8453) at wavelength of 417 nm.

7.2.7 Isotherm and kinetic models for RYD 145 adsorption

The adsorption of dye was calculated from Eq. (7.1) and removal efficiency (%) is calculated from Eq. (7.2).

$$q_e = \frac{(C_i - C_e) \times V}{m_a} \quad (7.1)$$

$$\text{Removal (\%)} = \frac{(C_i - C_e)}{C_i} \times 100 \quad (7.2)$$

Where q_e (mg/g) is amount of dye adsorbed by biochar, V (mL) is solution total volume of, m_a (g) is amount of BC, C_i (mg/L) is initial dye concentration and C_e (mg/L) is the final concentration of dye.

It is very important to study the relationship between adsorbent and adsorbate by using isotherm models. There are many isotherms that have been introduced and there are limitations of each isotherm. Adsorption of dye on biochar was studied by two parameter isotherms including Langmuir, Freundlich and Temkin models using the nonlinear equation to minimize the errors from the transformations to linear forms [38]. Isotherm model defined by Langmuir is suggests that the adsorbent has a homogeneous monolayer surface and energetically equivalent sites for adsorbate interaction [26]. The adsorbate molecules adhere to already adsorbed molecules of adsorbate, but only on the available surface of adsorbent. The Langmuir isotherm model is expressed by Eq. (7.3).

$$q_e = \frac{q_m C_e K}{1 + C_e K} \quad (7.3)$$

Where q_e (mg/g) is amount of dye adsorbed per mass of adsorbent, q_m (mg/g) is maximum adsorption capacity, C_e (mg/L) is equilibrium concentration and K (L/mg) is Langmuir constant.

A two parameter Freundlich isotherm is well known empirical model without any theoretical basis. This model is applicable to heterogeneous nature surface materials and expressed as given by Eq. (7.4) [26].

$$q_e = K_f C_e^{1/n} \quad (7.4)$$

Where K (mg/g) and 1/n are Freundlich constants related to adsorption capacity and sorption intensity, respectively.

Another two parameter model is Temkin isotherm, which is based on assumption that heat of adsorption of all molecules is directly related to adsorbent surface coverage. The adsorption is characterized by a uniform distribution of binding energies up to the maximum value [39]. This model is given by Eq. (7.5).

$$q_e = \frac{RT}{b_t} \ln(A C_e) \quad (7.5)$$

Where A (L/g) is equilibrium binding constant, b_t (J/mol) is isotherm constant for heat of sorption, R is the gas constant (8,314 J/mol. K) and T is the absolute temperature (K).

Adsorption kinetics is important to study the rate of adsorption, which are influenced by the surface complexity of the adsorbent, solute concentration, pH, temperature and flow. The widely used adsorption kinetic models are pseudo-first and second order given by Lagergren and Blanchard et al., respectively. The nonlinear forms are given as Eq. (7.6) and (7.7), respectively

$$\frac{dq_t}{dt} = k_{P-1}(q_e - q_t) \quad (7.6)$$

$$\frac{dq_t}{dt} = k_{P-2}(q_e - q_t)^2 \quad (7.7)$$

Where q_e (mg/g) and q_t (mg/g) are capacity of adsorbent to adsorb RYD 145 at equilibrium and at given time, respectively. k_{P-1} (1/min) and k_{P-2} (g/mg.min) are rate constants for pseudo first and second order, respectively while t (min) is time.

7.3 Results and Discussion

7.3.1 Main elemental composition of EMCRSW derived biochars

The effect of temperature on elemental composition of EMCRSW derived biochars were evaluated. Table 7.2 presents the main elemental composition of BC-

450, BC-550, BC-650 and previous studies from literature. It could be observed that temperature did not significantly altered the elemental composition among biochars sample. All biochars were of alkaline in nature. While pH was slightly increased from 8.3-9.1 with increasing temperature. Which is possible due to release of the alkali salts in ash as organic acids and carbonate decomposed during the pyrolysis process [26].

The carbon contents were observed as 10-10.5% in all prepared biochars and are in agreement with study of bird et al. [40] and other studies (Table 7.2). The ash contents were found highest for BC-650 while negligible difference for BC-450 and BC-550 was observed. The ash contents could be high at higher temperature due to loss of volatile matters and alkali metals decomposition. It is distinct feature of the algal biomass and its residue to have lower carbon contents than lignocellulosic biomass. Which is mainly correlated to higher ash and nitrogen contents [40-41] High ash in biochar could help to improve the adsorption process and adsorbent capacity [26]. The nitrogen is relatively higher than lignocelulosic biochars and is due to unconverted protein in algal biomass [42].

Biochar has three distinct classes based on the carbon content such as Class 1 deals with materials with 60% carbon or more, Class 2 have materials with 30-60% carbon and materials having 10-30% carbon are of Class 3 [43]. The carbon storage class estimates long-term (i.e., 100 year) soil carbon storage potential of a biochar. From elemental analysis as shown in Table 1 the biochars with 10- 10.5% carbon lied in class 3. The biochars having lower carbon, but higher oxygen and nitrogen are unique feature of algal biochar over lignocellulosic biochars. Although the algal biochars are less able to provide the carbon than lignocellulosic biochars, they can contribute direct nutrient benefits to soil and crop and are notably useful for application on acidic soil [40]. The higher heating value of biochars samples were found low and limiting their application as a fuel and as an alternative could be applied as an adsorbent for waste water treatment.

The yield of Biochar is mainly dependent on pyrolytic processing conditions, including temperature, heating rate, time and nitrogen flow rate. Generally, temperature is negatively correlated with the biochar yield. The biochar yield significantly decreased from 45% to 34% as temperature increased from 450 °C to 650 °C. It is obvious fact that mass loss occurs with rise in temperature due to carbohydrates, protein and other

contents cracking. The obtained yield of EMCRSW derived biochars is in a reasonable range reported from other studies in Table 3. Moreover, 20%-63% yield from biochar has been reported by Yu et al. in their recent review on algal biochars. The high yield of biochar from EMCRSW is showing its potential capability as a new feedstock.

7.3.2 Surface properties of biochars

The surface functional groups of an adsorbent play an important role for adsorption of pollutants. The surface functional groups of BC-450, BC-550 and BC-650 are presented in Fig. 7.2. The effect of temperature was observed as some peaks were disappeared in BC-650 sample. However, the overall main bands were almost similar in all samples. The peaks at 3448 cm⁻¹ and or 2925 cm⁻¹ were indicating the presence of O-H and C-H groups stretching, respectively [44]. This is also ensuring the presence of alcohol and methyl bands of alkenes. While band at 1640 cm⁻¹ was associated carboxylic compounds. The bands at 1422 and 1465 cm⁻¹ were features of C=C, while peaks at 1066, 1074 and 1093 were related to C-O stretch due to alcohols, ethers and phenols, respectively. The peaks at 617 cm⁻¹ and 591 cm⁻¹ are presenting MeX (M: metal, X: halogen) stretching vibrations in halogen compounds [44, 26]. The biochars surface produced at produced at different temperature was rich in O functional groups as evidenced from FTIR data and high O/C content.

The biochars samples were further analyzed for their surface area. It was observed that temperature greatly affected this property of biochar. Which is true in sense that with increase in temperature volatile loss occurs and increase the void space. The increase in surface area was observed (266 m²/g to 351 m²/g) with increasing temperature from 450 °C to 550 °C. Interestingly, as temperature increased to 650 °C the surface area decreased significantly to 151 m²/g. Which could be attribution of vapor condensation at the surface of biochar. The surface area of produced biochar and biochars derived from other materials is presented in Table 3 and Interestingly, the EMCRSW derived biochar has high surface from same class of biomass and even from some lignocellulosic materials as well. The high surface area is highly desired for material to be used as an adsorbent. Hence, EMCRSW derived biochars specifically BC-550 due to its highest surface area could be of attractive choice.

The iodine value is another important parameter which is closely interrelated with surface area of adsorbents. The iodine value of 120.12, 129.80 and 113.36 for BC-

450, BC-550 and BC-650, respectively are in well agreement with surface area result. The surface potential of biochars were determined and found as -11.81, -12.37 and -12.60 for BC-450, BC-550 and BC-650, respectively. Based on high surface area and other good features, BC-550 was selected for RYD 145 adsorption by ultrasonication.

7.3.3 BC-550 performance for ultrasonic adsorption of RYD-145

The effect of contact time, adsorbent dosage, concentration, pH and ultrasonic frequency on RYD-145 removal using BC-550 were evaluated.

7.3.3.1 Effect of contact time

The performance of BC-550 for RYD-145 removal was studied at variable time with 0.3 g/L adsorbent dose, 135 kHz, and 50 mg/L initial dye concentration at the solution pH of 7. From Fig.7.3 (a) it can be seen that the equilibrium times were observed at 1 minutes for RYD-145 removal. Where absorption of dye solution was nearly approaching zero. Not only shorter times, but also higher removal efficiencies were gain by ultrasonic adsorption. Sharifpour et al. 2018 [45] reported that ultrasonic technique was adopted for the adsorption of dye-safranin O, where equilibrium time was attained in shorter duration i.e in 5 min. The shorter adsorption time and higher efficiency obtained with ultrasonic adsorption is highly favorable for practical approach.

7.3.3.2 Effect of pH

The initial pH of solution has great importance in adsorption process. The effect of pH (3-7) was studied at fixed time, 50 mg/l concentration, 135 kHz and 0.3 g/l. There was negligible effect of pH on removal of RYD 145 was observed (not presented), which is in agreement with the study of Nautiyal et al [29]. Hence, remaining all other experiments were performed at pH of 7.

7.3.3.3 Effect of adsorbent dosage

The effect of adsorbent dosage was observed at 135 kHz, operating time 1 min and 50 mg/L solution concentration with pH 7. It could be observed from Fig.7.3 (b) that using 0.1 g/L adsorbent the RYD-145 was not completely removed as evidenced with absorption peak. However, with increased dosage to 0.3 g followed by 0.5 g, the absorption intensity reduced to nearly zero. Which confirmed that maximum dye has been removed form solution. Hence, 0.3 g/L of BC-550 was selected as an optimal choice.

7.3.3.4 Effect of initial dye concentration

The effect of initial dye concentration (50-300 mg/L) was evaluated at 135 kHz and optimized pH, time and adsorbent dosage. As depicted from Fig.7.3 (c), adsorption removal decreased with increase in dye concentration observed from peak intensity of solution at corresponding wavelength and is due to reduced vacant sites availability. The removal efficiency at 50 mg/L to 100 mg/L was highest and could be regarded as more than 95% as evidenced from absorption peak approaching to nearly zero.

7.3.3.5 Effect of ultrasound frequency

The effect of ultrasonic frequency for RYD-145 removal was performed at optimized time, pH, dye initial concentration and adsorbent dosage. The results from Fig. 7.3 (d) showing that BC-550 removed RDY-145 very effectively at both low (35 kHz) and high frequency (135 kHz). So, with economic point of concern ultrasonic adsorption process is recommended in this study.

7.3.4 Adsorption isotherm and kinetics

The adsorption data were analyzed according to Langmuir, Freundlich and Temkin models. The identified isotherm parameters and coefficient of determination (R^2) are given in Table 7.4 and the model based responses of q_e vs C_e are shown in Fig. 7.4. The application of the Langmuir, and Temkin models to the given set of experimental data gave a poor fit and are not suitable for the RYD 145 on BC-550 adsorbent. Freundlich model had the greater value of R^2 and fitted well. This finding is in well agreement with previous studies [2, 26, 29]. The Freundlich isotherm model fits well with high r-squared model value and presenting that BC-550 surface is of heterogeneous nature. The adsorption energy depends on the surface coverage [26]. The pseudo-first and second-order kinetic models were used to characterize mono-nuclear and binuclear adsorption processes, respectively. The results revealed that pseudo second order model with was better fit with R^2 value approaches near unity. Finally, the adsorption of RYD145 on BC-550 is well defined by second order kinetic model, which is associated to chemisorption. Which also conforms the exchange of electrons between the adsorbate and adsorbent.

Conclusion

Extracted marine *Chlorella* sp. residue was pyrolyzed at different temperatures to produce biochar and evaluated their properties. Temperature has significant influence on biochar surface area, while other properties such as pH, yield, zeta potential and elemental compositions were remained unaffected. All biochars possessed negative surface charge. Biochar produced at 550 °C with highest surface area of 355 m²/g was selected for dye removal by ultrasonication. BC-550 showed highly efficient adsorption (99% removal) of RYD 145 in much shorter time (1 min.). The adsorption mechanism was governed by Freundlich isotherm model and chemisorption of pseudo-second-order model well. The recycle of EMCRSW as the feedstock of biochar production and application as an efficient adsorbent is environmentally friendly approach and beneficial for biofuel and biomaterial industries.

Reference

- [1] L. Borah, M. Goswami, P. Phukan, Adsorption of methylene blue and eosin yellow using porous carbon prepared from tea waste: Adsorption equilibrium, kinetics and thermodynamics study, *J. Environ. Chem. Eng.* (2015). doi:10.1016/j.jece.2015.02.013.
- [2] S. Benkaddour, R. Slimani, H. Hiyane, I. El Ouahabi, I. Hachoumi, S. El Antri, S. Lazar, Removal of reactive yellow 145 by adsorption onto treated watermelon seeds: Kinetic and isotherm studies, *Sustain. Chem. Pharm.* (2018). doi:10.1016/j.scp.2018.08.003.
- [3] P. Gharbani, Modeling and optimization of reactive yellow 145 dye removal process onto synthesized MnOX-CeO₂ using response surface methodology, *Colloids Surfaces A Physicochem. Eng. Asp.* (2018). doi:10.1016/j.colsurfa.2018.03.046.
- [4] Y.C. Wong, Y.S. Szeto, W.H. Cheung, G. McKay, Equilibrium studies for acid dye adsorption onto chitosan, *Langmuir.* (2003). doi:10.1021/la030064y.
- [5] I. Khurana, A. Saxena, Bharti, J.M. Khurana, P.K. Rai, Removal of Dyes Using Graphene-Based Composites: a Review, *Water. Air. Soil Pollut.* (2017). doi:10.1007/s11270-017-3361-1.
- [6] A.A. Adeyemo, I.O. Adeoye, O.S. Bello, Adsorption of dyes using different

- types of clay: a review, *Appl. Water Sci.* (2015). doi:10.1007/s13201-015-0322-y.
- [7] N.P. Raval, P.U. Shah, N.K. Shah, Malachite green “a cationic dye” and its removal from aqueous solution by adsorption, *Appl. Water Sci.* (2016). doi:10.1007/s13201-016-0512-2.
- [8] G. Crini, Non-conventional low-cost adsorbents for dye removal: A review, *Bioresour. Technol.* (2006). doi:10.1016/j.biortech.2005.05.001.
- [9] M. El Haddad, R. Slimani, R. Mamouni, S. ElAntri, S. Lazar, Removal of two textile dyes from aqueous solutions onto calcined bones, *J. Assoc. Arab Univ. Basic Appl. Sci.* (2013). doi:10.1016/j.jaubas.2013.03.002.
- [10] M. Rafatullah, O. Sulaiman, R. Hashim, A. Ahmad, Adsorption of methylene blue on low-cost adsorbents: A review, *J. Hazard. Mater.* (2010). doi:10.1016/j.jhazmat.2009.12.047.
- [11] F.R. Oliveira, A.K. Patel, D.P. Jaisi, S. Adhikari, H. Lu, S.K. Khanal, Environmental application of biochar: Current status and perspectives, *Bioresour. Technol.* 246 (2017) 110–122. doi:10.1016/j.biortech.2017.08.122.
- [12] S. Rangabhashiyam, P. Balasubramanian, Characteristics, performances, equilibrium and kinetic modeling aspects of heavy metal removal using algae, *Bioresour. Technol. Reports.* 5 (2018) 261–279. doi:10.1016/j.biteb.2018.07.009.
- [13] R. Li, J.J. Wang, L.A. Gaston, B. Zhou, M. Li, R. Xiao, Q. Wang, Z. Zhang, H. Huang, W. Liang, H. Huang, X. Zhang, An overview of carbothermal synthesis of metal–biochar composites for the removal of oxyanion contaminants from aqueous solution, *Carbon N. Y.* 129 (2018) 674–687. doi:10.1016/j.carbon.2017.12.070.
- [14] Y.M. Chang, W.T. Tsai, M.H. Li, Chemical characterization of char derived from slow pyrolysis of microalgal residue, *J. Anal. Appl. Pyrolysis.* 111 (2015) 88–93. doi:10.1016/j.jaap.2014.12.004.
- [15] M.E. Fernandez, G.V. Nunell, P.R. Bonelli, A.L. Cukierman, Activated carbon developed from orange peels: Batch and dynamic competitive adsorption of basic dyes, *Ind. Crops Prod.* (2014). doi:10.1016/j.indcrop.2014.09.015.
- [16] A. Aygün, S. Yenisoy-Karakaş, I. Duman, Production of granular activated

- carbon from fruit stones and nutshells and evaluation of their physical, chemical and adsorption properties, *Microporous Mesoporous Mater.* (2003). doi:10.1016/j.micromeso.2003.08.028.
- [17] V.M. Esquerdo, T.R.S. Cadaval, G.L. Dotto, L.A.A. Pinto, Chitosan scaffold as an alternative adsorbent for the removal of hazardous food dyes from aqueous solutions, *J. Colloid Interface Sci.* (2014). doi:10.1016/j.jcis.2014.02.028.
- [18] M.A.M. Salleh, D.K. Mahmoud, W.A.W.A. Karim, A. Idris, Cationic and anionic dye adsorption by agricultural solid wastes: A comprehensive review, *Desalination.* (2011). doi:10.1016/j.desal.2011.07.019.
- [19] L. Ding, B. Zou, W. Gao, Q. Liu, Z. Wang, Y. Guo, X. Wang, Y. Liu, Adsorption of Rhodamine-B from aqueous solution using treated rice husk-based activated carbon, *Colloids Surfaces A Physicochem. Eng. Asp.* (2014). doi:10.1016/j.colsurfa.2014.01.030.
- [20] E. Akar, A. Altinişik, Y. Seki, Using of activated carbon produced from spent tea leaves for the removal of malachite green from aqueous solution, *Ecol. Eng.* (2013). doi:10.1016/j.ecoleng.2012.12.032.
- [21] K. Nuithitikul, S. Srikhun, S. Hirunpraditkoon, Influences of pyrolysis condition and acid treatment on properties of durian peel-based activated carbon, *Bioresour. Technol.* (2010). doi:10.1016/j.biortech.2009.07.040.
- [22] S. Hirunpraditkoon, N. Tunthong, A. Ruangchai, K. Nuithitikul, Adsorption Capacities of Activated Carbons Prepared from Bamboo by KOH Activation, *World Acad. Sci. Eng. Technol.* 5 (2011) 591–595.
- [23] J. Li, D.H.L. Ng, P. Song, C. Kong, Y. Song, P. Yang, Preparation and characterization of high-surface-area activated carbon fibers from silkworm cocoon waste for congo red adsorption, *Biomass and Bioenergy.* (2015). doi:10.1016/j.biombioe.2015.02.002.
- [24] A. Demirbas, Agricultural based activated carbons for the removal of dyes from aqueous solutions: A review, *J. Hazard. Mater.* (2009). doi:10.1016/j.jhazmat.2008.12.114.
- [25] Y. di Chen, S.H. Ho, D. Nagarajan, N. qi Ren, J.S. Chang, Waste biorefineries — integrating anaerobic digestion and microalgae cultivation for bioenergy production, *Curr. Opin. Biotechnol.* (2018). doi:10.1016/j.copbio.2017.11.017.

- [26] Y. di Chen, Y.C. Lin, S.H. Ho, Y. Zhou, N. qi Ren, Highly efficient adsorption of dyes by biochar derived from pigments-extracted macroalgae pyrolyzed at different temperature, *Bioresour. Technol.* 259 (2018) 104–110. doi:10.1016/j.biortech.2018.02.094.
- [27] N. Sanyano, P. Chetpattananondh, S. Chongkhong, Coagulation-flocculation of marine *Chlorella* sp. for biodiesel production, *Bioresour. Technol.* 147 (2013) 471–476. doi:10.1016/j.biortech.2013.08.080.
- [28] S. Paisan, P. Chetpattananondh, S. Chongkhong, Assessment of water degumming and acid degumming of mixed algal oil, *J. Environ. Chem. Eng.* 5 (2017) 5115–5123. doi:10.1016/j.jece.2017.09.045.
- [29] P. Nautiyal, K.A. Subramanian, M.G. Dastidar, Adsorptive removal of dye using biochar derived from residual algae after in-situ transesterification: Alternate use of waste of biodiesel industry, *J. Environ. Manage.* 182 (2016) 187–197. doi:10.1016/j.jenvman.2016.07.063.
- [30] A.M.P. Neto, R.A. Sotana de Souza, A.D. Leon-Nino, J.D. arc A. da Costa, R.S. Tiburcio, T.A. Nunes, T.C. Sellare de Mello, F.T. Kanemoto, F.M.P. Saldanha-Corrêa, S.M.F. Giancesella, Improvement in microalgae lipid extraction using a sonication-assisted method, *Renew. Energy.* 55 (2013) 525–531. doi:10.1016/j.renene.2013.01.019.
- [31] R. Maurya, C. Paliwal, T. Ghosh, I. Pancha, K. Chokshi, M. Mitra, A. Ghosh, S. Mishra, Applications of de-oiled microalgal biomass towards development of sustainable biorefinery, *Bioresour. Technol.* 214 (2016) 787–796. doi:10.1016/j.biortech.2016.04.115.
- [32] Y. Chisti, Biodiesel for microalgae, *Biotechnol. Adv.* 25 (2007) 294–306. doi:10.1016/j.biotechadv.2007.02.001.
- [33] N. Rashid, M.S.U. Rehman, J.I. Han, Recycling and reuse of spent microalgal biomass for sustainable biofuels, *Biochem. Eng. J.* 75 (2013) 101–107. doi:10.1016/j.bej.2013.04.001.
- [34] M.J. Ahmed, P.U. Okoye, E.H. Hummadi, B.H. Hameed, High-performance porous biochar from the pyrolysis of natural and renewable seaweed (*Gelidiella acerosa*) and its application for the adsorption of methylene blue, *Bioresour. Technol.* (2019). doi:10.1016/j.biortech.2019.01.054.

- [35] H. Zheng, W. Guo, S. Li, Y. Chen, Q. Wu, X. Feng, R. Yin, S.H. Ho, N. Ren, J.S. Chang, Adsorption of p-nitrophenols (PNP) on microalgal biochar: Analysis of high adsorption capacity and mechanism, *Bioresour. Technol.* 244 (2017) 1456–1464. doi:10.1016/j.biortech.2017.05.025.
- [36] K.M. Poo, E.B. Son, J.S. Chang, X. Ren, Y.J. Choi, K.J. Chae, Biochars derived from wasted marine macro-algae (*Saccharina japonica* and *Sargassum fusiforme*) and their potential for heavy metal removal in aqueous solution, *J. Environ. Manage.* 206 (2018) 364–372. doi:10.1016/j.jenvman.2017.10.056.
- [37] L. Nouri, O. Hamdaoui, Ultrasonication-assisted sorption of cadmium from aqueous phase by wheat bran, *J. Phys. Chem. A.* 111 (2007) 8456–8463. doi:10.1021/jp0721393.
- [38] S. Shahmohammadi-Kalalagh, H. Babazadeh, Isotherms for the sorption of zinc and copper onto kaolinite: Comparison of various error functions, *Int. J. Environ. Sci. Technol.* 11 (2014) 111–118. doi:10.1007/s13762-013-0260-x.
- [39] J.S. Piccin, G.L. Dotto, L.A.A. Pinto, Adsorption isotherms and thermochemical data of FDandC RED N° 40 Binding by chitosan, *Brazilian J. Chem. Eng.* 28 (2011) 295–304. doi:10.1590/S0104-66322011000200014.
- [40] M.I. Bird, C.M. Wurster, P.H. de Paula Silva, A.M. Bass, R. de Nys, Algal biochar - production and properties, *Bioresour. Technol.* 102 (2011) 1886–1891. doi:10.1016/j.biortech.2010.07.106.
- [41] M.I. Bird, C.M. Wurster, P.H. de Paula Silva, N.A. Paul, R. de Nys, Algal biochar: Effects and applications, *GCB Bioenergy.* 4 (2012) 61–69. doi:10.1111/j.1757-1707.2011.01109.x.
- [42] S.S. Kim, H.V. Ly, J. Kim, E.Y. Lee, H.C. Woo, Pyrolysis of microalgae residual biomass derived from *Dunaliella tertiolecta* after lipid extraction and carbohydrate saccharification, *Chem. Eng. J.* (2015). doi:10.1016/j.cej.2014.11.045.
- [43] D. Mohan, A. Sarawat, Y.S. Ok, C.U. Pittman, Organic and inorganic contaminants removal from water with biochar, a renewable, low cost and sustainable adsorbent - A critical review, *Bioresour. Technol.* 160 (2014) 191–202. doi:10.1016/j.biortech.2014.01.120.
- [44] E.B. Son, K.M. Poo, J.S. Chang, K.J. Chae, Heavy metal removal from

aqueous solutions using engineered magnetic biochars derived from waste marine macro-algal biomass, *Sci. Total Environ.* 615 (2018) 161–168. doi:10.1016/j.scitotenv.2017.09.171.

- [45] E. Sharifpour, M. Ghaedi, F. Nasiri Azad, K. Dashtian, H. Hadadi, M.K. Purkait, Zinc oxide nanorod-loaded activated carbon for ultrasound-assisted adsorption of safranin O: Central composite design and genetic algorithm optimization, *Appl. Organomet. Chem.* 32 (2018) 1–11. doi:10.1002/aoc.4099.

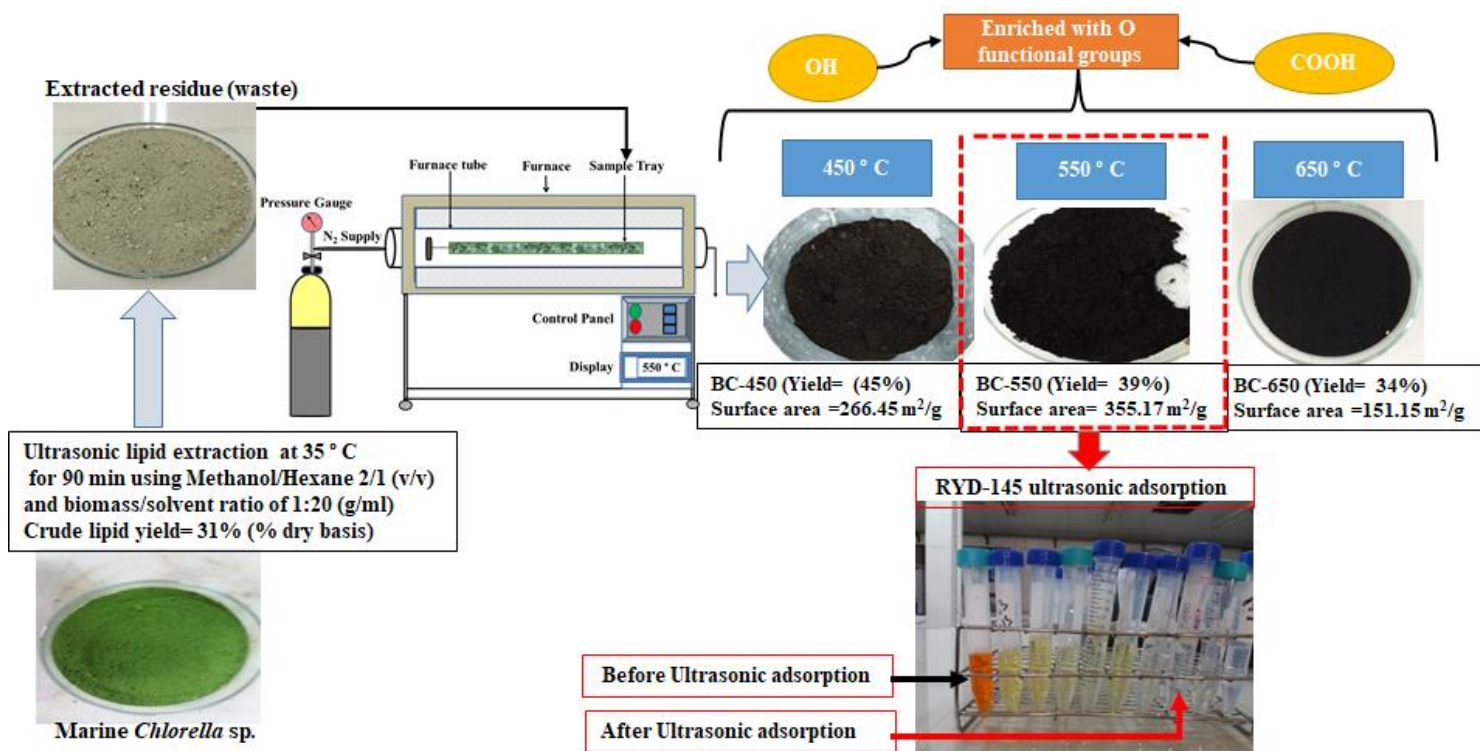


Figure.7.1 Overall processing scheme of biochar production from EMCRSW and its application for RYD 145 adsorption by ultrasonication

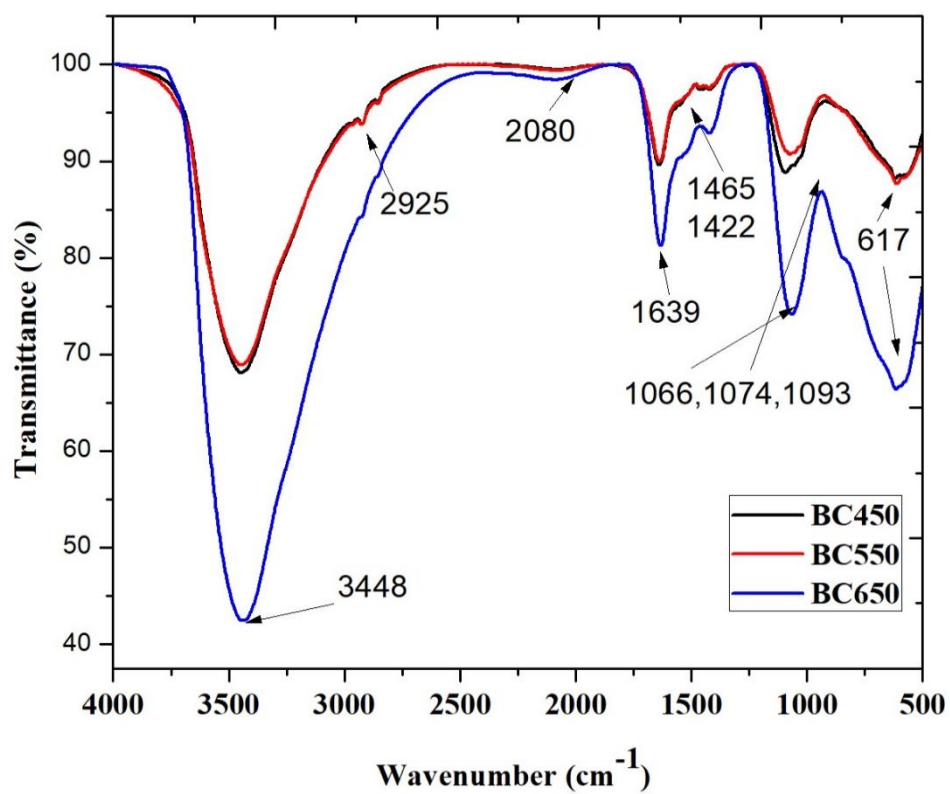


Figure. 7.2 FTIR profiles of EMCRSW derived biochar at different temperatures

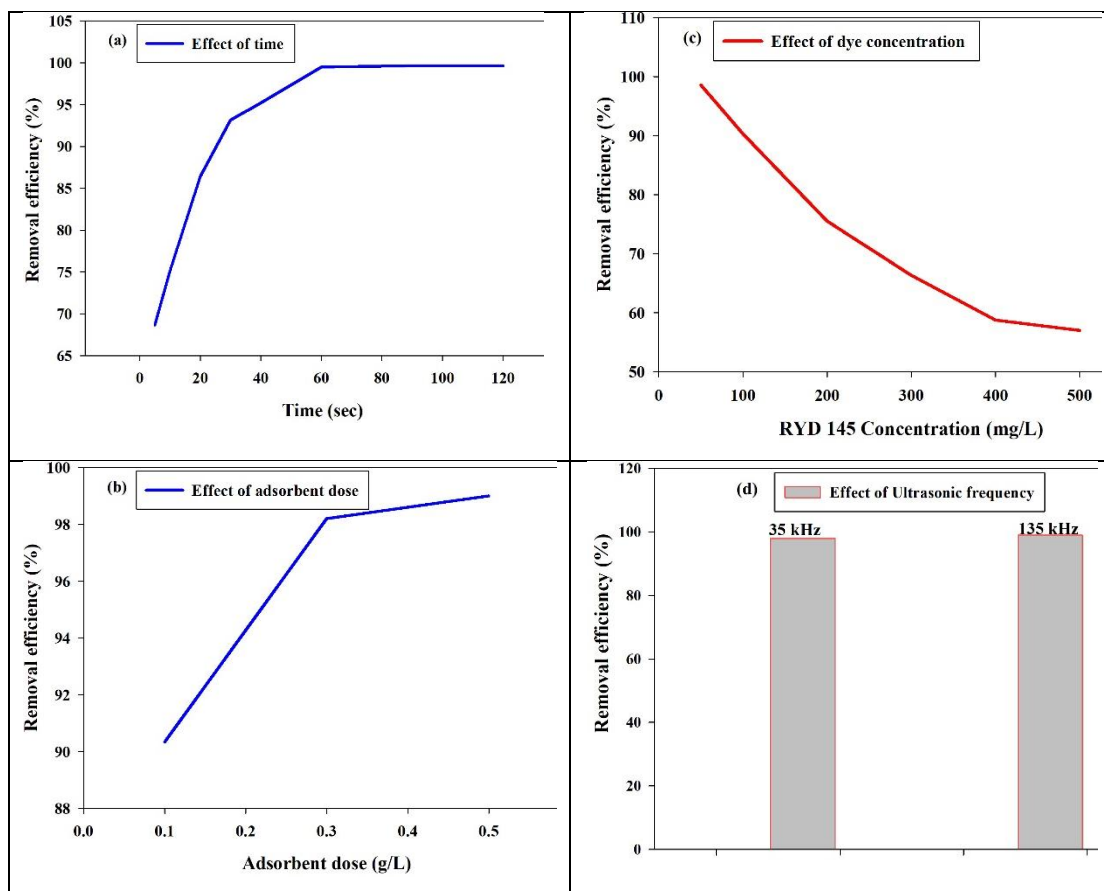


Figure 7.3. Removal efficiency of RYD-145 by BC-550 with ultrasonic adsorption to study effect of (a) contact time (b) adsorbent dosage and (c) initial concentration and (d) ultrasonic frequency.

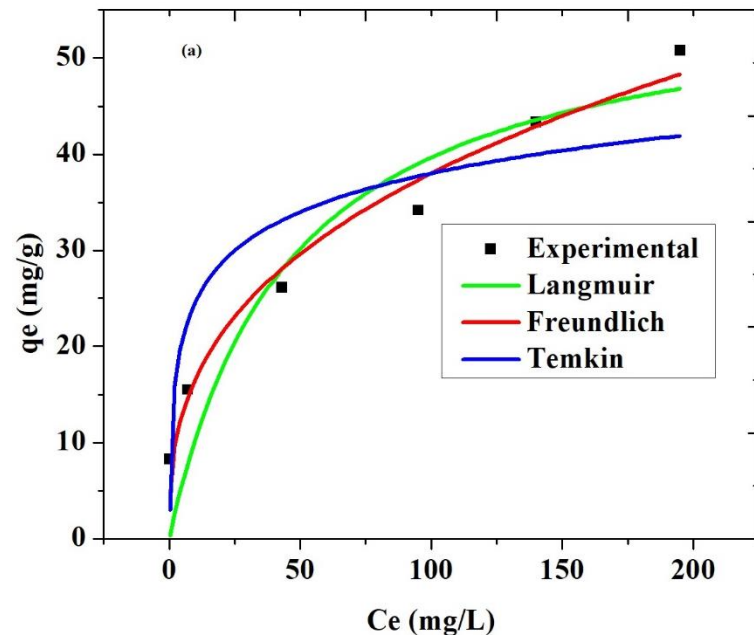


Figure. 7.4 Adsorption isotherm

Table 7.1 Adsorbate characteristics

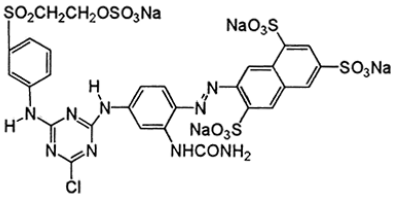
Formula	Molecular weight	Structure
$C_{28}H_{20}ClN_9Na_4O_{16}S_5$	1026.25 (g/mol)	 <p>The chemical structure is a complex organic molecule. It features a central benzimidazole ring system. One nitrogen of the benzimidazole is substituted with a 4-sulfonatephenyl group (SO₂CH₂CH₂OSO₃Na). The other nitrogen is substituted with a 2-amino-5-sulfonatephenyl group (NH₂ and NaO₃S). The 2-amino group is further substituted with a 4-sulfonatephenyl group (SO₃Na). The 5-sulfonate group is also present. The benzimidazole ring has a chlorine atom at the 4-position and a hydrogen atom at the 5-position. The overall structure is highly branched and contains multiple sulfur and oxygen atoms, consistent with the formula C₂₈H₂₀ClN₉Na₄O₁₆S₅.</p>

Table 7.2 Comparison of pH, and composition of EMCRSW derived biochars with other studies

Material	pH	C	H	N	S	O^a	Ash	H/C	O/C	C/N	HHV[#]
BC-450	8.3	10.5	4	1.6	1.0	26.1	56.8	4.6	1.7	6.5	5.6
BC-550	8.7	10	3.6	0.9	0.9	28.1	56.5	4.3	2.1	11.1	4.8
BC-650	9.1	10.1	2.9	0.8	0.9	22.3	63	3.5	1.7	12.6	4.5
FW algal BC	8.1	11.6	0.7	1.3	-	11.7	74.7	0.72	0.75	8.78	2.2
SW algal BC	6.1	17.4	1.8	3.3	-	18.1	59.4	1.22	0.78	5.32	5.1
<i>C. indica</i> BC	7.8	10.2	0.8	1.1	-	14.4	73.5	0.94	1.05	9.27	1.6
<i>Gracilaria</i> BC	7.6	30.9	2.2	2.8	4.4	16.5	43.2	0.85	0.40	11.03	15.6
<i>Eucheuma</i> BC	8.2	24.5	1.5	0.8	9.3	24.9	39	0.73	0.76	30.62	17.3

a by difference method

Higher heating value (MJ)=0.35 C+1.18H+1.10S-0.02N-0.10O-0.02Ash

Table 7.3 Comparison of yield and surface area of EMCRSW derived biochars with other biochars and materials from literature

Material	Condition	Yield (%)	S _{BET} (m ² /g)	Reference
BC-450	450 °C, 60 min	45	266	This study
BC-550	550 °C, 60 min	45	351	This study
BC-650	650 °C,, 60 min		151	
Conocarpus wastes	200 °C-800 °C	51-23	-	Wabel et al. [2012]
Peanut shell	300 °C, 700 °C	22, 37	5.61,448	Ahmed et al. [2012]
Rice straw	500 °C	29.77	34.73	Sew et al. [2016]
Korean cabbage	500 °C	34.19	11.44	
Wood chip	500 °C	21.27	<0.01	
<i>Chlorella</i> residue activated carbon	800 °C, 30 min 900 °C, 30 min	23-29	310 555	Chang et al. (2014)
<i>Gelidiella acerosa</i>			926.4	Ahmed et al. [2019]
<i>Chlorella</i> residue BC	450 °C, 20 min 450 °C, 60 min	44 34	-	Chang et al. (2015)
Pigments extracted algal residue BC	800 °C, 90 min	22	133	Chen et al. (2018)
<i>Spirulina platensis</i> BC	450 °C, 120 min	-	167	Nautiyal et al. (2016)
<i>Chlorella</i> sp. BC	600 °C, 30 min	-	6.16	Zheng et al. (2017)
Magnetic algal HBC	500 °C, 120 min	-	63	Son et al. (2018)
<i>S. japonica</i> BC	700 °C, 120 min 400 °C, 120 min	25 38	1.3 1.3	Poo et al. (2018)
<i>Eucheuma</i> sp. BC	450 °C, 60 min	57	34	Roberts et al.(2015)
<i>Sargassum</i> sp. BC	450 °C, 60 min	49	2.5-7.5	Roberts et al.(2015)
<i>Saccharina</i> sp. BC	450 °C, 60 min	45	1.3-8.5	Roberts et al.(2015)
Corn straw BC	600 °C, 120 min	-	13.08	Chen et al. (2011)
Empty fruit bunch BC	600 °C, 128 min	25	421	Zamani et al. (2017)
Peanut hull BC	450 °C, 60 min	-	24.01	Han et al. (2016)

Table 7.4 adsorption isotherm parameters

Adsorption parameter	Ultrasonic adsorption of RYD-145
Experimental q_{\max} (mg/g)	50.83
Langmuir	
q_{\max} (mg/g)	57.84
K_L	0.0218
R^2	0.85
Freundlich	
K_f	7.24
n	2.77
R^2	0.97
Temkin	
b_T (J/mol)	5.80
A_T (L/mg)	6.97
R^2	0.78

CHAPTER 8

Extraction and Quantification of Chlorophyll from Microalgae *Chlorella* sp.

M Amin^{1,2*}, P Chetpattananondh¹, M N Khan², F Mushtaq² and S K Sami²

¹Department of Chemical Engineering, Faculty of Engineering, Prince of Songkla University, 90112, Hat Yai, Thailand

²Department of Chemical Engineering, Faculty of Engineering and Architecture, BUITEMS, 87300, Quetta, Pakistan

*Corresponding author email: engr_amin63@yahoo.com

Abstract

Algal biomass emerged as a potential source of bioenergy and valuable derivatives in recent years. The major characteristics of microalgae such as high oil contents, carbon sequestration, high growth rate and valuable by-products are leading factors to compete with traditional resources. The aim of current study was (i) to extract and optimize chlorophylls (a and b) at temperature (30-40°C) and time (60-120 min) by ultrasonication assisted with methanol: hexane (2:1v/v) (ii) to find suitable dilution factor for chlorophyll analysis by UV spectroscopy considering 1:10, 1:15, 1:20 ml/ml and (iii) to determine suitability of dissolving methanol/hexane extract in different solvents for analysis and quantification by simultaneous equations. The full factorial design RSM was employed and found that model is well fitted (0.99 R²). Maximum recovery of total chlorophylls (a and b) was 17.15 µg/ml achieved at 30 °C and 120 min. The absorbance spectra peaks were found good with a dilution factor of 1:20 ml/ml. Dissolving the extract for analysis in same solvent is suitable choice even though acetone shows sharp peaks, but not in agreement with beer law. These pigments have a high market in pharmaceutical, dietary products, and food industry and recovery of these compounds can play an important role to make bioprocess industry more economical.

8.1 Introduction

Microalgae are considered as the 3rd generation resource for energy and received high focus in recent years. A microalga is unicellular organism, which possess the tendency to convert sun energy into chemical energy efficiently via photosynthetic process. A variety of strains available in algal class and *Chlorella* is one of them. Microalgae *Chlorella* sp. is single celled and green species with 2-10 μm [1]. It contains about 20, 45, 20 % fat, protein, carbohydrate [2,3], and 0.5-1 % pigments per weight of dry biomass [4]. The composition of biomass may vary due to different cultivation media and associated factors. *Chlorella* has oil contents of 28-32% [5] and abundantly available pigments due to photosynthetic action [6].

Chlorophyll is bioactive compound, which have wide application in pharmaceuticals, food and color industry [7]. Mainly there are two types of green pigments, namely chlorophyll-a and b, however excessive heat, light or air can destabilize the product [8]. This destabilization can degrade the chlorophyll product. The structure of chlorophyll is porphyrin macrocycle with four pyrrole rings, while presence of single isocyclic with pyrrole ring built phorbins structure. There are four carbons and a nitrogen atom in pyrrole ring. The position of nitrogen atoms easily attracts Mg^{+2} ions for binding. In chlorophyll-b, formyl group take over methyl group in ring, which differentiate it from chlorophyll-a. This structure difference between two classes of chlorophyll makes identification process easier by their peaks at respective wavelength and region (665 for Ch.-a, and 652 for Ch.-b) [8].

The downstream process of cell disruption for microalgal cell to release associated products is necessary, which could be achieved via physical or chemical method [9]. Earlier, soxhlet extraction procedure assisted with solvent was famous one, but it is time and energy intensive. The technological development in research and industrial sector introduced the new ways of disruption such as ultra-sonication and microwave. These methods do not only rupture the high dense cell very effectively but also conform short duration as well.

The use of ultrasonic as extractant method is of increased interest widely due to high efficiency and shorter time required [10]. The extraction process usually carried out with aid of chemicals such as chloroform, acetone, methanol and ethanol. A normal

protocol for chlorophyll extraction use acetone as effective solvent, however this is one of toxic solvent. The solvent selected for extraction process must be less harmful. Normally cell disruption of algal biomass release intercellular products, which comprised of lipids and chlorophylls mixture known as crude extract. Lipids are precursor of biodiesel production, which is not an objective of current study. Various studies conducted on lipid extraction from microalgae but limited data is found on quantification of chlorophylls in crude extract using different solvent. Current study focused on optimization of process and quantification of chlorophylls in crude extract, extracted via solvent assisted ultrasonic technique.

8.2 Material and Methodology

8.2.1. Material and Chemicals

A marine microalgae *Chlorella* sp. was cultivated in 20 m³ open aerated pond at National Institute of Coastal Aquaculture (NICA), Songkhla, Thailand as shown in Figure 1. The culture growth was attained using CO (NH₂)₂ and 16-16-16 fertilizer (16% N₂, 16% P and 16% K) as growth medium. Due to open cultivation scheme the other sources such as Light and CO₂ were provided naturally for photosynthetic action. Commercial grade n-hexane, methanol, ethanol and acetone were purchased from ACI Labscan Ltd., while aluminium sulphate was obtained from Saim chemical company Ltd. Thailand.



Figure 8.1. Marine *Chlorella* sp. cultivated in 20 m³ open pond system

8.2.2 Biomass harvesting and post processing

The cultured biomass attained peak growth phase in 7 days with cell density of 0.8 g/l was harvested using aluminium sulphate as flocculant agent. After harvesting biomass slurry was filtered using cheese cloth to remove any present contamination, filled in 20 L gallons and stored at 4 °C. The stored algal biomass slurry was washed thrice with DI water to remove salinity and pH was recorded as 7.5.

Cleaned biomass slurry was subjected to dewatering using vacuum filtration with GENVAC vacuum pump (PVL 3, 0.5 mbar, Italy). The slurry was stirred gently to enhance filtration rate. The wet paste as shown in Figure 2 was collected in zip locked air tight bags and stored at 4 °C for short period of time before starting extraction. 1gallon (20 L) slurry yields about 1 kg wet paste.



Figure 8.2. Fresh wet algae paste (10-12% dw solid biomass) after vacuum filtration

Extraction process was performed using ultrasonic bath (Crest power sonic, 45 kHz, CP 2600, USA). Experiment was conducted at different temperature (30-40 °C) and time (60-120 min) values. The Stored wet paste biomass was brought to room temperature firstly, then 10 gm (dw% basis) was placed in 250 ml Duran bottle. Organic solvent methanol: hexane (2:1 v/v) was mixed with sample and stirred for 1 minute. To prevent chlorophyll degradation due to light, sample bottles were covered with aluminium and placed in ultrasonic extraction bath at predefined condition. The extract after different time intervals were taken out and filtered using whatman 4 by vacuum application.

Residual biomass was stored for further processing, while filtrate was evaporated using Heidolph Laborta 4000 rotary evaporator for solvent recovery. The extract

obtained after solvent recovery was solid at ambient temperature. This solid was resuspended in methanol initially, instead of solvent mixture used for extraction, because developed simultaneous equation only deals with single solvent. Methanol was selected because of its higher proportion as extractant and have polar nature as well, which can easily dissolve green pigments. Optimum condition for chlorophyll quantity (previously using methanol) was determined, after that extract was dissolved in different solvents such as ethanol and acetone to perform analysis.

8.2.3 Analysis

The compositional analysis of wet paste biomass was performed according to standard procedures of Association of Official Analytical Chemist (AOAC). The AOAC protocols 991.20, 920.39, 942.05 were adopted to find out protein, crude fat and ash. Moisture contents were determined on the weight loss basis at 90-95 °C, while ANKOM²⁰⁰ analyzer was used to measure crude fiber contents at ADCET, PSU, Thailand. The carbohydrate and energy contents were determined by calculation method.

The UV-spectrophotometer (Agilent 8453, USA) was used for chlorophylls analysis. The sampling quartz of 1 cm was used in spectrophotometry. UV system was calibrated prior to analysis and blank reading was taken. Initially different dilutions 1:10, 1:15, 1:20 and 1:25 ml/ml (sample: solvent) were performed to get clear peaks at full spectrum range (100-800 nm). Further measurements were taken at best found dilution factor. Green pigments (chlorophyll a and b) absorb light in red and blue region. The developed simultaneous equations [Equation (8.1-8.3), for methanol, ethanol and acetone respectively were used to quantify chlorophylls from plants [11].

$$\begin{aligned} \text{Ch - a} &= 16.29A_{665.2} - 8.54A_{652.0} \\ \text{Ch - b} &= 30.68A_{652.0} - 13.58A_{665.2} \end{aligned} \quad (8.1)$$

$$\begin{aligned} \text{Ch - a} &= 13.36A_{664} - 5.19A_{649} \\ \text{Ch - b} &= 27.43A_{649} - 8.12A_{664} \end{aligned} \quad (8.2)$$

$$\begin{aligned} \text{Ch - a} &= 12.25A_{663.6} - 2.55A_{646.6} \\ \text{Ch - b} &= 20.31A_{646.6} - 4.91A_{663.6} \end{aligned} \quad (8.3)$$

The samples absorbance was recorded at desired wavelength as per above equation and quantity ($\mu\text{g/ml}$) of chlorophylls were calculated. The total quantity of

chlorophyll a and b was determined based on summing up the individual chlorophyll values and modeled as yield.

The 3^2 (2 factors 3 levels) full factorial response surface experimental design with 2 additional runs at centre point was selected to observe the effects on response (total quantity of chlorophylls). The design of the experiment, parametric analysis (ANOVA) by multiple regression and optimization was performed using Statistica version 10.0. Two factors temperature as X_1 (30, 35 and 40 °C) and time as X_2 (60, 90 and 120 min) were coded into three level as -1 (low), 0 (center) and +1 (high). The relationship between coded and actual value is presented in Equation (8.4).

$$X_i = \frac{x_i - x_o}{\Delta x} \quad (8.4)$$

Where X_i is coded value of independent variable; x_i is original factor; x_o is base value at center point and Δx is step change between low and high level. The experimental data were fitted according to Equation (8.5), which is the general form of the proposed model.

$$y = \beta_o + \sum_{i=1}^k \beta_i X_i + \sum_{i=1}^k \beta_{ii} X_i^2 + \sum_{i>j}^k \beta_{ij} X_i X_j + \varepsilon \quad (8.5)$$

Where y is response and β_o , β_i , β_{ii} , β_{ij} are linear, quadratic and interaction terms of model. The predictive response was studied for dependent variables and correlation equations were developed.

8.3 Results and discussion

8.3.1 Wet paste biomass compositional analysis

The compositional analysis of wet paste was determined by standard AOAC procedures. The composition of different microalgae strains is different, even same strain could have different composition due to diversity in culture. Moisture contents were found 90%, which means only 10% (dw) solid contents of algal biomass available. Fang et al., (2016) reported the findings for *Chlorella* sp. Wet biomass [12]. It is in normal range with respect to vacuum filtration application to concentrate biomass from 5-15%. Protein, crude fat, ash, carbohydrates and energy (kcal) contents were found 0.76, 0.8, 1.36, 1.59 and 9.43 respectively.

8.3.2 Ultrasonic extraction and optimization

The full factorial response surface methodology was adopted to design and optimize the ultrasonic extraction experiment. Response surface methodology is one of the most attractive tool for optimization of process [13]. The details of experiment such as coding and actual factors scheme, experimental and predicted response are presented in Table 1. The response fitted model regression analysis (ANOVA) is shown in Table 2. The data shows that experimental and predicted response is in good agreement and residual is minimal. Regression analysis was performed at 95% confidence level.

The model F value is good and making it significant, only 0.01% chance is there that error could be due to some unavoidable factor. Both linear, interaction and squared interaction terms are significant having p-value less than 0.05. Lack of test is non-significant with p-value of 0.91, which confirms the best fit of model. The R-squared of 0.99 very close to 1 is presenting good fit of model as well at 95% confidence.

On the other hand, adjusted and predicted R-squared value of 0.98 and 0.97, which are very close to R-squared value of 0.99 are well justifying the model. The standard deviation of 0.18, and 1.26% C.V leading to reliability of model. By backward elimination as setting confidence level at 0.95 a refined equation (8.6) in terms of coded factors was developed for response variable.

$$Y = 13.80 - 1.57X_1 - 0.95X_2 + 0.43X_1^2 - 1.17X_1X_2 + 1.12X_1^2X_2 \quad (8.6)$$

The selected solvent methanol shows high response in extracting these value-added products, as it was confirmed in our preliminary analysis as well. Some studies also reported methanol as consistent solvent for excellent capability of chlorophyll extraction compared to other solvents [14,15].

Response surface and contour plot of factors with respect to yield are given in Figure 3. Both factors showing significant effect on response, at 30 °C yield increased linearly with time increment but at 35 °C and 40 °C response yield trend was found in decreasing order as time increased. Kong et al.[16] study states that chlorophyll extraction via ultrasound increased linear with time at specific temperature, after that it started to decrease. This could be due to fact that chlorophylls start to degrade, if excessive heating applied [17]. The optimum condition was observed 30 °C and 120 min at which recovery was 17.19 (µg/ml). Two trials were performed at optimized condition to check accuracy and found ± 0.02 .

Table 8.1. Full factorial design runs with actual and model predicted response

Run	Actual Factors		A	A	Coded Factors		Total chlorophylls ($\mu\text{g/ml}$)	
	Temperature ($^{\circ}\text{C}$)	Time (min)	(665.2)	(652.0)	X ₁	X ₂	Experimental	Predicted
1	30	120	0.85	0.67	-1	1	17.20	17.15
2	35	120	0.62	0.51	0	1	12.90	12.8
3	35	90	0.70	0.54	0	0	13.80	13.85
4	35	90	0.75	0.54	0	0	14.0	13.80
5	30	60	0.80	0.56	-1	-1	14.50	14.45
6	40	120	0.59	0.46	1	1	11.70	11.67
7	35	60	0.91	0.56	0	-1	14.80	14.75
8	40	60	0.76	0.53	1	-1	13.70	13.67
9	40	90	0.64	0.49	1	0	12.60	12.67
10	35	90	0.82	0.51	0	0	13.50	13.8
11	30	90	0.98	0.59	-1	0	15.70	15.8

8.3.3 Dilution factor and dissolving of methanol/hexane extract in different solvents.

The dilution factor for spectroscopy analysis was investigated and 1:20 ml/ml factor is reasonable to produce clear peaks. Dissolving the methanol/hexane solvent extract in different single solvents (as per simultaneous equations) in methanol, ethanol, acetone was solely based on fact to plug data in available equations, and in case of suitability, choice of ethanol (non-toxic) as friendly solvent. It has been found that dissolving extract in different solvent (instead of extractant) is not good choice, however peaks were good but absorbance was more than 2, which sounds not good, because spectrophotometer linear absorbance range is between 0.1-1. Due to this fact chlorophyll calculated amount and absorbance values of sample diluted in ethanol and acetone are not presented here.

Table 8.2 Regression analysis

Source	SS	MS	F	df	p	significance
Model	22.69	4.54	144.82	5	<0.0001	significant
X ₁	14.73	14.73	470	1	<0.0001	significant
X ₂	1.80	1.80	57.61	1	0.0006	significant
X ₁ X ₂	5.52	5.52	176.25	1	<0.0001	significant
X ₁ ²	0.51	0.51	16.34	1	0.0099	significant
X ₁ ² X ₂	1.69	1.69	53.86	1	0.0007	significant
X ₁ X ₂ ² , X ₂ ²						Not significant
Residual	0.16	0.031		5		Not significant
LOF	0.30	1e ⁻²	0.16	3	0.91	
Pure error	0.13	0.063		2		
Total	22.85			10		
Precession	R²	R² Adj.	Std. Dev	Pred. R²	C.V %	
41.9	0.99	0.98	0.18	0.97	1.26	

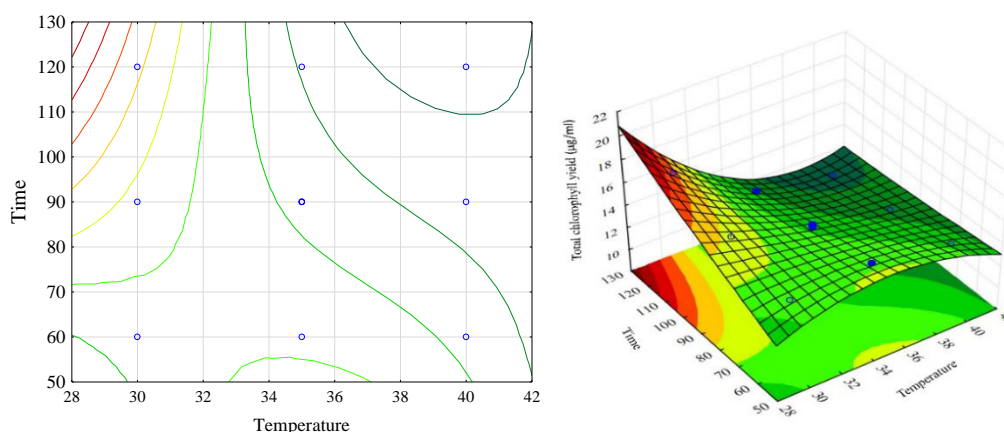


Figure 8.3. Surface and contour plots of fitted response for total chlorophyll yield ((µg/ml).

Conclusion

Current study presents that marine *Chlorella* sp. possess considerable amount of chlorophylls, which could be extracted and purified for wide range applications. High temperature was found not suitable for extraction as it might degrade pigments. Dissolving the extract (methanol/hexane) in methanol was found good, but it's

dissolving in ethanol and acetone was not accurate despite of producing clear peaks. It is concluded that same solvent (methanol in current study because of higher proportion with respect to hexane) utilized for extraction is best for dissolving again for analysis. More work is required in purification and developing simultaneous equation for mixed solvent.

Acknowledgment

The corresponding author is grateful to Graduate School Prince of Songkla University, Hat Yai, Thailand for the provision of Thailand's Education Hub for Southern Region of ASEAN Countries (THE-AC) scholarship, 2016.

References

- [1] Kelaiya S V., Chauhan P M and Akbari S H 2015 Fuel Property of Biodiesel Made From Microalgae (*Chlorella* sp.) *Curr. World Environ.* **10** 912–9
- [2] Phukan M M, Chutia R S, Konwar B K and Kataki R 2011 Microalgae *Chlorella* as a Potential bio-energy feedstock *Appl. Energy* **88** 3307–12
- [3] Kay R A and Barton L L 1991 Microalgae as Food and Supplement *Crit. Rev. Food Sci. Nutr.* **30** 555–73
- [4] D'Alessandro E B and Antoniosi Filho N R 2016 Concepts and studies on lipid and pigmentsof microalgae: A review *Renew. Sustain. Energy Rev.* **58** 832–41
- [5] Chisti Y 2008 Biodiesel from microalgae beats bioethanol *Trends Biotechnol.* **26** 126–31
- [6] Nurachman Z, H H, Rahmadiyah W R, Kurnia D, Hidayat R, Prijamboedi B, Suendo V, Ratnaningsih E, Panggabean L M G and Nurbaiti S 2015 Tropical marine *Chlorella* sp. PP1 as a source of photosynthetic pigments for dye-sensitized solar cells *Algal Res.* **10** 25–32
- [7] Borowitzka M A 2013 High-value products from microalgae-their development and Commercialisation *J. Appl. Phycol.* **25** 743–56
- [8] Halim R, Hosikian A, Lim S and Danquah M K 2010 Chlorophyll extraction from microalgae: A review on the process engineering aspects *Int. J. Chem. Eng.* **2010**
- [9] Lee J Y, Yoo C, Jun S Y, Ahn C Y and Oh H M 2010 Comparison of several methods for Effective lipid extraction from microalgae *Bioresour. Technol.* **101** S75--S77
- [10] Parniakov O, Apicella E, Koubaa M, Barba F J, Grimi N, Lebovka N, Pataro G, Ferrari G and Vorobiev E 2015 Ultrasound-assisted green solvent extraction of high-added value Compounds from microalgae *Nannochloropsis* spp. *Bioresour. Technol.* **198** 262–7
- [11] Sumanta N, Haque C I, Nishika J and Suprakash R 2014 Spectrophotometric Analysis of Chlorophylls and Carotenoids from Commonly Grown Fern Species by Using Various Extracting Solvents *Res. J. Chem. Sci. Res. J. Chem. Sci* **4**

2231–606

- [12] Yang F, Cheng C, Long L, Hu Q, Jia Q, Wu H and Xiang W 2015 Extracting lipids from Several species of wet microalgae using ethanol at room temperature *Energy and Fuels* **29** 2380–6
- [13] Li Y, Cui F, Liu Z, Xu Y and Zhao H 2007 Improvement of xylanase production by *Penicillium oxalicum* ZH-30 using response surface methodology *Enzyme Microb. Technol.*
- [14] Riemann B and Ernst D 1982 Extraction of chlorophyll a and chlorophyll b from Phytoplankton using standard extraction techniques *Freshw. Biol.*
- [15] Molnár É, Dóra Rippel-Pethő ! and Bocsi R 2013 Solid-Liquid Extraction of Chlorophyll From Microalgae From Photoautotroph Open-Air Cultivation *Hungarian J. Ind. Chem.Veszprém* **41** 119–22
- [16] Kong W, Liu N, Zhang J, Yang Q, Hua S, Song H and Xia C 2012 Optimization of ultrasound- Assisted extraction parameters of chlorophyll from *Chlorella vulgaris* residue after lipid Separation using response surface methodology *J. Food Sci. Technol.* **51** 2006–13
- [17] Schumann R, Häubner N, Klausch S and Karsten U 2005 Chlorophyll extraction methods for the quantification of green microalgae colonizing building facades *Int. Biodeterior. Biodegrad.* **55** 213–22

VITAE

Name Muhammad Amin

Student ID 5910130010

Educational Attainment

Degree	Name of Institution	Year of Graduation
Bachelor of Science (Chemical Engineering)	BUIITEMS	2010
Master of Science Chemical Engineering (Sustainable Process Development)	University of Moratuwa	2015

Scholarship Awards during Enrolment

1. Thailand's Education Hub for Southern Region of ASEAN Countries (THE-AC) scholarship, 2016
2. Research Thesis Grant, Graduate School, PSU, Thailand.

Work – Position and Address

Assistant Prof. Department of Chemical Engineering, BUIITEMS, Takatoo campus, airport road Quetta, Pakistan.

List of Publication and Proceeding

1. M. Amin, P. Chetpattananondh “Enhanced lipid recovery from marine *Chlorella* sp. by ultrasonication with an integrated process approach for wet and dry biomass” Bioenergy Research, 2019, 1-15.
2. M. Amin, P. Chetpattananondh, S. Ratanawilai “Application of extracted marine *Chlorella* sp. residue for bio-oil production as the biomass feedstock and microwave absorber” Energy Conversion and Management, 195 (2019):819-829.

3. M. Amin, P. Chetpattananondh “Biochar from extracted marine *Chlorella* sp. residue for high efficiency adsorption with ultrasonication to remove Cr (VI), Zn (II) and Ni (II)” *Bioresource Technology*, 289 (2019) 121578.
4. M Amin, P Chetpattananondh, M N Khan, F Mushtaq and S K Sami “Extraction and Quantification of Chlorophyll from Microalgae *Chlorella* sp.” *IOP Conf. Series: Material Science and Engineering* 414 (2018) 0120025.